Hawaii Ocean Time-series
Data Report 3
1991

Christopher Winn
Roger Lukas
David Karl
Eric Firing

University of Hawaii
School of Ocean and Earth Science and Technology
1000 Pope Road
Honolulu, Hawaii 96822
U. S.A.

SOEST
TECHNICAL REPORT
93-3

Preface

The Hawaii Ocean Time-series (HOT) project has been making repeated observations of the hydrography, chemistry and biology at a station north of Hawaii since October 1988. The objective of this research is to provide a comprehensive description of the ocean at a site representative of the central north Pacific Ocean. Cruises are made approximately once a month to the HOT deep-water station (22 45' N, 158W) located about 100 km north of Oahu, Hawaii. Measurements of the thermohaline structure, water column chemistry, currents, primary production and particle sedimentation rates are made over a 72-hour period on each cruise.

This document reports the data collected during 1991. However, we have included some data from 1988, 1989 and 1990 in order to place the data collected in 1991 within the context of our time-series observations. The data reported here are a screened subset of the complete data set. Summary plots are given for CTD, biogeochemical, optical, meteorological and ADCP observations.

In order to conserve paper and to provide easy computer access to our data, CTD data at the National Oceanographic Data Center (NODC) standard pressures for temperature, potential temperature, salinity, oxygen and potential density are provided in ASCII files on the enclosed diskette. Chemical measurements are also summarized in a set of Lotus 1-2-3™ files on the enclosed diskette. A more complete data set resides on a Sun workstation at the University of Hawaii. These data are in ASCII format, and can easily be accessed using anonymous ftp via Internet. Instructions for using the Lotus files and for obtaining the data from the network are presented in Section 8. The entire data set will also be submitted to the NODC and will eventually be available through that service.

Acknowledgements

Many people have participated in cruises sponsored by the HOT program. They are listed in Table 3.3. We gratefully acknowledge their contributions and support.

Special thanks are due to Chris Carrillo, John Dore, Dale Hebel, Marc Rosen, Terrence Houlihan, Ricardo Letelier and Jefrey Snyder for participating in most of the cruises and for the tremendous amount of time and effort they have put into the program. In addition, we would like to acknowledge the contributions made by Sharon DeCarlo for programming and data management, Willa Zhu, Julie Ranada and Xiaomei Zhou for ADCP processing and Lance Fujieki for programming and data processing. Fernando Santiago-Mandujano computed the final CTD calibration coefficients and assisted in compiling this report. Toshiaki Shinoda helped with the quality controlling of the WOCE bottle data. Carl Chun and Nava Zvaig provided additional computer support. Ursula Magaard performed many routine chemical analyses, including Winkler titrations. Ted Walsh performed salinity and nutrient analyses and Sean Kennan conducted the intercomparisons between salinometers. We also would like to thank the captains and crew members of the R/V MOANA WAVE, R/V ALPHA HELIX, and R/V WECOMA for their efforts and to thank Nancy Koike for producing this document. Without the assistance of these people, the data presented in this report could not have been collected, processed, analyzed and reported.

This data set was acquired with funding from the National Science Foundation (NSF) and the National Ocean and Atmospheric Administration (NOAA). The specific grants which have supported this work are NSF grants OCE-8717195 (WOCE), OCE-8800329 (JGOFS), and OCE-9016090 (JGOFS) and NOAA grant NA-90-RAH-0007.

1. Introduction

In 1987, the National Science Foundation established a special-focus research initiative termed 'The Global Geosciences Program.' This program is intended to support studies of the earth as a system of interrelated physical, chemical and biological processes that act together to regulate the habitability of our planet. The stated goals of this program are two-fold. The first goal is to understand the earth-ocean-atmosphere system and how it functions. The second goal is to describe, and eventually predict, major cause-and-effect relationships. Two components of the Global Geosciences Program are the World Ocean Circulation Experiment (WOCE) and the Joint Global Ocean Flux Study (JGOFS). The former is focused on physical oceanographic processes and the latter on biogeochemical processes.

The Hawaii Ocean Time-series (HOT) project has been funded under the sponsorship of both the WOCE and JGOFS programs to make repeated observations of the physics, chemistry and biology for five years at a station north of Hawaii. The objectives of HOT are to describe and understand the physical oceanography, and to identify and quantify the processes controlling biogeochemical cycling in the ocean at a site representative of the oligotrophic North Pacific Ocean.

Time-series cruises are made on approximately monthly intervals and two stations are occupied each month. The HOT deep-water station, also known as Station ALOHA (A Long-term Oligotrophic Habitat Assessment), is abou ies cruises t 100 km north of Kahuku Point, Oahu, Hawaii (Figure 1.1). Station ALOHA is at 22° 45' N, 158° W, and is defined as a 6 nautical mile radius from this position. All sampling at Station ALOHA is conducted within this circle. The maximum depth at Station ALOHA is 4750 m. A station is also occupied at 21° 20.6' N, 158° 16.4' W, near Kahe Point, Oahu, during the transit from Honolulu to Station ALOHA. The Kahe Point station is used primarily to test the CTD and other equipment, but it also provides additional time-series data at a near-shore site. The Kahe Point station is located in approximately 1500 m of water about 16 km from shore (Figure 1.1). Approximately 3 to 4 hours are spent at the Kahe Point station, and about 72 hours are spent at Station ALOHA during each cruise. The cruise length is dictated by the minimum time necessary to obtain reasonable estimates of particle flux using the free-floating sediment traps deployed at Station ALOHA. On HOT-31, October 19, 1992 through October 24, 1992, three extra stations were occupied along longitude 158°W as described in Section 3.

The JGOFS and WOCE components of the program measure a variety of parameters during the regular monthly sampling work at Station ALOHA (Table 1.1). JGOFS sampling includes primary production, particle flux, a variety of chemical determinations at discrete depths and continuous profiles of optical parameters. WOCE sampling includes a 36-hour burst of CTD casts at roughly 3-hour intervals to obtain temperature, salinity and oxygen profiles from 0 to 1000 dbar. WOCE sampling also includes a deep CTD cast as close to the bottom as possible.

Current measurements are made on HOT cruises using a shipboard Acoustic Doppler Current Profiler (ADCP) when a ship with the necessary equipment is available for monthly cruises. In addition, lowered ADCP measurements have been made on several HOT cruises.

This report presents data collected during the third year of the HOT Program (February-December 1991). During this period, 10 cruises were conducted using three research vessels (Table 3.1). The R/V MOANA WAVE, R/V ALPHA HELIX and R/V WECOMA are UNOLS vessels operated by the University of Hawaii, University of Alaska and Oregon State University, respectively.

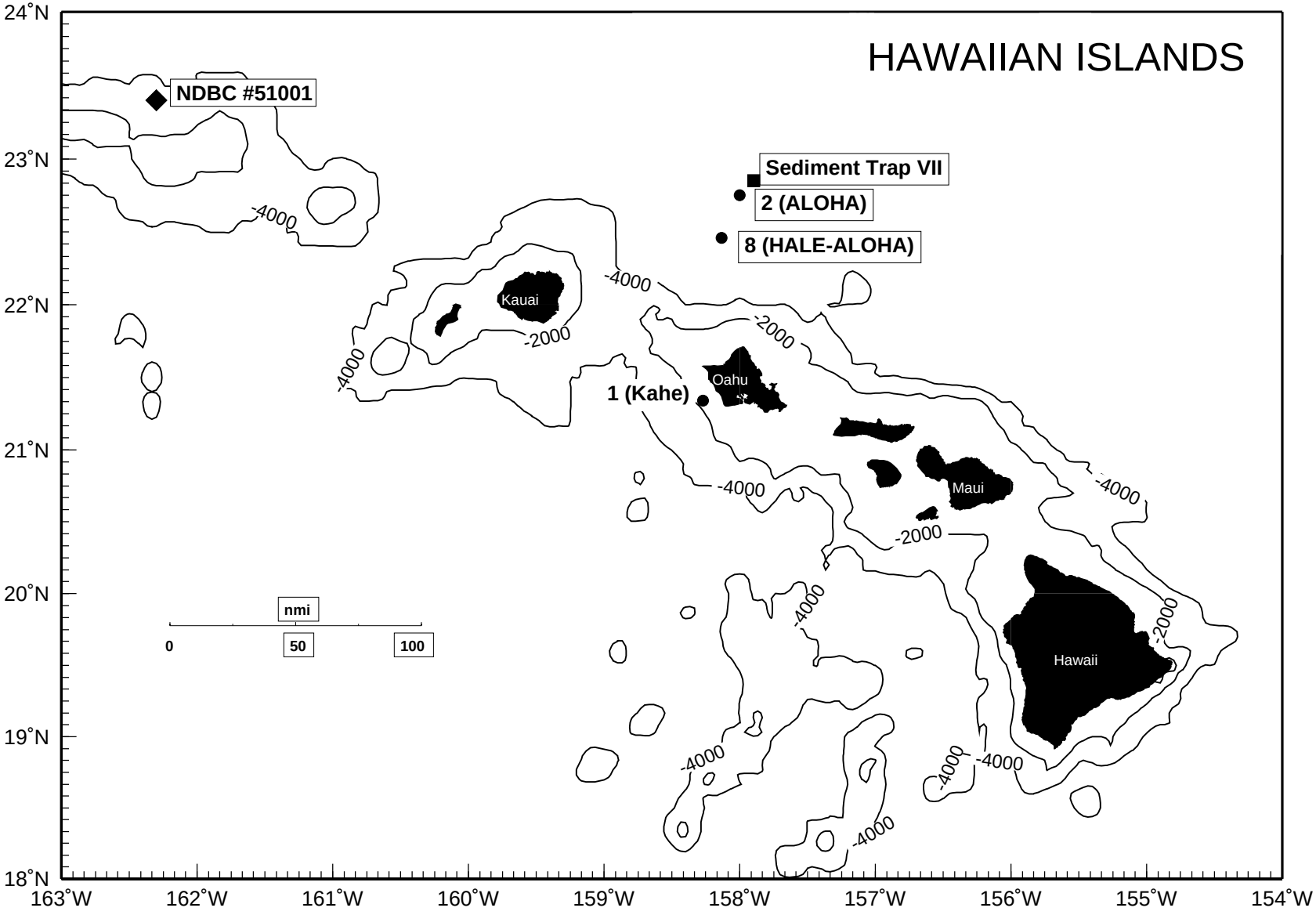

Figure 1.1: Map of Hawaiian Islands, showing Station ALOHA, the Kahe Point Station and NDBC Buoy. Isobaths are in meters

Table 1.1: Time-Series Parameters Measured at Station ALOHA

Parameter	Depth Range (m)	Analytical Procedure
1. CTD Measurements		
Temperature	0-4750	Thermistor on Sea-Bird CTD package with frequent calibration
Salinity	0-4750	Conductivity sensor on Sea-Bird CTD package, standardization with Guildline AutoSal #8400 against Wormley standard seawater
Oxygen	0-4750	Polarographic sensor on Sea-Bird CTD package with Winkler standardization
Fluorescence	0-1000	Sea-Tech Flash Fluorometer on Sea-Bird CTD package
Beam Transmission	0-1000	Sea-Tech 25 cm path length beam transmissometer on Sea-Bird CTD package
II. Optical Measurements		
Solar Irradiance (PAR)	Surface	Licor Cosine Collector and Biospherical 2 pi Collector
Underwater Irradiance (PAR)	0-150	Biospherical Profiling Natural Fluorometer 4 pi Collector
Solar Stimulated Fluorescence (683nm)	0-150	Biospherical Profiling Natural Fluorometer
III. Water Column Chemical Measurements		
Oxygen	0-4750	Winkler Titration
Total Dissolved Inorganic Carbon	0-4750	Coulometry
Titration Alkalinity	0-4750	Automated Titration
PH	0-4750	Potentiometry
Dissolved Inorganic Nitrate Plus Nitrite	0-4750	Autoanalyzer
Dissolved Inorganic Phosphorus	0-4750	Autoanalyzer
Dissolved Silica	0-4750	Autoanalyzer
Low Level Nitrate Plus Nitrite	0-200	Chemiluminescence
Low Level Phosphorus	0-200	Magnesium-induced Coprecipitation
Dissolved Organic Carbon	0-1000	Persulfate Wet Oxidation
Total Dissolved Nitrogen	0-1000	U.V. oxidation
Total Dissolved Phosphorus	0-1000	U.V. oxidation
Particulate Carbon	0-1000	High Temperature Combustion
Particulate Nitrogen	0-1000	High Temperature Combustion
Particulate Phosphorus	0-1000	High Temperature Combustion
IV. Water Column Biomass Measurements		
Chlorophyll *a* and Phaeopigments	0-200	Fluorometric Analysis
Chlorophyll *a, b*, *c* and Accessory Pigments	0-200	High Pressure Liquid Chromatography
Adenosine 5´-Triphosphate	0-1000	Firefly Bioluminescence
V. Carbon Assimilation and Particle Flux		
Primary Production	0-200	"Clean" ^{14}C Incubations
Carbon, Nitrogen, Phosphorus and Mass Flux	150, 300, 500	Free-Floating Particle Interceptor Traps
VI. Currents		
Acoustic Doppler Current Profiler	0-300	Hull Mounted, RDI #VM-150
Acoustic Doppler Current Profiler	0-4750	Lowered

2. Sampling Procedures and Analytical Methods

2.1. CTD Profiling

CTD data were collected with a Sea-Bird SBE-09 CTD, which had an internal Digiquartz pressure sensor and external temperature, conductivity and oxygen sensors. The Sea-Bird temperature-conductivity duct, which was used to circulate seawater through both the temperature and conductivity sensors, was used on all cruises during 1991. A Sea Tech flash fluorometer was also incorporated into the CTD sampling on the majority of the casts. In 1991 a Sea Tech beam transmissometer was added to the CTD system. The CTD was mounted in a rosette sampler, and the package was deployed on a conducting cable, which allowed for real-time data acquisition and data display. Water samples were taken on the upcasts for chemical analyses, and for calibration of the conductivity and oxygen sensors.

A CTD cast to approximately 1000 dbar was made at the Kahe Point Station on each cruise. At Station ALOHA, a burst of consecutive CTD casts to 1000 dbar was made over 36 hours to span the local inertial period (~31 hours) and three semi-diurnal tidal cycles. This sampling was designed so that energetic tidal and near-inertial variability during each cruise could be averaged to prevent these components from aliasing the longer time-scale signals. In order to satisfy WOCE requirements, one deep cast to near the bottom was made on each cruise. When cruises were made on a ship equipped with a 12-kHz echo sounder, a Benthos acoustic pinger attached to the rosette was used to make the cast to within 50 m of the sea floor (approximately 4750 m). When the research platform was not equipped with an echo sounder, this cast was made to 4500 dbar (unless cable length was shorter).

2.1.1. CTD Data Acquisition and Processing

CTD data were acquired at the instrument's highest sampling rate of 24 samples per second. Digital data were stored on a PC-compatible computer and, for redundancy, the analog CTD signal was recorded on VHS video tapes.

The raw CTD data were quality controlled and screened for spikes and missing data as described by Winn *et al.* (1991). The data were aligned as previously described, averaged to half-second values and the calibrations were applied. Salinity and oxygen were then computed in units of psu and μmol kg^{-1}, respectively. Details of these corrections are described in the following sections. A flowchart of the CTD processing is shown in Figure 2.1.

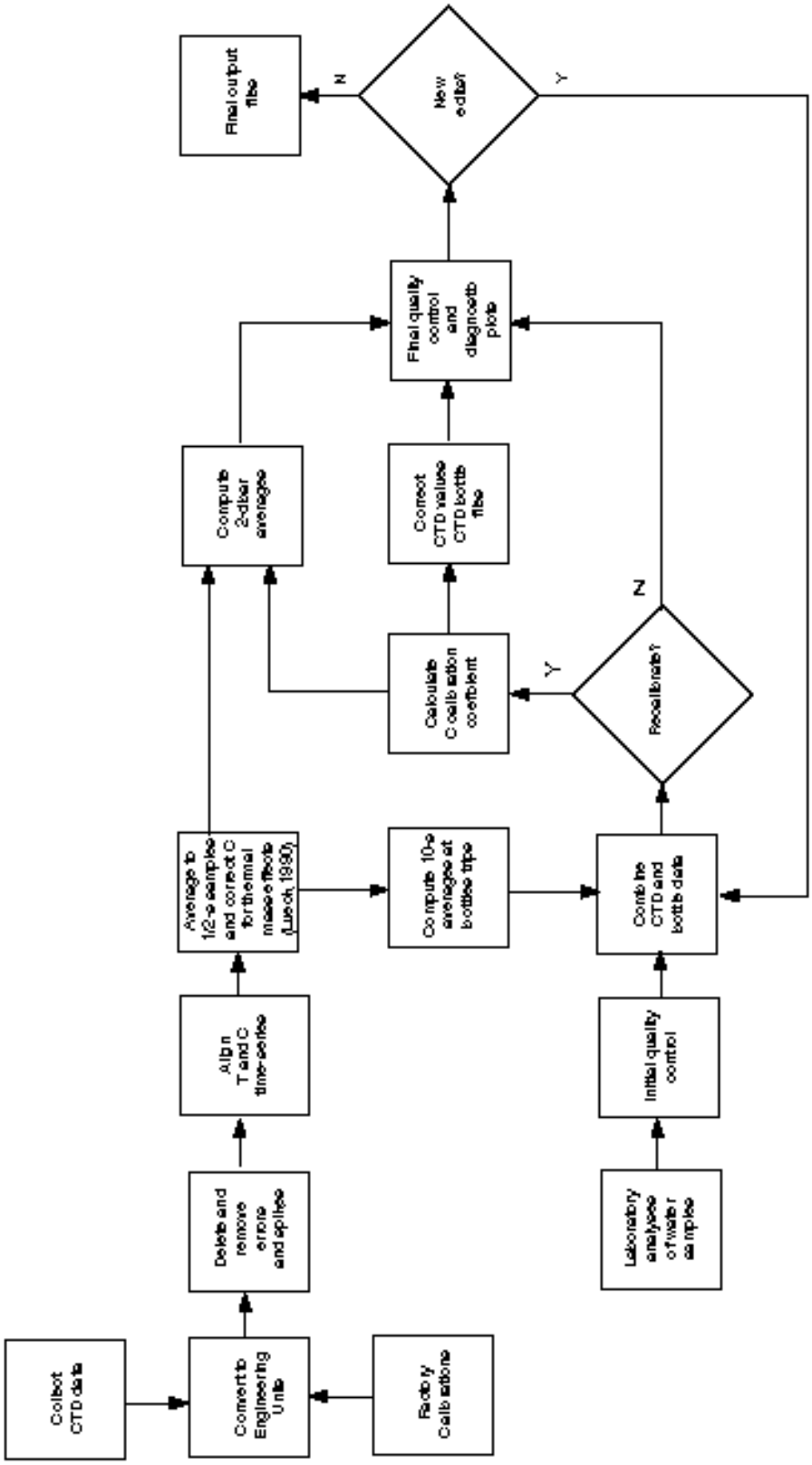

Figure 2.1: Flowchat of CTD data processing.

Eddy shed wakes, caused when the rosette entrains water, introduced salinity spikes in the CTD profile data. These contaminated data were handled using an algorithm which eliminated data collected when the CTD's speed was less than 0.25 m s^{-1} or its acceleration was greater than 0.25 m s^{-2}. The data were subsequently averaged into 2 dbar pressure bins. Temperature was reported in the ITS-90 scale. Salinity and all derived units were calculated using the UNESCO (1981) routines.

2.1.2. CTD Sensor Corrections and Calibration

2.1.2.1. Pressure

The pressure sensor calibration strategy was described in Winn *et al.* (1991). Briefly, this strategy used a high-quality quartz pressure transducer as the laboratory transfer standard and a Russka precision dead-weight pressure tester as a primary standard. The primary standard met National Bureau of Standards specifications and was operated under controlled conditions. The transfer standard was a Paroscientific Model 760 pressure gauge equipped with a 10,000 PSI transducer. The transfer standard was calibrated at the Oceanographic Data Facility at Scripps Institution of Oceanography in May of 1991.

Laboratory calibrations of the CTD pressure sensor were done using a dead weight pressure tester and a manifold to apply pressure simultaneously to the CTD pressure transducer and the transfer standard. Calibrations were done over a pressure range of 0-5000 dbar with points collected both as pressure was increased and as it was decreased.

Pressure transducer #26448 was used on all cruises in 1991. Subsequent calibrations against the transfer standard using its original calibration (Winn *et al.*, 1991) are given in Table 2.1. These results show that the bias of this pressure transducer relative to the transfer standard changed by approximately 0.5 dbar between February 1991 and June 1991. The drift in this sensor appeared to be relatively linear with time at least through 1992 (Table 2.1). An offset of 3 dbar was obtained after correction for the shift in the primary standard and was used for all cruises in 1991 (Note that this offset was only used for real-time data acquisition, as a more accurate offset was determined at the time that the CTD first enters the water on each cast). This shift was within the normal operating specifications of approximately 2 dbar/year for this sensor (N. Larson, Personal Communication, 1992).

Table 2.1: CTD Pressure Calibrations
(all units are in decibars)

Sea-Bird SBE-09 #91361 / Pressure Transducer #26448

Calibration date	Offset @ 0 dbar	slope offset @ max pressure	hysteresis
10 May 1989	-1.1	-0.6 @ 4500	N/A
10 July 1990	-1.65	-0.8 @ 5000	0.2
20 February 1991	-2.15	-0.9 @ 4800	0.25
27 June 1991	-2.7	-0.3 @ 4600	0.2
Final correction for 1991	3.0*	-0.9 @ 4600*	0.2
27 August 1992	-4.75	-0.1 @ 4500	0.1
27 August 1992	-4.9	-0.2 @ 4500	0.05
Mean	-4.83	-0.15	0.075
Final correction for 1992	-5.13[a]	-0.75[a]	0.075

[a]Adjusted for shift in lab pressure standard calibrated 16 May 1991 at SIO/ODF.

As described by Chiswell (1991), the indicated pressure from each profile was corrected for errors due to thermal disequilibrium during profiling. While the pressure error from this source can reach 7 dbar, the correction is good to better than 0.5 dbar. In September and October 1991, Sea-Bird upgraded our pressure transducers, virtually eliminating the thermal disequilibrium problem.

2.1.2.2. Temperature

Our strategy for CTD temperature calibration also relied upon the use of a transfer standard periodically recalibrated at a primary calibration center using techniques traceable to the National Bureau of Standards. As in 1990, three Sea-Bird SBE-3-02/F temperature transducers, serial numbers 741, 886 and 961 were available in 1991. These transducers were returned to Sea-Bird approximately once per year (recently increased to twice per year) for calibration by the Northwest Regional Calibration Center (NWRCC). The frequency of recalibration is a trade-off between confidence in the behavior of the sensor with time versus the risk of damage or loss during shipping to and from the calibration center. During 1991 sensor #741 was used only as a transfer standard during intercomparison runs with the other two sensors. Only sensor #886 was used at sea in 1991. Intercomparisons between #741 and #886 were done between each cruise to provide a check on the nature of the drift of sensor #886 relative to the transfer standard.

Primary calibrations

The calibrations at NWRCC typically have an RMS residual of 0.25-1.0 m°C (Table 2.2). Consistent with previous experience (Winn *et al.*, 1991) our sensors have exhibited a tendency towards higher temperature readings with time. Table 2.2 gives the calibration coefficients which were determined by NWRCC measurements. These coefficients were used in the following formula that gave the temperature (in °C) as a function of the frequency signal (f)

$$\text{Temperature} = 1/\{a+b[\ln(f_o/f)]\} = c[\ln^2(f_o/f)] + d[\ln^3(f_o/f)] - 273.15$$

Sensor #961

Sensor #961 was calibrated on 3 and 10 November 1989, on 12 and 21 December 1990 and again on 17 January 1992. Within each pair of calibrations, the mean difference between the calibrations over the 0-30°C range was 0.6 and 0.4 m°C, respectively. These differences are within the uncertainty of the calibrations. The maximum deviations in this temperature range associated with the slope and nonlinear terms in the calibration equation for these calibration pairs were 1.7 and 0.6 m°C and 1.8 m°C, respectively. The comparison of the 13 and 20 October 1989 calibrations showed differences up to 4 m°C, with a mean of 2.8 m°C. This large calibration shift was due to the replacement of an electronic component in the transducer. The quality of prior temperature measurements was not compromised by this shift.

Over the 13 months separating the first two calibration groups, the sensor drifted by 6.3 m°C. The sensor drifted 17.5 m°C during the 25 months separating the first group and the last calibration. We modeled the drift of sensor #961 as a linear function of time as per the experience of Sea-Bird over many years of working with these sensors. A linear fit to these offsets gave an intercept of 0.65 m°C with a slope of 2.101×10^{-5} °C day^{-1}. The RMS deviation of the offsets from this fit was 1.3 m°C. Maximum error from changes in the slope and nonlinear terms in the frequency to temperature conversion was estimated to be less than 1 m°C during 1991.

Table 2.2: Calibration Coefficients for Sea-Bird Temperature Transducers Determined at Northwest Regional Calibration Center. RMS Residuals from Calibration Give an Indication of Quality of the Calibration.

SN	YYMMDD	f_0	a	b	c	d	RMS (m°C)
961	920731	6782.47	3.67533E-3	6.00280E-4	151877E-5	2.26315E-6	0.05
961	920129	6789.88	3.67468E-3	6.00393E-4	1.56717E-5	2.72528E-6	0.10
961	920117	6609.38	3.67323E-3	6.00527E-4	1.64423E-5	3.44995E-6	0.10
961	901221	6596.33	3.67427E-3	6.00296E-4	1.50788E-5	1.90332E-6	0.28
961	901212	6555.62	3.67800E-3	6.00590E-4	1.54925E-5	2.33356E-6	0.27
961	891110	6593.31	3.67448E-3	6.00431E-4	1.54701E-5	2.26236E-6	1.42
961	891103	6570.80	3.67652E-3	6.00440E-4	1.54579E-5	2.39329E-6	0.48
961	891020	6584.74	3.67527E-3	6.00530E-4	1.60085E-5	2.99272E-6	0.80
961	891013	6569.50	3.67662E-3	6.00261E-4	1.45637E-5	1.50324E-6	0.26
961	890728	6585.62	3.67515E-3	6.00522E-4	1.58721E-5	2.82023E-6	0.81
886	920820	5935.78	3.67798E-3	5.95648E-4	1.41981E-5	1.94572E-6	0.61
886	920129	5969.00	3.67468E-3	5.95639E-4	1.45243E-5	2.12849E-6	0.20
886	920117	5753.52	3.67323E-3	5.96295E-4	1.60553E-5	3.39478E-6	0.12
886	910621	5734.40	3.67513E-3	5.95897E-4	1.39470E-5	1.18908E-6	0.71
886	901108	5736.72	3.67482E-3	5.95946E-4	1.44577E-5	1.86031E-6	0.72
886	891103	5720.16	3.67652E-3	5.96265E-4	1.52177E-5	2.50123E-6	0.57
886	891013	5719.06	3.67662E-3	5.96299E-4	1.50921E-5	2.19843E-6	0.30
886	881007	5738.95	3.67443E-3	5.96117E-4	1.52143E-5	2.58644E-6	0.42
741	920626	6246.37	3.67361E-3	6.01608E-4	1.48892E-5	2.32039E-6	0.61
741	911016	6233.18	3.67485E-3	6.01645E-4	1.46381E-5	1.87676E-6	0.17
741	910614	6242.89	3.67392E-3	6.01617E-4	1.44529E-5	1.67976E-6	0.96
741	891103	6215.18	3.67652E-3	6.01685E-4	1.44771E-5	1.74730E-6	0.26
741	870821	6233.01	3.67465E-3	6.01498E-4	1.43227E-5	1.70525E-6	0.37
741	870305	6227.60	3.67516E-3	6.01775E-4	1.52878E-5	2.58641E-6	0.48

Sensor #886

Sensor #886 was calibrated on the dates given in Table 2.2. Relative to the original calibration of this sensor, the 0-30°C average offset was 8.4 m°C on 13 October 1989, 10.1 m°C on 3 November 1989, 13.3 m°C on 8 November 1990, 19 m°C on 21 June 1991 and 23.8 m°C on 17 January 1992. A linear fit to these offsets gave an intercept of 0.89 m°C, with a slope of 1.871 x 10^{-5} °C day^{-1}. The RMS deviation of the offsets from this fit was 1.2 m°C.

The 21 June 1991 calibration was used to calculate temperature from the sensor frequency data obtained in 1991. When corrected for linear drift to 1 June 1991, this calibration gave the smallest deviation in the 0-5°C temperature range from the ensemble of all the calibrations available for this sensor (also corrected for linear drift to 1 June 1991). In the 0-5°C temperature range, the mean deviation of this calibration was approximately 0.5 m°C with less than a 1 m°C variation. The January 1992 calibration had a mean deviation of -0.15 m°C, while the November 1990 calibration had a mean deviation of -2.0 m°C. Thus, for the HOT cruises conducted in 1991, we placed an error bound of 1.4 m°C on deep water temperatures measured with this sensor.

Sensor #741

The calibration procedure as used for sensor #886 was also applied to sensor #741. The offsets over the range 0-30°C from the original calibration of this sensor in March 1987 were 1.6 m°C (21 August 1987), 11.8 m°C (3 November 1989), 16.8 m°C (14 June 1991), 18.2 m°C (16 October 1991) and 21.0 m°C (26 June 1992). Computing a linear fit to this drift yielded an intercept of 0.16 m°C, a drift of 1.081 x 10^{-5}°C day^{-1}, with an RMS residual of 0.50 m°C.

Laboratory calibrations

Our laboratory temperature sensor intercomparisons were done in an insulated water bath, using the CTD for data acquisition and sensor power. The water bath had a circulation system which drew water from the bottom of the tank and spread it across the top of the water column. It was unlikely that there were persistent temperature variations within the bath greater than 1 m°C, though we have not made exhaustive tests of this assertion. Short-term variations in temperature differences between sensors were less than ± 0.5 m°C. The bath was initially chilled to near 0°C, the CTD and sensors were inserted, the bath was closed, and over a period of 2 days the system slowly warmed to the lab temperature of 23-25°C. An initial period when the temperature of the CTD was coming into equilibrium with the bath (and was acting as a heat source) was readily identified. Averaging temperature transducer output over several minutes gave exceptionally stable temperature differences at a variety of bath temperatures.

Using sensor #741 as a reference, with the linear drift correction as described earlier,

sensor #886 showed a drift of 2.196 x 10^{-5} °C day^{-1}, with an RMS residual of 0.27 m°C for 4 laboratory intercomparisons. This was compared to the 1.871 x 10^{-5} °C day^{-1} linear drift estimated from the NWRCC calibrations.

Using the corrected #741 as a reference, 5 intercomparisons with sensor #9611 showed a linear drift of 2.0687 x 10^{-5} °C day^{-1} which was compared with the 2.101 x 10^{-5} °C day^{-1} estimated from the NWRCC calibrations. The close correspondence between these estimates provided us with added confidence in our drift correction procedures. The corrections applied to sensor #886 used during the 1991 HOT cruises are given in Table 2.3.

Table 2.3: Temperature and Conductivity Sensor Corrections

HOT	Temp #	T Correction °C	Cond #	α
23	886	0.0025	527	0.028
24	886	0.0020	527	0.028
25	886	0.0013	679	0.028
26	886	0.0008	679	0.028
27	886	0.0003	679	0.028
28	886	-0.0003	679	0.028
29	886	-0.0009	679	0.028
30	886	-0.0016	679	0.037
31	886	-0.0022	679	0.037
32	886	-0.0030	679	0.037

2.1.2.3 Conductivity

The conductivity cell was calibrated periodically at the NWRCC by varying the temperature of a saltwater bath as described by Winn *et al.* (1991). These nominal calibrations were used for data acquisition and final calibration was determined empirically by comparison with the salinities of discrete water samples acquired during each cast. Conductivity cells #527 and #679 were both used during 1991. Cell #527 was calibrated at NWRCC on 28 October 1988, on 2 May 1991 and again on 16 October 1991. Cell #679 was calibrated on 13 October 1989 and on 20 October 1990.

Prior to the empirical calibration of conductivity data with water bottle salinities, conductivity was corrected for the thermal inertia of the glass conductivity cell as described by Chiswell *et al*. (1990). Table 2.3 lists the value of α used for each cruise. No drift corrections were necessary during 1991.

Empirical calibration

Salinity was determined on discrete water samples as described in Section 2.2.1. Preliminary screening of the water sample salinities was done as described by Winn *et al.* (1991). Calibration of the conductivity cell was performed empirically by comparing its nominally calibrated output against the calculated conductivity values obtained from water sample salinities using the calibrated pressure and temperature of the CTD at the time of bottle closure. An initial estimate of bias and slope corrections to the nominal calibration were determined from a linear least squares fit to the ensemble of bottle-CTD conductivity differences as a function of conductivity, from all stations and casts during a particular cruise. This calibration was then used to screen suspect water samples.

The second iteration allowed for the possible addition of a quadratic term in the correction to conductivity, as well as a revised estimate of slope and bias. The final conductivity calibration coefficients are given in Table 2.4.

The quality of the CTD calibration is illustrated by Figure 2.2, which shows the differences between the corrected CTD salinities and the bottle salinities as a function of pressure for each cruise. Typically, the calibrations were best below 500 dbar, because the weaker vertical salinity gradients at depth lead to less error if the bottle and CTD pressures are slightly mismatched.

Table 2.4: Table of Conductivity Calibration Coefficients

Cruise	b0	b1
HOT-23	0.00207343318319	-0.00098102040688
HOT-24	0.00157308514800	-0.00084520383030
HOT-25	0.00152626456201	-0.00053079711518
HOT-26	0.00148415433267	-0.00062130748841
HOT-27	0.00203316767831	-0.00073369419722
HOT-28	0.00203234841543	-0.00080259573174
HOT-29	0.00202989823464	-0.00078001186357
HOT-30	0.00203580581331	-0.00084354215474
HOT-31	0.00236961792658	-0.00094021233001
HOT-32	0.001978289652239	-0.00088740367667

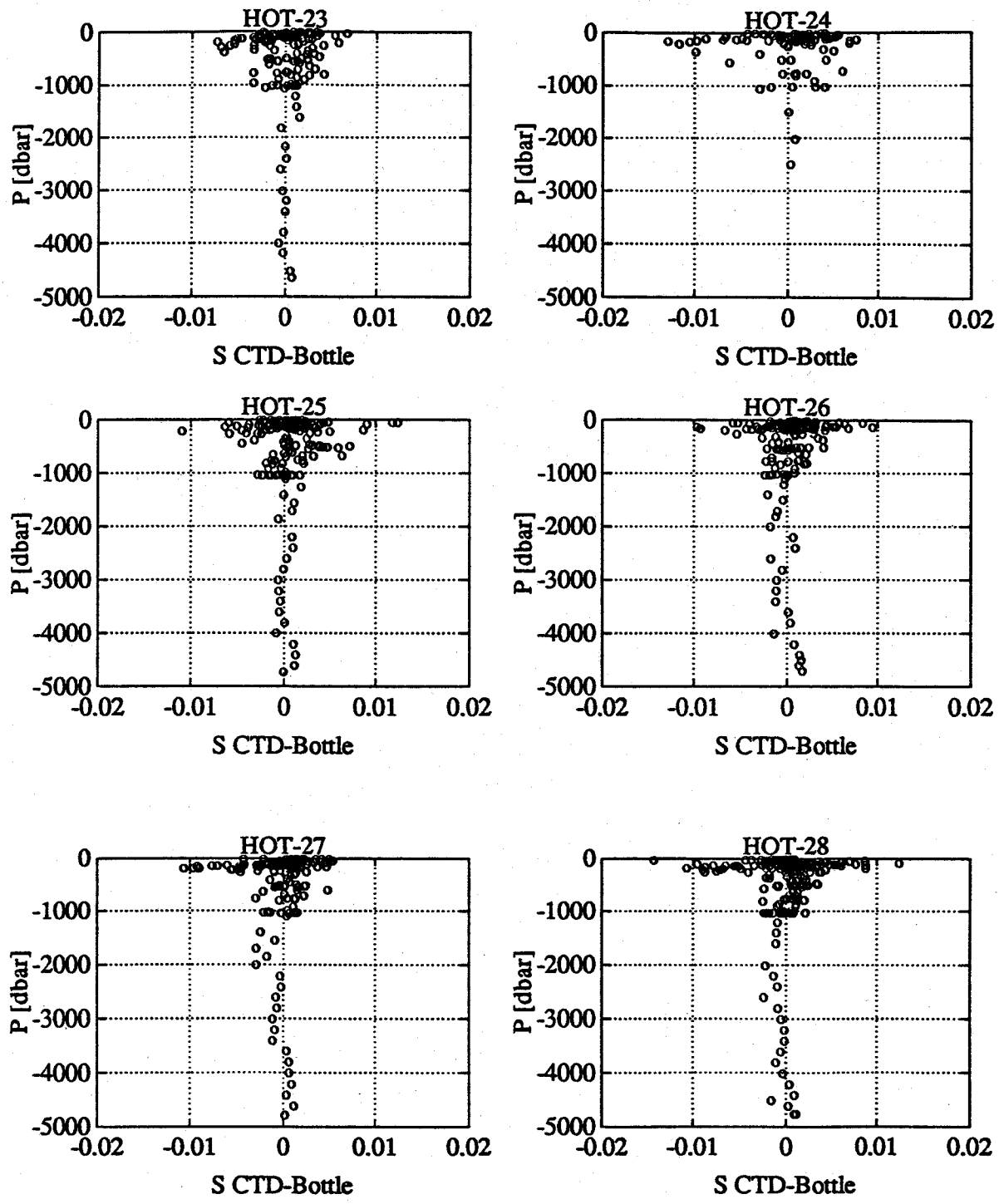

Figure 2.2: Differences between calibrated CTD salinities and bottle salinities for Station ALOHA, HOT-23 through 28.

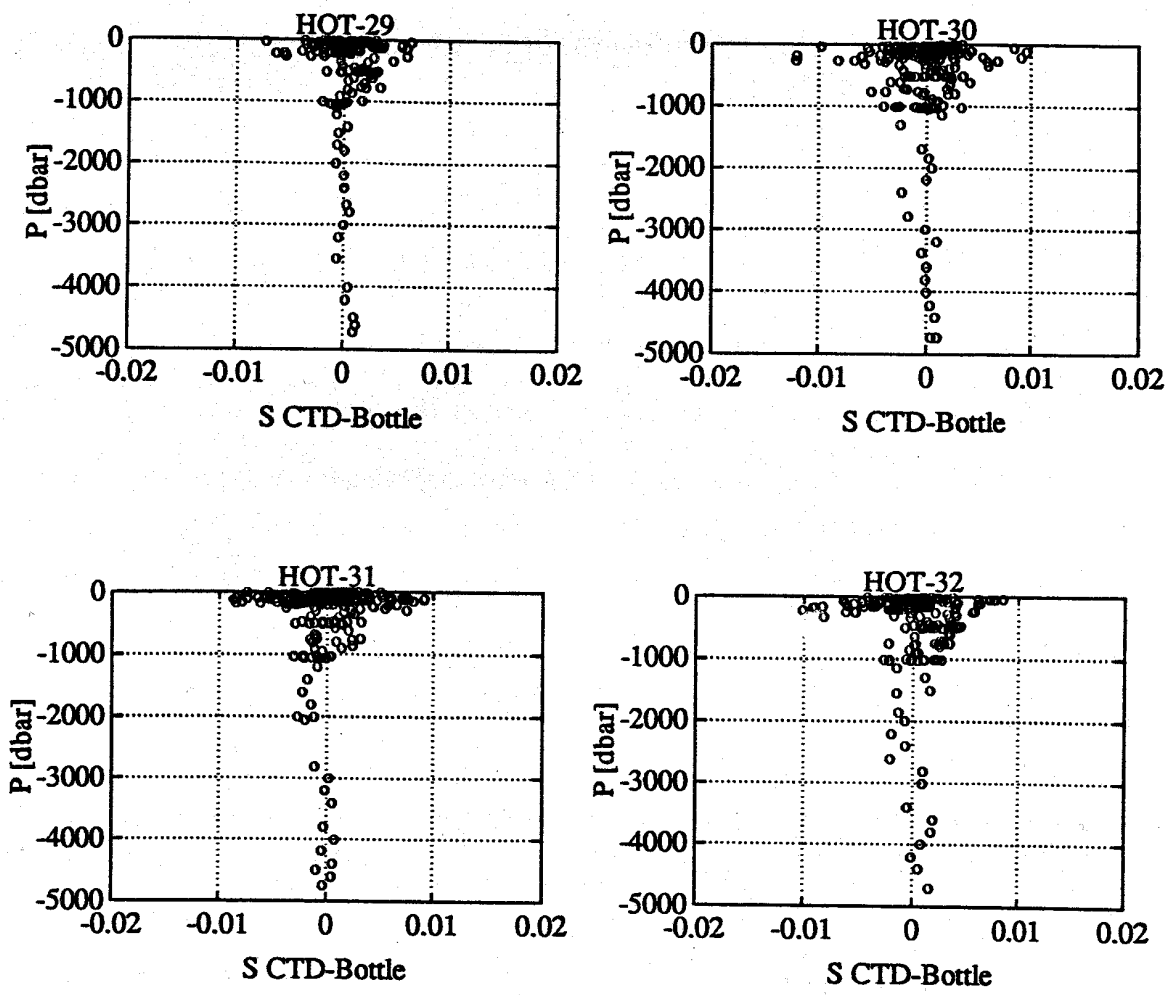

Figure 2.2 (continued): HOT-29 through 32.

The final step of the calibration was to perform a profile-dependent bias correction, to allow for drift during each cruise, or for sudden offsets due to fouling. This offset was determined by taking the median value of CTD-bottle salinity differences for each profile at temperatures below 5°C. Very few profiles collected during 1991 required adjustment in this way (Table 2.5.). Note that a change of 1 x 10^{-4} s m^{-1} in conductivity was approximately equivalent to 0.001 psu in salinity. Table 2.6 gives the mean and standard deviation for the final calibrated CTD values minus the water sample values. These values were comparable to the precision (0.001 psu) and accuracy (0.003 psu) estimated from the water sample salinities.

Table 2.5: Individual Cast Conductivity Offsets. Units are Siemens $m^{-1} \times 10^{-4}$

Cruise	Station	Cast	Offset
HOT-25	2	1	-0.9
HOT-26	2	2	1.6
	2	7	-0.8
	2	9	1.1
	2	10	1.2
	2	11	0.8
HOT-29	2	1	-0.7
	2	15	-1.8
HOT-32	2	1	-1.1
	2	2	-1.6
	2	16	0.9

Table 2.6: CTD-Bottle Salinity (psu) Comparison for Each Cruise

	0 < P < 4700		500 < P < 4700	
Cruise	Mean	St. Dev.	Mean	St. Dev.
HOT-23	0.0000	0.0025	0.0002	0.0016
HOT-24	0.0000	0.0043	0.0005	0.0028
HOT-25	0.0001	0.0029	0.0004	0.0019
HOT-26	0.0001	0.0027	-0.0001	0.0014
HOT-27	0.0000	0.0028	0.0002	0.0017
HOT-28	-0.0000	0.0032	0.0000	0.0013
HOT-29	0.0002	0.0022	0.0004	0.0013
HOT-30	-0.0000	0.0029	-0.0001	0.0018
HOT-31	-0.0000	0.0032	-0.0005	0.0015
HOT-32	0.0002	0.0030	0.0006	0.0017

2.1.2.4 Oxygen

As described in Winn *et al.* (1991), the Beckman polarographic oxygen sensor was used as the main oxygen sensor on HOT cruises 1 through 30. Because of the poor performance of the Beckman sensor in the upper 100 m of the water column, we have switched to the sensor produced by YSI Inc. These two sensors were cross calibrated for several cruises before we began to use the YSI as the primary sensor. Up to cruise 25, only the Beckman sensor was used for continuous oxygen profiling. On cruises 25 through 30 the YSI sensor was used as a backup to the Beckman and the results obtained from both sensors were compared. During this period, the YSI sensor provided slightly less resolution than the Beckman. However, consistent with our previous findings (Winn *et al.*, 1991), the results demonstrated that the YSI sensor was superior to the Beckman especially in the upper 100 m of the water column (Figure 2.3). Therefore, we used the YSI as the primary sensor beginning with HOT-31. Beginning with HOT-32 the gain on the YSI sensor was increased to double the resolution of this sensor. This change increased the precision of the YSI to approximately equal to that obtainable with the Beckman sensor. As described previously (Winn *et al.*, 1991), extra weight is generally given to oxygen values below 1000 m for the purpose of calibrating the O_2 sensor. This procedure was used on all cruises during 1991 with the exception of cruises 23, 25 and 26. On these cruises, the oxygen calibration above 1000 dbar was optimized when this weighting was not applied. On those cruises where the YSI was used as the primary sensor, the data from the upper 100 dbar was not discarded for the purpose of calibrating the sensor as was the practice with the Beckman sensor. Water bottle oxygen data were screened and both sensors were calibrated on all cruises during 1991 as described previously (Winn *et al.*, 1991).

Water sample analysis

Water samples were analyzed for oxygen as described in Section 2.2.2.

Screening of bottle samples

Bottle O_2 data were screened against the large historical data base generated for the Kahe Point and ALOHA sites by overplotting on the ensemble of all good data collected from each site. Both O_2 vs. pressure and O_2 vs. θ were inspected for suspicious values. Apparent rosette problems were investigated by looking at other water properties and resolved if possible.

The continuous O_2 profile from the CTD was also used for screening the bottle data. It was our experience that there was considerable finestructure in O_2, not always correlated with T-S finestructure. This was partly due to the biological processes which make O_2 a nonconservative tracer. Without the continuous profile to reveal this structure one might reject bottle oxygen values that were accurate. Thus, even though the sensor had some undesirable characteristics, it still provides useful information on the variability of O_2 on small scales.

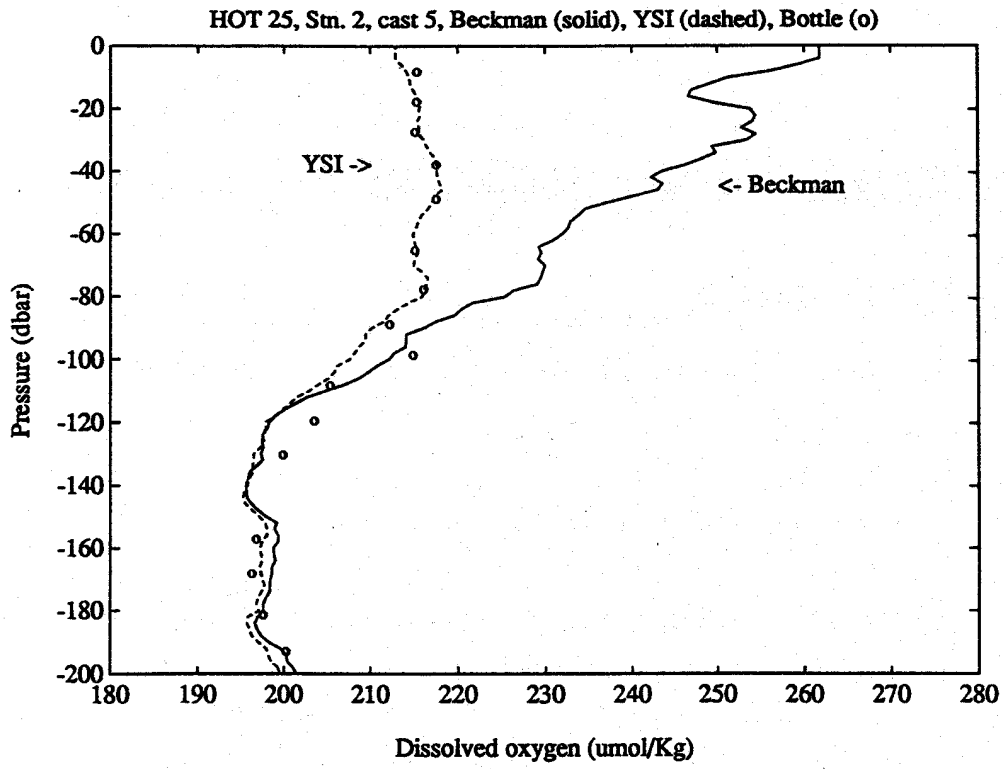

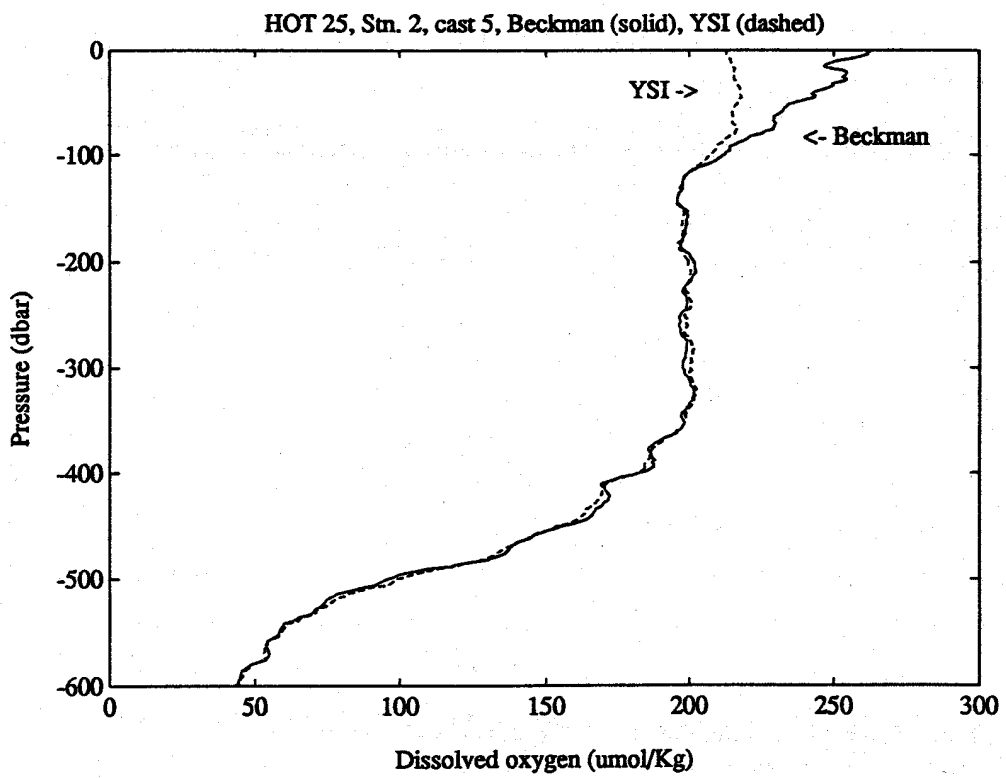

Figure 2.3: Calibrated Beckman and YSI oxygen profiles in the upper ocean for HOT-25. Upper panel: Calibrated YSI and Beckman profiles for the upper 200 dbar. Bottle data are represented by open circles. Lower panel: Calibrated YSI and Beckman profiles for upper 600 dbar on this same cruise showing good agreement at pressures greater than 125 dbar.

Empirical calibration

CTD O_2 calibration was performed following Owens and Millard (1985). Six parameters (B_{oc}, S_{oc}, tcor, pcor, τ, w_T) were fit to the CTD oxygen current (O_c), oxygen temperature (O_T), and O_c time variation $\left(\frac{d\,O_c}{d\,t}\right)$ by the equation:

$$OX = \left[\; S_{oc} \cdot \left(O_c + \tau \frac{dO_c}{dt}\right) + B_{oc} \right] \cdot OXSAT\,(T, S) \cdot \exp\,[tcor\,[T + w_T \cdot (T_o - T)] + pcor \cdot p]$$

where the OXSAT (oxygen saturation) was calculated from the CTD temperature and bottle salinity. (calibrated CTD salinities were used if the bottle salinity is absent or of suspect quality). The bottle O_2 values and the downcast CTD observations at the potential density of each bottle trip were grouped together for each cruise and used to find the best set of parameters using a nonlinear least squares algorithm based on the Levenberg-Marquardt method (Press *et al*., 1988). Two sets of parameters were obtained per cruise, corresponding to the casts at Station 1 (Kahe Pt.) and Station 2 (ALOHA). At Station 2, only WOCE casts were used for the fit. Data from deeper than 1000 m were assigned extra weight given that only one deep cast was obtained per cruise. This weighting was done by duplicating the data below 1000 m as many times as shallow (< 1000 m) casts were available for the calibration. The set of parameters obtained was used to calculate oxygen (OX) for all the CTD casts of this station. The quality of the O_2 sensor calibration was assessed from Table 2.7.

2.1.2.5. Flash Fluorescence and Beam Transmission

In situ flash fluorescence was measured during all three years of the time-series program using a flash fluorometer manufactured by Sea Tech Inc. (model ST0250). Fluorescence data were collected with the Sea-Bird CTD system described previously. As described in section 2.1.1 data were collected at 24 hz and averaged to 2 hz. The data were then processed to remove spikes and averaged in 2 dbar bins. The binned data were then quality controlled and quality flags were assigned to each 2 dbar bin. The quality controlled 2 dbar bin data set was too extensive to be included in this report. These data files are available via Internet (see Section 8).

Flash fluorescence traces were collected on as many of the 1000 m casts at both Station 1 and Station 2 as possible during 1991. Equipment problems prevented the collection of all but a single trace on HOT-24. Unfortunately, an absolute radiometric standard was not available for flash fluorometers. In order to correct for instrument drift over the three year program we have

Table 2.7: CTD-Bottle O_2 (µmol kg^{-1}) Comparison for Each Cruise

	Station 1, Kahe Point		Station 2, ALOHA			
	0 < P < 1100		0 < P < 4700		500 < P < 4700	
Cruise	Mean	St. Dev.	Mean	St. Dev.	Mean	St. Dev.
HOT-23	-0.02	2.56	0.28	2.99	0.32	2.95
HOT-24	---[a]	---[a]	-0.95	3.20	0.36	3.83
HOT-25	0.02	1.47	-0.11	2.44	-0.21	2.10
HOT 26	-0.09	2.29	0.08	3.21	0.06	2.76
HOT-27	0.00	2.33	-0.88	4.12	-0.94	2.70
HOT-28	-0.17	1.81	-0.25	2.02	-0.28	1.62
HOT-29	-0.06	2.51	0.18	1.93	0.47	1.34
HOT-30	-0.03	1.96	0.12	2.02	0.26	0.99
HOT-31	0.00	1.12	0.40	1.96	0.69	1.25
HOT-32	0.00	0.99	0.00[b]	2.40[b]	0.01[b]	1.54[b]
HOT-32			0.83[c]	3.22[c]	2.27[c]	2.64[c]

[a]No station due to bad weather

[b]Station 2, cast 1

[c]All other casts

checked the relative response of the instrument between each HOT cruise using fluorescent plastic sheeting. The sheeting was placed at a fixed distance (approximately 2 cm) from the instrument lamp in the dark. This procedure confirmed that the instrument was performing properly. As part of our maintenance program, the sensor was returned to the manufacturer for routine servicing on a regular basis. The instrument response changed slightly each time it was returned from servicing. Therefore, we normalized the instrument response each month using the voltage derived at two depths intervals (400-450 dbar and 900 to 1000 dbar). These depths were used because the fluorescence yield at these pressure horizons remained remarkably constant with time, and changed only when the instrument was serviced. A linear relationship of the form Vn = b Vo + a was used to convert all fluorescence data to a common voltage scale, where Vn is the corrected voltage, Vo is the output voltage and a and b are constants derived from the two deep water intervals. The constants used to correct the fluorescence data for all three years of the time-series program are given in Table 2.8.

In situ beam transmission was collected beginning on HOT-28, using a Sea Tech 25 cm path length instrument. No transmission data were collected on HOT 31 because of equipment problems. Transmission data were collected using the Sea-Bird CTD in a fashion analogous to that

Table 2.8: Fluorescence Calibration Factors

Cruise #	Station #	Cast #	a	b
1	0[a]	0[a]	-6.9427	1.0574
2	0	0	-6.9427	1.0574
3	0	0	-6.9427	1.0574
4	0	0	-6.9427	1.0574
5		0	-6.9427	1.0574
6	0	0	-6.9427	1.0574
7	0	0	-6.9427	1.0574
8	0	0	-6.9427	1.0574
9	0	0	-4.5734	2.0639
10	0	0	-4.5734	2.0639
11	0	0	-4.5734	2.0639
12	0	0	-4.5734	2.0639
13	0	0	-4.5734	2.0639
14	0	0	-4.5734	2.0639
15	0	0	0	1
16	0	0	0	1
17	0	0	0	1
18	0	0	0	1
19	0	0	0	1
20	0	0	0	1
22	0	0	0	1
23	0	0	0	1
24	0	0	0	1
25	0	0	0	1
26	0	0	0	1
27	0	0	0	1
28	0	0	0	1
29	0	0	0	1
30	0	0	0	1
31	0	0	0	1
32	0	0	0	1
32	1	1	0	0.5
32	2	8	0	0.5
32	2	9	0	0.5
32	2	13	0	0.5
32	2	15	0	0.5
32	3	1	0	0.5
32	3	2	0	0.5
32	5	1	0	0.5

[a]Zeros denote that the same calibration factors were used at all stations and casts on each HOT cruise.

described for flash fluorescence. The transmissometer was carefully calibrated as described by the manufacturer before each cruise to correct for instrument drift. The quality controlled 2 dbar binned data are also available via Internet (see Section 8).

2.2. Water Column Chemical Measurements

Samples for water column chemical analyses were collected at both Kahe Point and at Station ALOHA. Most of the samples were collected in the upper 1000 m. As much as possible, depth profiles of specific chemical constituents were collected on consecutive casts in order to minimize the effects of time-dependent variation within the water column. In addition, samples were collected near the same density or pressure horizons each month in order to facilitate comparisons between monthly profiles. Our strategy was to sample at density horizons within the main thermocline and at pressure horizons above and below this region (i.e., < 150 dbar and > 2000 dbar).

A detailed description of our sampling procedures and analytical methods was given in a separate report (Karl *et al.*, 1990). Abbreviated descriptions of these procedures were given in Chiswell *et al*. (1990). Beyond a general description of our analytical methods, only changes in the procedures described by Winn *et al*. (1991) are given in this report.

During 1991, water samples were collected using a 24-place aluminum rosette manufactured by Scripps Institution of Oceanography's Oceanographic Data Facility (ODF). Twelve-liter polyvinylchloride sampling bottles, also made by ODF, were used on this rosette. These sample
bottles were equipped with Buna-N rubber O-rings, Teflon-coated steel springs and standard General Oceanics sampling valves.

The primary objective of the Hawaii Ocean Time-series program is to assess variability in the central Pacific Ocean on annual and interannual time scales. One of our most important concerns, therefore, is to ensure that the highest possible precision and accuracy is consistently maintained for all water column chemical measurements. In order to achieve the highest possible data quality, we have instituted a quality-assurance/quality-control program (see Karl *et al.*, 1990), and have attempted to collect all ancillary information necessary to ensure that our data are not biased by sampling artifacts.

Although approximately 20% of our chemical analyses are replicated (see Karl *et al*., 1990), only mean values are reported in the data sets provided with the report. To assist in the interpretation of these data and to save users the time needed to estimate the precision of individual chemical analyses, we have summarized precision estimates from replicate determinations for each constituent on each HOT cruise during 1991. Whenever possible, we have also monitored the consistency of our analytical results between cruises by maintaining reference materials and by monitoring the concentration of the chemical of interest in the deep

sea where month-to-month variability is believed to be small.

2.2.1. Salinity

Salinity samples were collected in 250 ml glass bottles and stored at room temperature in the dark for analysis in our shore-based laboratories. The time between sample collection and analysis was about one week. Prior to analysis, each sample was allowed to equilibrate to laboratory temperature.

Salinity determinations reported for HOT cruises 23 to 26 were run on an AGE Minisal using the same procedures as described in Chiswell *et al.* (1990). For HOT cruises 27-32 a Guildline Autosal #8400 was used as the primary analytical instrument, but samples were run on both instruments to ensure that analytical consistency was maintained. The results of duplicate salinity determinations using both instruments are given in Tables 2.9 and 2.10. Table 2.9 presents the results of direct comparisons of replicate samples. Table 2.10 shows the results of the analysis of laboratory standards run with each set of monthly samples. No significant differences were observed between the salinities determined with both instruments. Typical precision (one standard deviation of triplicate samples from the same Niskin bottle) during 1991 was about 0.001 psu for both instruments.

Table 2.9: Salinity Results by Cruise: Autosal - Minsal

HOT	# Outliers Removed	Mean S Diff. (mpsu)	N (Samples)
25	4	-0.7 ± 1.4	49
26	1	0.1 ±1.8	60
27	1	-0.2 ± 1.7	81
28	5	1.5 ± 1.3	76
29	3	1.0 ± 1.7	78
30	3	1.6 ± 1.9	97
31	2	0.5 ± 2.9	55
32	13	1.6 ± 2.3	62

Table 2.10: Results for Lab-substandards by Cruise

HOT	Mean Salinity (psu) & # of samples			
	Autosal	#	Minisal	#
24	35.1655 ± 0.0006	3	35.1654 ± 0.005	4
25	35.1664 ± 0.0005	8	35.1665 ± 0.0017	4
26	35.1672 ± 0.0001	4	35.1682 ± 0.0011	3
27	34.5486 ± 0.0008	16	34.5549 ± 0.0111	7
28	34.5507 ± 0.0004	22	34.5509 ± 0.0009	2
29	34.5511 ± 0.0003	17	34.5524 ± 0.0012	4
30	34.4374 ± 0.0003	25	34.4377 ± 0.0015	3
31	34.4363 ± 0.0002	22	34.4375 ± 0.0010	4
32	34.4686 ± 0.0003	18	34.4683 ± 0.0010	4

2.2.2. Oxygen

Oxygen samples were drawn as soon as possible after the rosette arrived on deck and before any other samples were taken. These samples were collected in calibrated 125-ml iodine flasks, and were fixed immediately for subsequent analysis in the laboratory. Oxygen concentrations were determined using the Winkler titration method of Carpenter (1965) as described by Winn *et al*. (1991).

The mean precision of our oxygen analysis during 1991 was 0.15% (Table 2.11). Oxygen concentrations measured over the first three years of the program are plotted at constant density horizons in the deep ocean in Figure 2.4. Oxygen analyses differed by approximately 5 µmol kg^{-1} in deep water, indicating that analytical consistency was maintained throughout the first three years of the program.

Oxygen concentrations are reported in units of µmol kg^{-1}. These concentrations were computed assuming that the samples come to the surface adiabatically (i.e., they were drawn into the 125 ml flasks at their *in situ* potential temperature). As was described previously (Winn *et al*., 1991), this procedure can introduce a systematic error in oxygen concentration because the water sample warms enroute to the surface.

Table 2.11: Precision of Winkler Titration

Cruise	Average of all Triplicate Measurements CV (%)[a]	N[b]
23	0.14	8
24	0.06	5
25	0.07	8
26	0.06	8
27	0.31	8
28	0.13	7
29	0.22	10
30	0.17	8
31	0.12	11
32	0.18	9

[a]Coefficient of variation expressed as the difference between replicates expressed as a percentage of the mean when duplicate samples were collected, and expressed as the standard deviation as a percentage of the mean for samples collected in triplicate.

[b]Number of depths from which replicates were collected. Only replicates from depths where oxygen concentrations exceed 100 μmol kg^{-1} were included in the analysis.

In order to evaluate the magnitude of this error, and to allow for the calculation of oxygen concentrations with the greatest accuracy, we measured the temperature of the seawater sample within individual Niskin bottles at the time that the iodine flask was filled (i.e., oxygen sample temperature). Oxygen sample temperatures were measured on all HOT cruises during 1991 using a standard glass mercury thermometer or a digital thermistor. Because of the rough sea-state frequently encountered at the time-series site, the precision of on-deck temperatures measured as described above was about ± 1°C.

Figure 2.5 (top panel) shows a plot of the difference between oxygen sample (on-deck) temperature and potential temperature computed from *in situ* temperature at the time of bottle trip versus pressure. The bottom panel of this figure shows a plot of the difference between oxygen concentrations computed using on-deck and potential temperatures for all samples collected during 1990 and 1991. The scatter observed in delta temperature below 500 m is due primarily to the speed with which the CTD is raised through the thermocline. The depth dependent variability in delta oxygen was a result of the time-series sampling strategy as described by Winn *et al.* (1991).

Figure 2.4: Oxygen versus time at three density horizons at Station ALOHA. Oxygen concentration at potential densities of 27.782, 27.758 and 27.675.

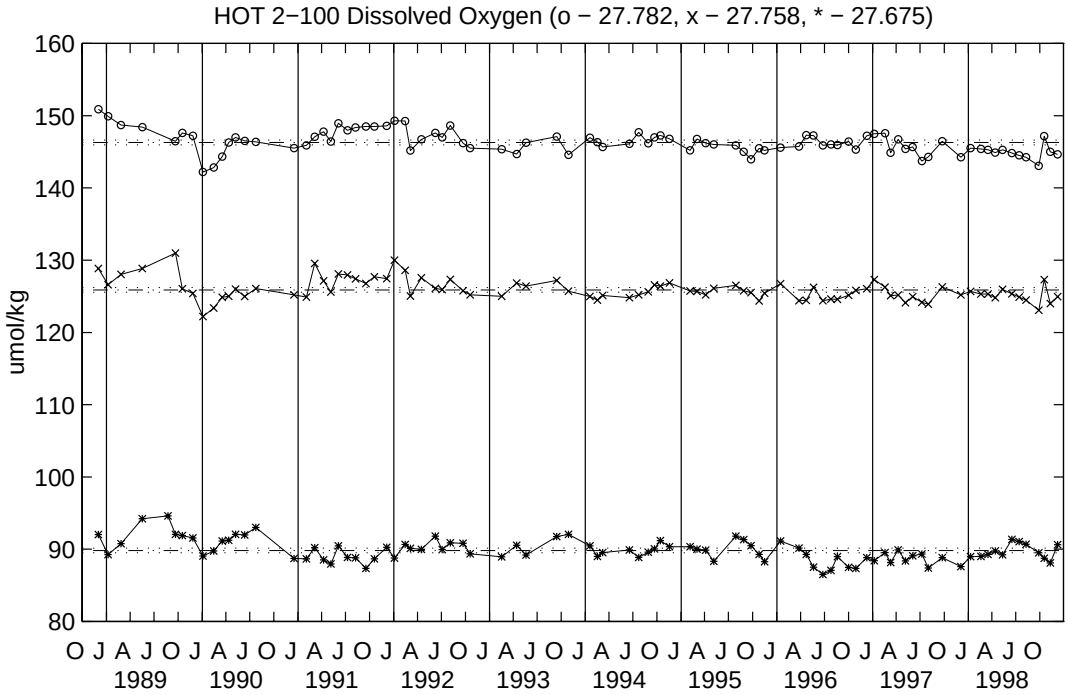

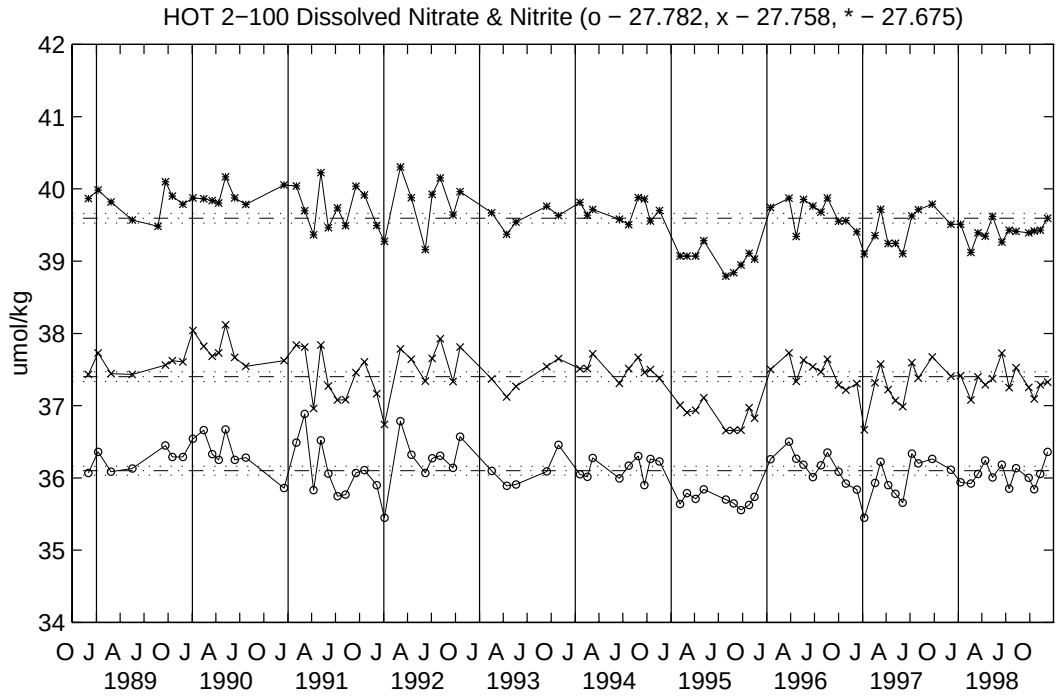

Figure 2.6: As in Figure 2.4, except for concentrations of dissolved [nitrate+nitrite]

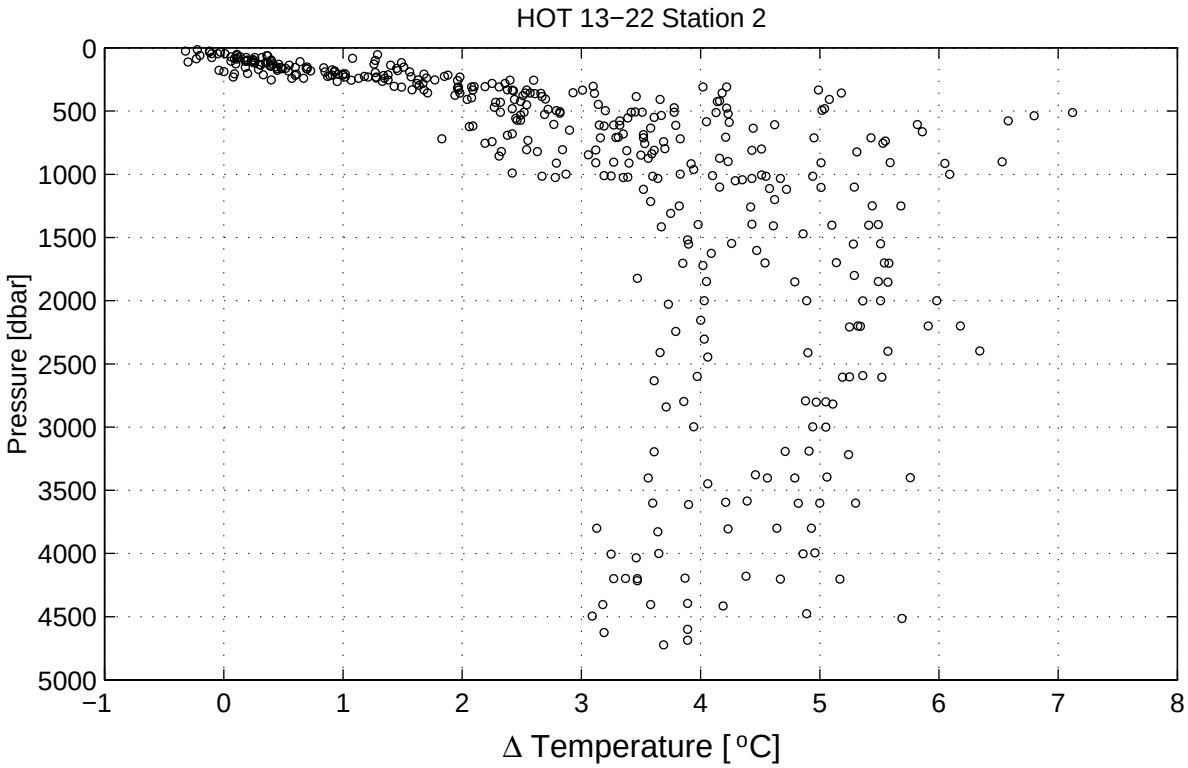

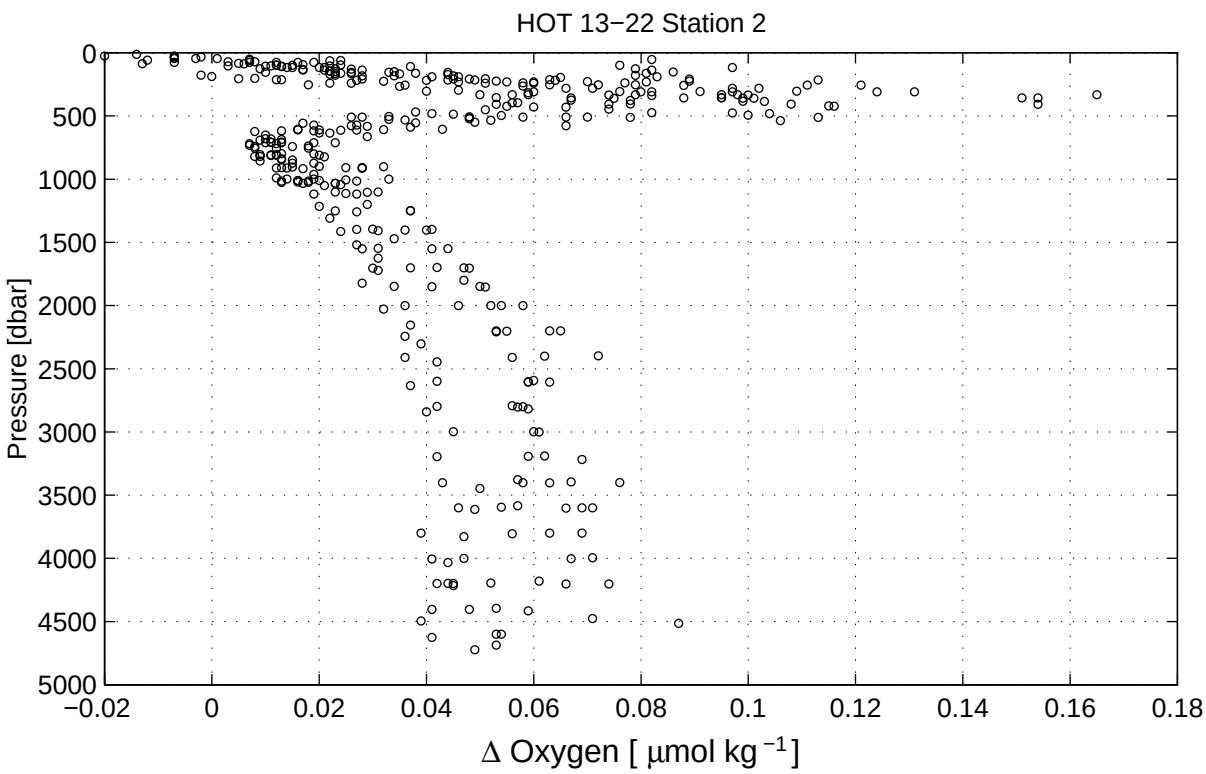

Figure 2.5: Upper Panel: Difference between sample temperature at the time of sample collection and potential temperature calculated from *in situ* temperature at the time of bottle trip. Lower panel: Difference in oxygen concentration in units of μmol kg^{-1} using temperatures measured at the time of sample collection and potential temperature computed from *in situ* temperature.

2.2.3. Dissolved Inorganic Carbon

Samples for dissolved inorganic carbon (DIC) were measured using a commercial coulometer modified for high-precision measurements as described by Chiswell *et al.* (1990). During 1991 we were provided with primary DIC standards by Dr. Andrew Dickson to help ensure the accuracy of coulometric analyses. The results of these analyses indicated that the precision of our analytical work is excellent and that our determinations are accurate to within 1 µmole per kg (Table 2.12).

Table 2.12: Analysis of Dissolved Inorganic Carbon Standards
(A. Dickson; Batch #10)

Sample	Date	µmol/kg
1	7 May 1992	1961.28
2	15 May 1992	1962.78
3	18 May 1992	1962.26
4	17 Jun 1992	1959.00[a]
5	16 Jul 1992	1961.42
6	17 Jul 1992	1961.02
7	22 Jul 1992	1962.44
8	7 Sep 1992	1962.09
9	9 Sep 1992	1962.63

[a]This sample was greater than 2 standard deviations from the mean and was not included our calculation of analytical precision.

2.2.4. Titration Alkalinity

Titration alkalinity was determined using the Gran titration method of Edmond (1970) as modified by Bradshaw and Brewer (1988), except that an open titration cell was used. Samples were titrated with approximately 0.1 N HCl using a Dosimat 665 digital burette, a Corning semi-micro combination pH electrode and Orion model 940 pH meter. The titration system was computer controlled to automate the procedure. The second end point (V_2) was determined with a modified Gran plot, which was corrected for the influence of sulfate and fluoride. The electrode was calibrated with seawater (Tris) buffer (Hansson, 1973; Dickson, 1993). The electrode slope and ε° were determined by an iterative procedure which minimized the residuals of the Gran function over the pH range of 3.5 to 3.0.

The precision of our titration procedure was approximately 2 µequiv/kg. Unfortunately, anabsolute alkalinity standard was not available, and the accuracy was established primarily by the value determined for the normality of the titrant. We have intercalibrated the determination between our acid normality with that of Dickson's laboratory at Scripps Institution of

Oceanography, where high-precision coulometric methods are used for this purpose.

2.2.5. pH

pH was determined using standard potentiometric techniques. Water samples were drawn from the Niskin bottles directly into 125-ml high density polypropylene bottles. These bottles were filled completely and capped immediately. The samples were then placed in a water bath and equilibrated at 25° C. pH was measured with a Corning semi-micro combination electrode, and an Orion 940 pH meter. In 1991 the electrode was standardized with NBS buffers (pH 7 and 10) obtained from Fisher Scientific. The pH data for 1991 are therefore on the NBS scale at 25°C. Beginning in January 1992 the electrode was calibrated with seawater buffers (Tris and Bis; Dickson, 1993), and pH determinations were therefore on the seawater scale.

2.2.6. Inorganic and Organic Nutrients

Samples for the determination of nutrient concentrations were collected in acid-washed 125-ml polyethylene bottles, and immediately frozen for transport to the laboratory. Analyses were conducted at room temperature on a four-channel Technicon Autoanalyzer II continuous flow system, using slight modifications of the Technicon procedures for the analysis of seawater samples (Winn *et al*., 1991; Karl *et al*., 1990). A summary of the precision of our dissolved inorganic nutrient analyses during HOT-23 through HOT-32 is shown in Table 2.13. In Figures 2.6-2.8, nutrient concentrations measured at three density horizons are presented. Nitrate plus nitrite (Figure 2.6) and phosphate (Figure 2.7) plotted at constant density show little cruise-to-cruise variability, indicating that analytical consistency was maintained for these analyses. Deep-water silica values (Figure 2.8) show larger cruise-to-cruise variability, up to 5 µmol kg^{-1} at 3000 m. However, this variability represents less than 4% of the absolute value at this depth, indicating that reasonably good analytical consistency was also maintained for this analysis.

2.2.6.1. Nitrate plus Nitrite and Dissolved Total Nitrogen

The sum of [nitrate+nitrite] was measured after reduction of nitrate to nitrite in a copperized cadmium reduction column on the autoanalyzer as described by Chiswell *et al.* (1990) and Karl *et al.* (1990). Total dissolved nitrogen (TDN) was determined following ultraviolet (UV) light oxidation (Armstrong *et al.*, 1966; Walsh, 1989). Dissolved organic nitrogen (DON) was determined from the difference between TDN and the sum of [nitrate+nitrite].

Figure 2.7: As in Figure 2.4 except for dissolved phosphate.

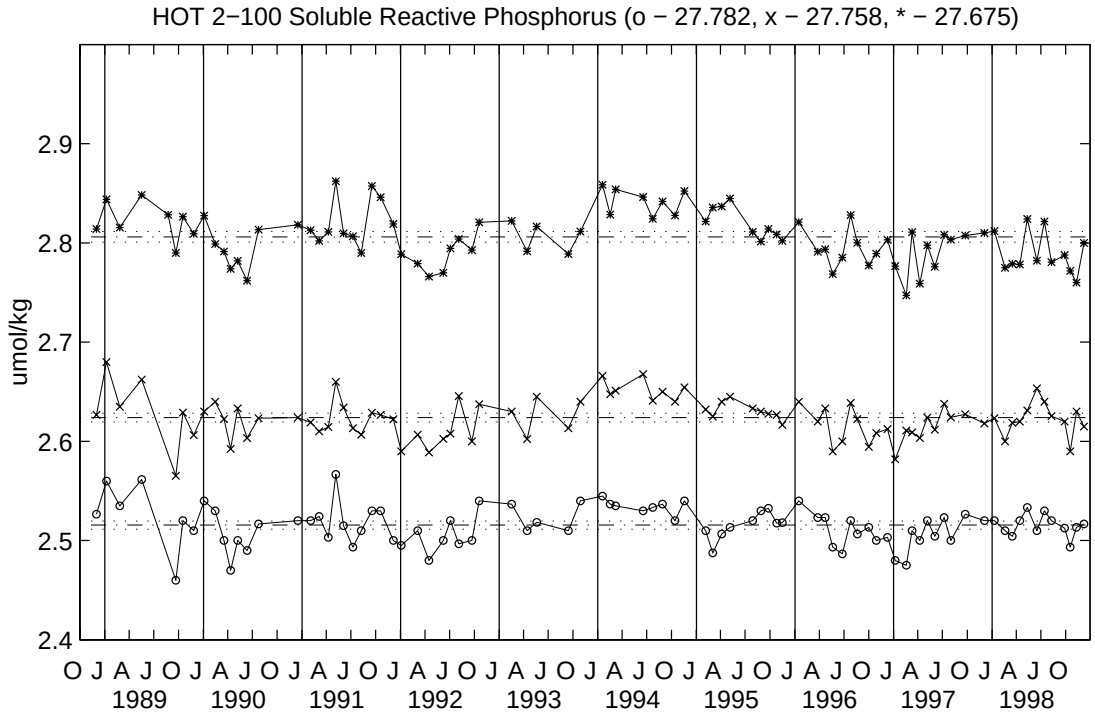

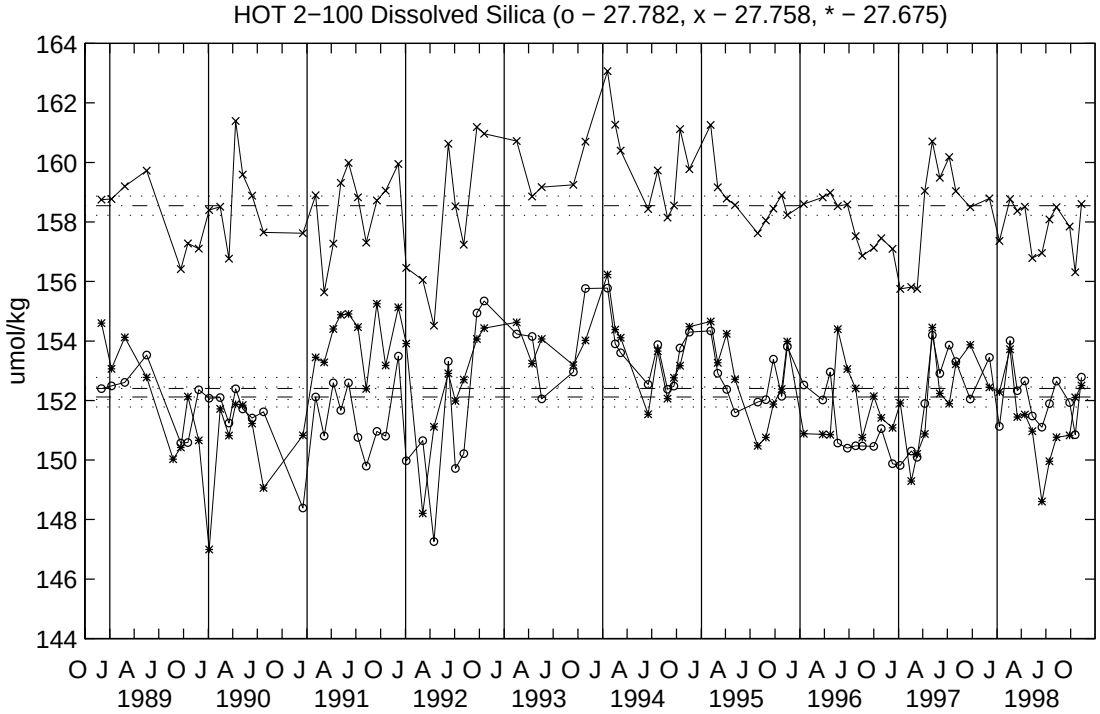

Figure 2.8: As in Figure 2.4 except for dissolved silica.

Table 2.13: Precision of Dissolved Nutrient Analyses

Cruise	Phosphorus		Nitrate + Nitrite		Silica	
	Analytical[a]	Field[b]	Analytical[a]	Field[b]	Analytical[a]	Field[b]
23	0.1 (.003)c	0.4 (.011)	1.2 (.073)	0.6 (0.13)	9.7 (0.26)	4.2 (0.39)
24	0.7 (.010)	0.2 (.010)	2.1 (0.18)	0.5 (0.15)	5.6 (0.19)	0.9 (0.19)
25	0.4 (.006)	0.4 (.009)	0.3 (.079)	0.3 (.045)	0.1 (.16)	1.8 (.21)
26	0.4 (.007)	0.4 (.007)	0.4 (.097)	0.5 (.049)	1.3 (.11)	1.8 (.25)
27	0.0 (0)	0.4 (.006)	0.5 (.050)	0.6 (.037)	0.1 (.12)	2.5 (.22)
28	0.5 (.006)	0.3 (.011)	0.4 (.106)	0.7 (.062)	0.2 (.21)	0.9 (.68)
29	0.0 (0)	0.2 (.004)	0.1 (.009)	0.3 (.034)	0.1 (.10)	0.2 (.13)
30	0.3 (.010)	0.4 (.004)	0.4 (.073)	0.3 (.035)	0.4 (0.36)	3.1 (0.44)
31	0.6 (.005)	0.6 (.010)	0.2 (.033)	0.4 (.034)	1.3 (.37)	2.4 (.21)
32	0.8 (.009)	0.7 (.012)	0.2 (.042)	0.3 (.027)	0.4 (.32)	4.6 (.22)

[a]Average coefficient of variation (i.e., standard deviation as a percentage of the mean) for analytical replicates (i.e., replicate analysis of a single sample) for phosphate concentrations 0.4 µM, [nitrate+nitrite] concentrations 0.2 µM, and silica concentrations 0.2 µM.

[b]Average coefficient of variation for field replicates (i.e., analysis of replicate samples from the same Niskin) for the above concentration ranges.

[c]Numbers in parentheses are the mean absolute differences, in µM, between replicates.

2.2.6.2. Soluble Reactive and Total Dissolved Phosphorus

Soluble reactive phosphorus (SRP) was measured by reaction with acidified molybdate reagent and potassium antimonyl tartrate, followed by the subsequent reduction with ascorbic acid. Total dissolved phosphorus was measured by ultraviolet photo-oxidation, followed by analysis of the oxidation products (Chiswell *et al.*, 1990). Dissolved organic phosphorus (DOP) is measured as the difference between TDP and SRP as described by Chiswell *et al.* (1990).

2.2.6.3. Silica

Soluble reactive silica was measured by reaction with ammonium molybdate at low pH,

followed by reduction with ascorbic acid as described by Chiswell *et al.* (1990).

2.2.6.4. Dissolved Organic Carbon

Dissolved organic carbon (DOC) was determined with the persulfate oxidation method as described in Winn *et al.* (1991). A summary of the precision of organic nutrient analyses are given in Table 2.14.

Table 2.14: Precision of Dissolved Organic Nutrient Analyses

CV (%) Dissolved Organic Nutrients						
	DOC		DON		DOP	
Cruise	CV(%)[a]	n[b]	CV(%)	n	CV(%)	n
23	nd		nd		nd	
24	3.9 (1.0)[c]	3	4.3 (0.18)	3	10.8	2
25	nd		10.5 (0.81)	3	27.1	3
26	2.9 (0.9)	4	13.7 (0.31)	4	7.6	3
27	0.8 (0.2)	3	16.0 (0.44)	3	13.1	3
28	nd		32.5 (0.51)	1	16.7	4
29	nd		14.12 (0.31)	4	20.4	2
30	nd	nd	6.0 (0.19)	4	4.6	3
31	nd		13.9 (0.82)	5		
32	nd		13.6 (0.38)	4		

[a]Average coefficient of variation (i.e., standard deviation as percentage of the mean for replicate samples.)

[b]Number of replicates analyzed.

[c]Number in parentheses are the mean absolute differences, in µM, between replicates.

In April 1991 an NSF-sponsored DOC/DON interlaboratory comparison study was conducted at Station ALOHA. The persulfate method described above was compared with several high-temperature techniques employing platinum catalysts. On average, the high-temperature methods yielded DOC concentrations that were 2- to 3-fold higher than the persulfate oxidation technique. Consequently, we have begun to use a commercially available high-temperature instrument for DOC analyses and discontinued the persulfate oxidation analysis

of DOC following HOT-27. We are presently perfecting the high temperature analysis of DOC for our routine time-series measurements.

2.2.6.5. Low Level Nitrate Plus Nitrite

Surface water samples (<100 m) have [nitrate+nitrite] concentrations below the approximately 0.03 µM detection limit of the Technicon Autoanalyzer. To achieve high-precision high-accuracy measurements at these low levels, we employed the chemiluminescent method of Cox (1980) and Garside (1982). In this method, nitrite and nitrate were chemically reduced to gaseous nitric oxide by an acidic solution of concentrated sulfuric acid, ferrous ammonium sulfate and ammonium molybdate. The reduced nitric oxide was carried by an inert carrier gas (argon) through a series of traps to remove acid and water vapors and then into an Antek model 720 chemiluminescent nitrogen analyzer. The nitrogen analyzer combined nitric oxide with ozone to produce a metastable nitrogen dioxide. The nitrogen dioxide subsequently emitted a photon as it returned to ground state, and the emitted light was detected by a photomultiplier tube. The integrated electrical signal produced by the photomultiplier is proportional to the content of [nitrate+nitrite] in the sample. The calibration of the low level nitrate/nitrite analysis was performed using a stock solution of KNO_3 (10 mM) in deionized distilled water (DDW). Working standards were prepared fresh by volumetric dilutions of the stock using acid-washed glass pipettes and flasks. In order to maintain the accuracy of the analysis, serial dilutions of a certified reference standard (CSK) are included in every sample run, in case stock solutions become contaminated or microbially altered during storage. The detection limit for [nitrate+nitrite] was approximately 1-2 nM, while precision and accuracy of the analysis were approximately 2-3 nM.

2.2.6.6. Low Level Soluble Reactive Phosphorus

Phosphate concentrations in the euphotic zone were also below the approximately 0.2 µM detection limit of the Technicon autoanalyzer. In order to resolve variability in phosphate concentrations in the euphotic zone we employed the "MAGIC" procedure of Karl and Tien (1992). With this method, soluble reactive phosphate was concentrated by co-precipitation with $Mg(OH)_2$ and the standard molybdenum blue color reaction was used to quantify the orthophosphate in the concentrated samples. Samples were collected in acid wash 500 ml polyethylene containers and frozen immediately for transport to the laboratory.

2.2.7. Particulate Carbon and Nitrogen

Samples for particulate carbon (PC) and particulate nitrogen (PN) were prefiltered through a 202-µm Nitex mesh, collected onto a combusted GFF filter and analyzed using a commercial CHN analyzer (Chiswell *et al*., 1990).

2.2.8. Particulate Phosphorus

Samples for particulate phosphorus (PP) were prefiltered through a 202-µm Nitex mesh, collected onto a combusted GFF filter and oxidized by high temperature ashing. The resultant

orthophosphate was measured spectrophotometrically (Chiswell *et al.* 1990).

2.2.9. Pigments

Chlorophyll *a* and phaeopigments were measured fluorometrically using standard techniques (Strickland and Parsons, 1972). Analytical precision for fluorometric chlorophyll *a* on replicate field sample determinations in 1991 are summarized in Table 2.15. Integrated values for pigment concentrations were calculated using the trapezoid rule. In addition to the fluorometric determination of pigments, we also measured chl *a* and accessory photosynthetic pigments (Table 2.16) by high-performance liquid chromatography (HPLC) according to the procedure described by Bidigare *et al.* (1990). A known amount of canthaxanthin was added to each sample as an internal standard and all pigments were quantified using external standards provided during the JGOFS pigment intercalibration exercises.

Table 2.15: Precision of Fluorometric Analyses of Chlorophyll *a* and Phaeopigment

Cruise	Chl *a* CV(%)[a]	Phaeo CV(%)[a]
13	7.39	16.30
14	9.45	9.10
15	8.03	11.12
16	5.58	11.38
17	4.31	7.19
18	1.85	4.67
19	1.76	4.94
20	1.91	5.04
22	3.00	6.34

[a]Coefficient of variation as a percent of the mean of all triplicate determinations for each cruise.

Table 2.16: HPLC Pigment Analysis

Pigment	RF[a]	RT[b]
Chlorophyll c_3	.000441	
Chlorophyll (c_1 + c_2) & Mg 3,8 DVP4A5	.000441	
Peridinin	.000593	.316
19'-Butanoyloxyfucoxanthin	.000398	.380
Fucoxanthin	.000443	.415
19'-Hexanoyloxyfucoxanthin	.000336	.450
Prasinoxanthin	.000512	.487
Diadinoxanthin	.000285	.635
Zeaxanthin	.000275	.766
Chlorophyll *b*	.00156	.888
Chlorophyll *a*	.000729	1.000
Chlorophyll c_4	.000441	
Carotens	.000264	1.612

[a]RF - Response Factor (mg pigment per unit absorbance peak area at 436 nm).
[b]RT - Retention Time (relative to chlorophyll *a*)

2.2.10. Adenosine 5'-Triphosphate

Water column adenosine 5'-triphosphate (ATP) concentrations were determined as described by Winn *et al.* (1991). The precision of ATP determinations in 1991 are given in Table 2.17.

Table 2.17: Precision of ATP Analyses

Cruise	ATP CV(%)[a]
23	11.5
24	16.1
25	9.7
26	8.7
27	16.4
28	15.3
29	12.3
30	16.3
31	15.0
32	16.7

[a]Coefficient of variation as the percent of mean of all triplicate determinations for each cruise.

2.3. Biogeochemical Rate Measurements

2.3.1. Primary Productivity

Photosynthetic production of organic matter was measured by the carbon-14 method. Incubations were conducted *in situ* using a free-floating array equipped with a VHF transmitter and a strobe light as described by Winn *et al.* (1991). Twelve-hour *in situ* incubations were conducted during 1991 on all cruises on which it was possible to do primary production experiments. Integrated carbon assimilation rates were calculated using the trapezoid rule. In all cases, the shallowest values were extended to 0 m. The deepest primary production measurements were extrapolated to a value of zero at 200 m.

2.3.2. Particle Flux

Particle flux was measured using sediment traps deployed on a free-floating array for approximately 72 hours each month. Sediment trap design and sample collection methods, as well as sample analysis, were performed as previously described in Winn *et al*. (1991).

2.4. ADCP Measurements

Shipboard ADCPs were available and used on all HOT cruises in 1991. RDI model VM-150 instruments were used on the R/V MOANA WAVE (HOT-23, -30) and on the R/V WECOMA (HOT-31, -32). An RDI model VM-300 instrument was used on the R/V ALPHA HELIX (HOT-24, -25, -26, -27, -28, and -29). ADCP depth range is roughly inversely proportional to the frequency, so the range on the R/V ALPHA HELIX, with a 306-kHz profiler, was about half the range on the R/V MOANA WAVE and the R/V WECOMA, with their 153-kHz profilers. The performance of the R/V WECOMA installation was superior to that on the R/V MOANA WAVE; the R/V WECOMA appears to generate much less acoustic noise when underway.

ADCP and navigation data were recorded successfully throughout all cruises except HOT-24 and the first leg of HOT-27. Only on-station data were available from HOT-24, and only the last day on station plus the transit to Honolulu were available from the first leg of HOT-27. The temperature sensor on the ADCP transducer on the R/V ALPHA HELIX failed during HOT-27; data from that and the following R/V ALPHA HELIX cruises were corrected for the erroneous sound speed used by the Data Acquisition System to calculate the water velocity from the Doppler shift.

Navigation on all cruises was almost entirely from GPS. The raw reference layer velocity estimates were noisy on the R/V ALPHA HELIX because only fixes averaged over each ensemble were available on a regular basis. Shifting the average fix time to the middle of the ensemble succeeded in reducing much of this noise. Gaps in the R/V MOANA WAVE GPS record on HOT-30 were caused by a malfunction in the Magnavox 1157 GPS/Transit receiver. A Magnavox 4200 receiver was installed on the R/V WECOMA for HOT-31 and following cruises, and the 1-Hz fix updates were logged by the ADCP Data Acquisition system using our own user

exit program. The raw reference layer velocities on HOT-31 are extraordinarily clean and smooth, reflecting the accuracy with which GPS was capable in the absence of Selective Availability (SA), the deliberate degradation of GPS signals by the Defense Department. The relatively noisy reference layer velocities on HOT-32 showed the effects of SA, which was turned on between these two cruises.

2.5. Optical Measurements

Incident irradiance at the sea surface was measured on each HOT cruise with a Licor LI-200 data logger and cosine collector. Irradiance levels were averaged over 10-minute intervals and integrated over the daylight period during the primary production experiment. Vertical profiles of Photosynthetically Available Radiation (PAR) were also obtained on most cruises during 1990 with a Biospherical Instruments model PNF-300 optical profiler. These data sets were too large to be included in this report. The entire data set is available via internet as described Section 8.

2.6. Meteorology

Meteorological data were collected at four-hour intervals while on station. Wind speed and direction, atmospheric pressure, wet- and dry- bulb air temperature, sea surface temperature, cloud cover and sea state were recorded as described in Chiswell *et al*. (1990). In this report we compared these data to those collected at the nearest NDBC (National Data Buoy Center) buoy. The buoy data was available from the National Oceanic Data Center.

2.7. XBT

XBT casts were generally made spaced seven minutes of latitude apart during the transit to or from the deep-water site. Sippican T-7 probes having a maximum depth of 750 m were used. The files were screened for bad and missing data, and no corrections were applied.

3. Cruise Summaries

3.1. HOT-23; S. Chiswell, Chief Scientist

HOT-23 departed Snug Harbor on the R/V MOANA WAVE at 1800 on 1 February 1991 and returned at approximately 1800 on 6 February. Kahe Point was visited enroute to Station ALOHA, and XBTs were dropped during the transit from Kahe Point to Station ALOHA. Regular sampling work was conducted at Station ALOHA. Inverted echo sounders (IES) were deployed during this cruise, and 6 extra stations were completed near the deployment sites.

Sampling

All WOCE and JGOFS chemical sampling was completed on this cruise. Both the WOCE deep cast and the 36 hour CTD burst sampling were completed successfully.

Primary Production and Sediment Trap Measurements.

Both the primary production and sediment trap measurements were made on this cruise

without problems.

Ancillary Projects.

S. Chiswell deployed Inverted Echo Sounders near the ALOHA Station, and extra CTD stations were occupied near these deployment sites. Plankton net tows were done for R. Letelier.

3.2. HOT-24; D. Karl, Chief Scientist

HOT-24 departed Snug Harbor at 0900 on 5 March 1991 on the R/V ALPHA HELIX and returned at 0730 on 9 March. The cruise was shorter than usual because of the extremely rough weather encountered on this cruise.

Sampling

Although Kahe Point was visited on this cruise, no samples were collected because of a breakdown in the winch hydraulics. Rough weather, and a propensity for the R/V ALPHA HELIX to roll, prevented the collection of the CTD burst sampling at Station ALOHA. CTD work on this cruise was restricted to daylight hours and a total of 7 casts were obtained at Station ALOHA. The WOCE deep cast was one of these 7 casts. In spite of the restricted number of casts obtained at Station ALOHA, all of the primary WOCE and GOFS chemical sampling was obtained on this cruise.

CTD Operations

Because of the failure of a hydraulic line at Kahe Point, the primary CTD winch was not used, and the R/V ALPHA HELIX winch and conducting cable were for CTD profiling used on this cruise. The R/V ALPHA HELIX winch had a single conductor cable instead of the standard three conductor wire we normally use. This resulted in more spikes in the CTD data than normal. In addition, the rough weather and several violent collisions with the ship during recovery and deployment of the CTD caused the loss of some CTD data on this cruise. For example, all data collected on the WOCE deep cast were deemed bad.

Primary Production and Particle Flux

No primary production data were collected on this cruise because of rough weather. The drifting sediment trap array was deployed and recovered successfully. However, all of the 300 m data was lost when the traps overturned after recovery. In addition, fewer replicates than usual were collected at 150 and 500 meters because of broken collars and overturned PITS at these depths.

3.3. HOT-25; R. Lukas, Chief Scientist

The R/V ALPHA HELIX departed from Snug Harbor at 0930 HST on 8 April 1991, and returned approximately 1430 on 11 April. The return was one day early because the GOFS

drifting sediment trap array was not deployed (see below).

The weather was very good, with light trade winds prevailing. There remained a swell from the previously strong trades, and the swell caused occasional excessive rolling of the vessel.

With the exception of the sediment trap deployment, the cruise achieved all other scientific objectives. All the standard WOCE and JGOFS chemical samples were obtained. The WOCE deep cast and CTD burst sampling was completed and 2 casts were made at the Kahe Point station. The GOFS primary productivity array was successfully deployed and recovered. Several net tows were made for students working in the JGOFS component of the program.

Primary Production and Particle Flux

The JGOFS primary productivity array was successfully deployed and recovered. However, during the final stage of the deployment of the sediment trap array, the surface spar buoy swung into the side of the ship breaking off the weighted end. There was no means to repair this damage, so the array was recovered and the deployment abandoned.

3.4. HOT-26; C. Winn, Chief Scientist

We departed Snug Harbor at 0900 on 6 May 1991 aboard the R/V ALPHA HELIX. We returned to Snug Harbor on 10 May at 1700. The return trip was unusual because we rounded the southeast end of Oahu. This course saved us about two hours of transit time because the sediment traps drifted about 25 miles east of Station ALOHA.

Sampling

All WOCE and GOFS chemical sampling was completed on HOT-26. The WOCE deep cast was obtained and both the sediment trap and primary production experiments were completed. However, the WOCE 36 hour burst sampling was not completed as planned. Although CTD casts were collected over the entire period spent at station ALOHA, due to adverse weather, CTD casts were not obtained on three hour intervals over a contiguous 36 hour period. CTD operations were halted for approximately 12 hours on 8 May due to rough seas (i.e., 3-4 m seas and 25 to 30 knot winds). The CTD cart and tail-weight was used for all CTD deployments. The new tail-weight deployment system proved very effective in reducing the CTD motion during recovery. However, it was necessary to add wooden braces to the cart in order to prevent the CTD from shifting.

Primary Production and Particle Flux

The primary production array was deployed and recovered without problems. However, the recovery of the sediment trap spar buoy was a problem again on HOT-26 because of the large JGOFS spar buoy. It should be replaced with a smaller one on the remaining R/V ALPHA

HELIX cruises. In addition, the sediment trap crosses at all four depths slipped on this cruise. At all depths except 500 meters the crosses were prevented from moving significantly downward by the hose clamp used to stabilize the crosses. The 500 meter cross slipped all the way down to the tail weight.

3.5. HOT-27; R. Lukas, Chief Scientist

HOT-27 was conducted on R/V ALPHA HELIX in two parts. ALPHA HELIX departed from Snug Harbor for Leg 1 at 0945 HST on 3 June 1991, and returned approximately 1030 on 6 June. Leg 2 departed from Snug Harbor at 1200 on 8 June and returned to Snug Harbor at 1200 on 9 June.

The weather was generally good, with light easterly trade winds prevailing. Occasional rain squalls were encountered, and the first two days of Leg 1 were fairly cloudy.

The work went smoothly on Leg 1. All scheduled casts were done, and the sediment traps were deployed without mishap. The primary productivity cast took longer than normal due to pre-tripping of the go-flos on the first attempt. The *in situ* array was deployed and recovered with no problems. Some net tows were conducted between hydrographic casts.

The sediment traps were recovered on Leg 2 at approximately 0100 on 9 June. With the exception of a mishap on the part of the ship's crane operator, the sediment trap recovery went very smoothly. The crane operator's error resulted in the headache ball falling from the crane onto the ship deck. Fortunately, no none was injured when the ball hit the deck.

A new spar buoy recovery strategy was used on Leg 2. This strategy involved tying the top of the spar buoy to the deck before lifting the spar out of the water. This resulted in the spar buoy being lifted onto the deck in a horizontal position and made for a much smoother recovery. We will employ this strategy as much as possible on future cruises.

One PNF cast was conducted at Kahe Point and four at Station ALOHA. LICOR data were logged on 4 June through 6 June.

3.6. HOT-28; C. Winn, Chief Scientist

We departed Snug Harbor on the R/V ALPHA HELIX at 1030 on 8 July 1991 after a 1.5 hour delay for barge traffic. Other than the delayed departure, the cruise schedule did not deviate significantly from plan. We returned to Snug Harbor at 1600 on 12 July.

Sampling

All WOCE and GOFS hydrographic and chemical sampling was completed on HOT-28. The JGOFS primary production and sediment trap experiments were also successful. However,

the WOCE 36 burst sampling was interrupted after approximately 30 hours because of the failure of the Markey winch.

CTD Operations

The Markey winch failed with approximately 1000 m of wire out. As a result, about 1000 m was cut from the hydrowire. We attempted to recover the CTD using wire clamps and the ship's crane before cutting the wire. This attempt was abandoned when the wire clamp, which was not designed specifically for our wire, broke strands in the hydrowire. After the hydrowire was cut, the package was recovered by spooling on the R/V ALPHA HELIX winch. Following an 8 to 10 hour delay to reconfigure the system, CTD operations were resumed using the R/V ALPHA HELIX wire and winch. The 1000 m piece of cut wire was discarded at approximately 22° 45.22'N, 158° 01.54'W.

Sediment trap and Primary production Work

The sediment trap and primary production work went smoothly on this cruise. The R/V ALPHA HELIX crew was primarily responsible for recovering and deploying the sediment trap gear. Although the recovery of the large spar buoy continues to be a problem on the R/V ALPHA HELIX, the seas were relatively calm on this cruise, and the deployment and recovery of the spar was accomplished without major problems.

3.7. HOT-29; D. Hebel, Chief Scientist

HOT 29 was conducted aboard the RV ALPHA HELIX 8-12 August 1991. We departed Snug Harbor on 8 August 1991 at approximately 0900 hours and returned at 1600 on 12 August.

Sampling

All WOCE and GOFS chemical sampling was completed on this cruise. The WOCE deep cast was obtained and the WOCE burst sampling was completed without incident. No significant equipment problems were encountered on this cruise.

Primary Production and Particle Flux

Primary production and particle flux samples were collected without significant problems on this cruise.

3.8. HOT-30; C. Winn, Chief Scientist

HOT-30 departed Snug Harbor on the R/V MOANA WAVE on Monday 16 September at 0900. Departure was delayed for approximately one hour due to ship traffic. Both Station ALOHA and the Kahe Point station were visited on this cruise. HOT-30 returned to Snug Harbor

at 1300 on Friday 20 September. The sea-state was calm during on the first two days at Station ALOHA. We noticed that *Trichodesmium* sp. was relatively abundant in the upper water column (see below).

WOCE and GOFS Sampling

All chemical sampling was completed on this cruise at both Kahe Point and Station ALOHA. The WOCE deep cast was obtained and the WOCE CTD burst sampling was accomplished without significant problems. The GOFS sediment trap collections and the GOFS primary production work was also completed without significant problems.

Continuous Profiling

CTD operations also went extremely well on this cruise, and there were no significant problems to report. The addition of the transmissometer to the optical profiler made the package too heavy to recover easily by hand and it was recovered using the windlass attached to the winch.

Sediment Trap and Primary Production

The sediment traps were deployed and recovered without serious problems on HOT-30. The traps drifted approximately 25 kilometers to the southwest. A new filtration system was used on this cruise to filter the sediment trap samples. This pressure filtration system reduced the time required to process these samples from the approximately 18 hours on most recent cruises to approximately 8 hours. The primary production experiment was also successful. However, several light bottles were lost. This appeared to be due primarily to the poor condition of the lanyards on the light bottles.

Trichodesmium sp.

During the calm weather encountered on the first two days at Station ALOHA, we noticed an accumulation of *Trichodesmium* sp. in spherical colonies at the surface. Net tows were done at several depths above 100 m in an attempt to evaluate the vertical distribution of these colonies. In addition, 10-liter samples were collected at several depths with the rosette sampler. Unfortunately, few colonies were observed in the 10-liter samples at any depth. Also, opening and closing nets were not available on this cruise, making interpretation of the net tow data problematic.

3.9. HOT-31; E. Firing, Chief Scientist

We departed Snug Harbor on the R/V WECOMA at 1000 on 19 October after a delay of about 3 hours for fueling and another half hour to retrieve a missing piece of equipment. We

returned to Snug Harbor at 1000 on 23 October.

Weather

Weather was good throughout the cruise. Winds were light easterlies for the first part and increased to moderate east-northeasterlies at the end. On the last day we felt a swell from stronger trades to the northeast of us. There were only a few brief showers.

Sampling

The Kahe Point station took over 6 hours because of problems with the CTD and with the level wind on the winch. The latter was fixed on the way to ALOHA. Work at ALOHA proceeded at a good pace with no major problems. All of the WOCE and GOFS chemical sampling was completed. Both the WOCE deep cast and CTD burst sampling were successful. Four LADCP casts were made: one to 4600 m and three to 2000 m. Good data quality was obtained on all.

CTD Sampling

The CTD was equipped with Marlin Atkinson's Morita O_2 sensor for the first time. At Atkinson's request, the CTD was therefore powered up almost continuously, and an effort was made to keep the Morita flushed with seawater and the rest of the SeaBird plumbing flushed with freshwater. However, because of leaks in the plumbing, sensors were frequently exposed to air.

Primary Production and Particle Flux

The primary production and particle flux measurements were made without problems. The sediment traps drifted north and east, consistent with the prevailing currents measured with the shipboard ADCP.

Additional CTD Stations

A new element was added on this cruise. CTD stations were occupied on 158°W at 23°25'N, 21°57.8'N, and 21°46.6'N. The first of these, Station 3, is 40 miles north of ALOHA. Station 4 is about 10 miles offshore of the 400-m isobath at Kahuku, and Station 5 is near that isobath. Each of these stations was conducted with the 24-place rosette and with sampling like that at Kahe Point. The 100-mile section to Kahuku on 158°W was filled in with T-7 XBTs at 10-mile intervals from Station 3 to 22°35'N, and at 5-mile intervals from there to 21°50'N. Including one failure, this required 16 probes (15 T-7 and 1 T-4). The last probe was launched slightly later than intended and hit bottom at 500 m; a T-4 would have sufficed.

After leaving Station 5, the ship proceeded along the North Shore approximately following the 300-m isobath so as to provide bottom-track calibration of the shipboard ADCP

and gyrocompass.

3.10. HOT-32; C. Winn, Chief Scientist

We left Snug Harbor on the R/V WECOMA on 4 December at 1030 hr after an approximately 40-minute delay to complete the hydrowire termination and to complete securing loose gear. We returned to Snug Harbor at 0730 on 9 December.

Sampling

All routine sampling was completed on this cruise. The WOCE deep cast and burst CTD sampling (30 hours) was completed without problems.

CTD Operations

CTD operations were suspended because of moderately rough weather beginning at 1800 on 6 December. CTD burst sampling was therefore restricted to approximately 30 hours.

Primary Production and Particle Flux

Upon arriving at Station ALOHA the sediment traps were deployed on the southeast edge of Station ALOHA, and CTD operations commenced after transiting to the center of the station area. The *in situ* primary production array was deployed and recovered without problems. The sediment traps were recovered 72 hours after deployment. The sediment trap array drifted only a few miles on this cruise.

Additional CTD Stations

CTD Stations 3, 4 and 5 were occupied on 158°W at 23° 25'N, 21° 57.8'N, and 21° 46.6'N as on HOT-31. XBTs were dropped at regular intervals during the transit from Station 3 to Station 5. Water samples were drawn for nutrients, chlorophyll and salinity at each of these stations. In addition, the flash fluorometer and the transmissometer were deployed on each of these casts.

The ship proceeded along the 300 m isobath from Station 5 to Kaena Point, to provide for calibration of the ADCP. Between Kaena Point and Snug Harbor the ship moved several miles offshore to pump the bilge. We arrived at Snug Harbor at approximately 0730.

Table 3.1: Summary of HOT Cruises, 1991

HOT	Ship	Depart	Return
23	R/V MOANA WAVE	1 February 1991	6 February 1991
24	R/V ALPHA HELIX	5 March 1991	9 March 1991
25	R/V ALPHA HELIX	8 April 1991	11 April 1991
26	R/V ALPHA HELIX	6 May 1991	10 May 1991
27	R/V ALPHA HELIX	3 June 1991	6 June 1991
28	R/V ALPHA HELIX	8 July 1991	12 July 1991
29	R/V ALPHA HELIX	7 August 1991	12 August 1991
30	R/V MOANA WAVE	16 September 1991	20 September 1991
31	R/V WECOMA	19 October 1991	24 October 1991
32	R/V WECOMA	4 December 1991	9 December 1991

Table 3.2: Ancillary Projects Supported by HOT

HOT	Principal Investigator	Institution / Program
23-32	Charles Keeling	Scripps Inst. of Oceanography
23-32	Steve Emerson	University of Washington
23-32	Paul Quay	University of Washington
23-32	Daniel Vaulot and Lisa Campbell	University of Hawaii

Table 3.3: University of Hawaii Cruise Personnel

	23	24	25	26	27	28	29	30	31	32
S. Chiswell, P. I.	■									
E. Firing, P. I.									■	
D. Karl, P. I.		■								
R. Lukas, P. I.			■		■					
C. Winn, P. I.			▒	■		■		■		■
I. Hamann, Scientist										▒
D. Hebel, Scientist	▒	▒	▒	▒	▒		■	▒	▒	▒
B. Popp, Scientist								▒		
L. Tupas, Scientist									▒	▒
A. Adam, Technician			▒							
C. Carrillo, Technician					▒	▒	▒	▒	▒	
K. Constantine, Technician										▒
T. Houlihan, Technician		▒	▒	▒	▒	▒	▒	▒	▒	▒
J. Kirshtein, Technician									▒	
U. Magaard, Technician	▒							▒		
R. Muller, Technician										▒
L. Pozzi, Technician		▒								
M. Rosen, Technician	▒	▒	▒	▒						
J. Snyder, Technician	▒	▒	▒	▒	▒	▒	▒	▒	▒	
F. Thomas, Technician										▒
J. Christian, Graduate Student	▒		▒				▒	▒	▒	▒
J. Constantinou, Graduate Student							▒		▒	
M. Cremer, Graduate Student				▒						
J. Dore, Graduate Student		▒	▒	▒	▒				▒	
L. Fujieki, Graduate Student					▒					
S. Kennan, Graduate Student	▒			▒		▒	▒			
E. Kotler, Graduate Student								▒		▒
S. Krothapalli, Graduate Student							▒	▒		
R. Letelier, Graduate Student	▒	▒	▒	▒		▒	▒		▒	
H. B. Liu, Graduate Student										▒
S. McCarthy, Graduate Student								▒	▒	▒
C. Moyer, Graduate Student					▒					
J. Pietrazek, Graduate Student										▒
T. Rust, Graduate Student								▒		
F. S.-Mandujano, Graduate Student	▒	▒			▒	▒	▒			
C. Sabine, Graduate Student	▒	▒			▒			▒		
D. Sadler, Graduate Student		▒				▒	▒		▒	▒
T. Shinoda, Graduate Student		▒		▒		▒				
M. Ver, Graduate Student	▒		▒							
	23	24	25	26	27	28	29	30	31	32

Shaded area = cruise participant Solid area = Chief Scientist

4. Results

4.1. Hydrography

4.1.1. 1991 CTD Profiling Data

Continuous profiles of temperature, salinity, oxygen and σ_θ (sigma theta) were collected at both Kahe Point and Station ALOHA. The data collected for Station ALOHA during 1991 are presented in Figures 6.1.1-18. The results of bottle determinations of oxygen, salinity and inorganic nutrients are also shown on these figures. In addition, stack plots of CTD temperature and salinity profiles for all 1000 m casts conducted at Station ALOHA are presented. The temperature, salinity and oxygen profiles obtained from the deep casts at Station ALOHA during 1991 are presented in Figures 6.1.19-21. In general, results are similar to those collected in 1988 through 1990 (Winn *et al.*, 1991).

4.1.2. Time-series Hydrography, 1988-1991

The hydrographic data collected during the first three years of HOT are presented in a series of contour plots (Figures 6.2.1-14). These figures show the data collected in 1991 within the context of the larger time-series database. The CTD data used in these plots are obtained by averaging the data collected by monthly burst sampling. Therefore, much of the variability which would otherwise be introduced by tidal and near inertial oscillations in the upper ocean has been removed. Figures 6.2.1 and 6.2.2 show the contoured time-series record for potential temperature and density in the upper 1000 dbar for all HOT cruises through 1991. Seasonal variation in temperature for the upper ocean is apparent in the maximum of near-surface temperature of about 26°C and the minimum of approximately 23°C. Oscillations in the depth of the 5°C isotherm below 500 m appear to be relatively large with displacements up to 75 m. The main pycnocline is observed between 100 and 600 dbar, with a seasonal pycnocline developing between June and December in the 50-100 dbar range (Figure 6.2.2). The cruise-to-cruise changes between February and July 1989 in the upper pycnocline illustrate that variability in density is not always resolved by our quasi-monthly sampling.

Figures 6.2.3-6 show the contoured time-series record for salinity in the upper 1000 dbar for all HOT cruises through 1991. The plots show both the CTD and bottle results plotted against pressure and σ_θ. Most of the differences between the contoured sections of bottle salinity and CTD salinity are due to the coarse distribution of bottle data in the vertical as compared to the CTD observations. Some of the bottles in Figure 6.2.6 are plotted at density values lower than the indicated sea surface density. This is due to surface density changing from cast to cast within each cruise, and even between the downcast and upcast during a single cast.

Surface salinity is variable from cruise-to-cruise, with no obvious seasonal cycle. The salinity maximum is generally found between 50 and 150 dbar, and within the potential density range 24-25 kg m^{-3}. A salinity maximum region extends to the sea surface in the latter part of 1988 and 1990, as indicated by the 35.2 psu contour reaching the surface. This contour nearly reaches the surface late in 1989. The maximum value of salinity in this feature is subject to short-

term variations of about 0.1 psu, which are probably due to the proximity of the HOT site to the region where this water is formed at the sea surface (cf. Tsuchiya, 1968). The salinity minimum is found between 400 and 600 dbar (26.35-26.85 kg m^{-3}). There is no obvious seasonal variation of this feature, but there are distinct periods of higher than normal minimum salinity in early 1989 and in the fall of 1990. These variations are related to the episodic appearance at the HOT site of energetic finestructure and submesoscale water mass anomalies (Lukas and Chiswell, 1991).

Figures 6.2.7 and 6.2.8 show contoured time-series for oxygen in the upper 1000 dbar at the HOT site. The oxygen data show a strong oxycline between 400 and 625 dbar (26.25-27.0 kg m^{-3}), and an oxygen minimum centered near 800 dbar (27.2 kg m^{-3}). During 1988-89, there was a persistent oxygen maximum near 300 dbar (25.75 kg m^{-3}), which appeared only weakly and intermittently during 1990. This feature reappears in 1991. The oxygen minimum exhibited some interannual variability as well, with values less than 30 µmol kg^{-1} appearing in the last half of 1989 and the first half of 1990 and then reappearing, less intensely, in 1991. The surface layer shows a seasonality in oxygen concentrations, with highest values in the winter. This roughly corresponds to the minimum in surface layer temperature (Figure 6.2.1). An oxygen maximum at about 100 m appears in the latter half of 1991.

Figures 6.2.9-14 show [nitrate+nitrite], phosphate and silica at the HOT site plotted against both pressure and potential density. The nitricline is located between about 200 and 600 dbar (25.75-27 kg m^{-3}; Figures 6.2.9-10). Most of the variations seen in these data are associated with vertical displacements of the density structure, and when [nitrate+nitrite] is plotted versus potential density, most of the contours are level. The upper reaches of the water column show considerable variability in density space. There is some indication of an annual cycle with a depression in both [nitrate+nitrite] and in phosphate at the top of the nutricline in the spring of 1990 and 1991. This variability is probably due to a combination of biological and physical processes at the base of the euphotic zone. A third exception is found during March-April 1990 when elevated levels of [nitrate+nitrite] are seen between 25.5 and 26.25 kg m^{-3}.

The phosphate (Figures 6.2.11 and 6.2.12) and silica (Figures 6.2.13-14) contour plots are, in general, similar to the [nitrate+nitrite] plot.

4.2. Fluorescence and Beam Transmission

Stack plots of the flash fluorescence and beam transmission results from each HOT cruise in 1991 are presented in Figures 6.3.1-10. Percent transmission data were collected starting on HOT-28. No transmission data was collected on HOT-31 because of equipment problems. *In situ* flash fluorescence profiles show the fluorescence maximum at the base of the euphotic zone, characteristic of the central North Pacific Ocean. Percent transmission profiles consistently show

increased attenuation due to increased particle load at depths shallower than 100 dbar. Both fluorescence and beam transmission profiles show the influence of internal waves when plotted against pressure, but remain relatively constant within a cruise when plotted in density space. However, both data sets show substantial cruise-to-cruise variability in these properties.

Representative fluorescence profiles for a period of three years are shown in Figures 6.3.11 and 12. In order to facilitate comparison, only night-time profiles are presented after normalization to the average density profile obtained from the CTD burst sampling for each cruise. Month-to-month variability in the average depth of the fluorescence maximum is apparent. This is particularly evident in year 3 where the depth of the fluorescence maximum appears to increase in mid to late summer (Figure 6.3.11). Beam transmission profiles for cruises in 1991 are shown in Figure 6.3.13. These profiles were collected at approximately midnight and were normalized to the average density profile obtained for each cruise. Although only a few monthly observations are available, beam transmission profiles show considerable variability on monthly time scales.

4.3. Biogeochemistry

Biogeochemical data collected during 1991 are summarized in Figures 6.4.1. In some cases the results from the first year of the program have been combined with the 1990 results to produce these figures.

4.3.1. Dissolved Inorganic Carbon and Titration Alkalinity

Dissolved inorganic carbon (DIC) and titration alkalinity measured in the upper 1000 dbar of the water column over the first 3 years of the time-series program are presented in Figures 6.4.1-5. Time-series of titration alkalinity and DIC in the mixed layer are presented in Figure 6.4.1. Titration alkalinity normalized to 35 ppt salinity averages approximately 2305 μ equivalents/kg and, within the precision of the analysis, appears to remain relatively constant at Station ALOHA. This observation is consistent with the results of Weiss *et al.* (1982) which predict that titration alkalinity normalized to salinity remains constant in both the North and South Pacific Subtropical Gyres. In contrast to titration alkalinity, the concentration of dissolved inorganic carbon varies annually. DIC in the mixed layer is highest in winter and lowest in summer. This oscillation is consistent with an exchange of carbon dioxide across the air-sea interface driven by temperature dependent changes in mixed layer pCO_2.

Figures 6.4.2-5 show contoured time-series for DIC and titration alkalinity in the upper 1000 dbar for all HOT cruises through 1991. DIC, whether normalized to 35 ppt salinity or not, remains relatively constant below 100 dbar with time (Figures 6.4.2-3). Titration alkalinity (Figure 6.4.4) shows considerable time dependent variability around the shallow salinity maximum, centered at about 125 dbar, and the salinity maximum, centered at about 400 dbar. These variations are largely associated with variability in salinity at these depths and disappear when alkalinity is normalized to 35 ppt (Figure 6.4.5). Titration alkalinity normalized to 35 ppt

salinity is elevated in surface waters in spring of 1990. This corresponds to the appearance of mesoscale eddies at Station ALOHA at this time (Winn *et al.*, 1991).

4.3.2. Low Level Nutrient Profiles

Because euphotic zone nutrient concentrations are at or below autoanalyzer detection limits particularly for nitrogen and phosphorus, these data provide little insight into the temporal variability in upper reaches of the water column. Figures 6.4.6 and 6.4.7 show the profiles obtained from our low level nutrient analyses in 1991. Low level [nitrate+nitrite] measurements were initiated on HOT-26. Low level phosphate profiles are available for all cruises in 1991. At depths shallower than 100 dbar, phosphate is typically less than 150 nmol kg^{-1}. Phosphate concentrations appear to vary by at least 3-fold in this region (Figure 6.4.6). Concentrations of [nitrate+nitrite] between 0-100 dbar at less than 100 dbar are always less than 20 nmol kg^{-1} and are often less the 5 nmol kg^{-1} (Figure 6.4.7).

4.3.3. Pigments

A contour plot of chlorophyll *a* concentrations measured by using standard fluorometric techniques from 0 to 200 dbar over the first three years of the program is shown in Figure 6.4.8. As expected a chlorophyll maximum with concentrations up to 300 µg m^{-3} is observed at approximately 100 dbar. No obvious seasonal cycle is observed in the chlorophyll maximum layer. The chlorophyll concentrations at depths shallower than 50 dbar appear to have steadily decreased from January 1989 to mid 1990. There is some indication that the chlorophyll concentrations in the surface waters are increasing again toward the end of 1991.

4.3.4. Particulate Carbon, Nitrogen and Phosphorus

Particulate carbon (PC), nitrogen (PN) and phosphorus (PP) in the surface ocean over the first three years of the program are shown in Figures 6.4.9-11. PC varies between 1.6 - 3.0 µmol kg^{-1}, PN between 0.15 -0.45 µmol kg^{-1} and PP between 12 - 30 nmol kg^{-1} in the upper 50 dbar of the water column. PC and PN show a clear annual cycle with peaks in particulate concentrations in summer of 1989, 1990 and 1991.

4.4. Biogeochemical Rate Measurements

4.4.1. Primary Productivity

The results of the carbon-14 incubations and pigment determinations for samples collected on Go-Flo casts in 1991 are presented in Tables 4.4.1 and 4.4.2. Table 4.4.1 presents the primary production and pigment measurements made at individual depths on all 1991 cruises. Table 4.4.2 presents integrated values for irradiance, pigment concentration and primary production rates. The pigment concentrations and carbon-14 incorporation rates reported are the average of triplicate determinations. Integrated primary production rates measured over all three years of the program are shown in Figure 6.5.1 in order to place the 1991 results within the context of the time-series data set.

Table 4.4.1: Primary Production and Pigment Summary

Cruise[a]	Depth (m)	Mean Chl *a* [b] mg m^{-3}	Std. Dev. Chl *a* [c] mg m^{-3}	Mean Phaeo[b] mg m^{-3}	Std. Dev. Phaeo[c] mg m^{-3}	Light[d] mg C m^{-3} Rep #1	Light[d] mg C m^{-3} Rep #2	Light[d] mg C m^{-3} Rep #3	Dark[d] mg C m^{-3} Rep #1	Dark[d] mg C m^{-3} Rep #2	Dark[d] mg C m^{-3} Rep #3
23	5	0.068	0.001	0.015	0.001	6.73	4.71		0.08	0.06	0.11
23	25	0.059	0.005	0.015	0.003	4.73	6.50	5.19	0.07	0.07	0.08
23	45	0.128	0.027	0.052	0.001	6.11	7.22	5.67	0.09	0.08	0.08
23	75	0.102	0.001	0.037	0.006	2.58	2.62		0.07	0.08	0.07
23	100	0.139	0.002	0.022	0.004	0.94	0.94	1.02	0.05	0.04	0.06
23	125	0.129	0.016	0.192	0.003	0.57	0.55	0.53	0.03	0.04	0.03
23	150					0.07	0.07	0.06	0.04	0.01	0.03
23	175					0.01	0.05	0.00	0.03	0.03	0.04
25	5	0.088	0.002	0.068	0.001	5.83	4.25		0.09	0.11	0.09
25	25	0.090	0.001	0.070	0.002	6.03	6.30	7.63	0.11	0.11	0.10
25	45	0.091	0.003	0.082	0.004	5.47	4.84	4.96	0.13	0.13	0.14
25	75	0.131	0.002	0.099	0.007	2.44	3.00	3.12	0.15	0.15	0.13
25	100	0.187	0.006	0.216	0.004	1.62	1.50	1.60	0.09	0.08	0.07
25	125	0.228	0.003	0.390	0.012	0.75	0.71	0.71	0.05	0.05	0.07
25	150	0.063	0.001	0.162	0.005	0.11	0.11	0.11	0.04	0.04	0.04
25	175	0.042	0.003	0.076	0.009	0.04	0.04	0.05	0.03	0.03	0.03
26	5	0.092	0.002	0.068	0.001	11.32		11.45	0.13	0.14	0.14
26	25	0.110	0.001	0.070	0.002	11.11	10.91	10.05	0.26	0.14	0.19
26	45	0.107	0.013	0.082	0.004	7.86	7.32	6.72	0.16	0.16	0.16
26	75	0.142	0.004	0.099	0.007	4.27	4.53	4.04	0.09	0.11	0.13
26	100	0.181	0.001	0.216	0.004	2.12		2.39	0.07	0.07	0.08
26	125	0.218	0.002	0.390	0.012	1.67	1.75	1.67	0.05	0.05	0.05
26	150	0.141	0.005	0.162	0.005	0.28		0.32	0.06	0.05	0.04
26	175	0.103	0.002	0.076	0.009		0.07	0.06	0.03	0.04	0.04
27	5	0.101		0.064			3.45	8.97	0.23	0.26	0.12
27	25	0.099	0.005	0.066	0.007	8.89	8.18		0.12	0.14	0.11
27	45	0.101		0.078		6.96	7.24	6.95	0.12	0.10	0.09
27	75	0.119		0.087		3.09	2.98	3.54	0.10	0.13	0.10
27	100	0.164	0.001	0.152	0.005	1.49	1.32	1.56	0.13	0.11	0.11
27	125	0.209	0.018	0.365	0.021	0.81	0.82	0.71	0.07	0.05	0.04
27	150	0.090		0.234				0.17	0.06	0.05	0.06
27	175	0.021		0.040			0.04	0.03	0.06	0.07	0.05

Table 4.4.1: (continued)

Cruise[a]	Depth (m)	Mean Chl *a* [b] mg m^{-3}	Std. Dev. Chl *a* [c] mg m^{-3}	Mean Phaeo[b] mg m^{-3}	Std. Dev. Phaeo[c] mg m^{-3}	Light[d] mg C m^{-3} Rep #1	Light[d] mg C m^{-3} Rep #2	Light[d] mg C m^{-3} Rep #3	Dark[d] mg C m^{-3} Rep #1	Dark[d] mg C m^{-3} Rep #2	Dark[d] mg C m^{-3} Rep #3
28	5	0.066	0.008	0.059	0.006	3.65	4.35	5.76	0.02	0.14	0.13
28	25	0.064	0.002	0.063	0.002	6.11	6.40	6.70	0.12	0.13	0.13
28	45	0.087	0.002	0.069	0.001	5.00	4.13	3.59	0.16	0.16	0.15
28	75	0.136	0.005	0.138	0.003	3.43	3.00	4.09	0.13	0.13	0.15
28	100	0.224	0.016	0.209	0.008	1.95	1.87	1.94	0.09	0.09	0.09
28	125	0.198	0.020	0.431	0.008	0.87	0.91	0.81	0.03	0.04	0.03
28	150	0.064	0.012	0.202	0.026	0.14	0.14	0.15	0.02	0.03	0.02
28	175	0.072	0.003	0.128	0.008	0.08	0.07		0.05	0.06	0.05
29	5	0.070	0.003	0.070	0.010	6.96	6.61	7.30	0.12	0.20	0.12
29	25	0.067	0.007	0.064	0.003	7.38	7.32	5.54	0.11	0.09	0.09
29	45	0.074	0.003	0.070	0.006	6.15	4.82		0.16	0.13	0.13
29	75	0.146	0.002	0.120	0.003	3.11		3.19	0.10	0.16	0.13
29	100	0.198	0.004	0.204	0.006	1.28	1.24	1.29		0.08	
29	125	0.195	0.008	0.405	0.013	0.71	0.83	0.67	0.04	0.04	0.04
29	150	0.079	0.004	0.221	0.003	0.14	0.18	0.14			
29	175	0.026	0.002	0.096	0.006	0.07	0.05	0.05	0.04	0.06	0.05
30	5	0.074		0.055		7.41		7.54	0.18	0.19	0.18
30	25	0.069		0.055		8.31	8.01	7.16	0.17	0.19	0.17
30	45	0.085		0.070			6.69	5.17	0.17	0.16	0.19
30	75	0.169		0.146		3.43		3.67	0.14	0.16	0.11
30	100	0.224		0.352		1.40	1.46	1.56	0.04	0.06	0.04
30	125	0.152		0.459		0.53	0.52	0.55	0.07	0.05	0.06
30	150	0.075		0.223		0.03	0.07	0.07	0.05	0.05	0.04
30	175	0.082		0.159		0.11	0.10	0.11	0.07	0.08	0.08
31	5	0.076	0.008	0.067	0.007	9.11		10.07	0.18	0.16	0.14
31	25	0.079	0.005	0.059	0.003	6.87	6.39	6.10	0.13		
31	45	0.091	0.002	0.092	0.007	4.72	5.48	5.50	0.20	0.18	0.18
31	75	0.201	0.004	0.209	0.010	2.67	2.37	2.81	0.10	0.11	0.11
31	100	0.287	0.007	0.405	0.014	0.91	0.87	0.96	0.06	0.07	0.05
31	125	0.109	0.010	0.300	0.008	0.23	0.20	0.22	0.03	0.03	0.03
31	150	0.073	0.002	0.195	0.008	0.05	0.05	0.06	0.03	0.02	0.04
31	175	0.081	0.014	0.058	0.014	0.15	0.14		0.16	0.07	0.15

Table 4.4.1: (continued)

Cruise[a]	Depth (m)	Mean Chl *a* [b] mg m^{-3}	Std. Dev. Chl *a* [c] mg m^{-3}	Mean Phaeo[b] mg m^{-3}	Std. Dev. Phaeo[c] mg m^{-3}	Light[d] mg C m^{-3} Rep #1	Light[d] mg C m^{-3} Rep #2	Light[d] mg C m^{-3} Rep #3	Dark[d] mg C m^{-3} Rep #1	Dark[d] mg C m^{-3} Rep #2	Dark[d] mg C m^{-3} Rep #3
32	5	0.124		0.070		5.25	4.72	5.35	0.09	0.12	0.11
32	25	0.107	0.004	0.060	0.004		5.40		0.12	0.11	0.10
32	45	0.108		0.083		3.55	4.72	4.31	0.10	0.11	0.11
32	75	0.182		0.172		1.85	2.23	1.52	0.08	0.08	0.05
32	100	0.215	0.006	0.399	0.010	0.75	0.75	0.75	0.04	0.05	0.04
32	125	0.127	0.008	0.287	0.019	0.19	0.19	0.16	0.03	0.04	0.04
32	150	0.044		0.122		0.05	0.05	0.05	0.02	0.04	0.03
32	175	0.057		0.102		0.05	0.04	0.04	0.04	0.03	0.05

[a]No data from HOT-24. All samples are from daylight *in situ* incubations (see text).

[b]Average of 2 or more replicates

[c]Std. Dev. (standard deviation) computed only at depths with three replicate subsamples

[d]Incorporation during *in situ* incubation period. Incubation times are approximations only (i.e., half day or full day). Actual incubation time for each measurement is given in Table 4.4.2.

Table 4.4.2: *In Situ* Primary Production and Pigment Summary
Integrated Values 0-200 m

Cruise	Incident Irradiance ($E\ m^{-2}\ d^{-1}$) cosine[a]	hemi[b]	Pigments ($mg\ m^{-2}$) Chl *a*	Phaeo	Incubation Duration (hrs)	Carbon Assimilation Rates ($mgC\ m^{-2}\ d^{-1}$) light	dark[c]
23	37.8	87.0	17.50	12.50	12.0	465	20
24	44.7	ND[d]	ND	ND	ND	ND	ND
25	47	ND	24.21	30.14	13.3	476	29
26	51.5	ND	28.58	30.14	13.1	793	33
27	54.7	89.5	21.40	26.41	15.3	589	28
28	55.7	ND	24.00	33.46	15.2	474	27
29	52.1	90	22.53	32.39	13.3	518	31
30	48.5	88.9	24.55	39.03	14.0	569	34
31	40.4	109	24.29	34.17	13.2	509	29
32	32.6	91.5	22.75	31.78	12.3	366	23

[a]cosine collector
[b]hemispherical collector
[c]extrapolated to daily rates
[d]ND = not determined

Variability in rates of primary production, integrated over the euphotic zone during the first three years of the time-series program, appear to be stochastic with no evidence of a seasonal cycle. Measured rates ranged between approximately 150 and 1100 mgC m^{-2} day^{-1} with the highest rate being observed in August 1989. This high rate of primary production coincided with a cyanobacterial bloom observed in surface waters near Station ALOHA on HOT cruise #15 (Karl *et al*., 1992). This variability, with a range of almost a factor of 7, is surprisingly large. However, the majority of the primary production estimates were between 250 and 600 mgC m^{-2} day^{-1}, and the average rate of primary production was approximately 450 mgC m^{-2} day^{-1}. Although this value is higher than historical measurements for the central ocean basins (Ryther, 1969), it is consistent with more recent measurements using modern methodology (Martin *et al*., 1987; Knauer *et al*., 1990).

4.4.2. Particle Flux

Particulate carbon (PC), nitrogen (PN), phosphorus (PP) and mass fluxes (150, 300 and 500 m) are presented in Table 4.4.3 and fluxes at 150 m for the first 3 years of the program are shown in Figures 6.5.2-5.

Table 4.4.3: Station ALOHA Sediment Trap Flux Data

		Carbon			Nitrogen			Phosphorus			Mass Flux		
Cruise	Depth (m)	Mg m^{-2} day^{-1}	St. Dev.[a]	n	mg m^{-2} day^{-1}	St. Dev.[a]	n	mg m^{-2} day^{-1}	St. Dev.[a]	n	mg m^{-2} day^{-1}	St. Dev.[a]	n
23	150	17.7	2.2	6	2.8	0.2	6	0.24	0.04	3	28.6	3.7	3
23	300	10.6	1.3	6	1.4	0.3	6	0.18	0.05	2	19.4	2.8	3
23	500	9.2	3.3	6	1	0.4	6	0.17		1	10.1	3.1	3
24	150	17.9	6.2	5	2.9	1.1	5	0.30	0.03	3	46.5	2.2	2
24	500	10.4	1.9	3	0.9	0.6	3	0.22	0.14	2	43.3	23.3	2
26	150	41.5	6	5	6.4	1	5	0.65	0.11	3	124.9	49.1	3
26	300	11.9	3.2	6	1.5	0.3	6	0.16	0.03	3	44.6	11.6	3
26	500	11.7	6.4	6	1.4	0.3	6	0.15	0.03	3	26.9	7.7	3
27	150	49.5	3.7	5	7.9	0.7	5	0.71	0.08	3	90.0	3.0	3
27	300	14.5	3.2	6	1.5	0.4	6	0.13	0.01	3	27.2	5.8	3
27	500	9	1.6	6	1	0.3	6	0.08	0.02	3	20.3	5.3	3
28	150	22.3	1.5	3	3.7	0.5	3	0.44	0.28	3	46.1	34.3	3
28	300	15.8	5.5	5	2.2	0.4	5	0.16	0.05	3	13.6	5.0	3
28	500	8.8	1.9	6	0.8	0.1	5	0.08	0.02	2	22.6	11.4	3
29	150	30.2	4.3	6	5.4	0.9	6	0.45	0.08	3	70.3	13.7	3
29	300	27	9.9	6	3.8	1.3	6	0.24	0.03	3	46.8	19.5	3
29	500	14.3	4.5	6	1.7	0.5	6	0.11	0.01	3	40.1	1	3
30	150	26.8	5.5	6	4.6	0.7	6	0.49	0.11	3	72	25.3	3
30	300	16.6	3.3	6	2.3	0.1	6	0.21	0.05	3	44.4	14.2	3
30	500	7.4	1.7	5	1.2	0.1	5	0.36	0.20	3	80.7	13.6	3
31	150	13.4	2.2	6	2.2	0.3	6	0.30	0.05	3	59.3	14.8	3
31	300	8.5	6	6	1.5	0.3	6	0.10	0.04	3	30.1	6.7	3
31	500	16.1	1.5	6	1.5	0.3	6	0.13	0.04	3	24.8	2.3	3
32	150	22	2.3	6	3.3	0.4	6	0.26	0.06	3	42.4	4.3	3
32	300	12.5	1.4	6	1.8	0.2	6	0.04	0.00	3	29.7	5.7	3
32	500	8.3	2.9	6	0.8	0.3	6	0.02	0.04	2	26.9	13.7	3

[a]When n □ 3, the variability is expressed as standard deviation (St. Dev.); when n = 2 variability is expressed as the difference

Carbon flux displays a clear annual cycle with peaks in both the early spring and in the late summer months (Figure 6.5.2). The magnitude of particle flux varies by a factor of approximately 3. With the exception of anomalous PP fluxes measured on the first two HOT cruises, temporal variability in PN, PP and mass flux show similar temporal trends, and also vary between cruises by about a factor of three (Figures 6.5.2-5). Elemental ratios of carbon and nitrogen at 150 m are typically between 6 - 10 at 150 m and show no obvious temporal pattern. These particle flux measurements and elemental ratios are consistent with those measured in the central North Pacific Ocean by the VERTEX program (Martin *et al*., 1987). Nitrogen flux at 150 m, as a percent of photosynthetic nitrogen assimilation (calculated from carbon-14 primary production values assuming a C:N ratio [by atoms] of 6.6) ranges between 2 - 10%. The average value (approximately 6.5%) is consistent with the estimate of new production for the oligotrophic central gyres made by Eppley and Peterson (1979) and with field data from the VERTEX program (Knauer *et al*., 1990).

Average fluxes of PC, PN, PP and mass at 150, 300 and 500 m from the first three years of the time-series observations are shown in Figures 6.5.6-9. For carbon, nitrogen, phosphorus and total mass, the flux declines rapidly with depth, presumably due to the rapid dissolution and remineralization of organic particles sinking through the water column. The flux of carbon at 500 m is less than 50% of the flux at 150 m.

4.5. ADCP Measurements

An overview of the shipboard ADCP data is given by the plots of reference layer velocity versus time (Figures 6.6.1-10), the velocity as a function of time and depth (Figures 6.6.11a-22a) and the velocity as a function of position and depth (Figures 6.6.11b-22b). As during the previous two years, currents were highly variable from cruise to cruise and within each cruise. Mean currents near the surface on station were southeast on HOT-23, north on HOT-24, east on HOT-25, -26 and -32, southwest on HOT-27, -28 and -30, north on HOT-29 and northeast on HOT-31.

4.6. Meteorology

The meteorological data collected by the HOT program include atmospheric pressure, sea-surface temperature and wet and dry bulb air temperature. These data are presented in Figures 6.7.1-3. As described by Winn *et al.* (1991), parameters show evidence of annual cycles, although the daily and weekly ranges are nearly as high as the annual range for some variables. Wind speed and direction are also collected on HOT cruises. These data, as well as the simultaneous measurements of these parameters at NDBC buoy #51001 (Figure 1.1) during the

period covered by this report, are presented in Figures 6.7.4-13.

4.7. Light Measurements

Integrated irradiance measurements made with the on-deck cosine collector on days that primary production experiments were conducted are presented in Table 4.2.

4.8. NDBC Buoy and Shipboard Observations

An NDBC buoy is located about 400 km west of Station ALOHA. This buoy collects hourly observations of air temperature, sea surface temperature, atmospheric pressure, wind velocity and significant wave height. Because continuous observations of atmospheric and surface ocean conditions may be valuable in the interpretation of our time-series observations, we have examined the coherence in the data sets collected at hourly intervals at the buoy and at approximately monthly intervals on the time-series cruises. In order to examine the coherence in these sets of observations, meteorological data collected on HOT cruises 14-30 (years 2 and 3) were compared to buoy data collected over the same time interval. Both air temperature time-series records show an annual cycle, and a high correlation is observed between the buoy and cruise data (Figure 6.6.22). The root mean square (RMS) of the residuals is approximately 0.7°C. A close relationship is displayed between sea-surface temperatures (Figure 6.6.22), with a residual RMS of only 0.34°C. Atmospheric pressure shows two distinct relationships (Figure 6.6.24). The points with higher pressures at Station ALOHA were obtained on the 4 SSP Kaimalino cruises conducted in 1990. Separate linear fits to each relationship produce high correlation coefficients and a RMS difference of about 1 mbar. These data show that the pressures measured on the R/V KAIMALINO are off by about 7 mbar with respect to the buoy data. Wind speed measured by the buoy and on the HOT cruises show a relatively weak correlation with a correlation coefficient of 0.66 and a residual RMS of more than 2 m/sec (Figure 6.6.24). Wind direction is slightly better, with a correlation coefficient of nearly 0.8 and an RMS of about 35 degrees (Figure 6.6.25). Cross correlations between buoy data and ship-based measurements of air temperatures, sea-surface temperatures and atmospheric pressure were used to check for existence of a time delay between these datasets. No lagged correlations between these parameters were observed. A time delay was observed in wind direction during HOT-23 (Figure 6.6.26) where buoy winds lead the ship observations by 2 hours. This lag was not observed in wind speed. We conclude from these analyses, that buoy data can be used to get useful estimates of air temperature, sea-surface temperature and atmospheric pressure at Station ALOHA.

5. References

Armstrong, F.A.J., P.M. Williams and J.D.H. Strickland, 1966: Photo-oxidation of organic matter in sea water by ultraviolet radiation, analytical and other applications. *Nature*, **211**, 481-483.

Bidigare, R.R., J. Marra, T.J. Dickey, R. Iturriaga, K.S. Baker, R.C. Smith and H. Pak, 1990: Evidence for phytoplankton succession and chromatic adaptation in the Sargasso Sea during Spring 1985. *Marine Ecology Progress Series*, **60**, 113-122.

Bradshaw, A.L. and P.G. Brewer, 1988: High precision measurements of alkalinity and total carbon dioxide in seawater by potentiometric titration: Presence of unknown protolytes? *Marine Chemistry,* **23**, 69-86.

Carpenter, J.H., 1965: The accuracy of the Winkler method for dissolved oxygen analysis. *Limnology and Oceanography*, **10**, 135-140.

Chiswell, S.M., 1991: Dynamic response of CTD pressure sensors to temperature. *Journal of Atmospheric and Oceanic Technology*, **8**, 659-668.

Chiswell, S.M., E. Firing, D. Karl, R. Lukas, C. Winn, 1990: Hawaii Ocean Time-series Program Data Report 1, 1988-1989. School of Ocean and Earth Science and Technology Report 1, University of Hawaii, 269 pp.

Cox, R.D., 1980: Determination of nitrate at the parts per billion level by chemiluminescence. *Analytical Chemistry*, **52**, 332-335.

Dickson, A., 1993: pH buffers for sea water media based on the total hydrogen ion concentration scale. *Deep-Sea Research*, **40**, 107-118.

Edmond, J.M., 1970: High precision determination of titration alkalinity and total carbon dioxide content of seawater by potentiometric titration. *Deep-Sea Research*, **17**, 737-750.

Eppley, R.W. and B.J. Peterson, 1979: Particulate organic matter flux and planktonic new production in the deep ocean. *Nature*, **282**, 677-680.

Garside, C., 1982: A chemiluminescent technique for the determination of nanomolar concentrations of nitrate and nitrite in seawater. *Marine Chemistry*, **11**, 159-167.

Hansson, I., 1973: A new set of pH-scales and standard buffers of sea water. *Deep-Sea Research,* **20**, 479-491.

Karl, D. M., R. Letelier, D. V. Hebel, D. F. Bird and C. D. Winn, 1992: *Trichodesmium* blooms and new nitrogen in the North Pacific gyre. In: E. J. Carpenter et al. (eds.), *Marine Pelagic Cyanobacteria: Trichodesmium and Other Diazotrophs*, pp. 219-237. Kluwer Academic Publishers, Netherlands.

Karl, D.M. and G. Tien, 1992: MAGIC: A sensitive and precise method for measuring dissolved phosphorus in aquatic environments. *Limnology and Oceanography*, **37**, 105-116.

Karl, D.M., C.D. Winn, D.V.W. Hebel and R. Letelier, 1990: Hawaii Ocean Time-series Program Field and Laboratory Protocols, September 1990.

Knauer, G.A., D.G. Redalje, W.G. Harrison and D.M. Karl, 1990: New production at the VERTEX time-series site. *Deep-Sea Research*, **37**, 1121-1134.

Lukas, R. and S. Chiswell, 1991: Submesoscale water mass variations in the salinity minimum of the north Pacific near Hawaii. *WOCE Notes*, **3(1)**, 1,6-8.

Martin, J.H., G.A. Knauer, D.M. Karl and W.W. Broenkow, 1987: VERTEX: Carbon cycling in the northeast Pacific. *Deep-Sea Research*, **34**, 267-285.

Owens, W.B. and Millard, R.C., 1985: A new algorithm for CTD oxygen calibration. *Journal of Physical Oceanography*, **15**, 621-631.

Press, W., B. Flannery, S. Teokolsky, W. Vetterling, 1988: Numerical recipes in C. Cambridge U. Press, 735 pp.

Ryther J. H., 1969: Photosynthesis and fish production in the sea: The production of organic matter and its conversion to higher forms of life vary through the world ocean. *Science*, **166**, 72-76.

Strickland, J.D.H. and T.R. Parsons, 1972: A practical handbook of seawater analysis. Fisheries Research Board of Canada, 167 pp.

Tsuchiya, M., 1968: Upper waters of the intertropical Pacific Ocean. *Johns Hopkins Oceanographic Studies*, **4**, 49 pp.

UNESCO, 1981: Tenth report of the joint panel on oceanographic tables and standards. *UNESCO Technical Papers in Marine Science*, No. 36, UNESCO, Paris.

Walsh, T.W., 1989: Total dissolved nitrogen in seawater: a new high-temperature combustion method and a comparison with photo-oxidation. *Marine Chemistry*, **26**, 295-311.

Weiss, R.F., R.A. Jahnke and C.D. Keeling, 1982: Seasonal effects of temperature and salinity on the partial pressure of CO_2 in seawater. *Nature*, **300**, 511-513.

Winn, C., S.M. Chiswell, E. Firing, D. Karl, R. Lukas: Hawaii Ocean Time-series Program Data Report 2, 1990. School of Ocean and Earth Science and Technology Report 2, University of Hawaii, 175 pp.

6. Figures
6.1. CTD Profiles

Figures 6.1.1a-10a: CTD and nutrient data collected at Station ALOHA. Upper left panel: Temperature, salinity, oxygen and density (σ_{θ}) as a function of pressure for WOCE deep cast. Salinity and oxygen water bottle data are also plotted. Upper right panel: Nutrients ([NO_3 + NO_2], PO_4 and silica) and oxygen as a function of potential temperature for all water samples. Lower left panel: CTD temperature and salinity profiles plotted as a function of pressure. Lower right panel: Salinity and oxygen from CTD and water samples plotted as a function of potential temperature.

Figures 6.1.1b-10b: Stack plots of temperature and salinity against pressure to 1000 dbar for all CTD casts. Upper panel: Potential temperature versus pressure to 1000 dbar. Lower panel: Salinity versus pressure to 1000 dbar.

Figure 6.1.11: 1991 potential temperature profiles. Upper panel: Potential temperature versus pressure for all deep casts in 1991. Lower panel: Potential temperature for all deep casts in 1991 plotted from 2500 dbar.

Figure 6.1.12: 1991 temperature-salinity plots. Upper panel: Potential temperature versus salinity for all deep casts collected during 1991. Lower panel: Potential temperature versus density on same casts in the 1-5°C range.

Figure 6.1.13: 1991 oxygen profiles. Upper panel: Oxygen values derived from calibrated CTD sensor data versus potential temperature for all deep casts collected during 1991. Lower panel: Oxygen versus potential temperature for 1991 deep casts within the 1-5°C range.

Station ALOHA HOT 23

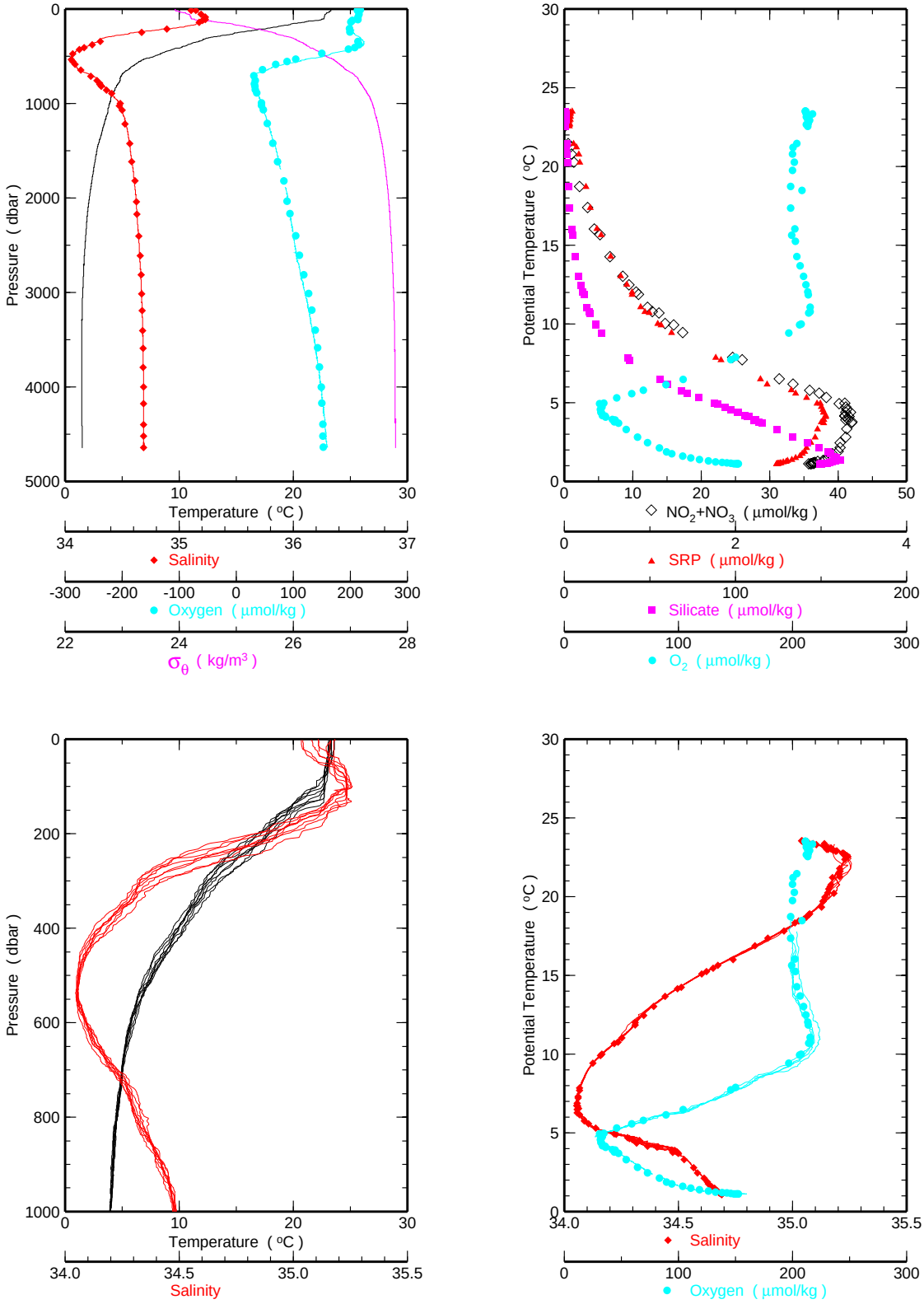

Figure 6.1.1a

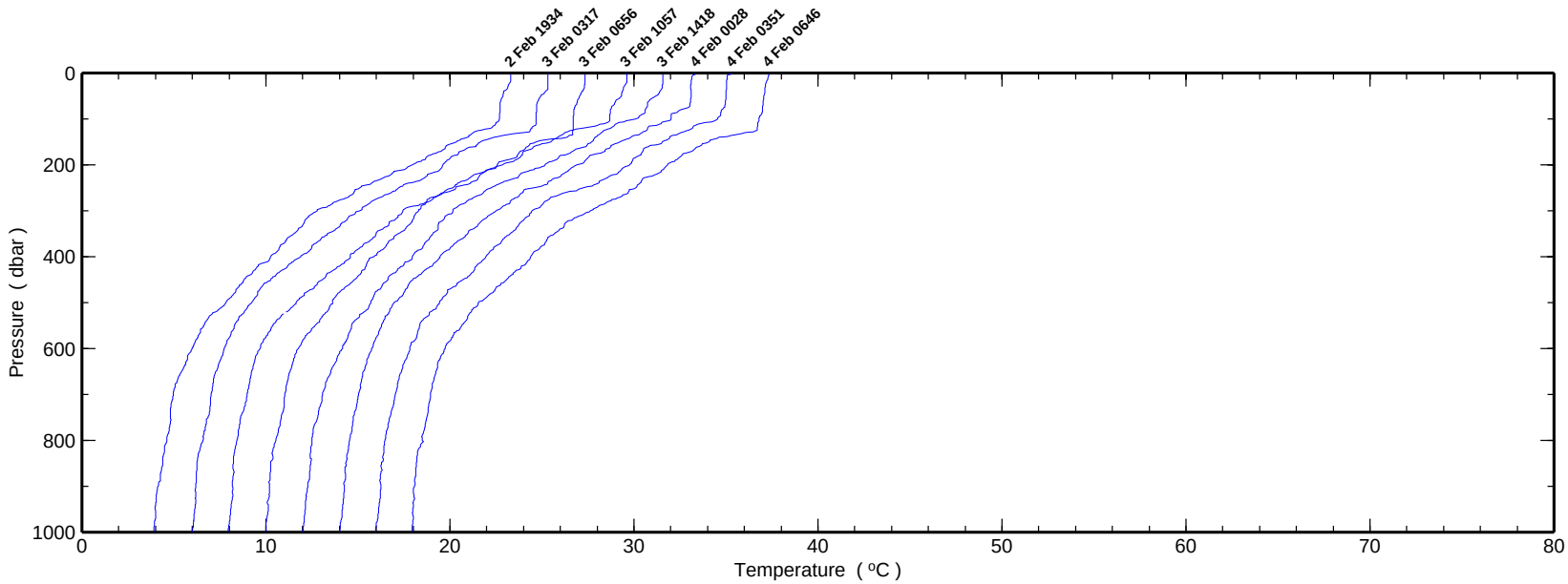

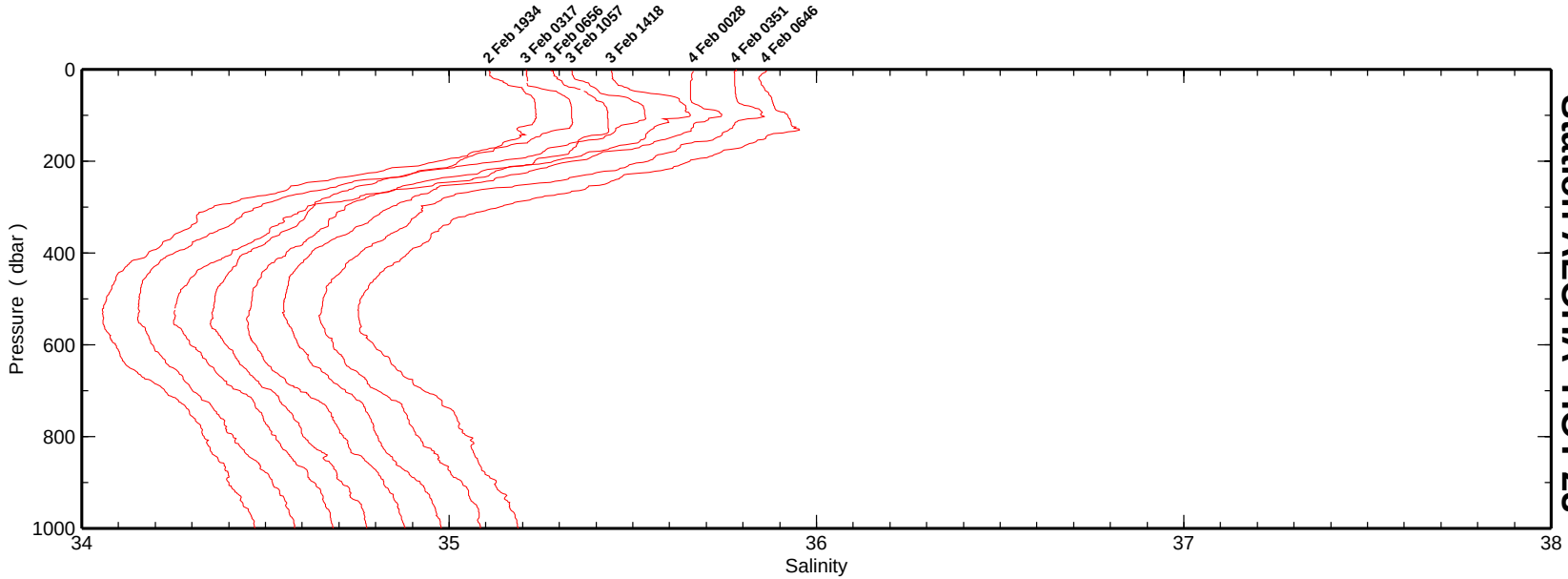

Figure 6.1.1b

Station ALOHA HOT 23

Station ALOHA HOT 24

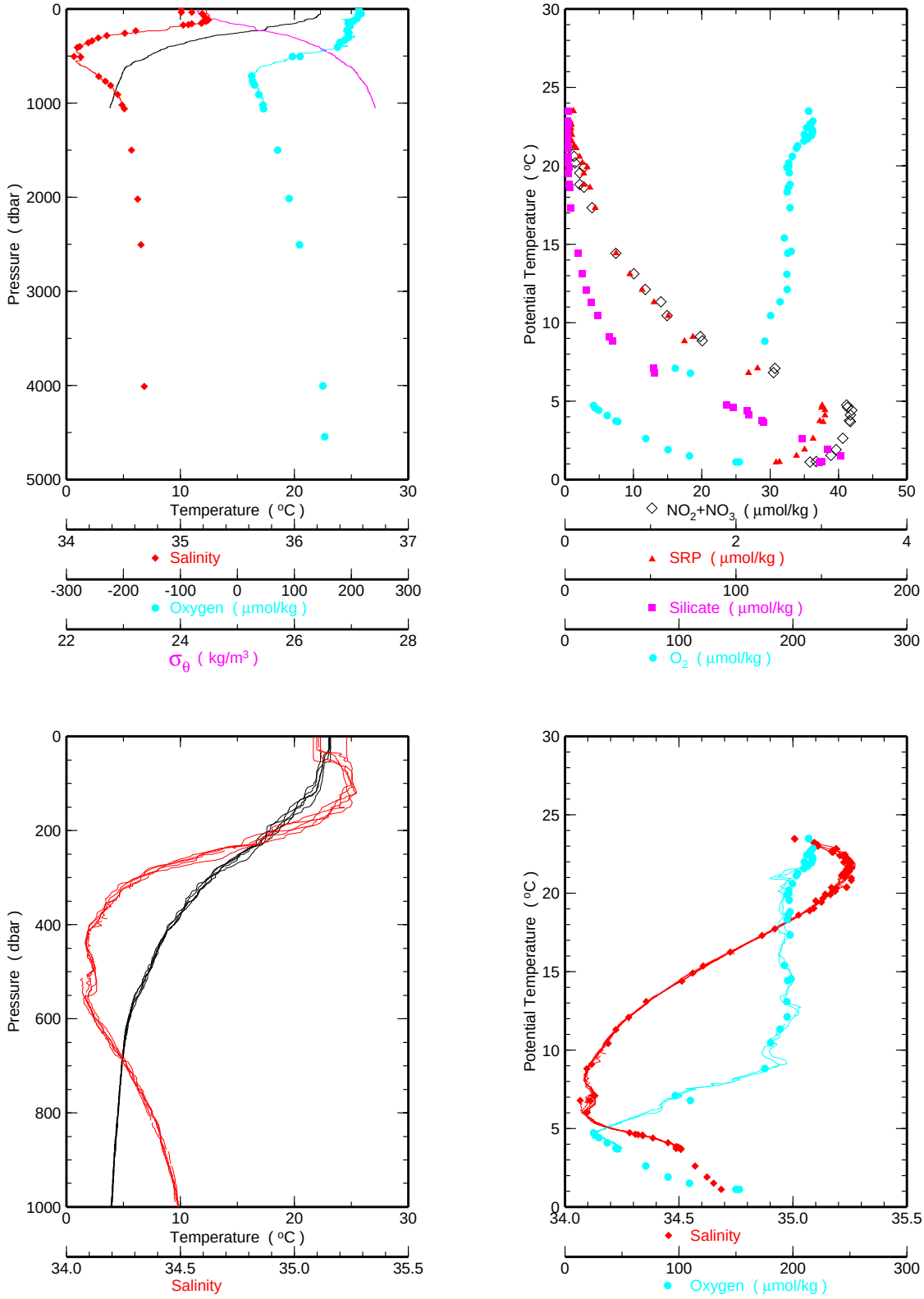

Figure 6.1.2a

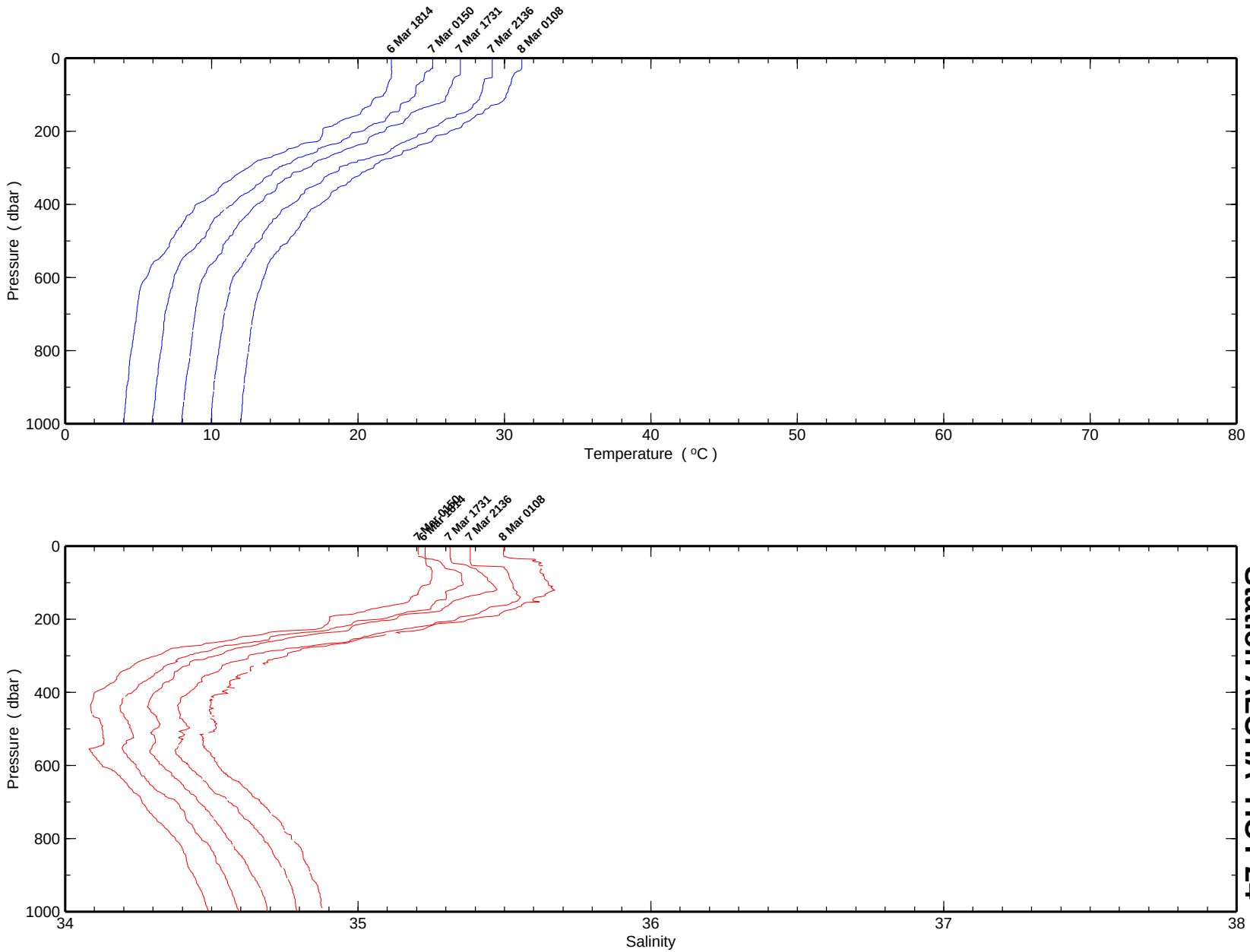

Figure 6.1.2b

Station ALOHA HOT 24

Station ALOHA HOT 25

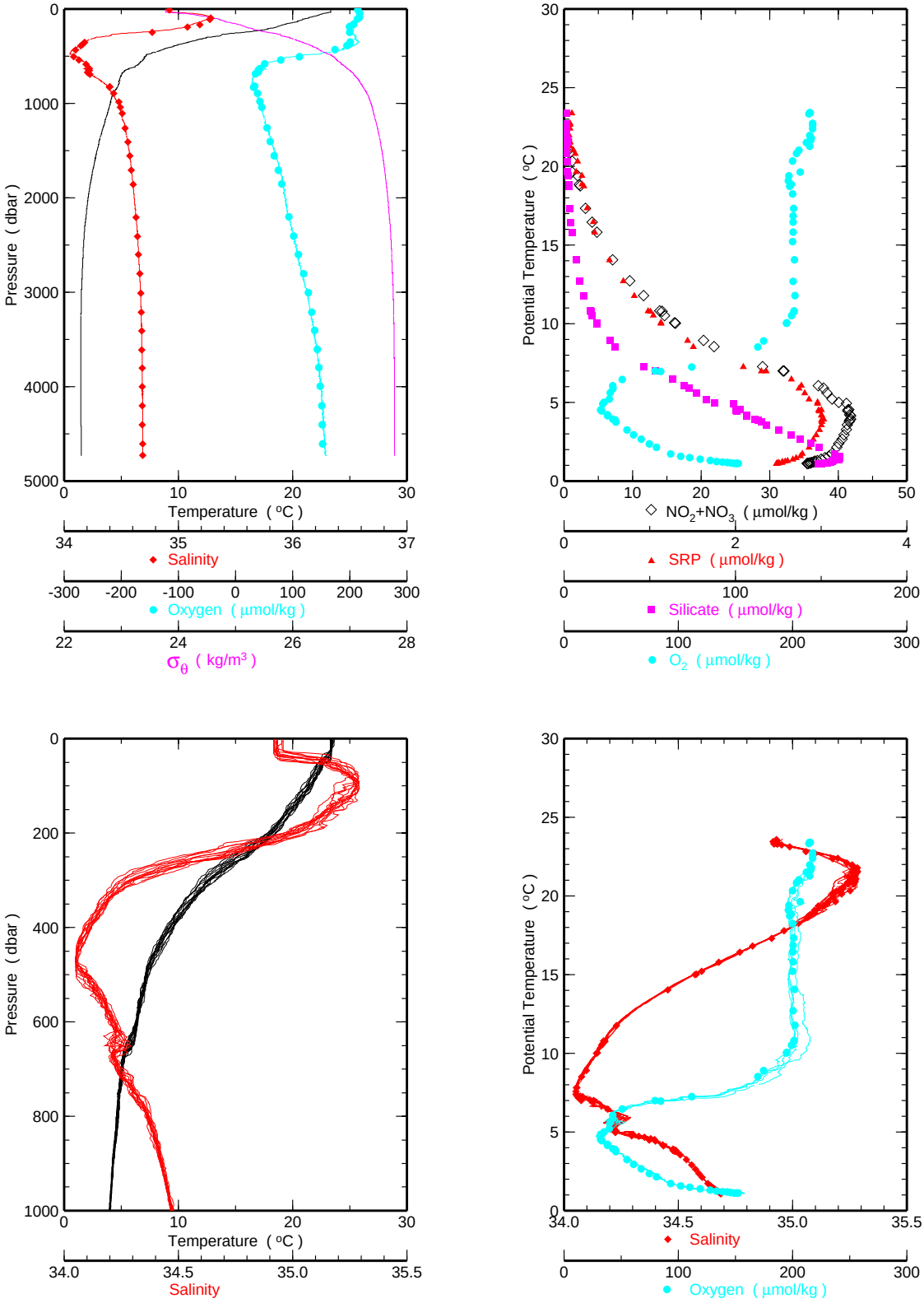

Figure 6.1.3a

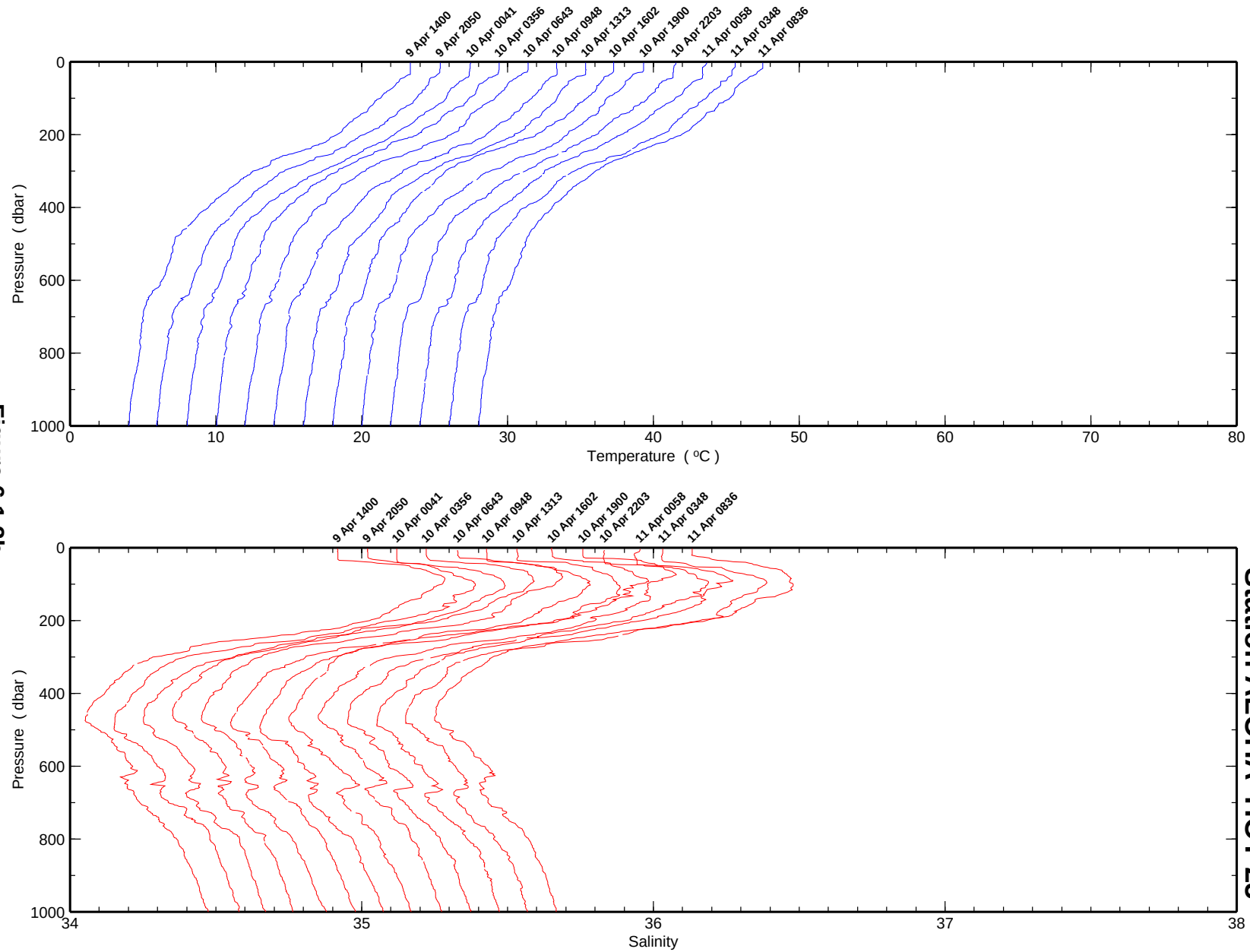

Figure 6.1.3b

Station ALOHA HOT 25

Station ALOHA HOT 26

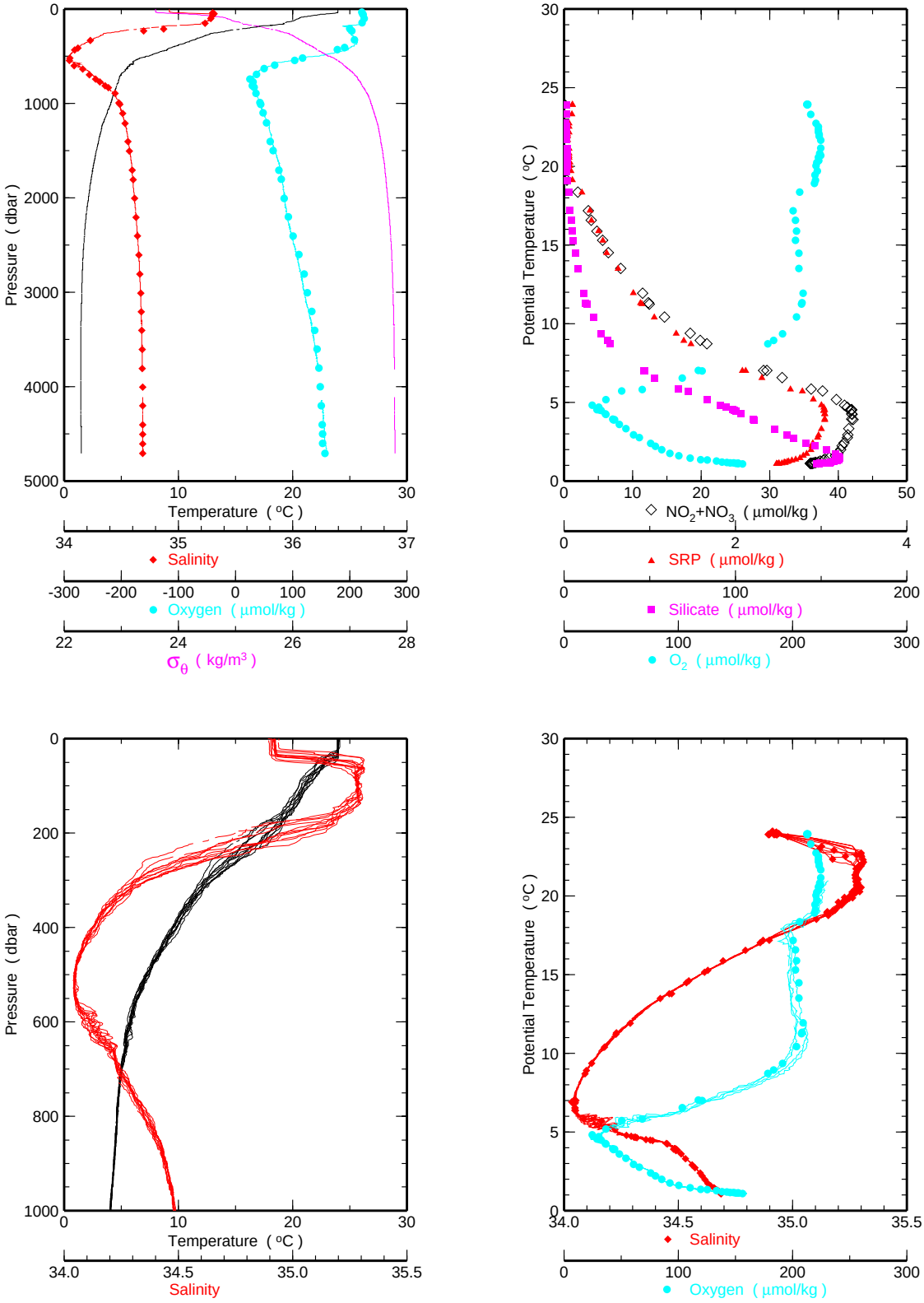

Figure 6.1.4a

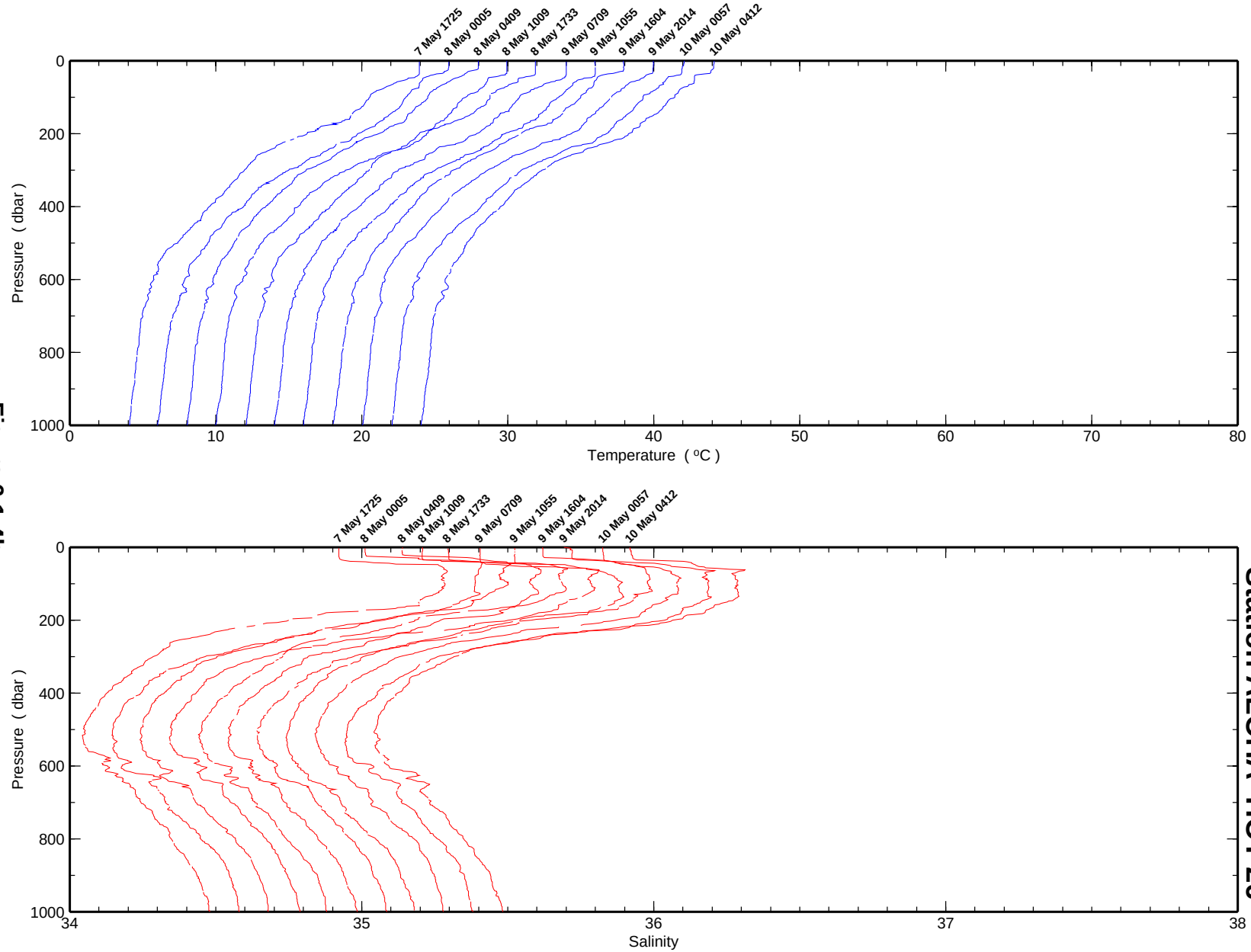

Figure 6.1.4b

Station ALOHA HOT 26

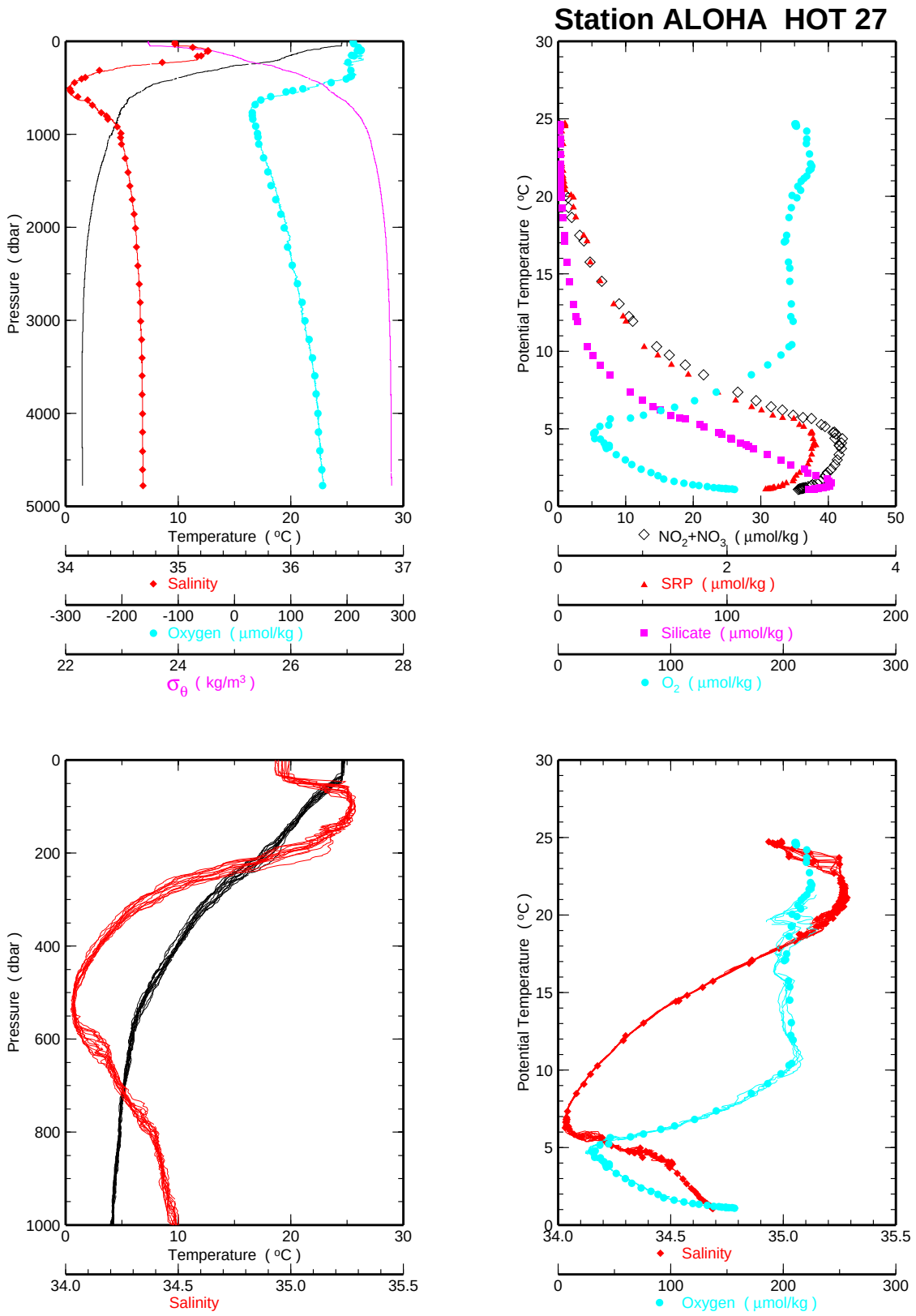
Station ALOHA HOT 27
Pressure (dbar)
Temperature (°C)
Salinity
Oxygen (µmol/kg)
σθ (kg/m³)
Potential Temperature (°C)
NO2+NO3 (µmol/kg)
SRP (µmol/kg)
Silicate (µmol/kg)
O2 (µmol/kg)
Pressure (dbar)
Temperature (°C)
Salinity
Potential Temperature (°C)
Salinity
Oxygen (µmol/kg)

Figure 6.1.5a

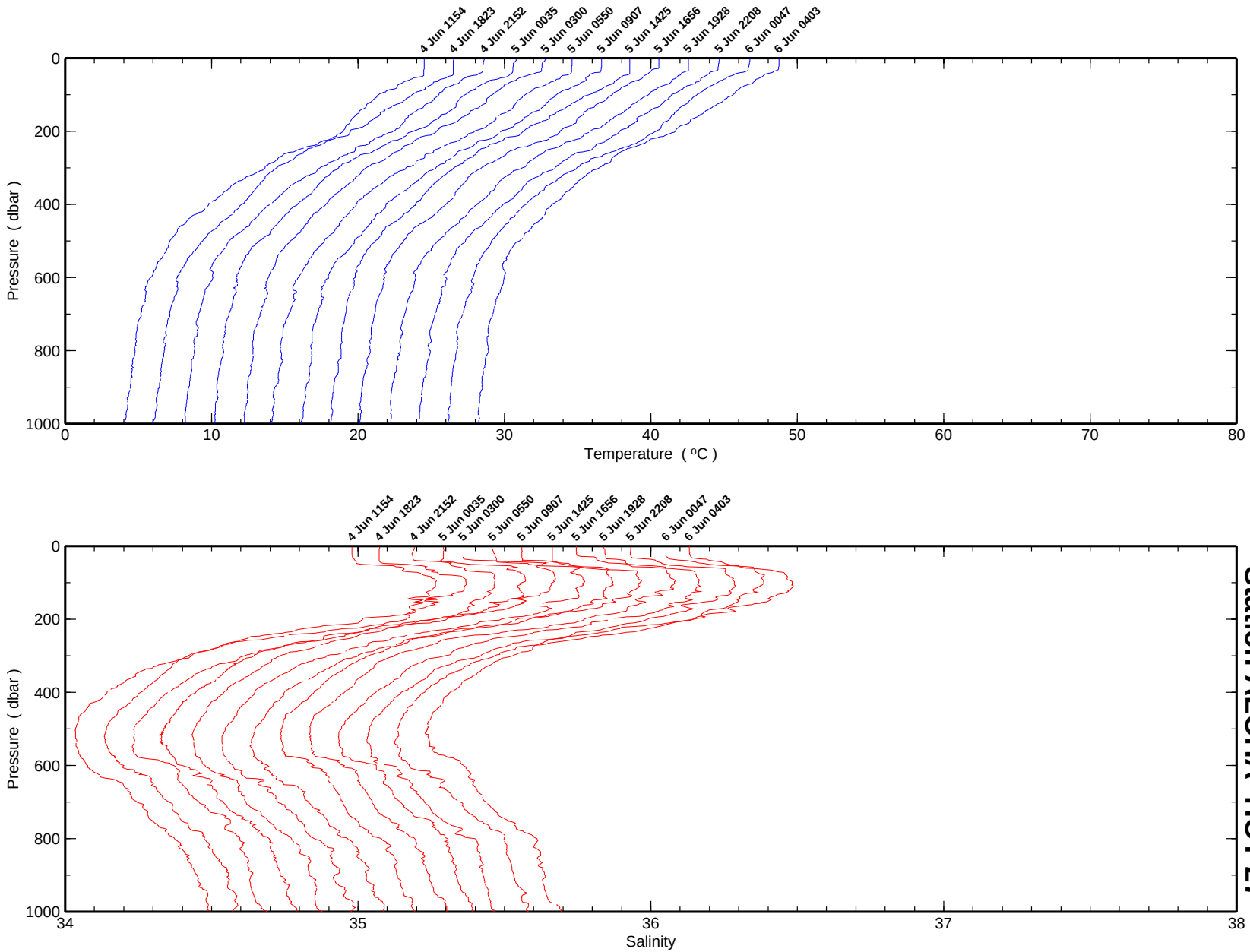

Figure 6.1.5b

Station ALOHA HOT 27

Station ALOHA HOT 28

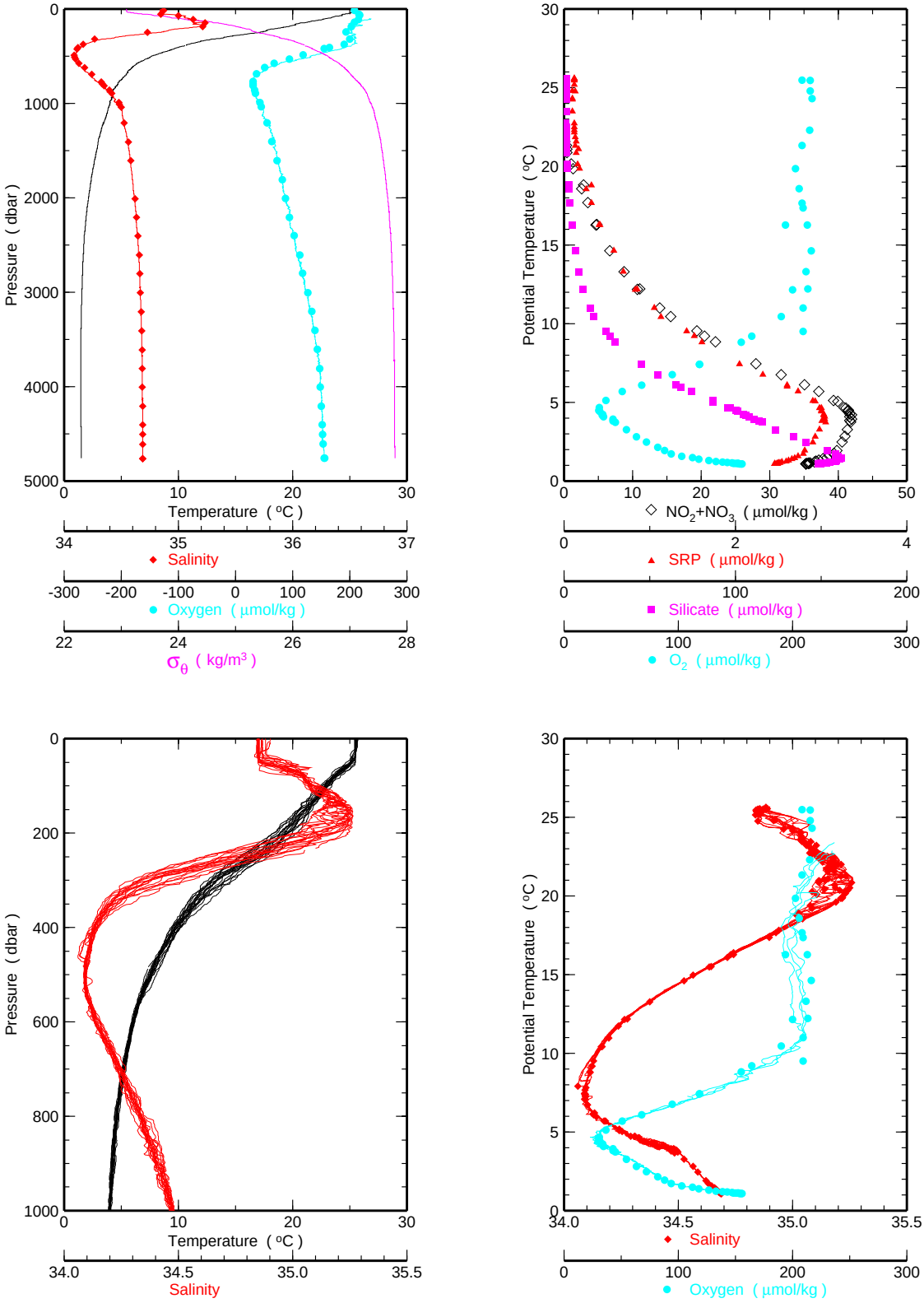

Figure 6.1.6a

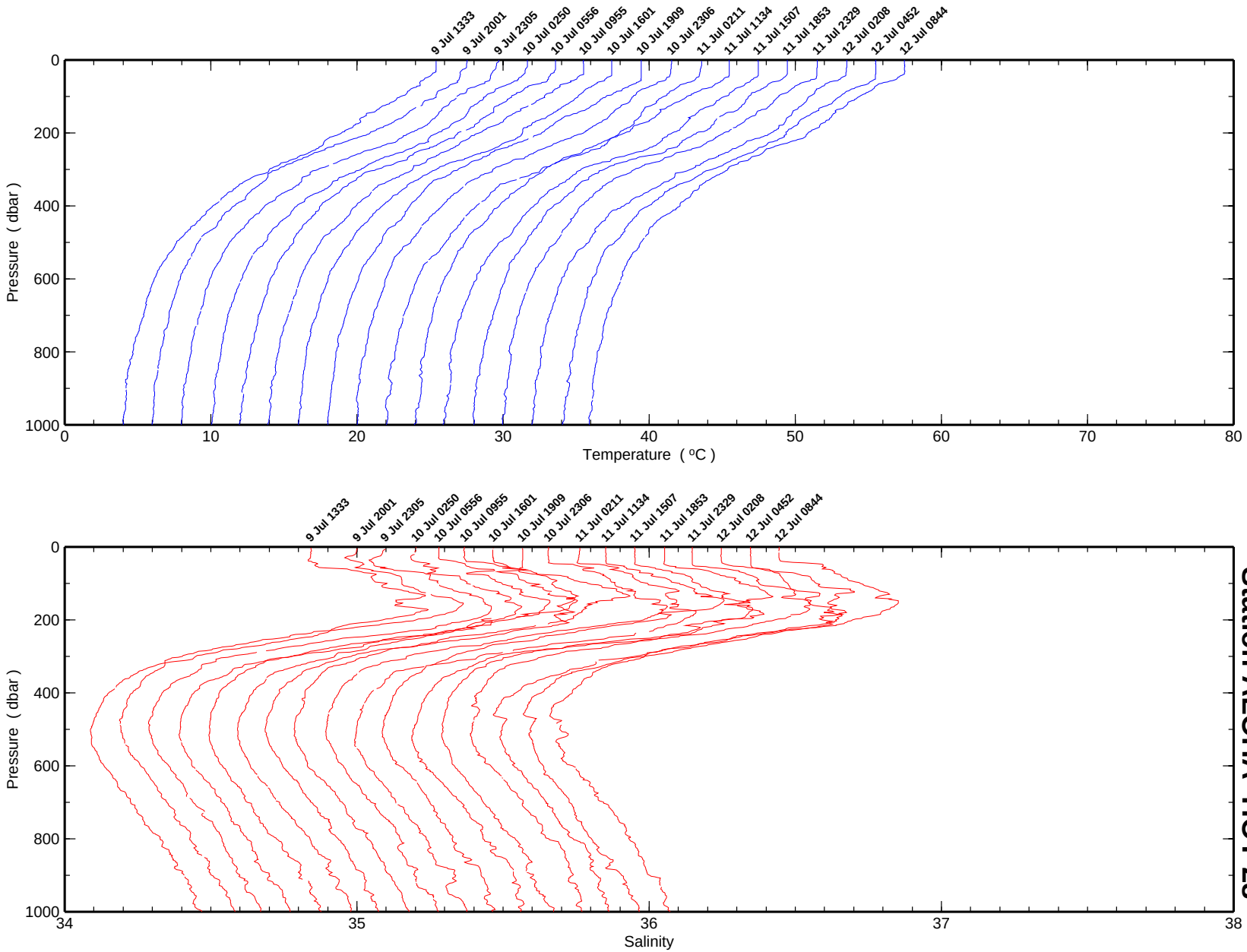

Figure 6.1.6b

Station ALOHA HOT 28

Station ALOHA HOT 29

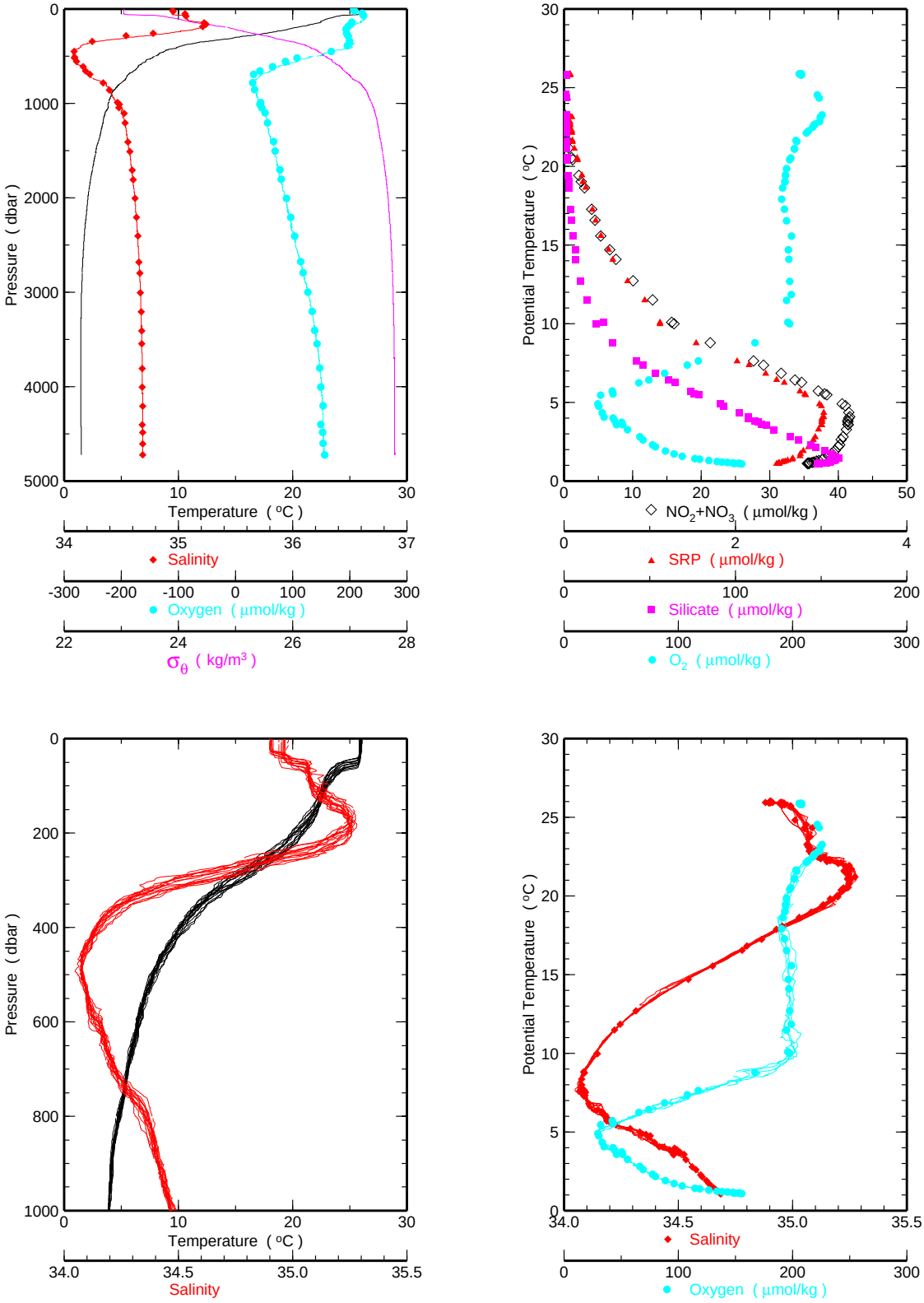

Figure 6.1.7a

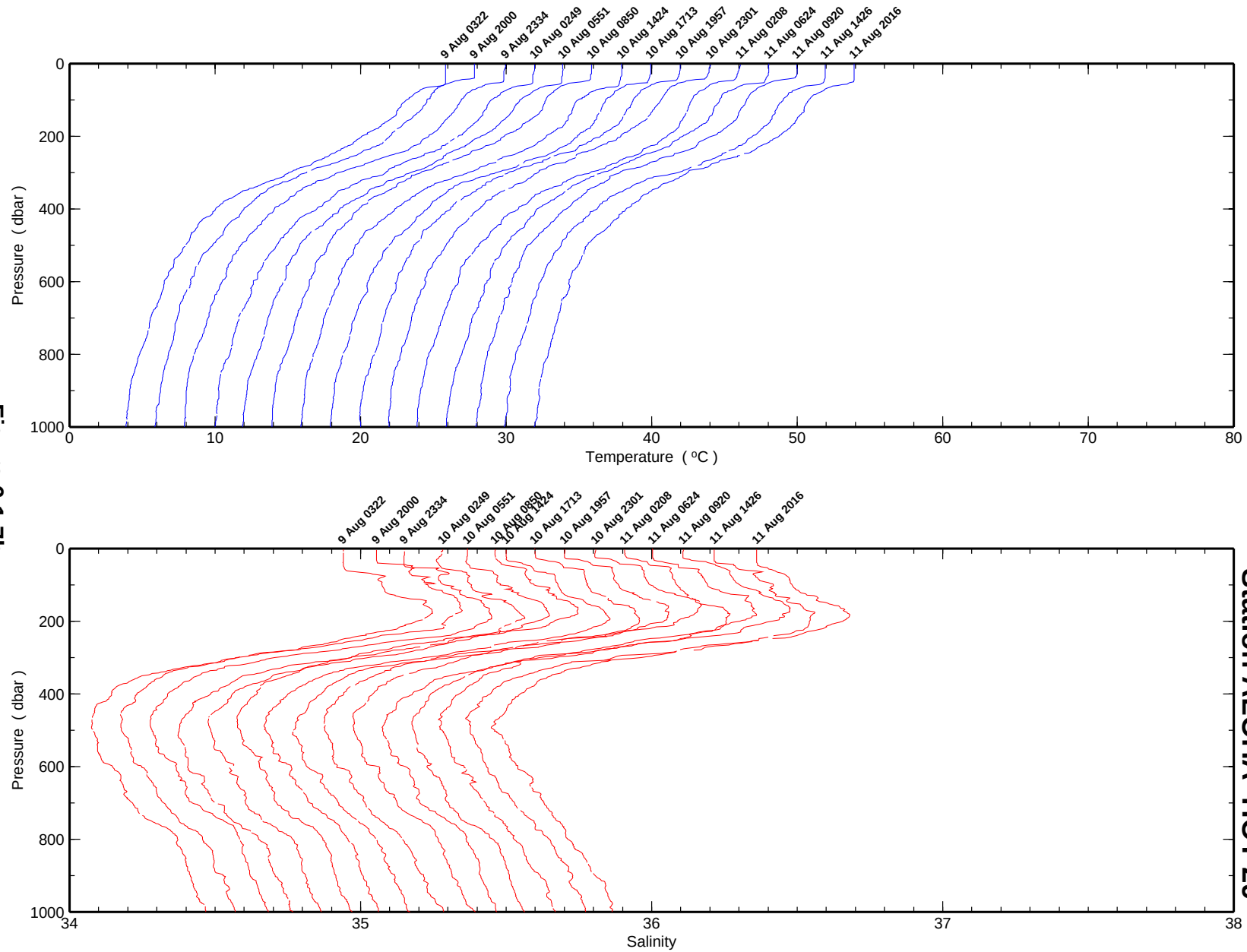

Station ALOHA HOT 29

Figure 6.1.7b

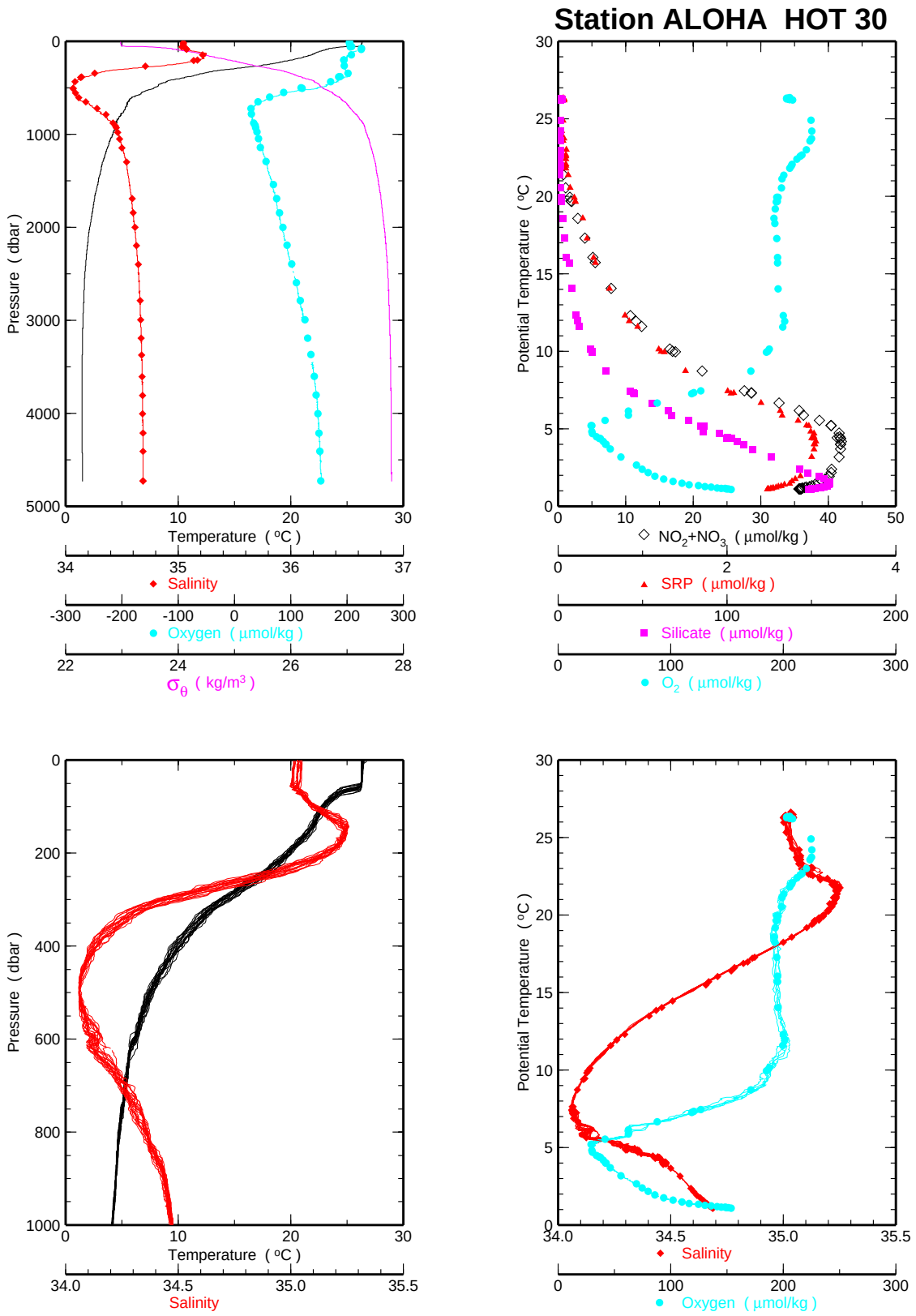
Station ALOHA HOT 30
Pressure (dbar)
Temperature (°C)
Salinity
Oxygen (µmol/kg)
σθ (kg/m³)
Potential Temperature (°C)
NO2+NO3 (µmol/kg)
SRP (µmol/kg)
Silicate (µmol/kg)
O2 (µmol/kg)
Pressure (dbar)
Temperature (°C)
Salinity
Potential Temperature (°C)
Salinity
Oxygen (µmol/kg)

Figure 6.1.8a

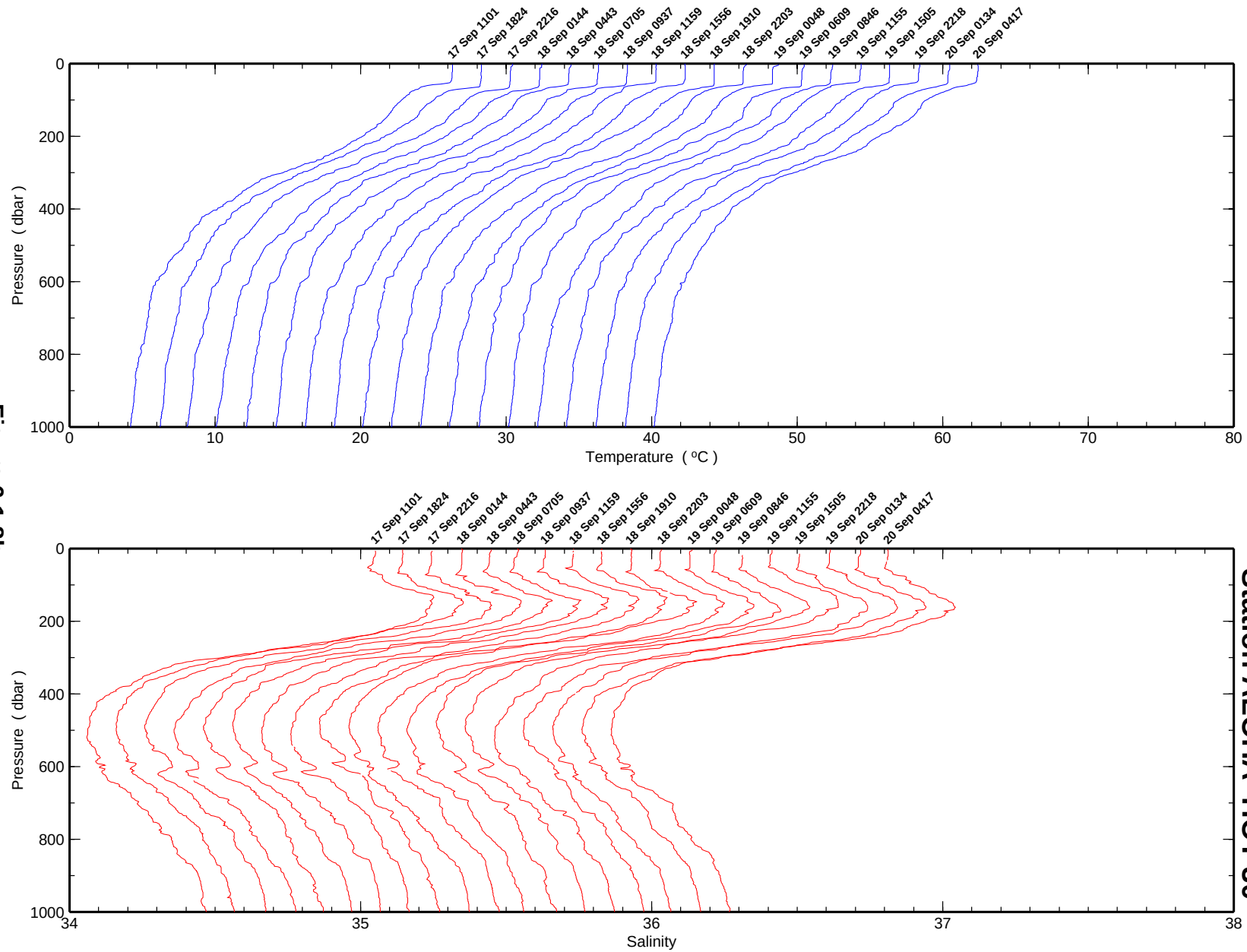

Station ALOHA HOT 30

Figure 6.1.8b

Station ALOHA HOT 31

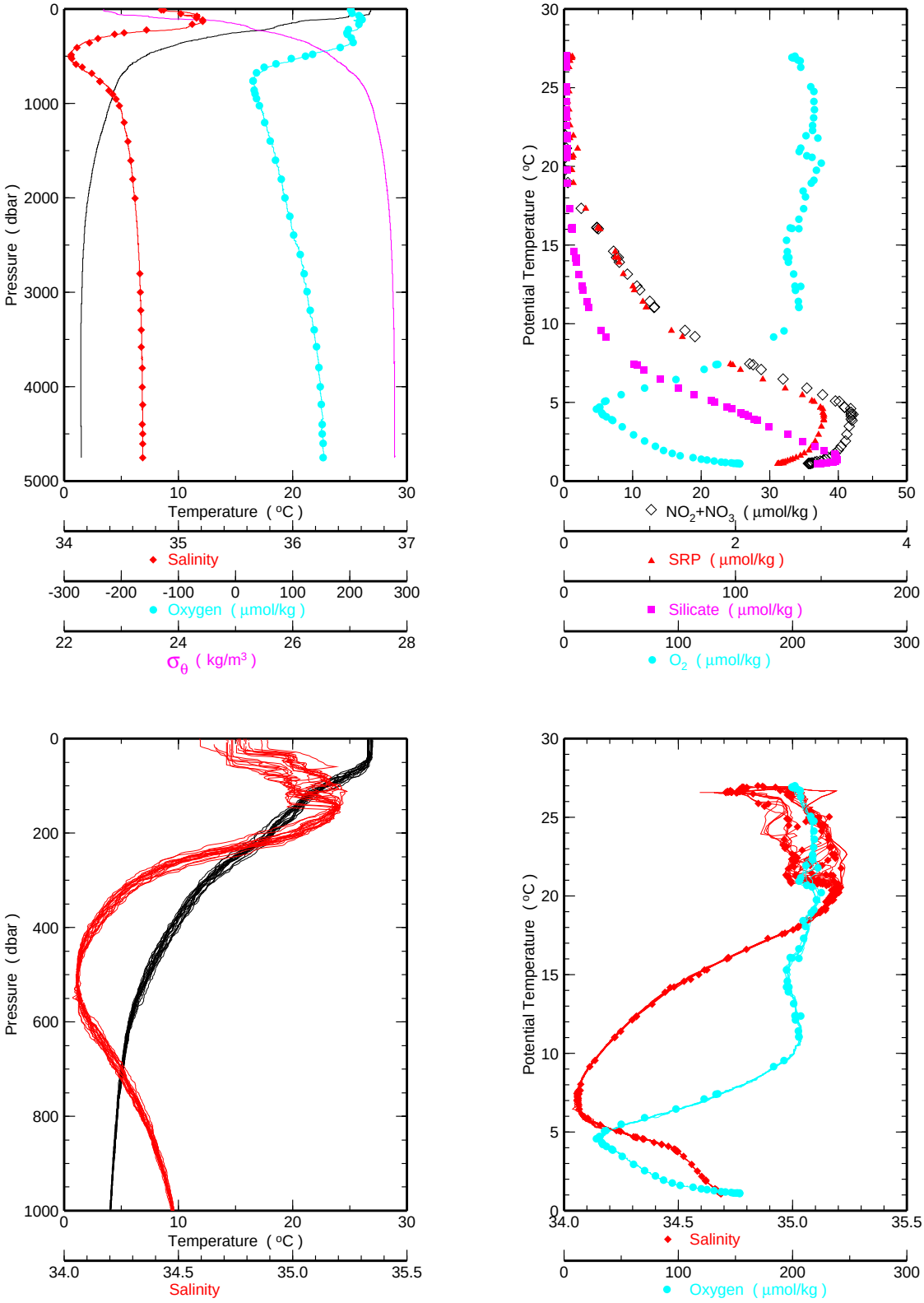

Figure 6.1.9a

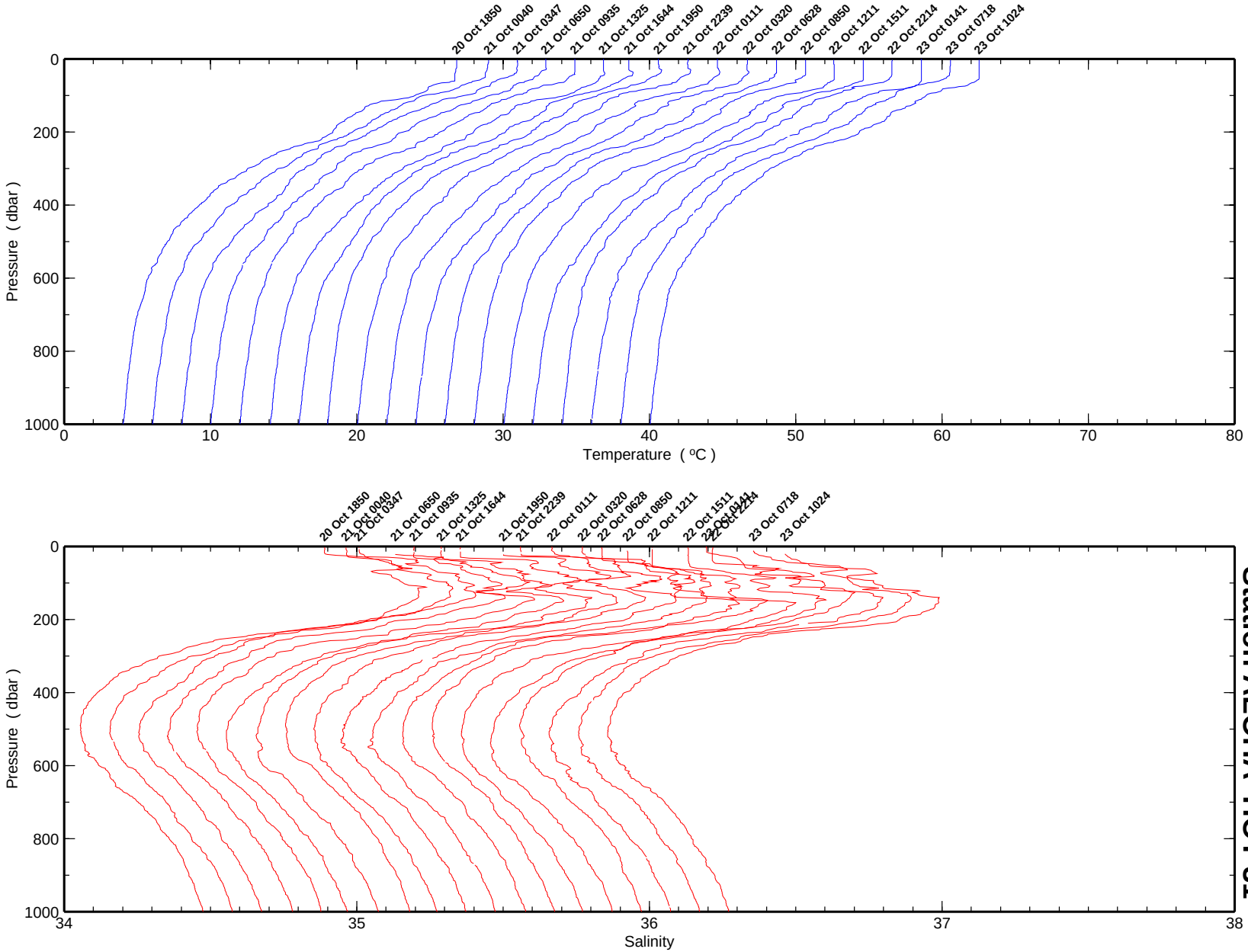

Figure 6.1.9b

Station ALOHA HOT 31

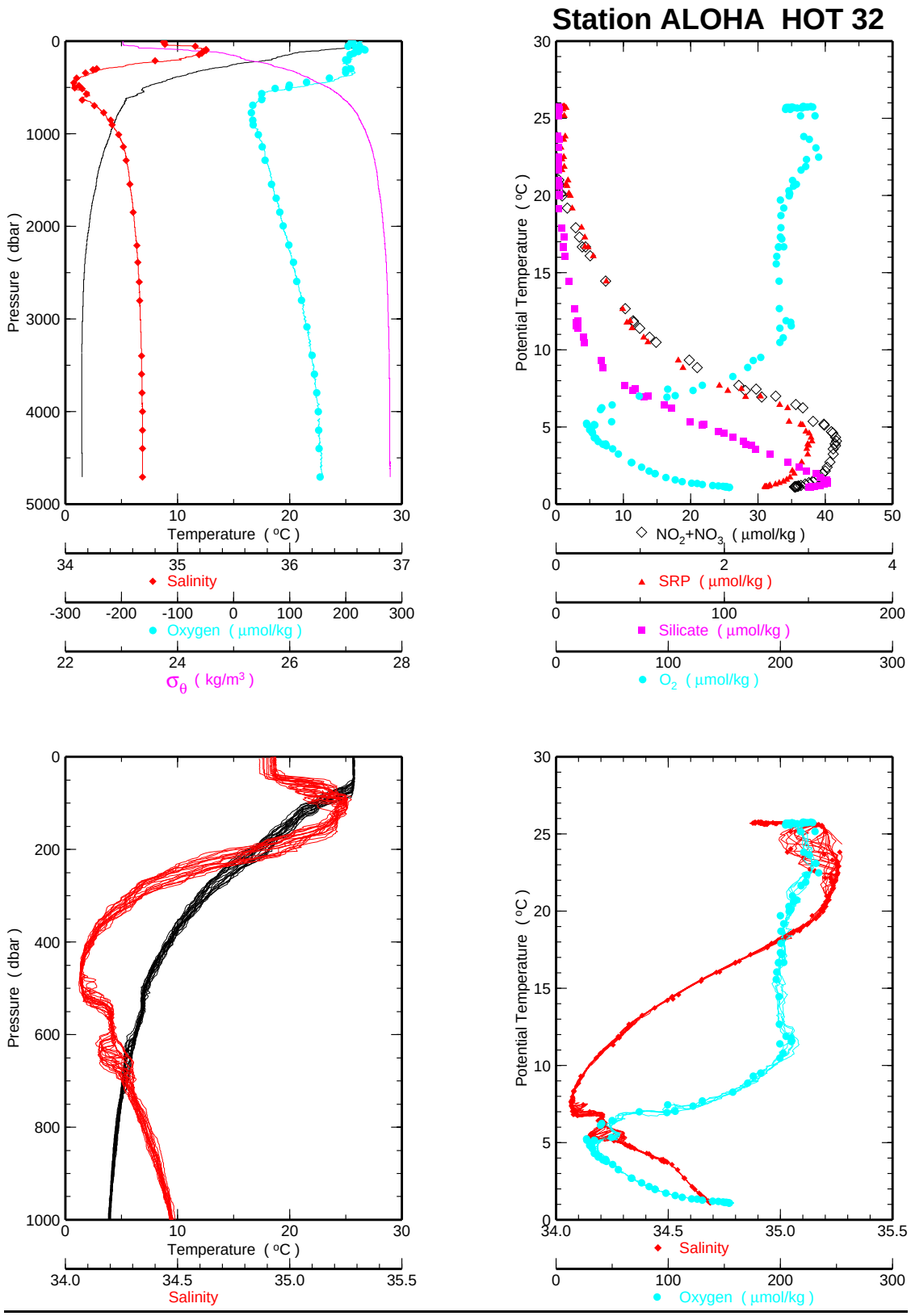

Figure 6.1.10a

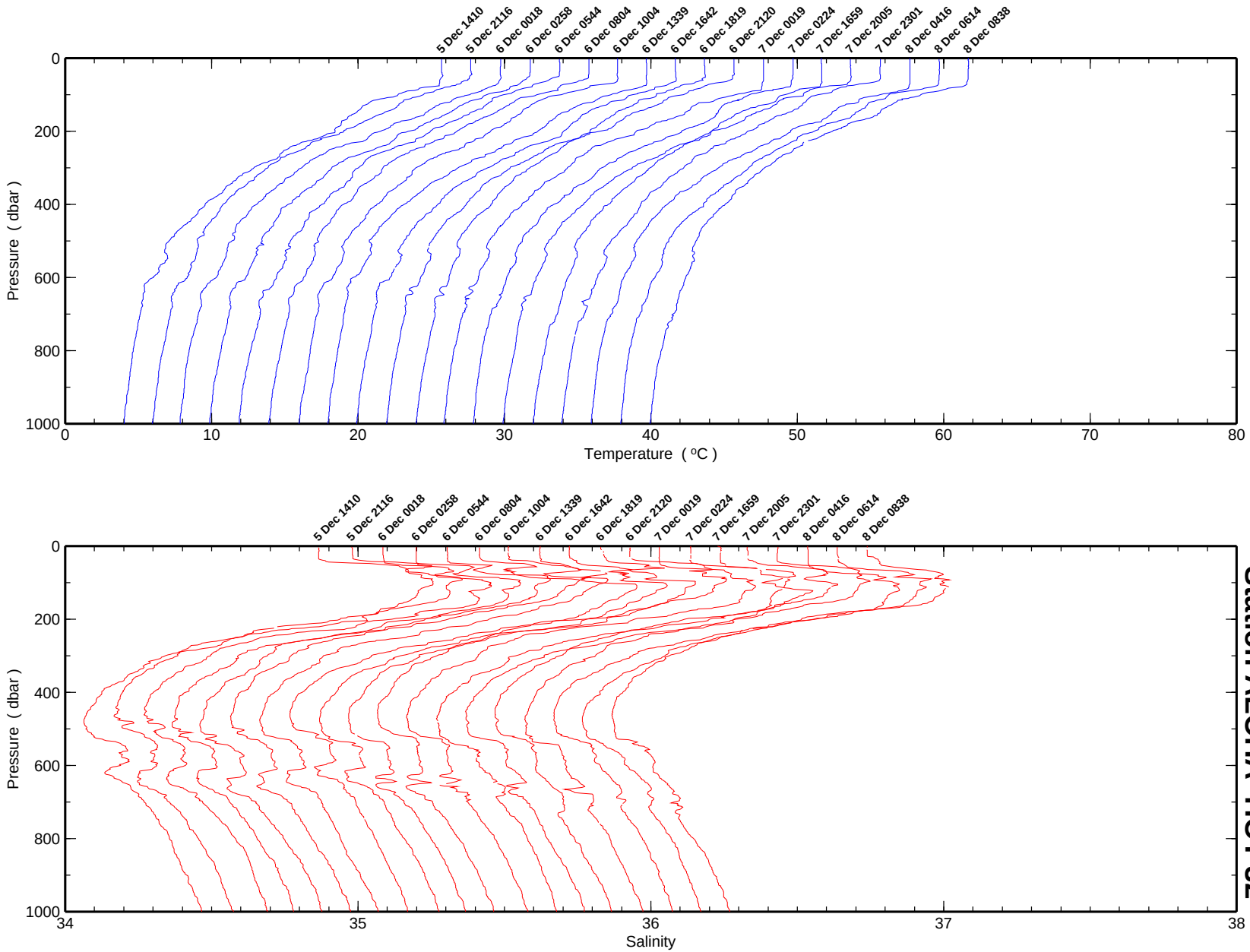

Figure 6.1.10b

Station ALOHA HOT 32

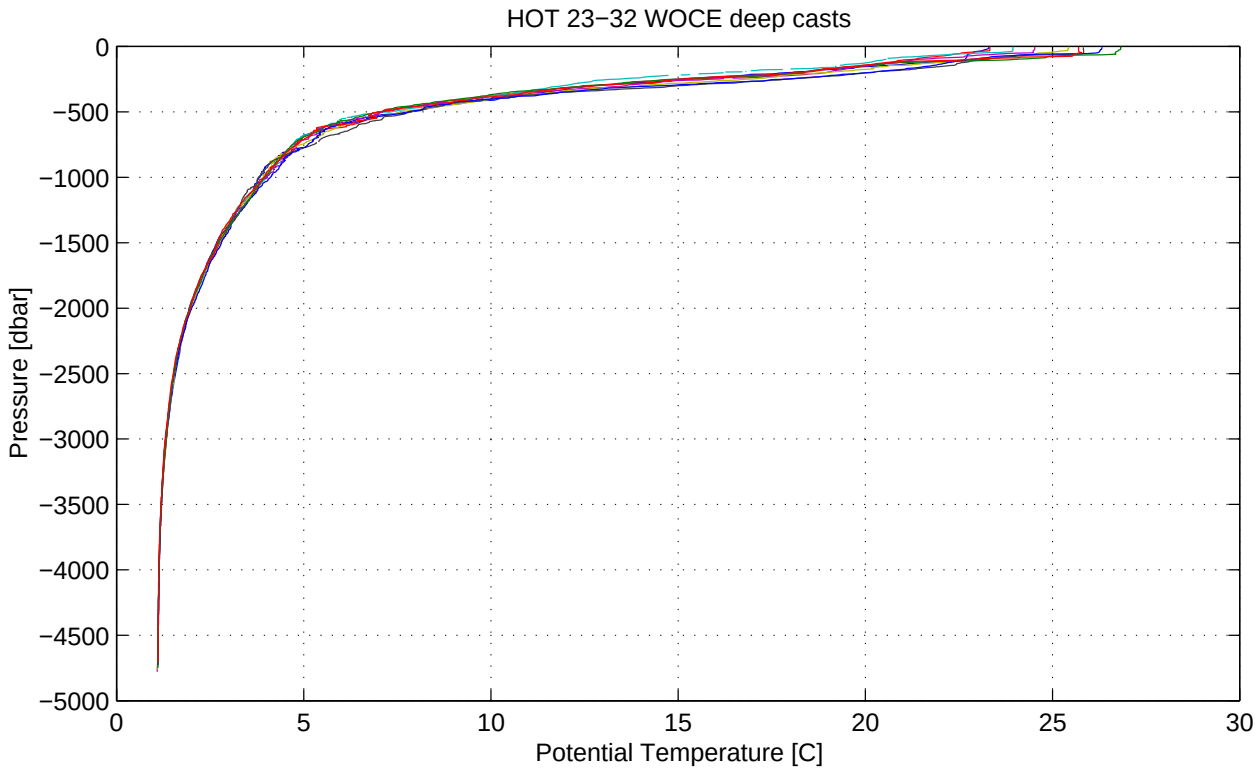
HOT 23−32 WOCE deep casts
Pressure [dbar]
Potential Temperature [C]
0
−500
−1000
−1500
−2000
−2500
−3000
−3500
−4000
−4500
−5000
0
5
10
15
20
25
30

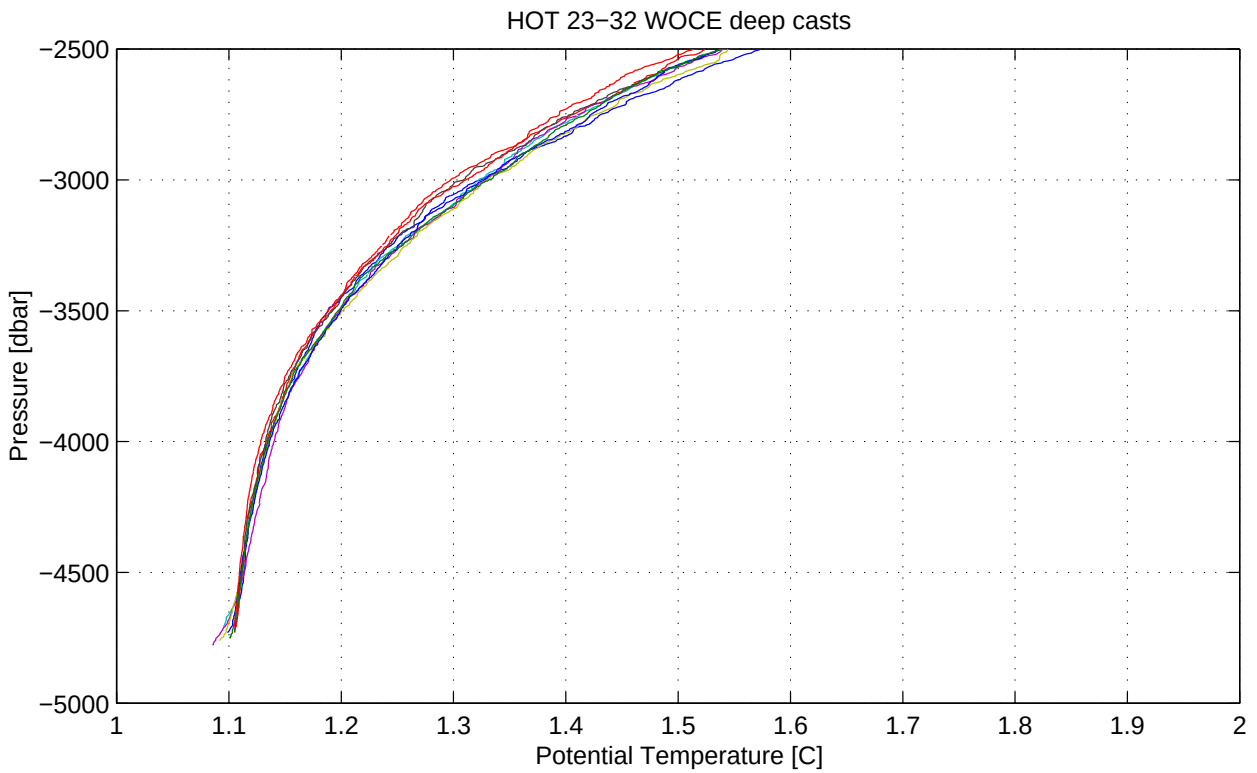
HOT 23−32 WOCE deep casts
Pressure [dbar]
Potential Temperature [C]
−2500
−3000
−3500
−4000
−4500
−5000
1
1.1
1.2
1.3
1.4
1.5
1.6
1.7
1.8
1.9
2

Figure 6.1.11

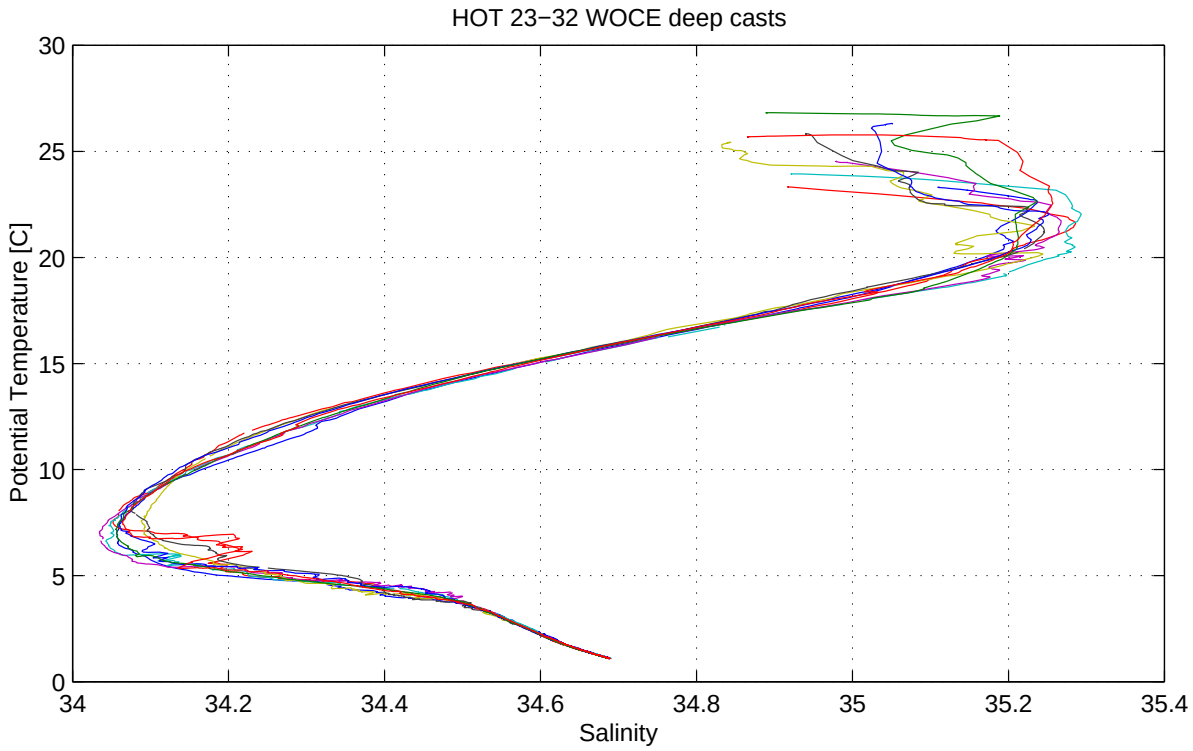
HOT 23−32 WOCE deep casts
Potential Temperature [C]
Salinity
30
25
20
15
10
5
0
34
34.2
34.4
34.6
34.8
35
35.2
35.4

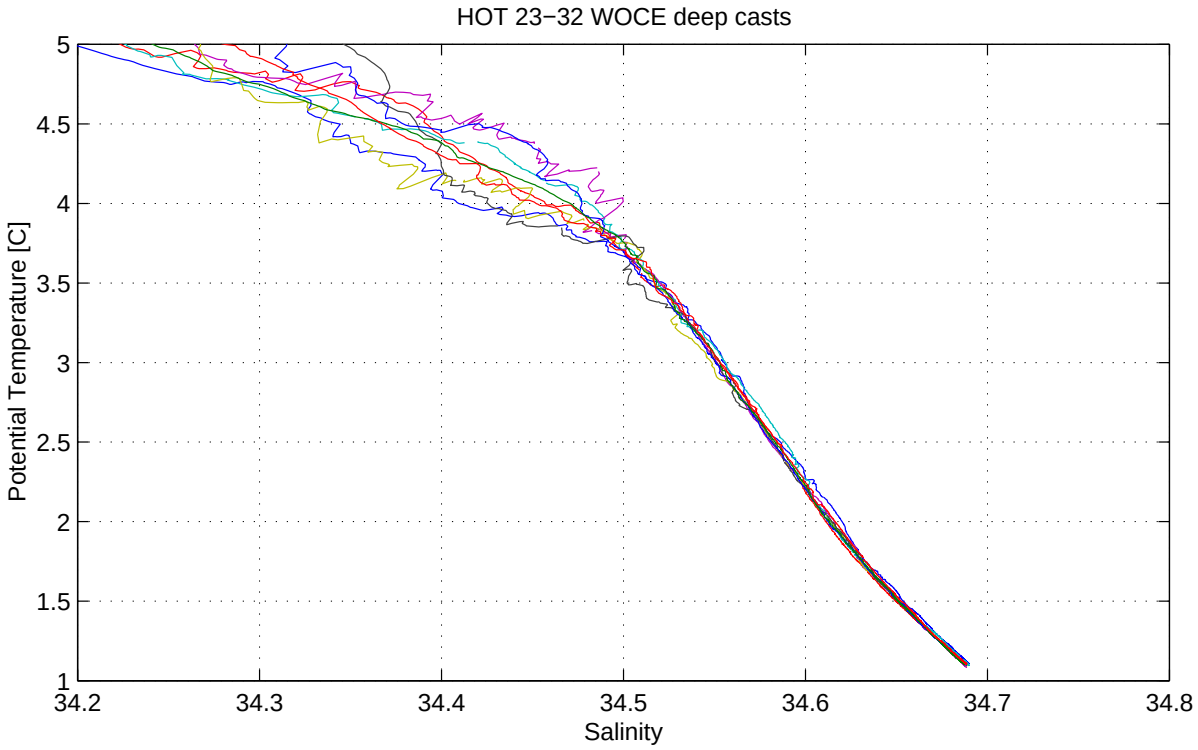
HOT 23−32 WOCE deep casts
Potential Temperature [C]
Salinity
5
4.5
4
3.5
3
2.5
2
1.5
1
34.2
34.3
34.4
34.5
34.6
34.7
34.8

Figure 6.1.12

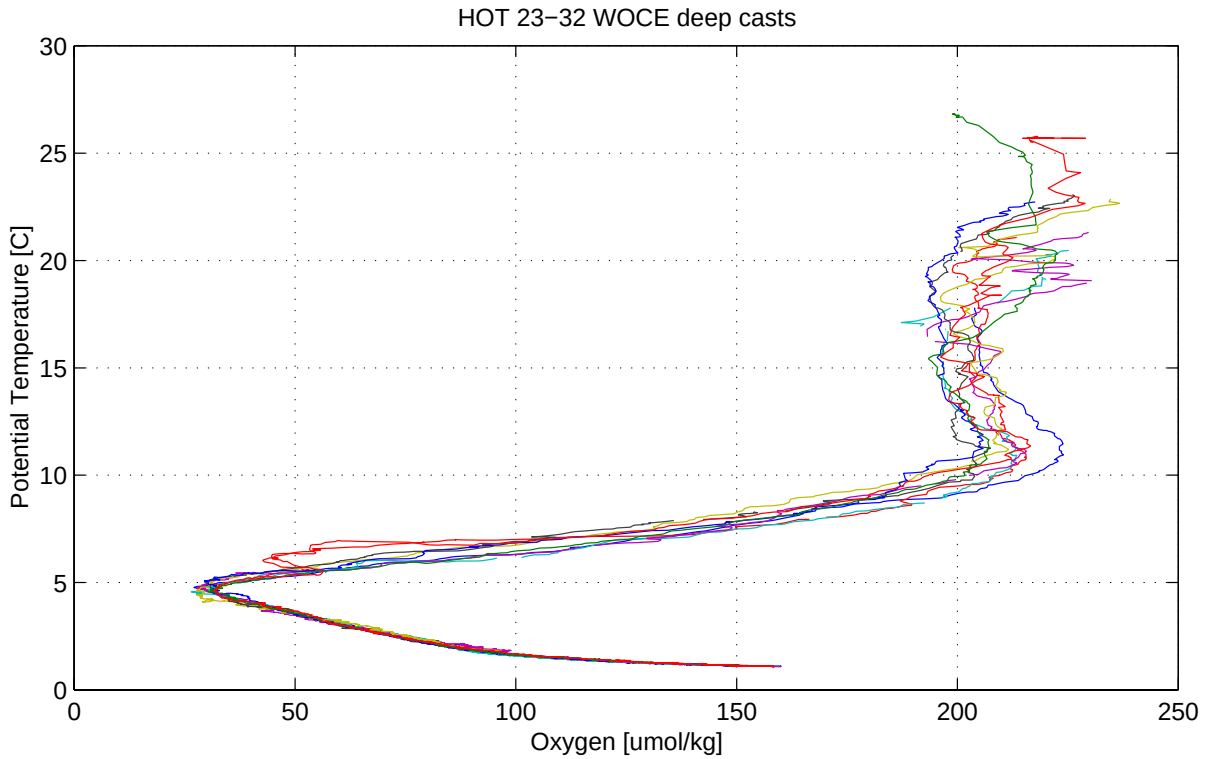
HOT 23−32 WOCE deep casts
Potential Temperature [C]
Oxygen [umol/kg]
0
5
10
15
20
25
30
0
50
100
150
200
250

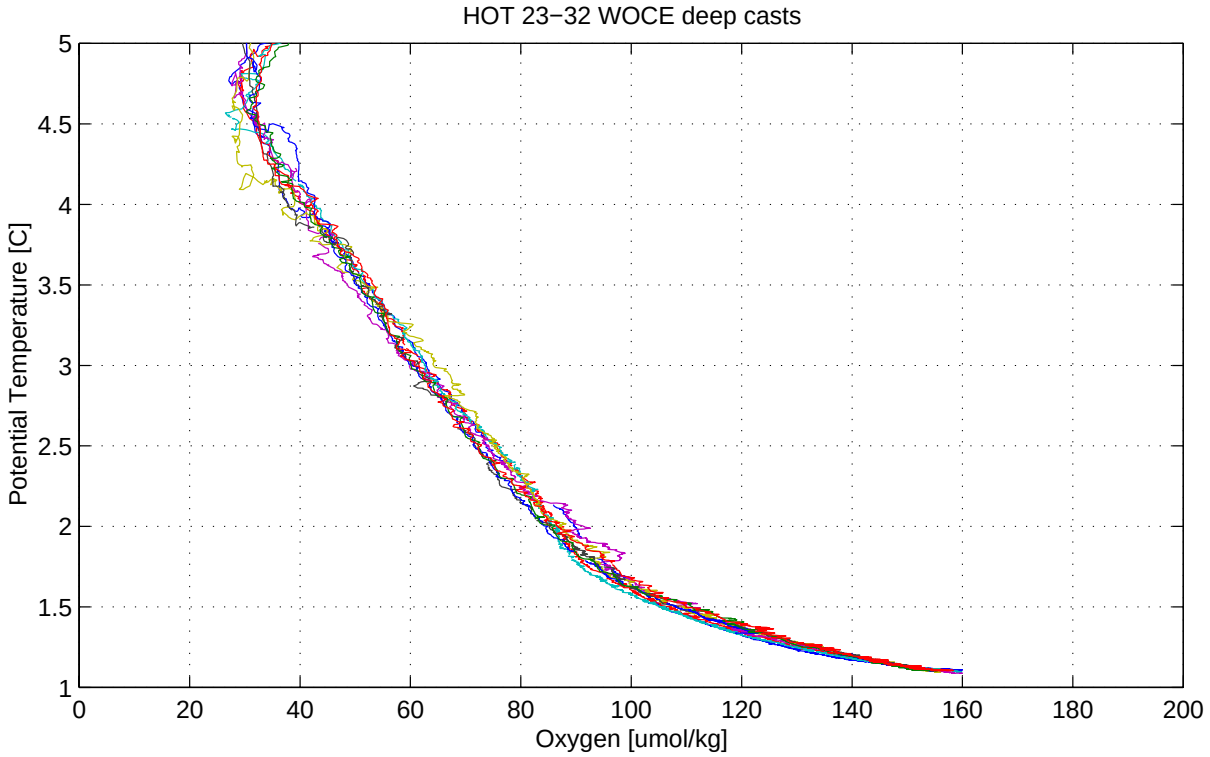
HOT 23−32 WOCE deep casts
Potential Temperature [C]
Oxygen [umol/kg]
1
1.5
2
2.5
3
3.5
4
4.5
5
0
20
40
60
80
100
120
140
160
180
200

Figure 6.1.13

6.2. Contour Plots

Figures 6.2.1-14 show data from HOT 1-32. Time of each cruise is indicated by a symbol along the time axis.

Figure 6.2.1: Potential temperature measured by CTD plotted versus pressure. All casts at the HOT site are averaged for each cruise.

Figure 6.2.2: Potential density, calculated from CTD measurements of pressure, temperature and salinity, plotted versus pressure. All casts at the HOT site are averaged for each cruise.

Figure 6.2.3: Salinity measured by CTD plotted versus pressure. All casts at the HOT site are averaged for each cruise.

Figure 6.2.4: Salinity measured by CTD plotted versus potential density. All casts at the HOT site are averaged for each cruise. The average density of the sea surface for each cruise is connected by a heavy line.

Figure 6.2.5: Salinity from discrete water sample analyses plotted versus pressure. Locations of bottle closures are indicated by dots.

Figure 6.2.6: Salinity from discrete water sample analyses plotted versus potential density. The average density of the sea surface .for each cruise is connected by a heavy line. Locations of bottle closures are indicated by dots.

Figure 6.2.7: Oxygen from discrete water sample analyses plotted versus pressure. Locations of bottle closures are indicated by dots.

Figure 6.2.8: Oxygen from discrete water sample analyses plotted versus potential density. The average density of the sea surface for each cruise is connected by a heavy line. Locations of bottle closures are indicated by dots.

Figure 6.2.9: Nitrate plus nitrite from discrete water sample analyses plotted versus pressure. Locations of bottle closures are indicated by dots.

Figure 6.2.10: Nitrate plus nitrite from discrete water sample analyses plotted versus potential density. The average density of the sea surface for each cruise is connected by a heavy line. Locations of bottle closures are indicated by dots.

Figure 6.2.11: Phosphate from discrete water sample analyses plotted versus pressure. Locations of bottle closures are indicated by dots.

Figure 6.2.12: Phosphate from discrete water sample analyses plotted versus potential density. The average density of the sea surface for each cruise is connected by a heavy line. Locations of bottle closures are indicated by dots.

Figure 6.2.13: Silicate from discrete water sample analyses plotted versus pressure. Locations of bottle closures are indicated by dots.

Figure 6.2.14: Silicate from discrete water sample analyses plotted versus potential density. The average density of the sea surface for each cruise is connected by a heavy line. Locations of bottle closures are indicated by dots.

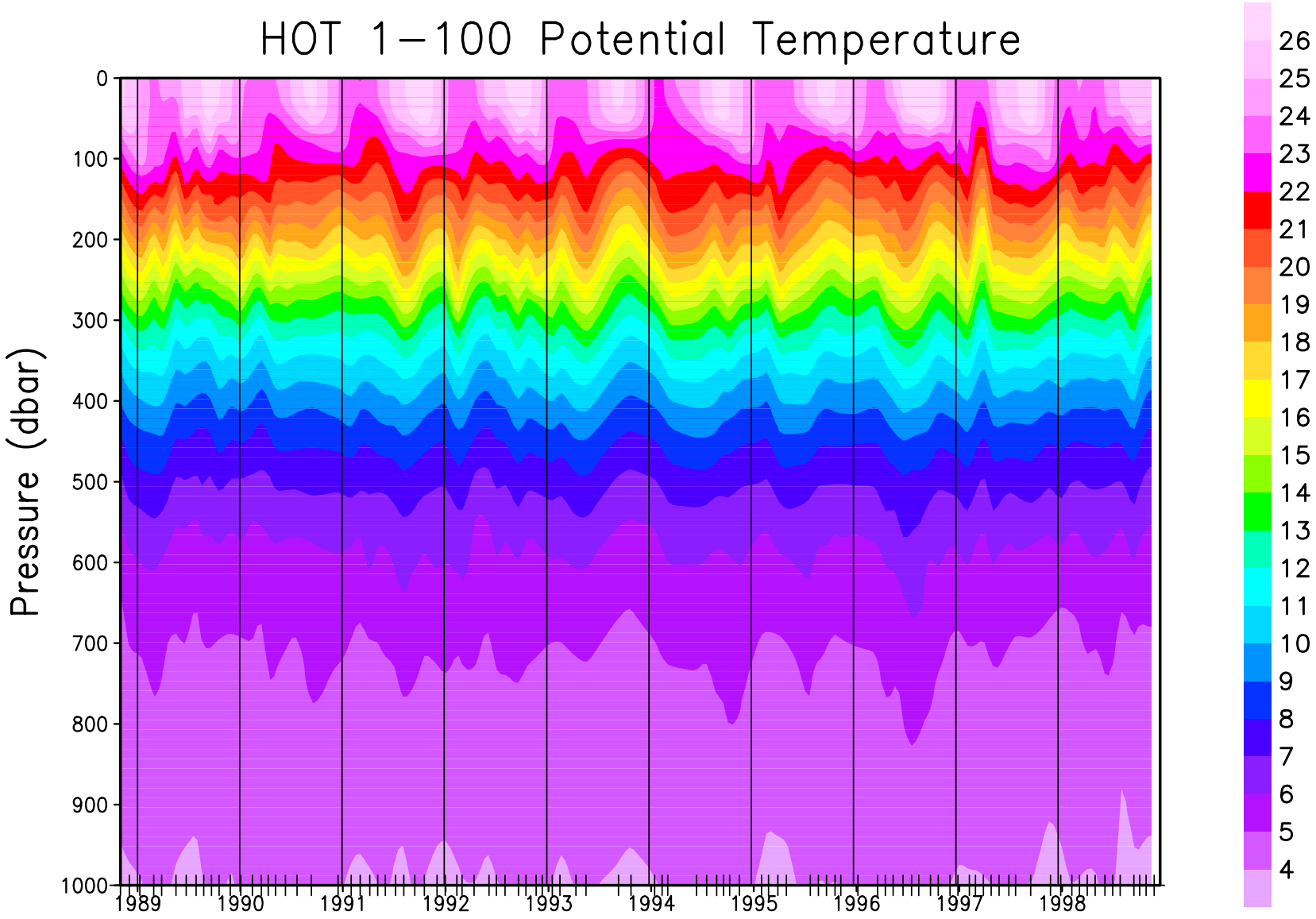

Figure 6.2.1: Contour plot of CTD potential temperature versus pressure for HOT cruises 1-100.

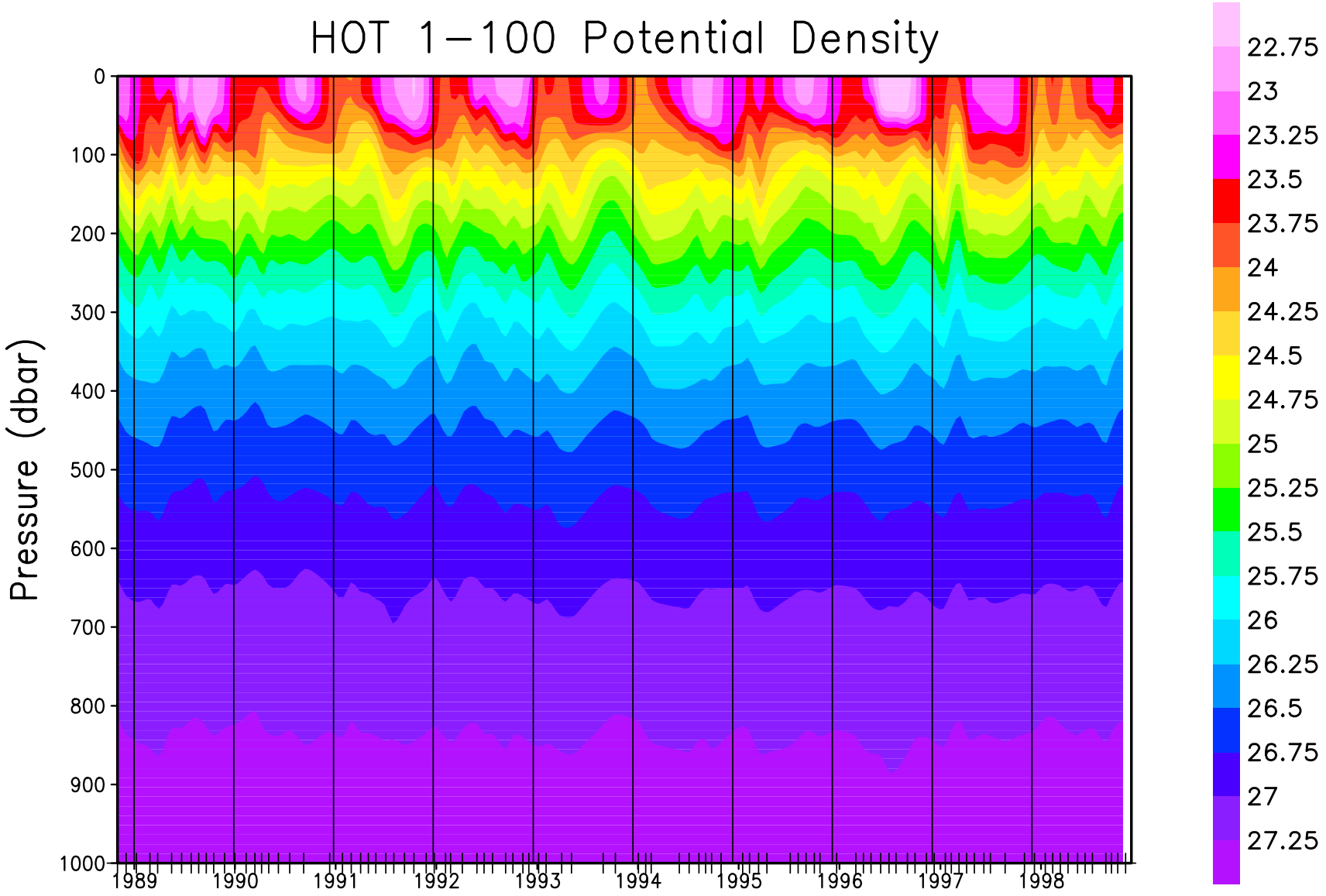

Figure 6.2.2: Contour plot of potential density (σ_θ), calculated from CTD pressure, temperature and salinity, versus pressure for HOT cruises 1-100.

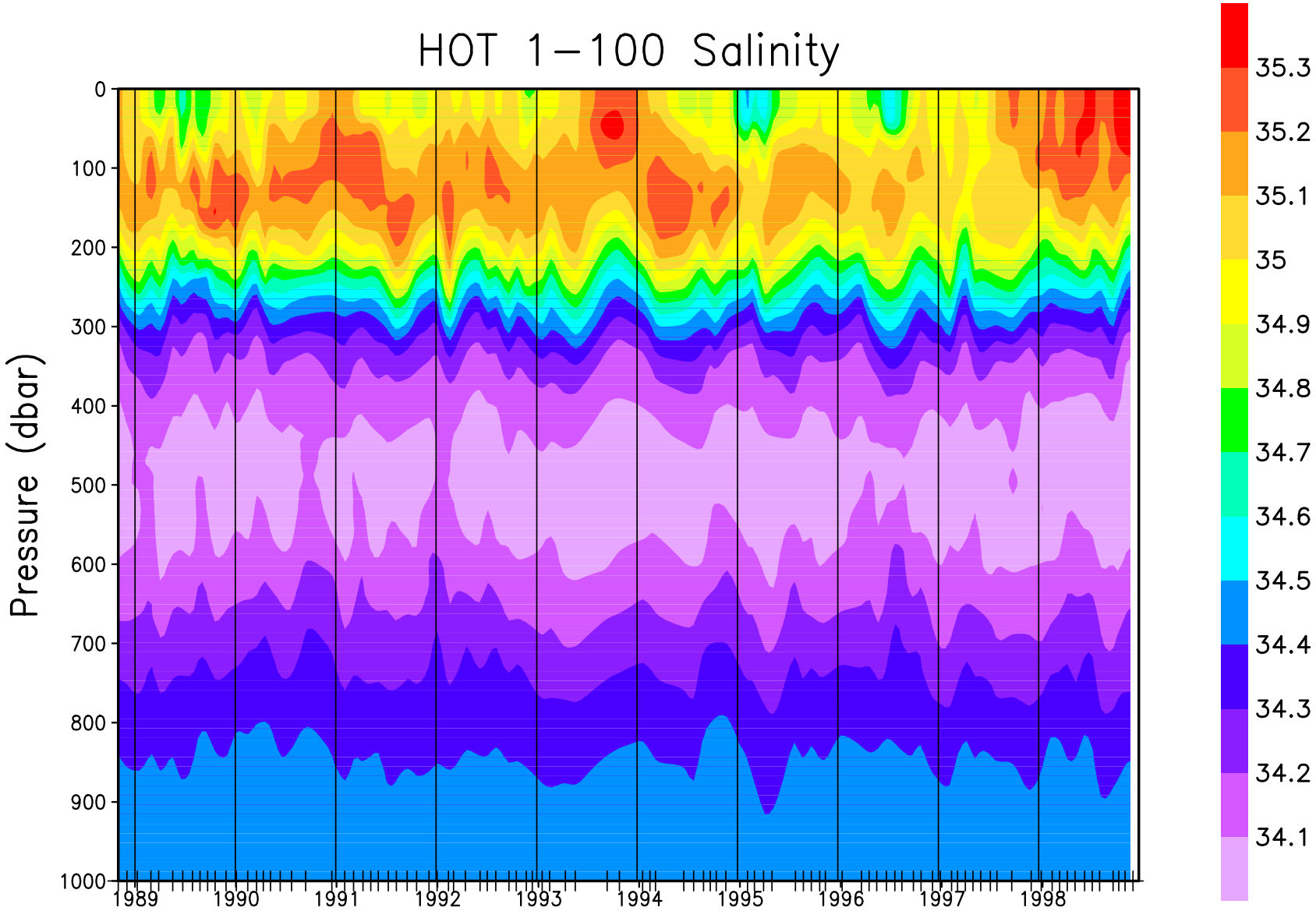

Figure 6.2.3: Contour plot of CTD salinity versus pressure for HOT cruises 1-100.

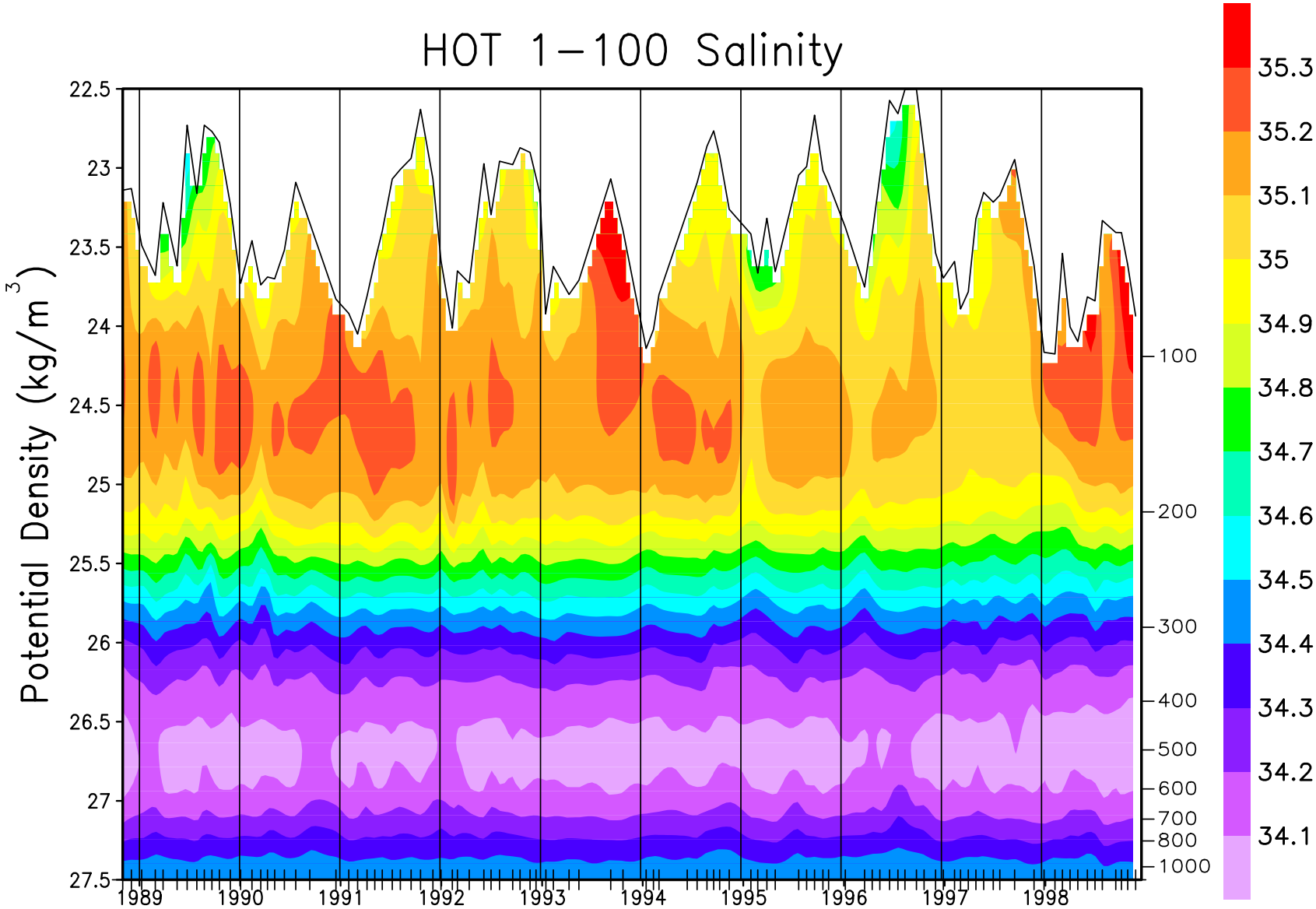

Figure 6.2.4: Contour plot of CTD salinity versus potential density (σ_θ) to 27.5 kg m^{-3} for HOT cruises 1-100. The average density of the sea surface is connected by the heavy line.

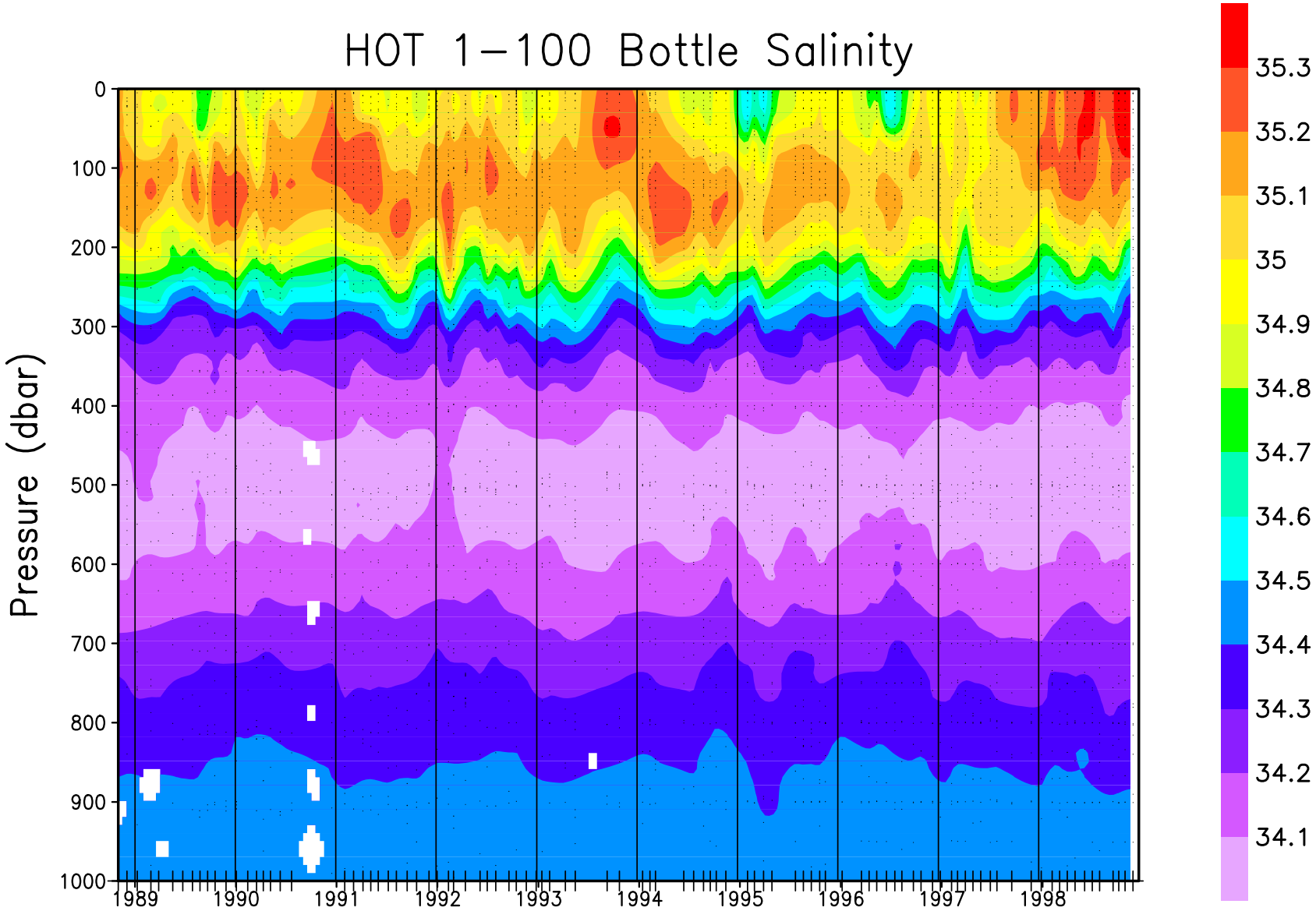

Figure 6.2.5: Contour plot of bottle salinity versus pressure for HOT cruises 1-100. Location of samples in the water column are indicated by the solid circles.

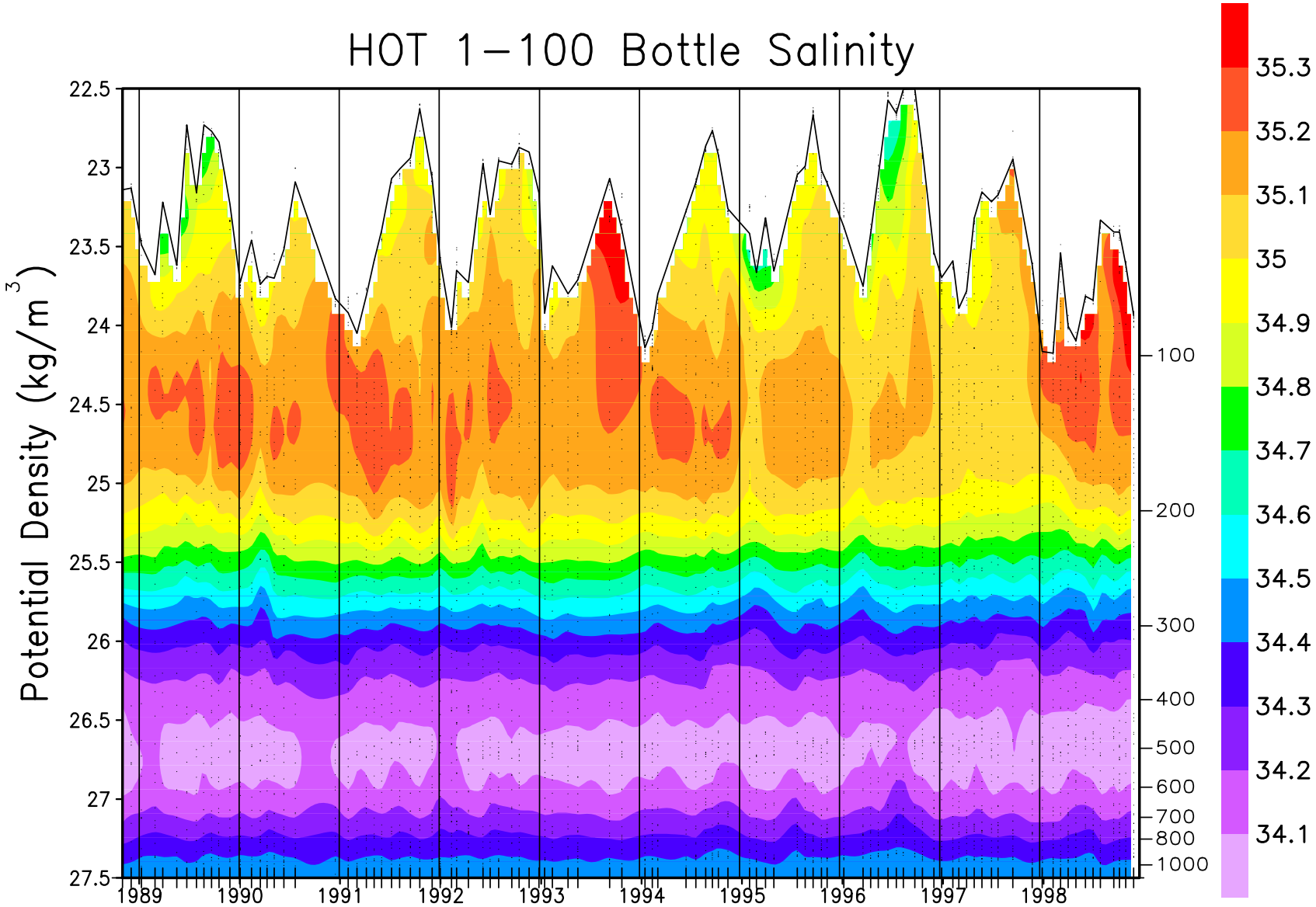

Figure 6.2.6: Contour plot of bottle salinity versus potential density (σ_θ)to 27.5 kg m^{-3} for HOT cruises 1-100. The average density of the sea surface is connected by the heavy line.

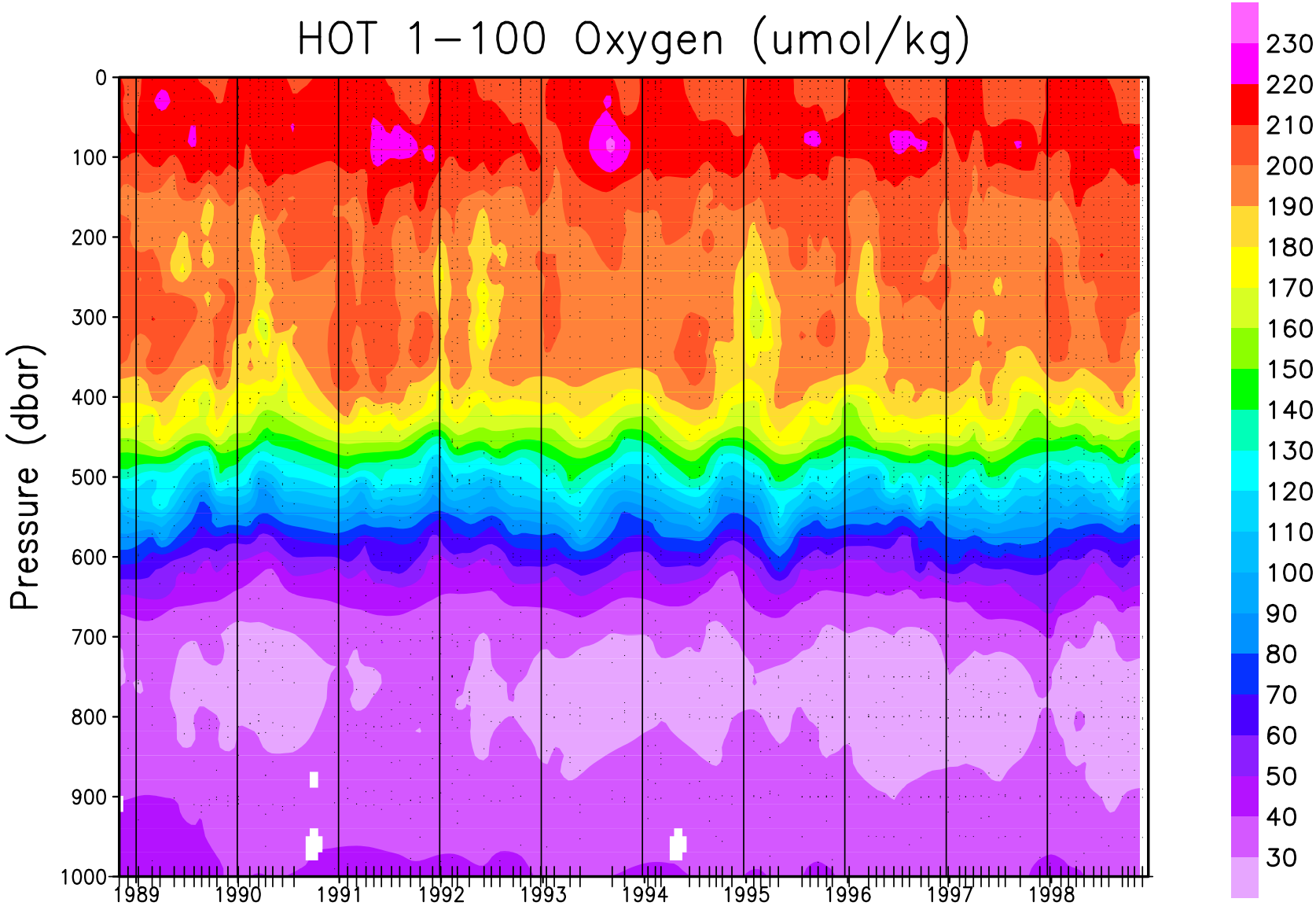

Figure 6.2.7: Contour plot of bottle oxygen versus pressure for HOT cruises 1-100. Location of samples in the water column are indicated by the solid circles.

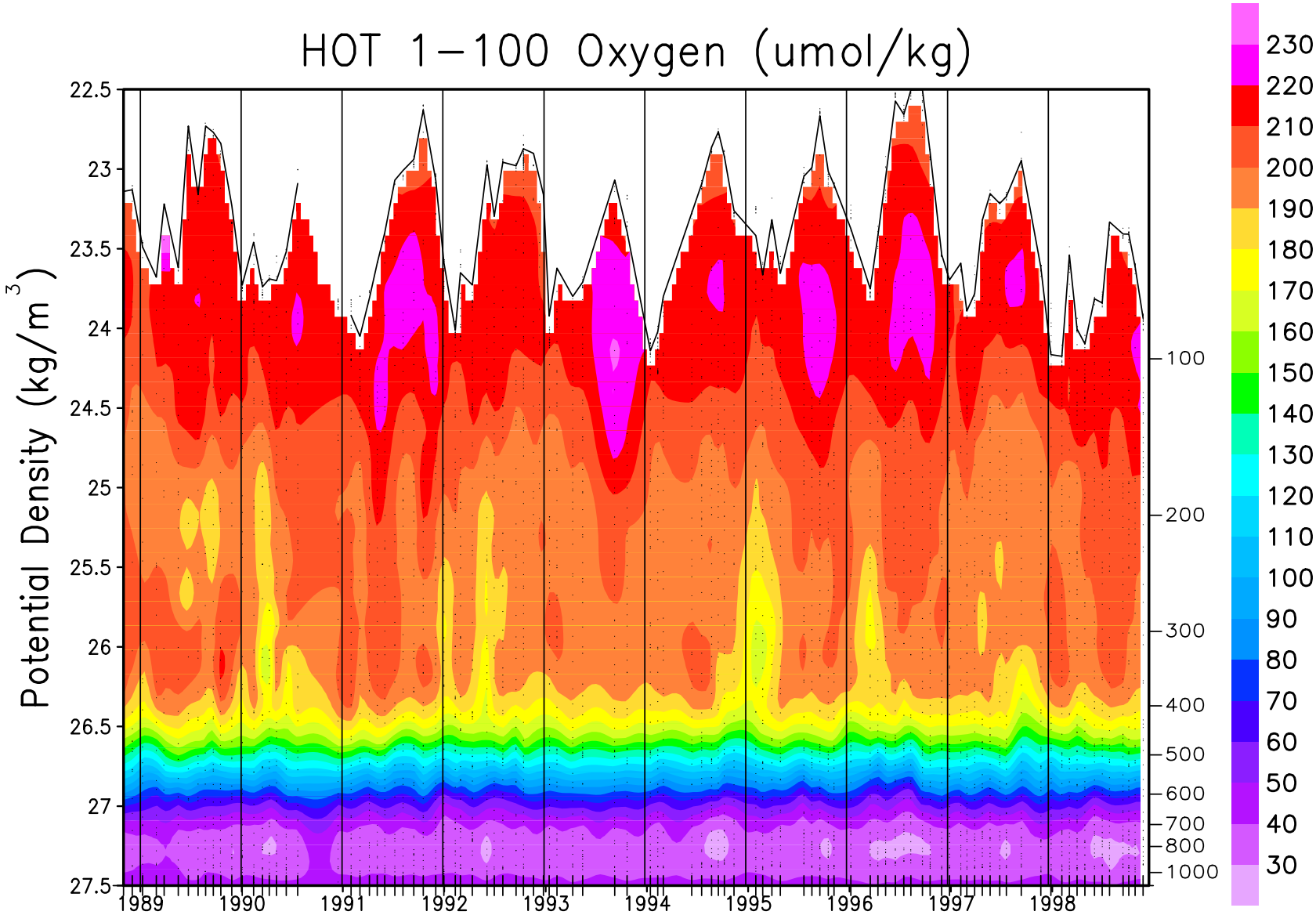

Figure 6.2.8: Contour plot of bottle oxygen versus potential density (σ_θ) to 27.5 kg m^{-3} for HOT cruises 1-100. The average density of the sea surface is connected by the heavy line.

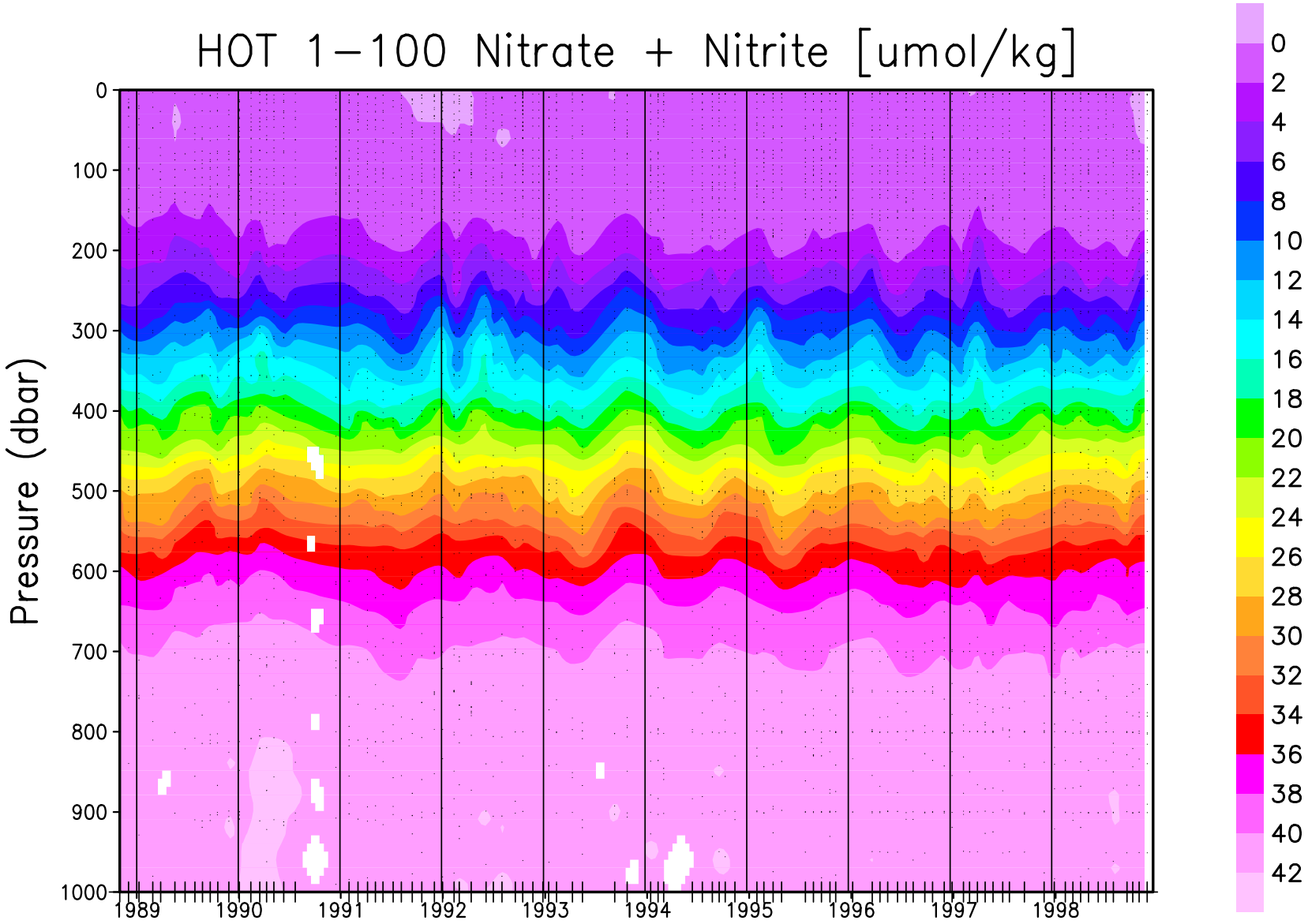

Figure 6.2.9: Contour plot of [nitrate + nitrite] versus pressure for HOT cruises 1-100. Location of samples in the water column are indicated by the solid circles.

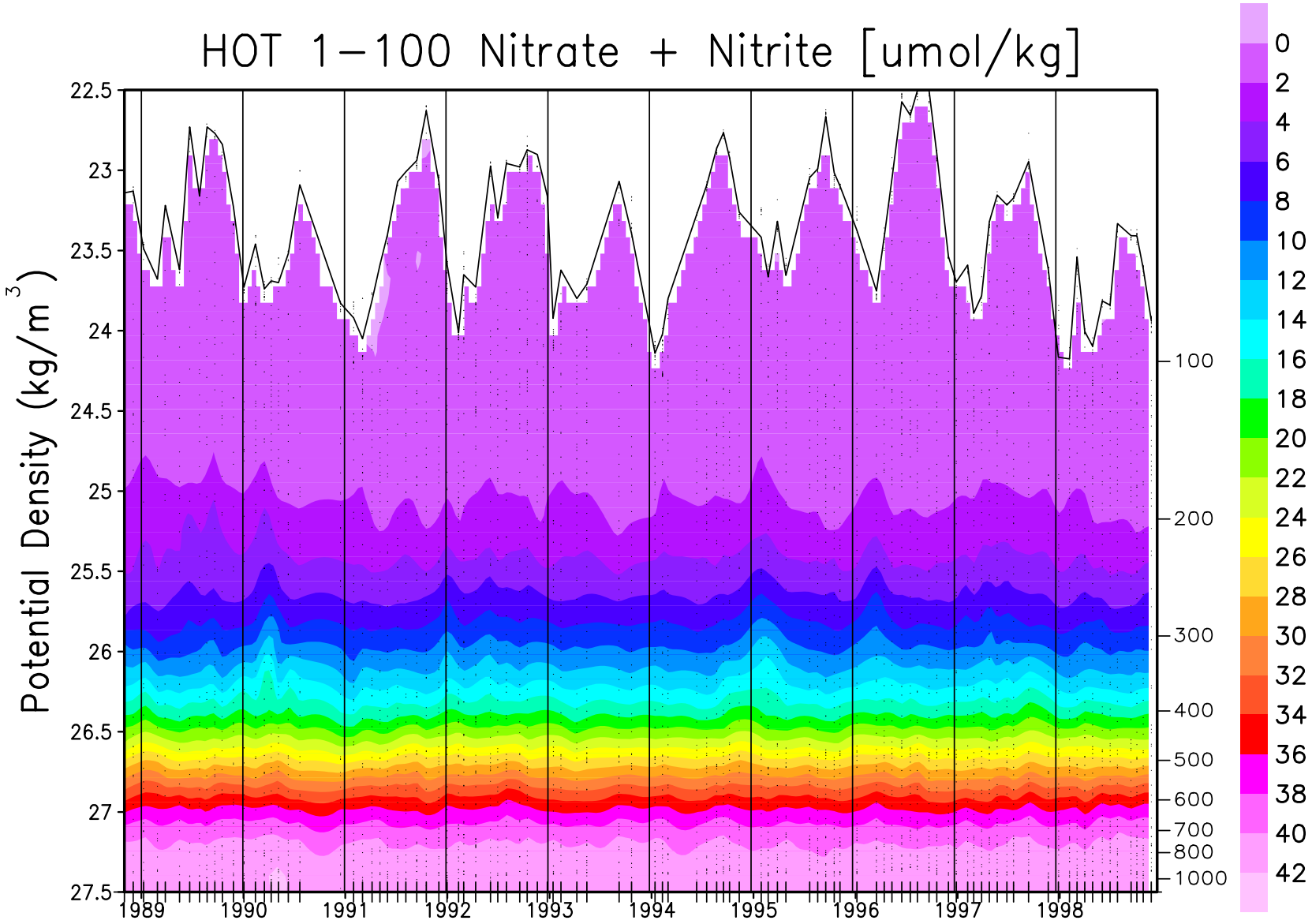

Figure 6.2.10: Contour plot of [nitrate + nitrite] versus potential density (σ_θ) to 27.5 kg m^{-3} for HOT cruises 1-100. The average density of the sea surface is connected by the heavy line.

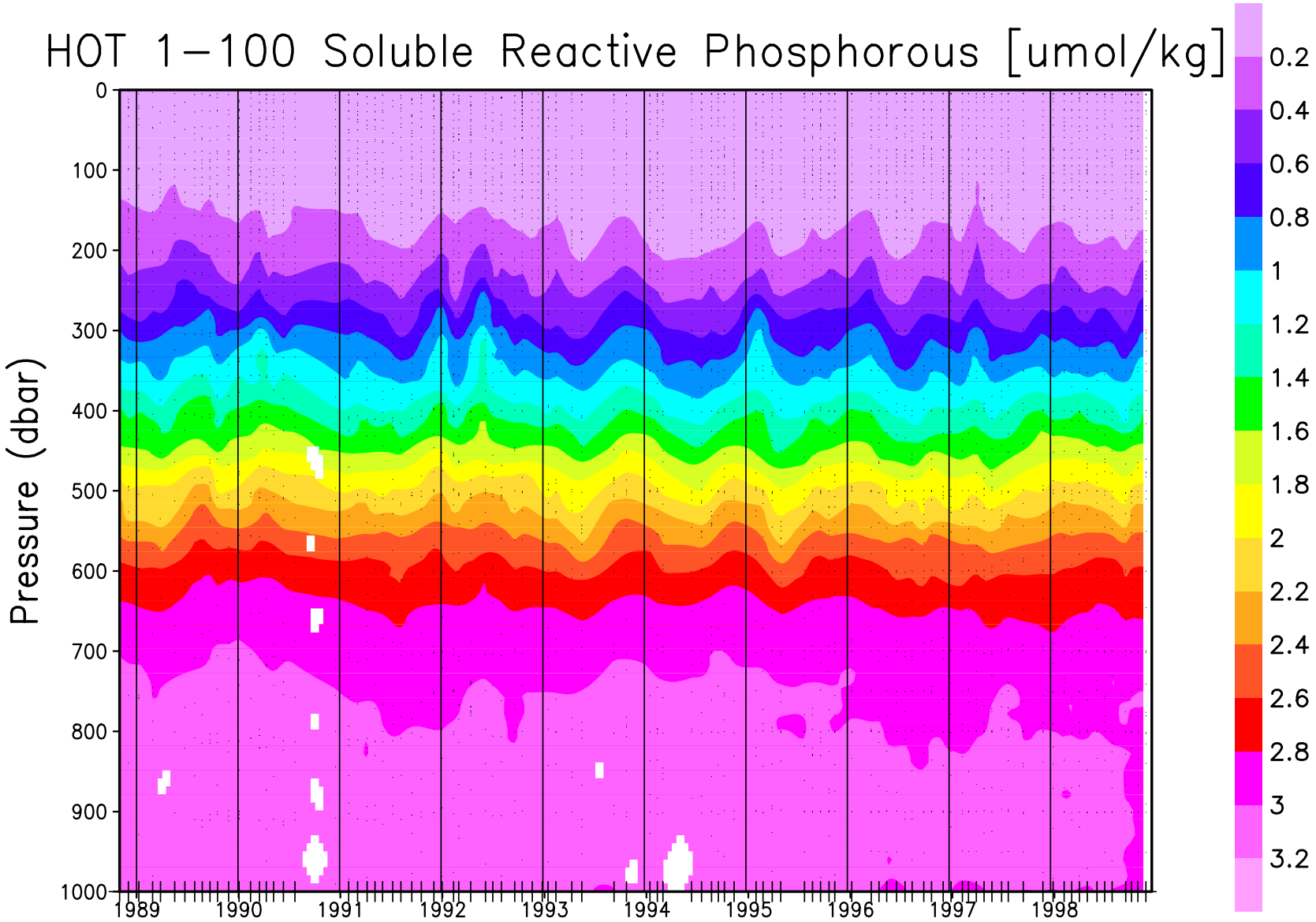

Figure 6.2.11: Contour plot of soluble reactive phosphate versus pressure for HOT cruises 1-100. Location of samples in the water column are indicated by the solid circles.

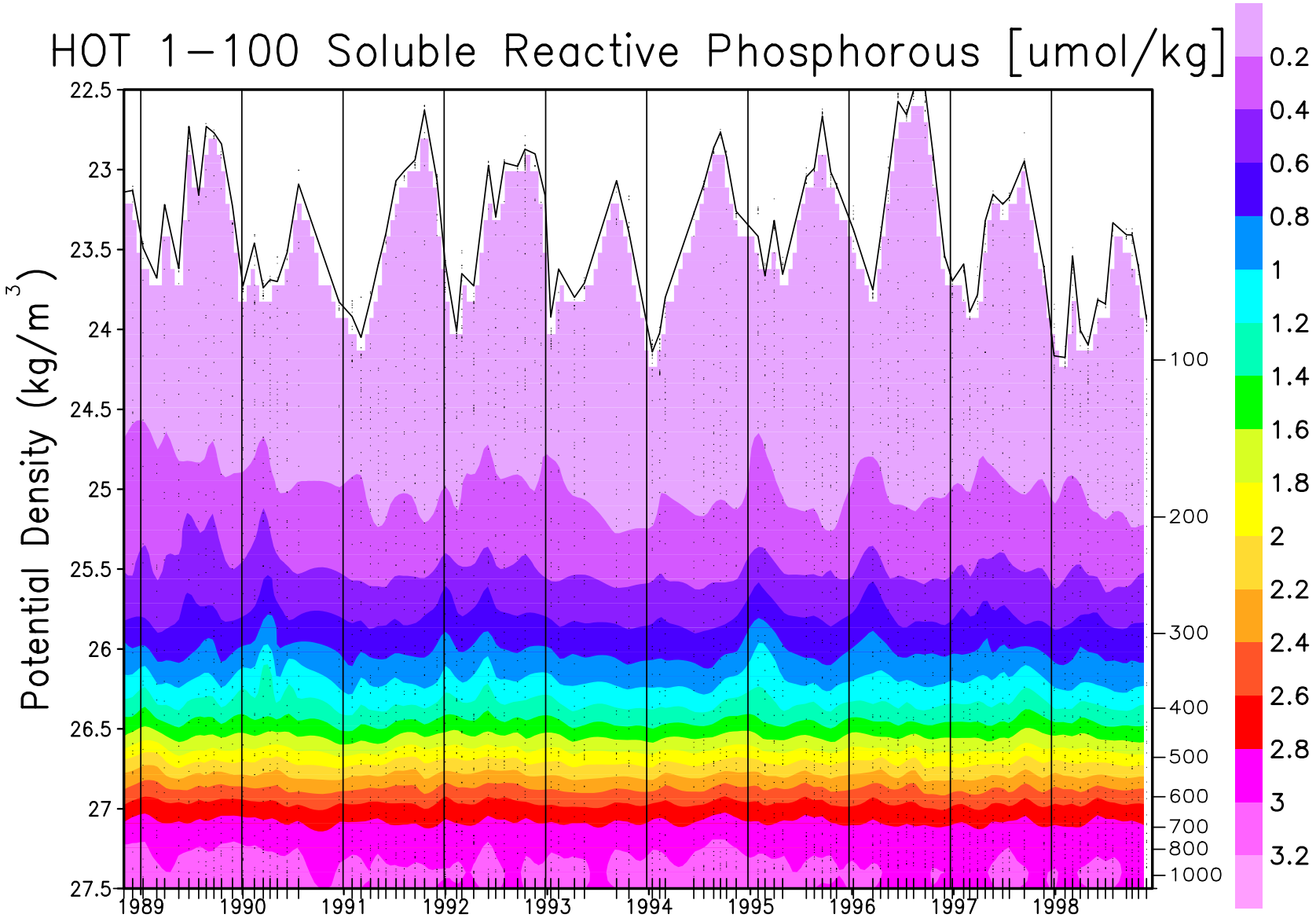

Figure 6.2.12: Contour plot of soluble reactive phosphate versus potential density (σ_θ) to 27.5 kg m^{-3} for HOT cruises 1-100. The average density of the sea surface is connected by the heavy line.

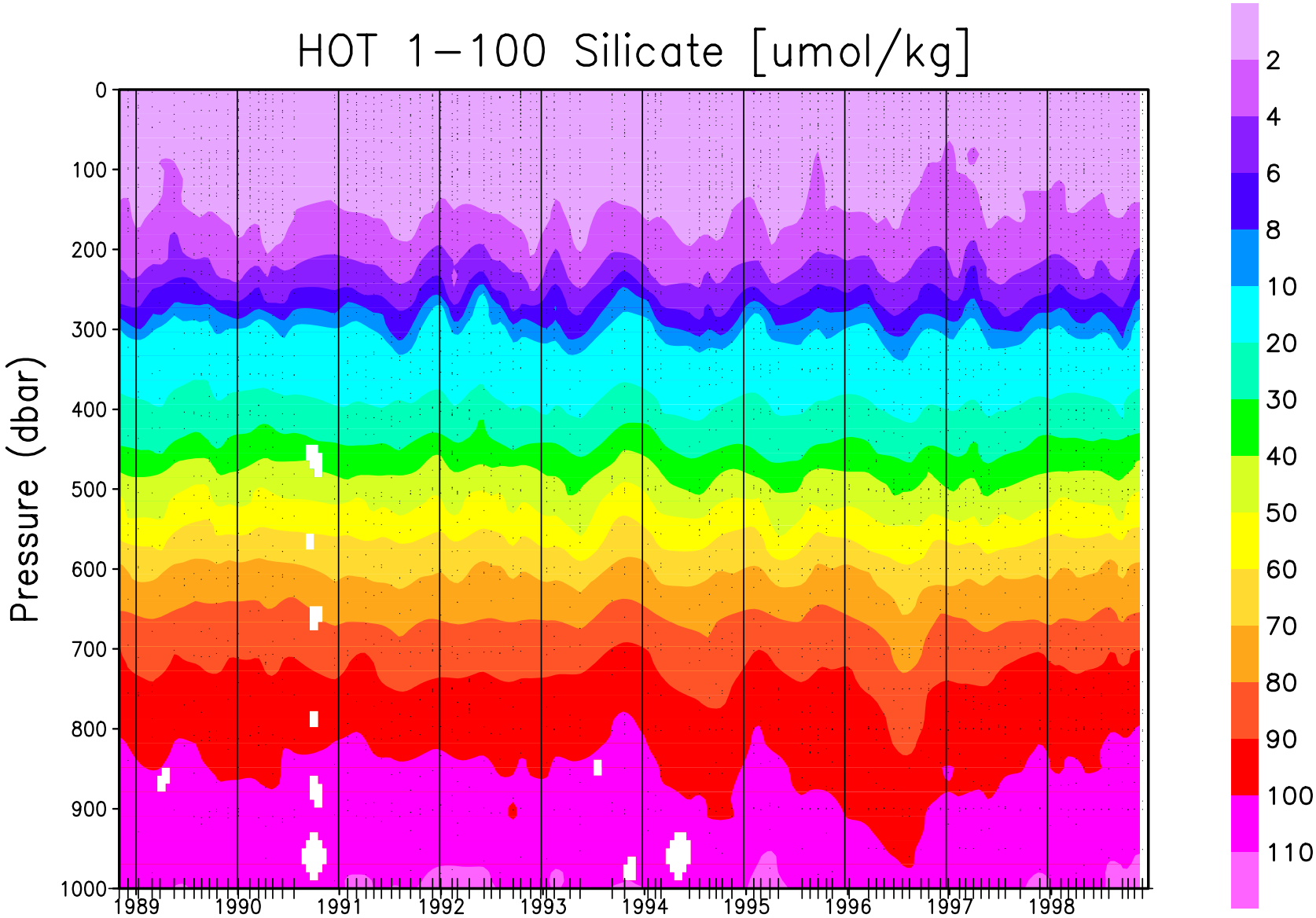

Figure 6.2.13: Contour plot of silicate versus pressure for HOT cruises 1-100. Location of samples in the water column are indicated by the solid circles.

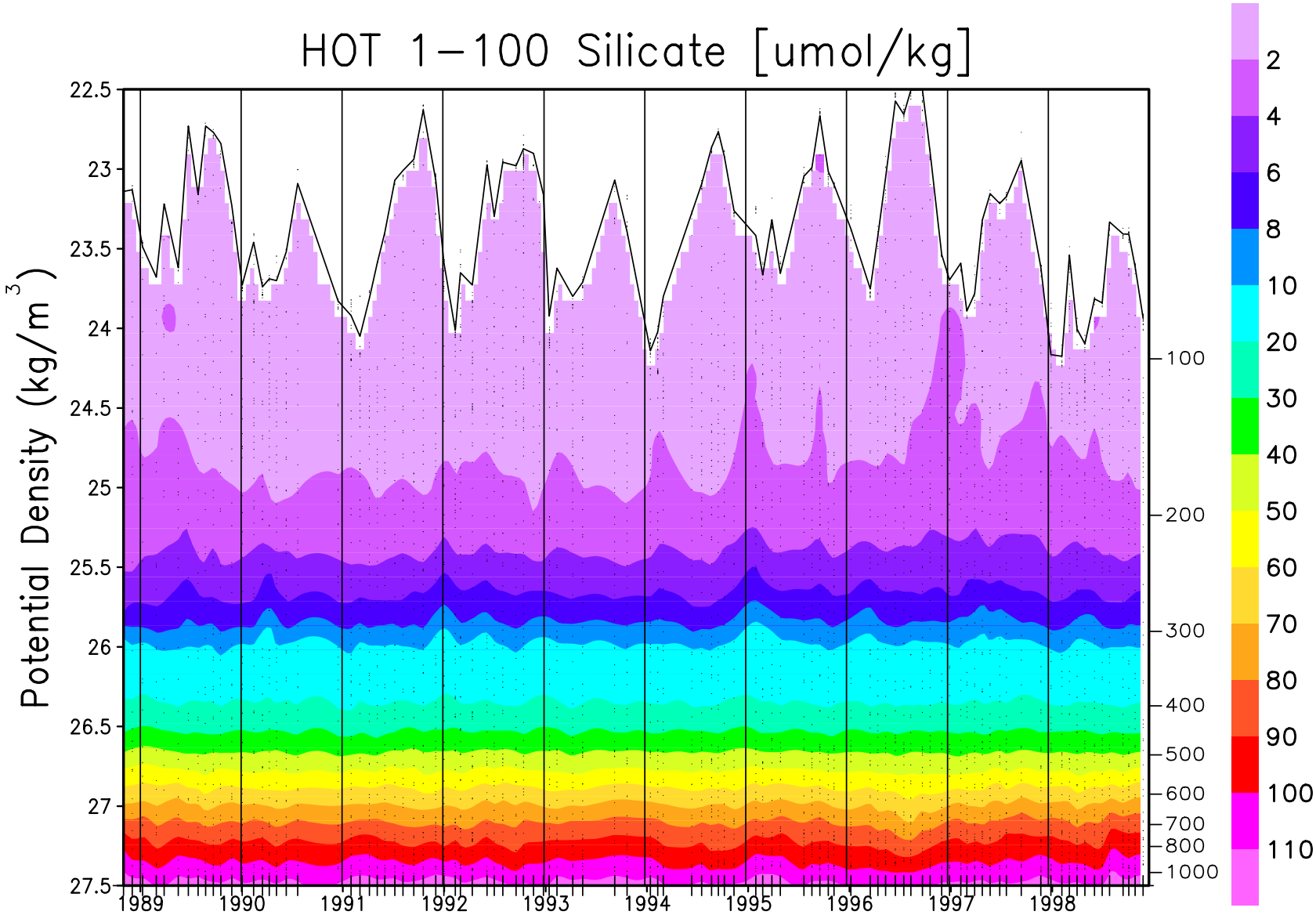

Figure 6.2.14: Contour plot of silicate versus potential density (σ_θ) to 27.5 kg m^{-3} for HOT cruises 1-100. The average density of the sea surface is connected by the heavy line.

6.3. Flash Fluorescence and Beam Transmission

Figures 6.3.1-10: Stack plots of flash fluorescence and beam transmission (when available) collected at Station ALOHA on HOT 23-32. Upper two panels show flash fluorescence data collected on each cruise plotted versus pressure to 250 dbar and potential density to 26 σ_θ.

Figure 6.3.11: Stack plots of averaged night-time fluorescence profiles plotted versus pressure to 250 dbar collected on each HOT cruise in from 1988 through 1991. Upper panel shows averaged profiles collected in 1988 and 1989. Middle panel shows profiles collected in 1990. Lower panel shows profiles collected in 1991. The data collection date is shown at the top of each panel.

Figure 6.3.12: As in 6.3.11, except profiles are plotted versus potential density to 26 σ_θ.

Figure 6.3.13: Stack plots of averaged beam transmission profiles collected in 1991. Upper panel shows profiles plotted versus pressure to 250 dbar. Lower panel shows profiles plotted versus potential density to 26 σ_θ. The data collection dates are shown at the top of each panel.

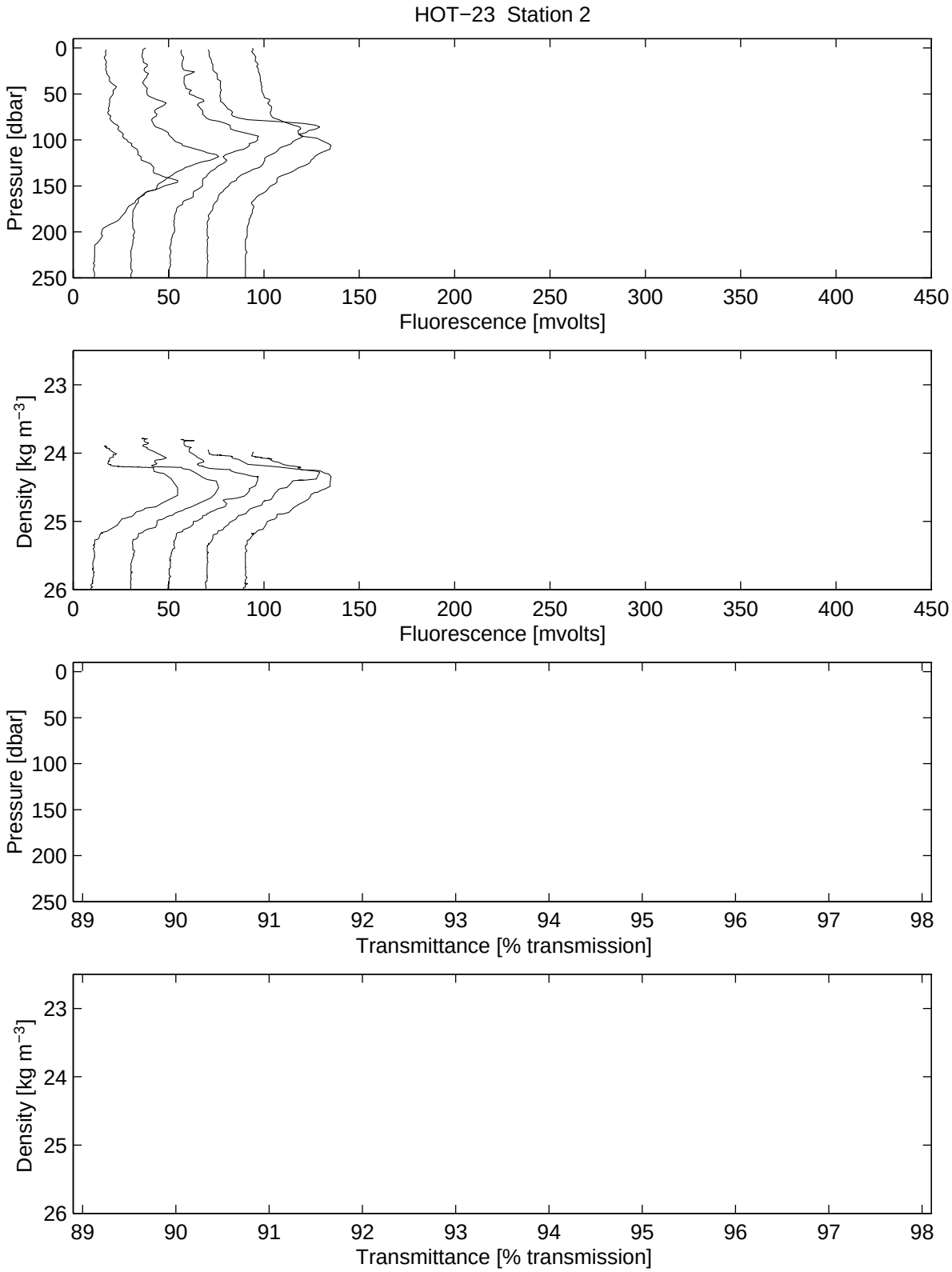
HOT−23 Station 2
Pressure [dbar]
Fluorescence [mvolts]
Density [kg m−3]
Fluorescence [mvolts]
Pressure [dbar]
Transmittance [% transmission]
Density [kg m−3]
Transmittance [% transmission]

Figure 6.3.1

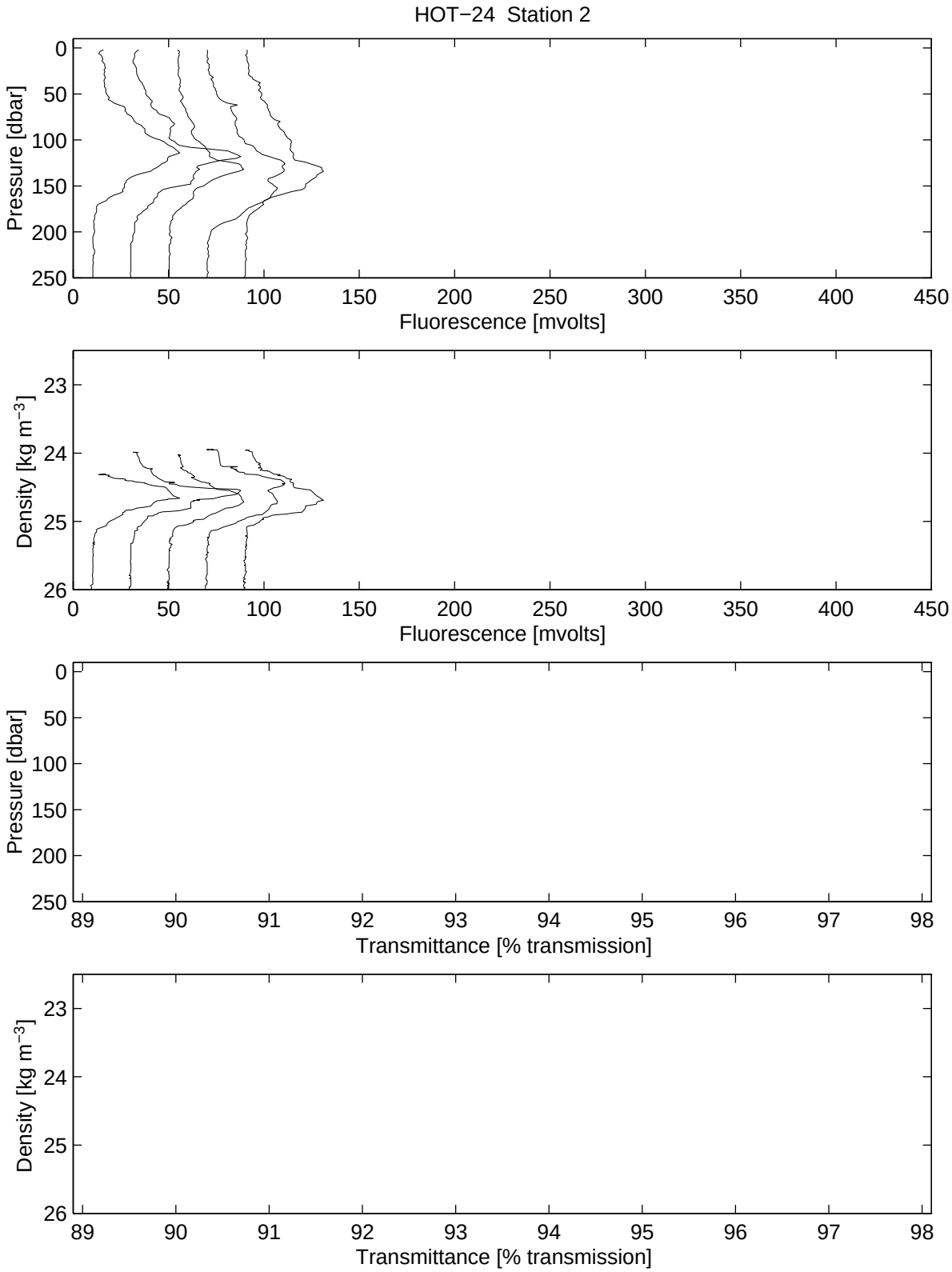
HOT−24 Station 2
Pressure [dbar]
Fluorescence [mvolts]
Density [kg m−3]
Fluorescence [mvolts]
Pressure [dbar]
Transmittance [% transmission]
Density [kg m−3]
Transmittance [% transmission]

Figure 6.3.2

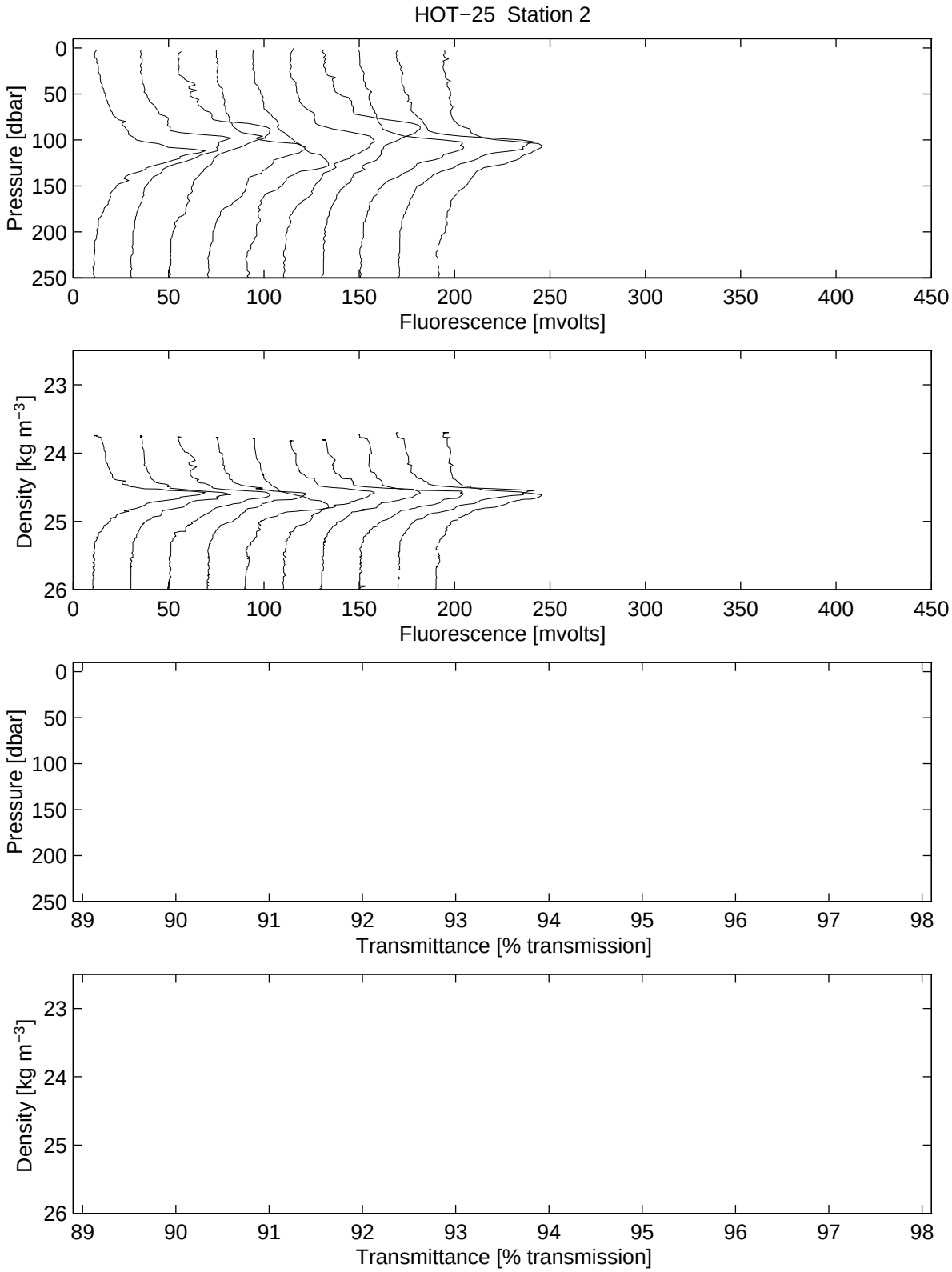
HOT−25 Station 2
Pressure [dbar]
Fluorescence [mvolts]
Density [kg m−3]
Fluorescence [mvolts]
Pressure [dbar]
Transmittance [% transmission]
Density [kg m−3]
Transmittance [% transmission]

Figure 6.3.3

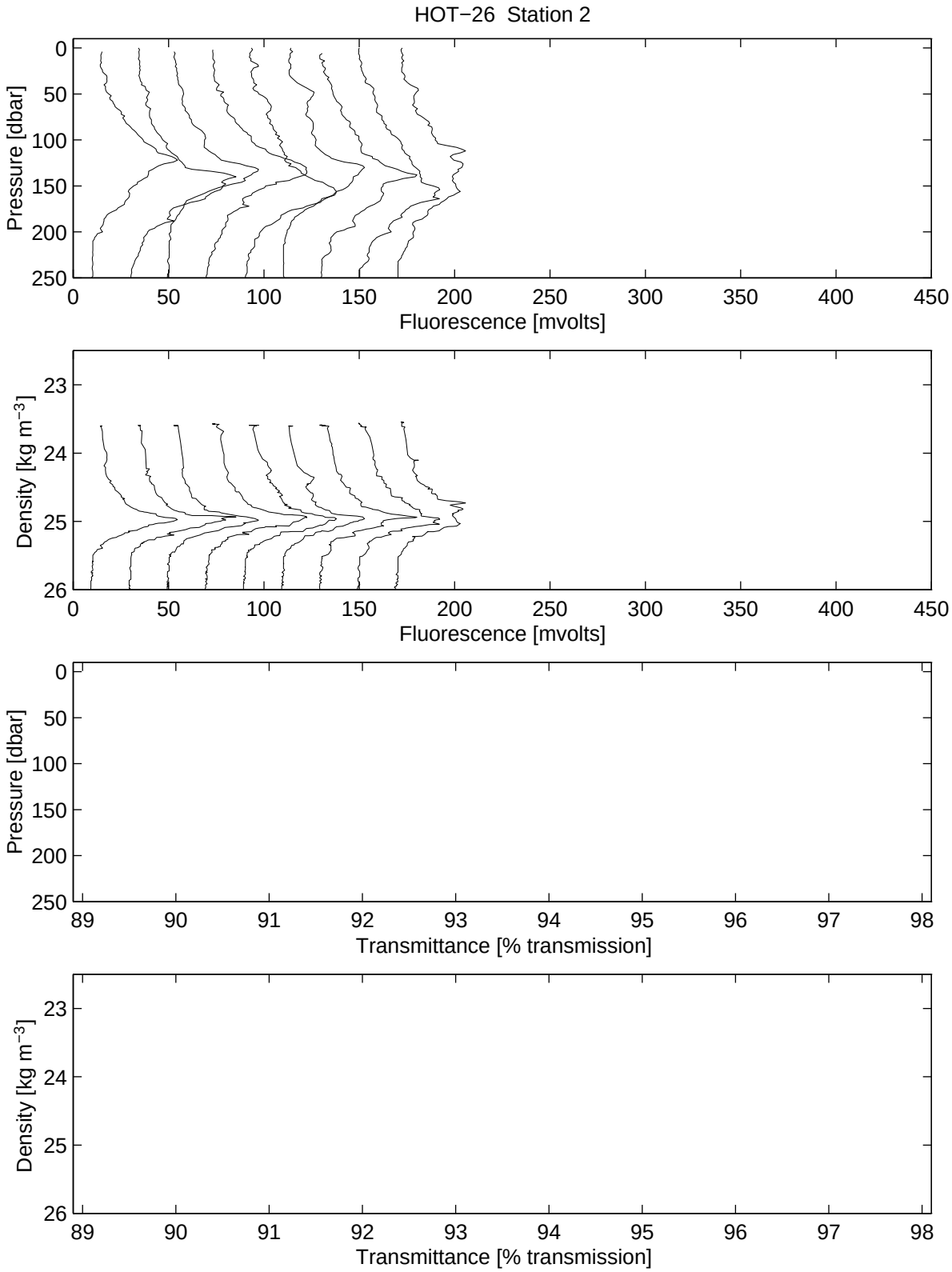
HOT−26 Station 2
Pressure [dbar]
Fluorescence [mvolts]
Density [kg m−3]
Fluorescence [mvolts]
Pressure [dbar]
Transmittance [% transmission]
Density [kg m−3]
Transmittance [% transmission]

Figure 6.3.4

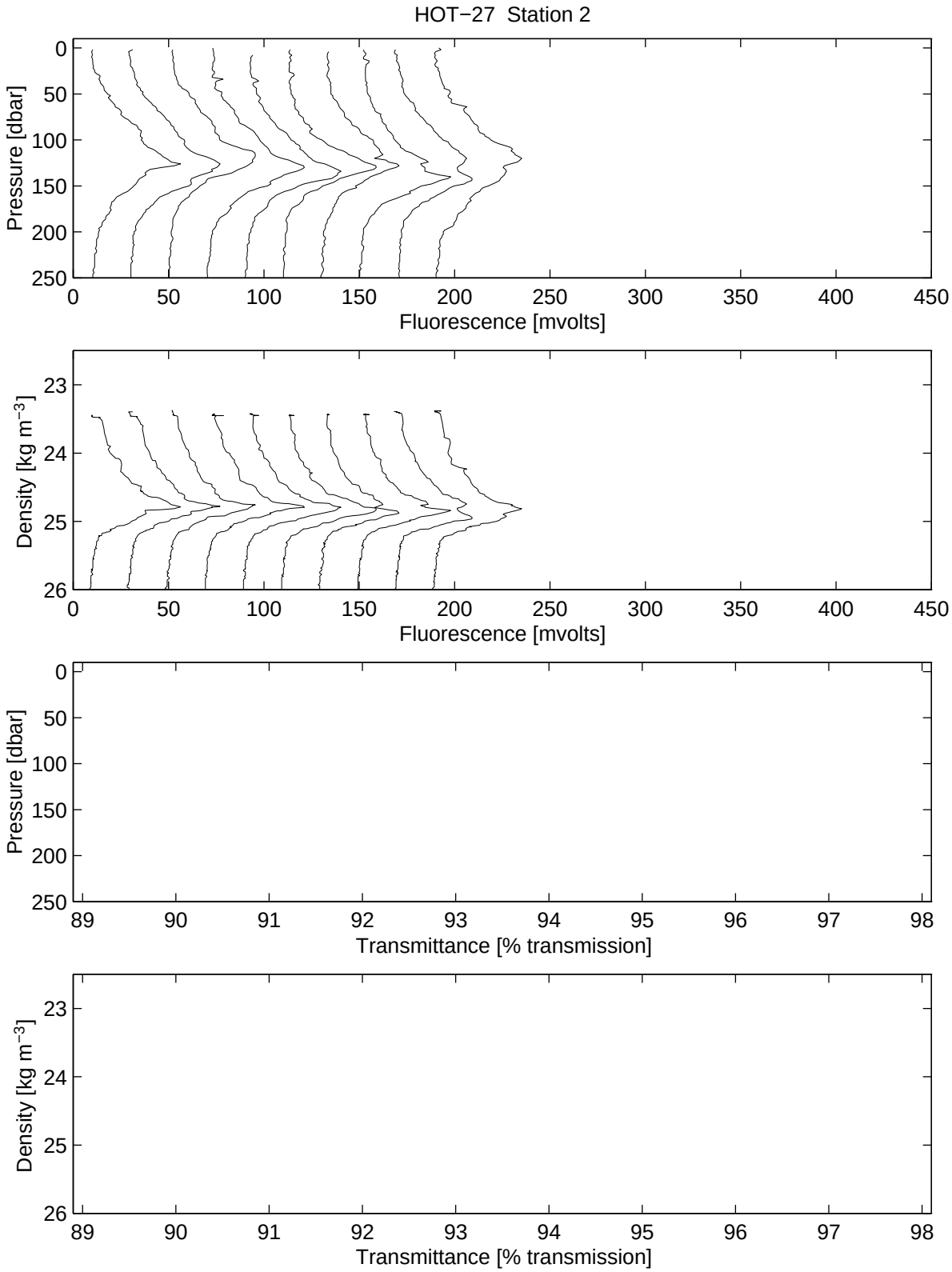
HOT−27 Station 2
Pressure [dbar]
Fluorescence [mvolts]
Density [kg m−3]
Fluorescence [mvolts]
Pressure [dbar]
Transmittance [% transmission]
Density [kg m−3]
Transmittance [% transmission]

Figure 6.3.5

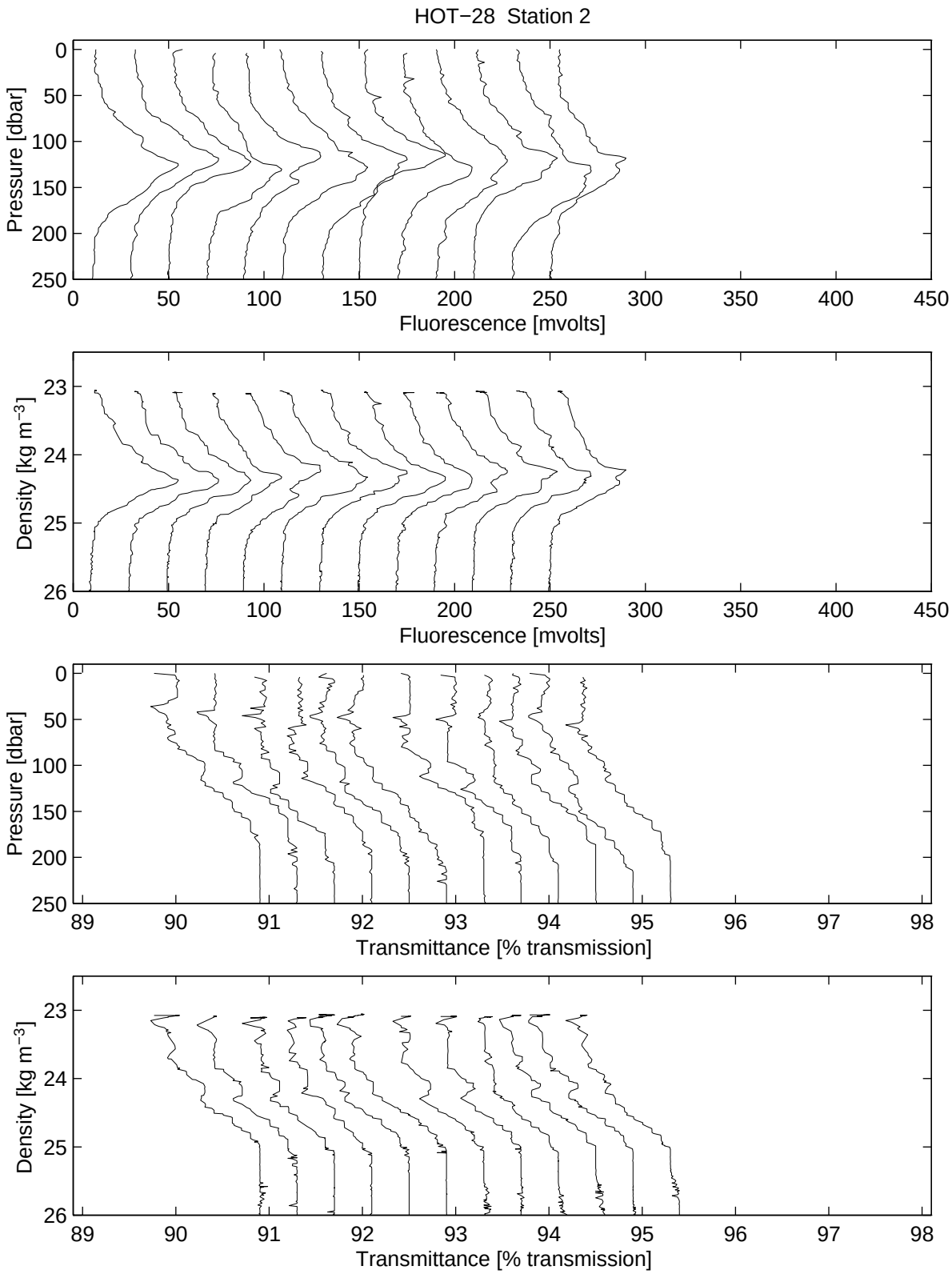
HOT−28 Station 2
Pressure [dbar]
Fluorescence [mvolts]
Density [kg m−3]
Fluorescence [mvolts]
Pressure [dbar]
Transmittance [% transmission]
Density [kg m−3]
Transmittance [% transmission]

Figure 6.3.6

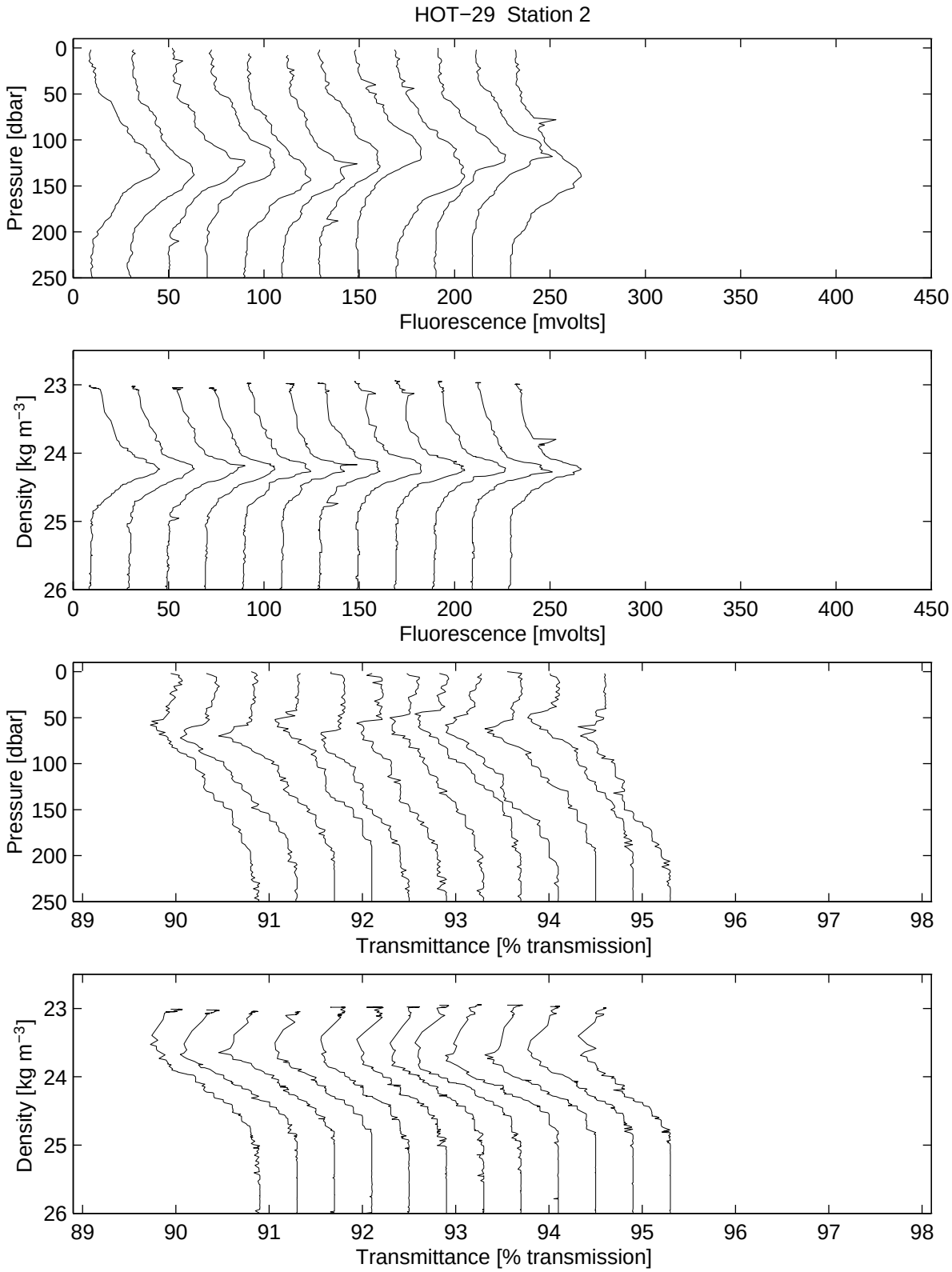
HOT−29 Station 2
Pressure [dbar]
Fluorescence [mvolts]
Density [kg m−3]
Fluorescence [mvolts]
Pressure [dbar]
Transmittance [% transmission]
Density [kg m−3]
Transmittance [% transmission]

Figure 6.3.7

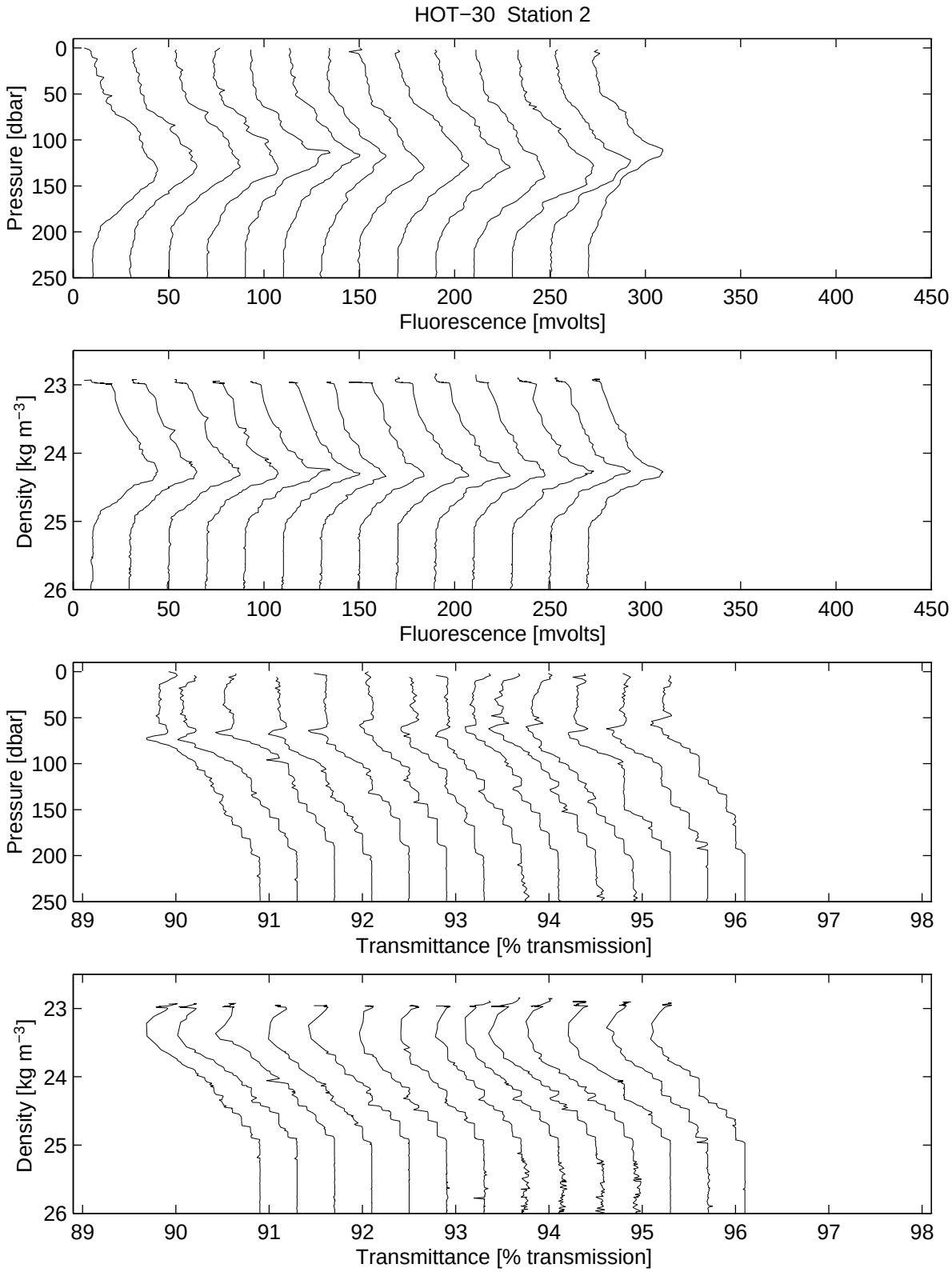
HOT−30 Station 2
Pressure [dbar]
Fluorescence [mvolts]
Density [kg m−3]
Fluorescence [mvolts]
Pressure [dbar]
Transmittance [% transmission]
Density [kg m−3]
Transmittance [% transmission]

Figure 6.3.8

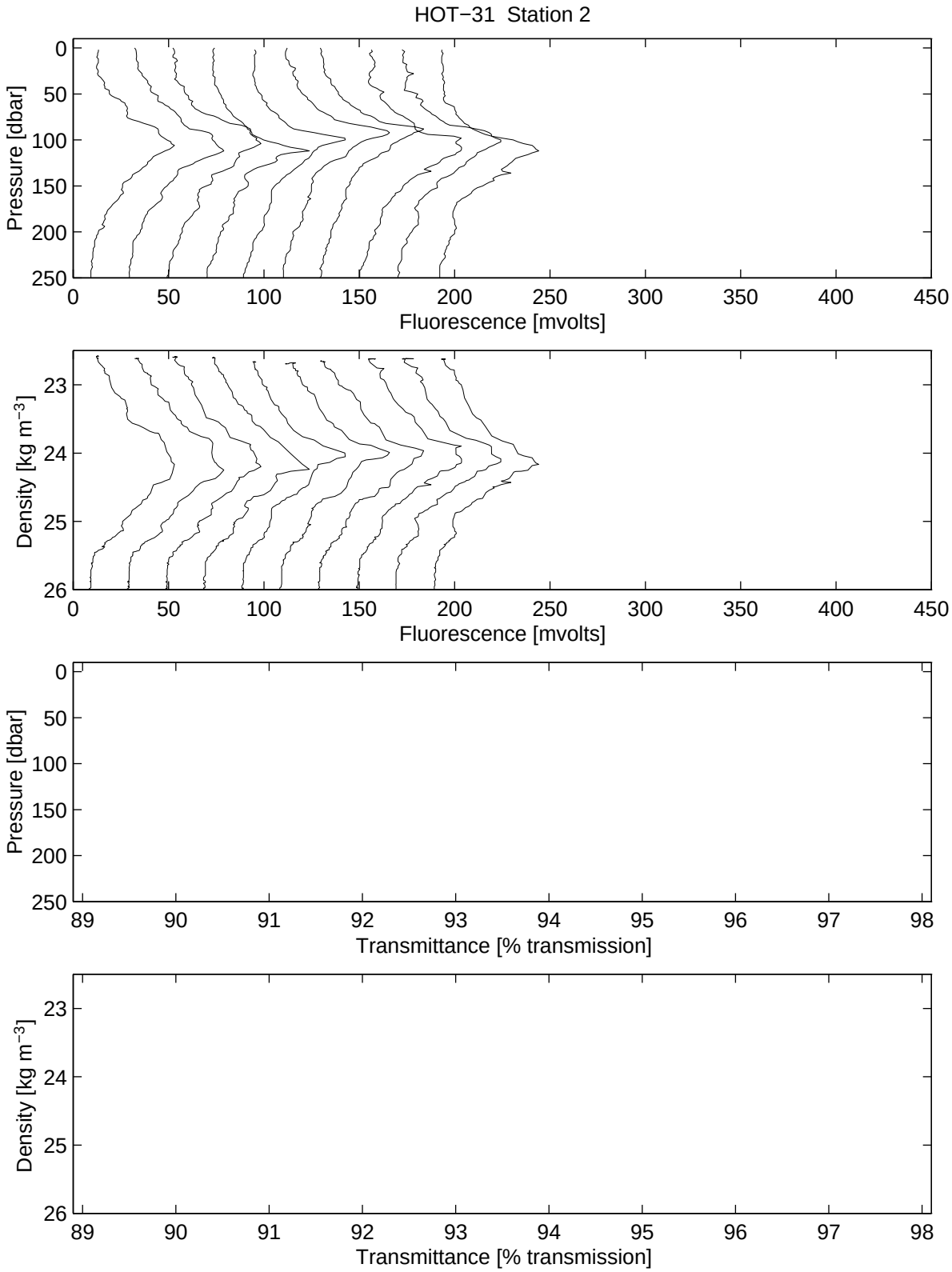
HOT−31 Station 2
Pressure [dbar]
Fluorescence [mvolts]
Density [kg m−3]
Fluorescence [mvolts]
Pressure [dbar]
Transmittance [% transmission]
Density [kg m−3]
Transmittance [% transmission]

Figure 6.3.9

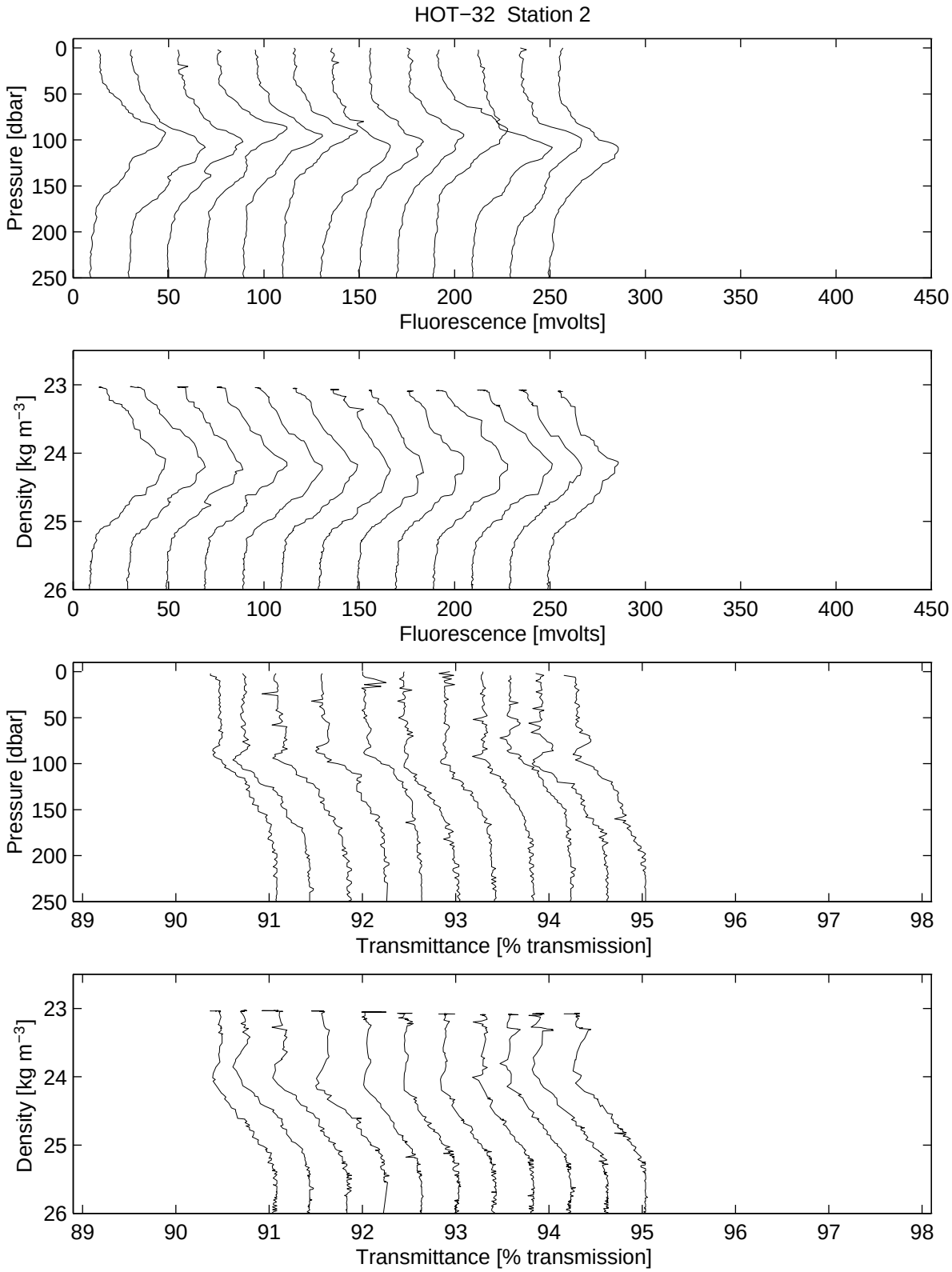
HOT−32 Station 2
Pressure [dbar]
Fluorescence [mvolts]
Density [kg m−3]
Fluorescence [mvolts]
Pressure [dbar]
Transmittance [% transmission]
Density [kg m−3]
Transmittance [% transmission]

Figure 6.3.10

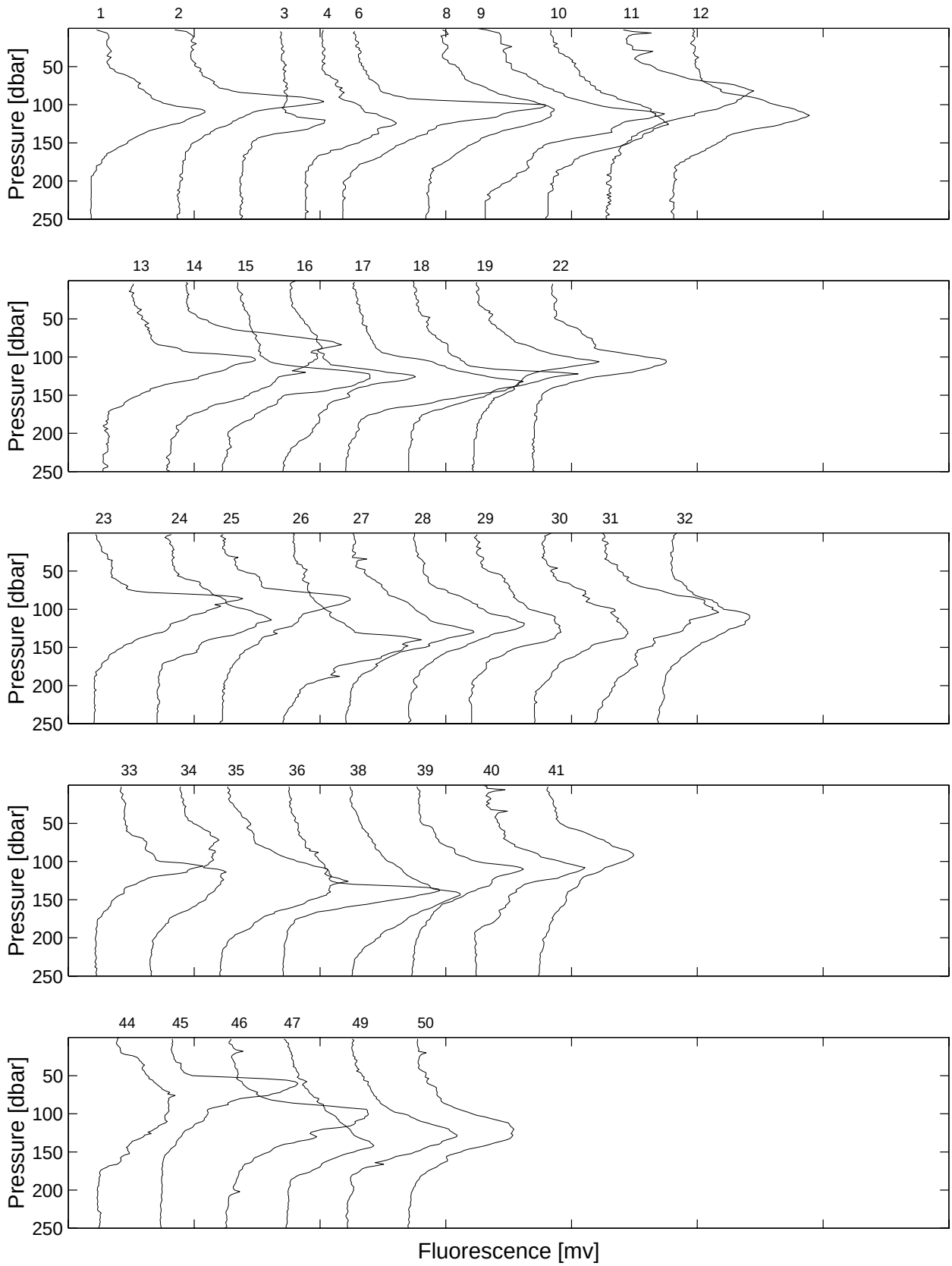
1 2 3 4 6 8 9 10 11 12
13 14 15 16 17 18 19 22
23 24 25 26 27 28 29 30 31 32
33 34 35 36 38 39 40 41
44 45 46 47 49 50
Pressure [dbar]
50
100
150
200
250
Fluorescence [mv]

Figure 6.3.11

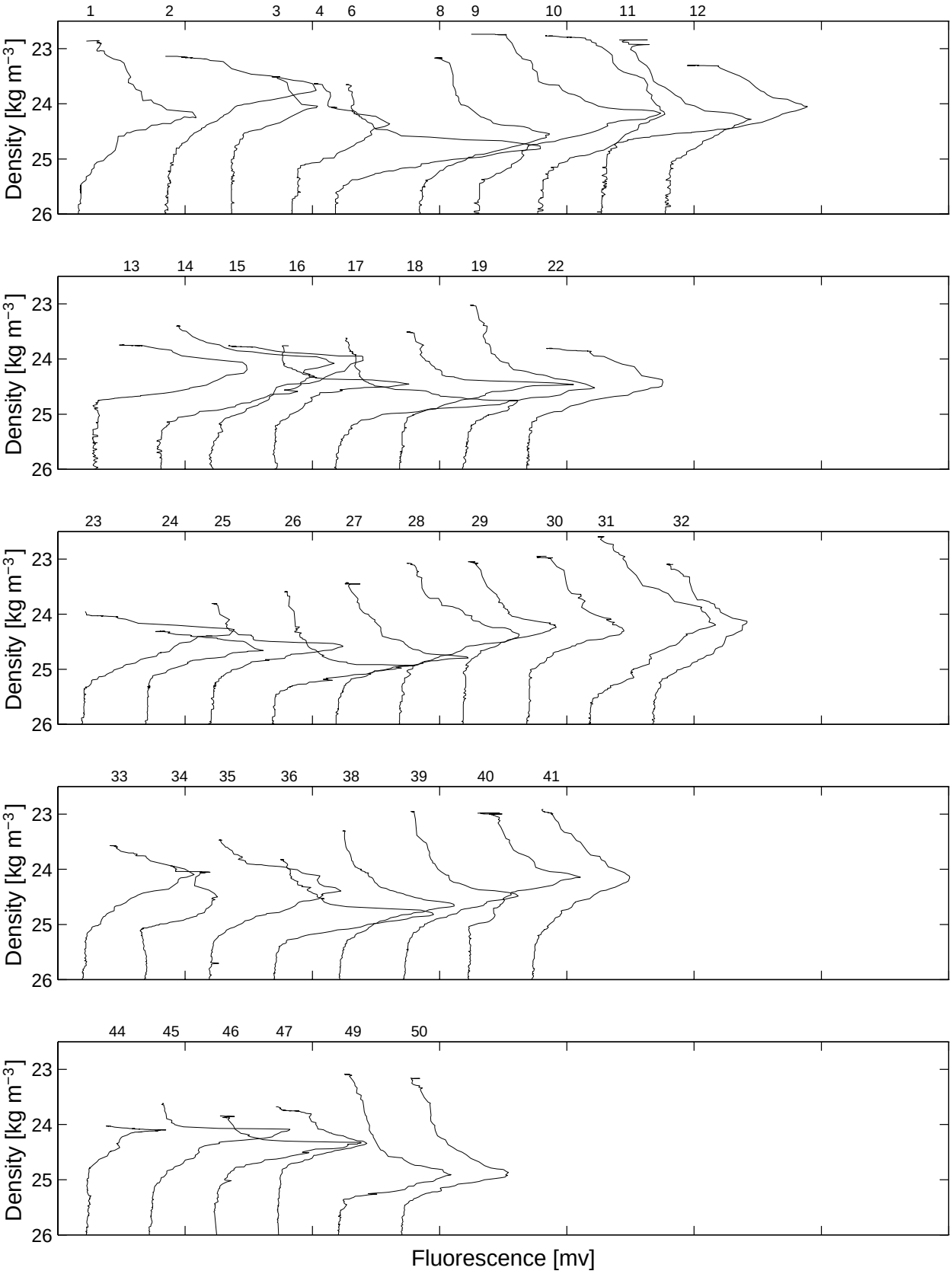
1 2 3 4 6 8 9 10 11 12
13 14 15 16 17 18 19 22
23 24 25 26 27 28 29 30 31 32
33 34 35 36 38 39 40 41
44 45 46 47 49 50
Density [kg m−3]
23
24
25
26
Fluorescence [mv]

Figure 6.3.12

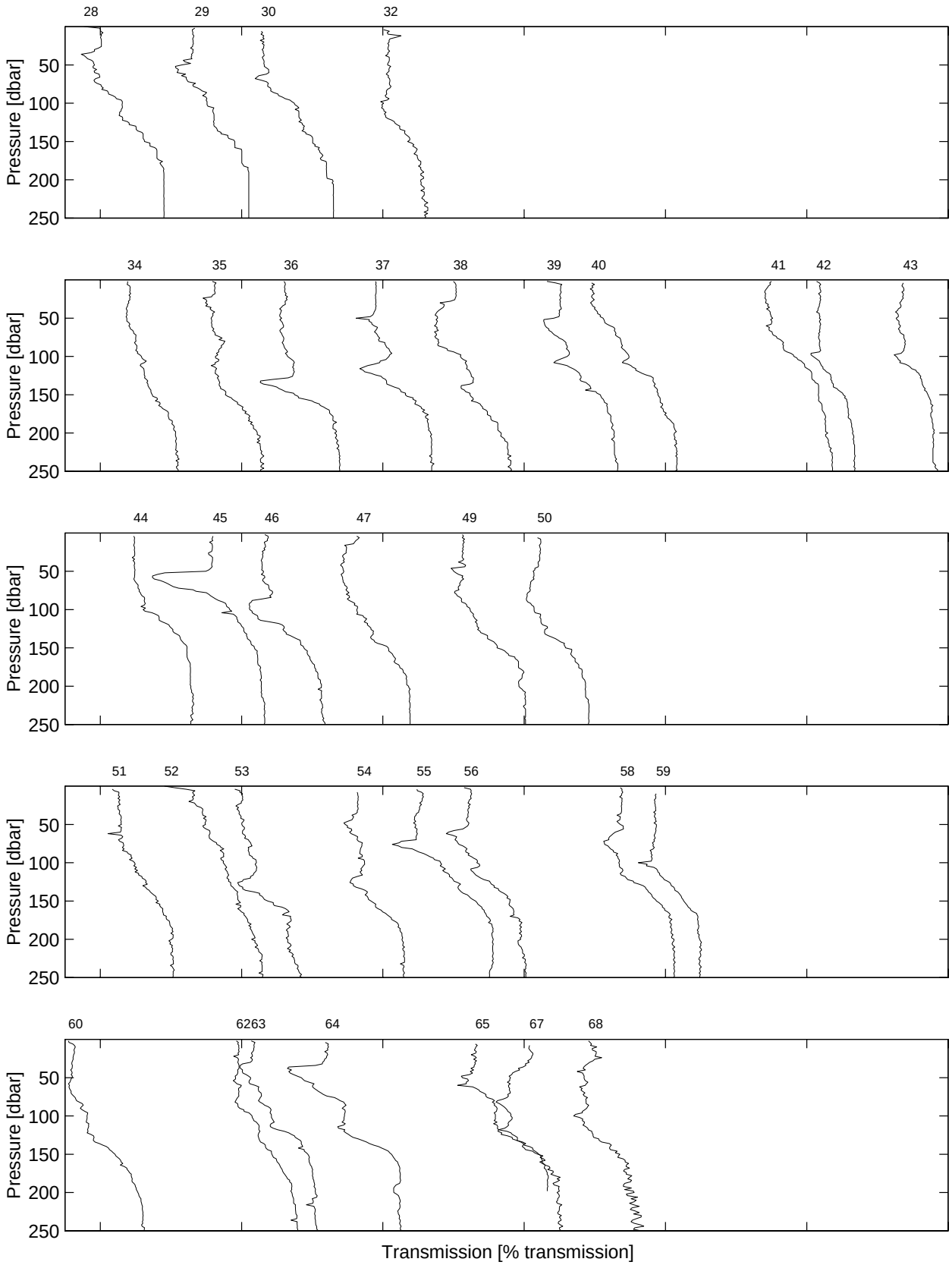
28
29
30
32
34
35
36
37
38
39
40
41
42
43
44
45
46
47
49
50
51
52
53
54
55
56
58
59
60
6263
64
65
67
68
Pressure [dbar]
50
100
150
200
250
Transmission [% transmission]

Figure 6.3.13

6.4. Biogeochemistry

Figure 6.4.1: Titration alkalinity and DIC in surface waters (0-50 dbar) at Station ALOHA. Upper panel: Titration alkalinity plotted versus time for all HOT cruises. Error bars represent standard deviation of pooled samples collected between at less than 50 dbar. Lower panel: As in upper panel except for DIC.

Figure 6.4.2: Contoured time-series of DIC in the upper 1000 dbar at Station ALOHA.

Figure 6.4.3: As in Figure 6.4.2, except DIC has been normalized to 35 ppt salinity.

Figure 6.4.4: Contoured time-series of titration alkalinity in the upper 1000 dbar at Station ALOHA.

Figure 6.4.5: As in Figure 6.4.4, except titration alkalinity has been normalized to 35 ppt salinity.

Figure 6.4.6: Soluble reactive phosphorus measured by the MAGIC procedure in the upper 250 dbar at Station ALOHA on each HOT cruise where data are available.

Figure 6.4.7: Nitrate plus nitrite measured by the nitrogen oxides analyzer in the upper 250 dbar at Station ALOHA in 1991.

Figure 6.4.8: Contoured time-series of chlorophyll *a* in the upper 200 dbar for all HOT cruises.

Figure 6.4.9: Particulate carbon at Station ALOHA on all HOT cruises. Upper panel: Mean particulate carbon concentration in the upper 50 dbar. Error bar represents the standard deviation of pooled samples collected. Lower panel: As in upper panel but for 50 to 100 dbar.

Figure 6.4.10: As in Figure 6.4.9 except for particulate nitrogen.

Figure 6.4.11: As in Figure 6.4.10 except for particulate phosphorus.

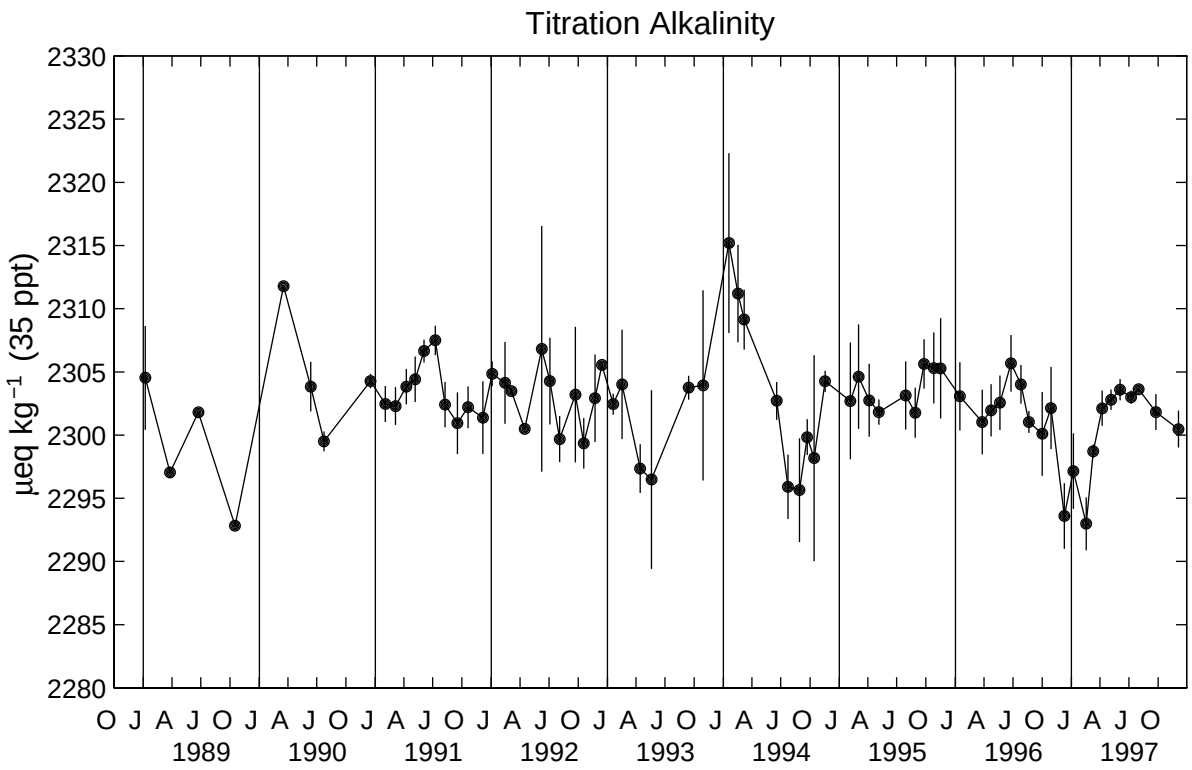
Titration Alkalinity
µeq kg⁻¹ (35 ppt)
2330
2325
2320
2315
2310
2305
2300
2295
2290
2285
2280
O J A J O J A J O J A J O J A J O J A J O J A J O J A J O J A J O J A J O J A J O
1989
1990
1991
1992
1993
1994
1995
1996
1997

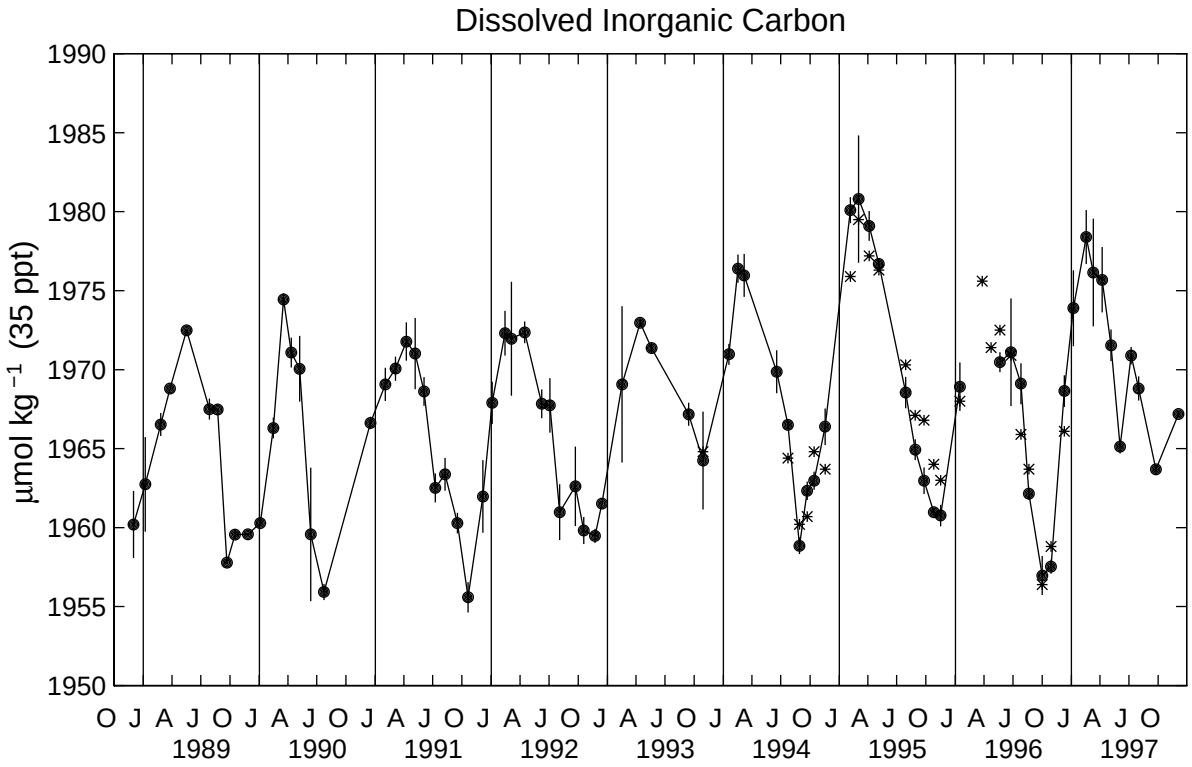
Dissolved Inorganic Carbon
µmol kg⁻¹ (35 ppt)
1990
1985
1980
1975
1970
1965
1960
1955
1950
O J A J O J A J O J A J O J A J O J A J O J A J O J A J O J A J O J A J O J A J O
1989
1990
1991
1992
1993
1994
1995
1996
1997

Figure 6.4.1

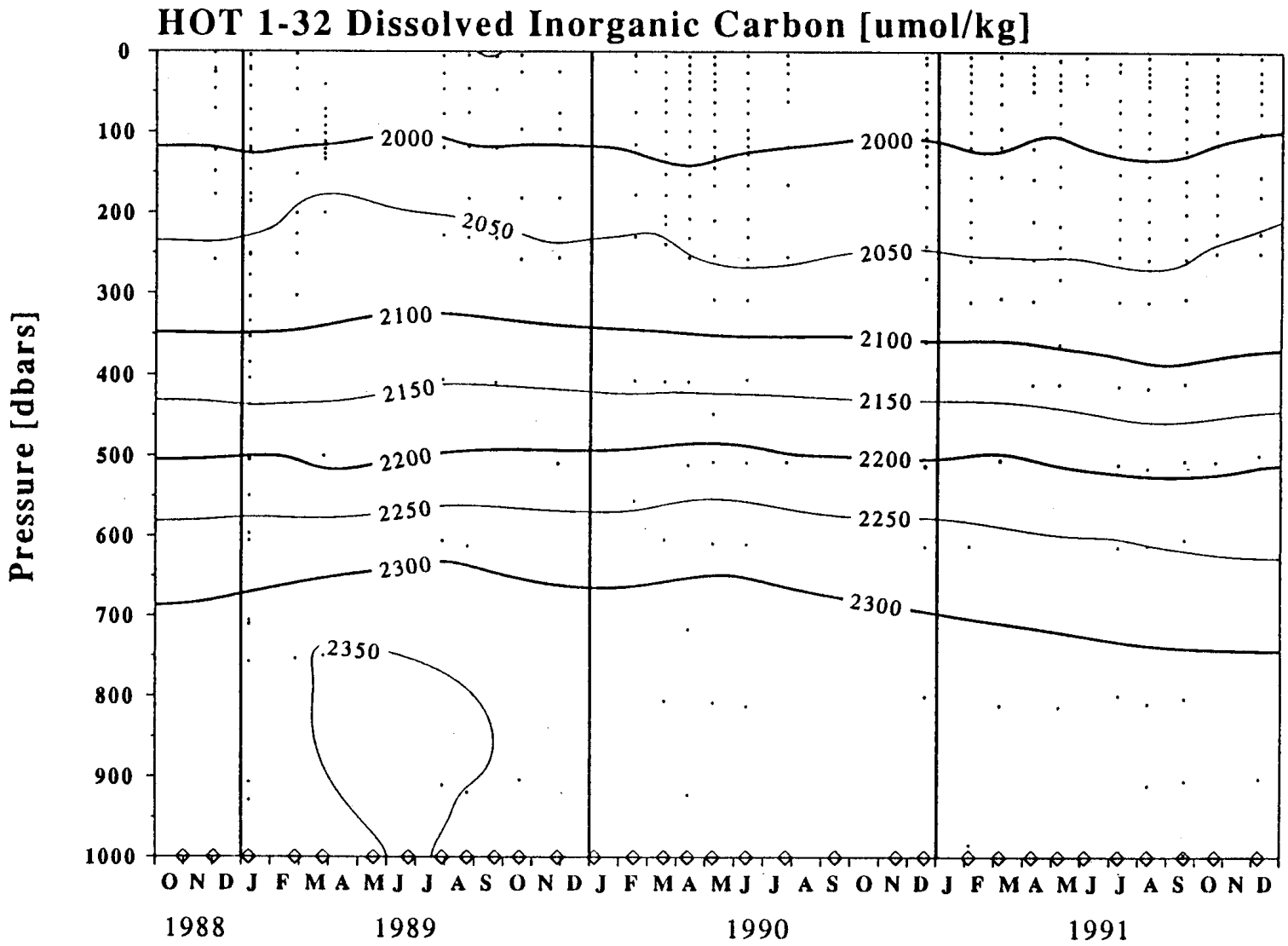
HOT 1-32 Dissolved Inorganic Carbon [umol/kg]
Pressure [dbars]
0
100
200
300
400
500
600
700
800
900
1000
2000
2050
2100
2150
2200
2250
2300
2350
O N D J F M A M J J A S O N D J F M A M J J A S O N D J F M A M J J A S O N D
1988
1989
1990
1991

Figure 6.4.2

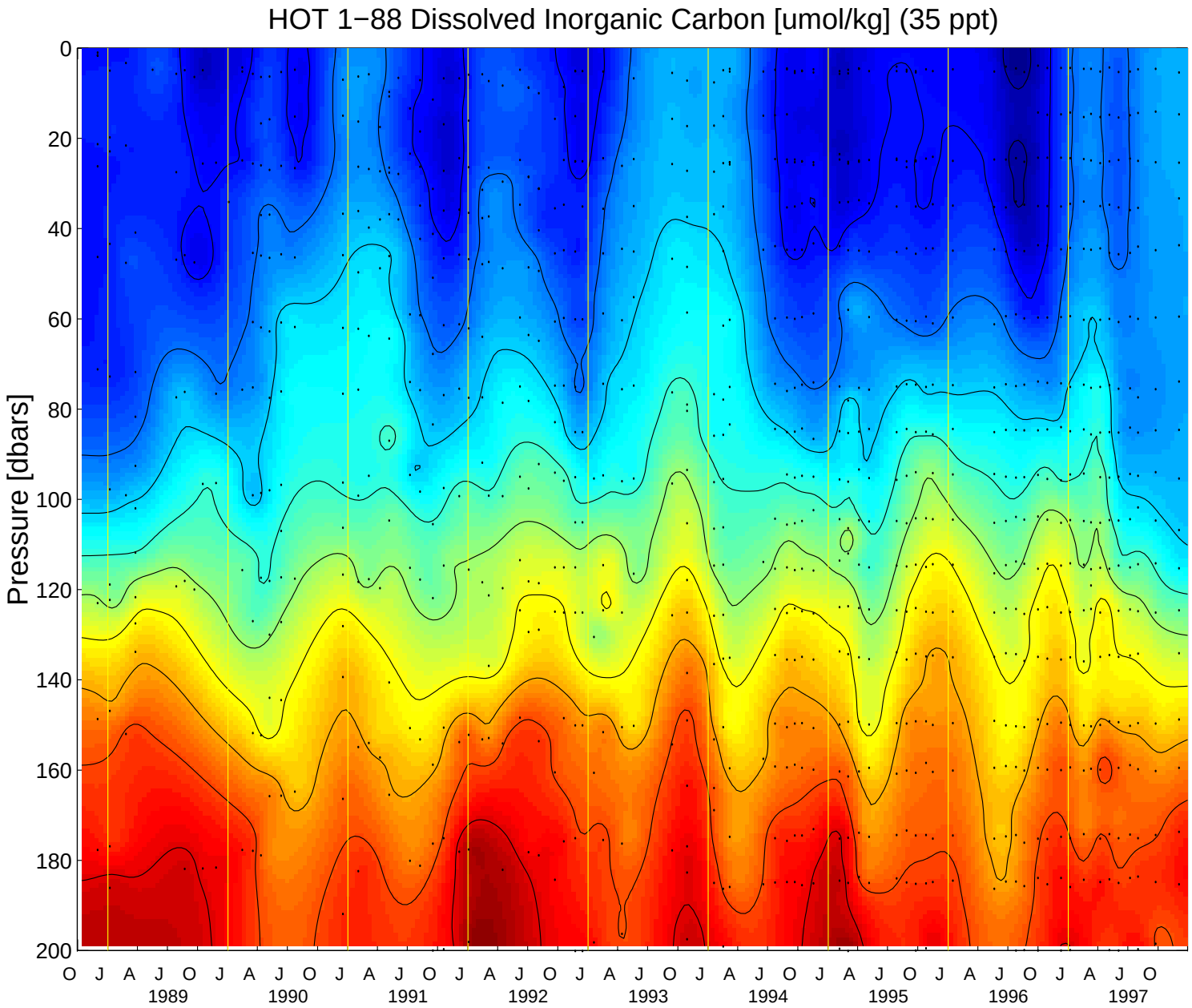
HOT 1−88 Dissolved Inorganic Carbon [umol/kg] (35 ppt)
Pressure [dbars]
0
20
40
60
80
100
120
140
160
180
200
O J A J O J A J O J A J O J A J O J A J O J A J O J A J O J A J O J A J O J A J O
1989
1990
1991
1992
1993
1994
1995
1996
1997

Figure 6.4.3

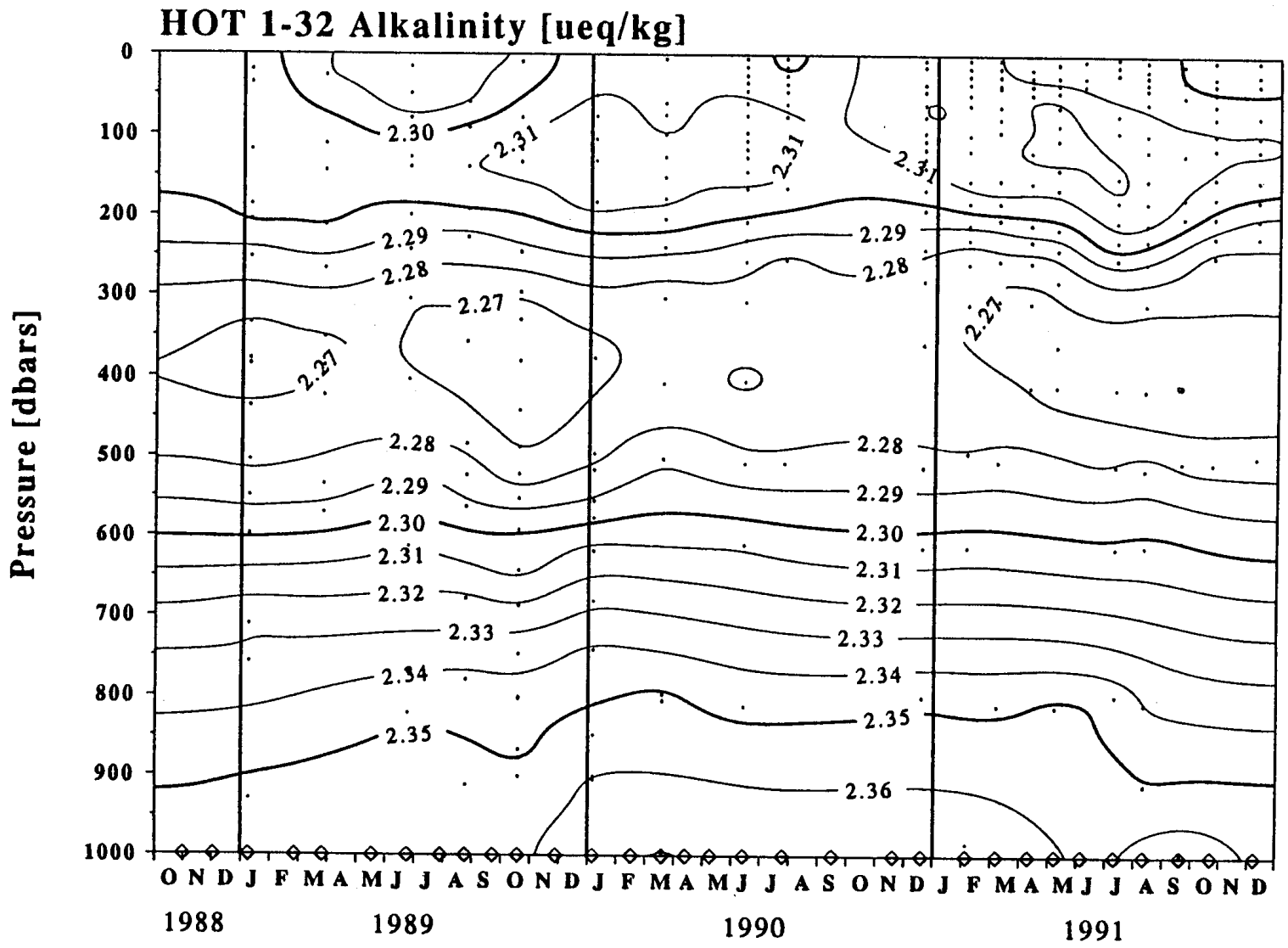
HOT 1-32 Alkalinity [ueq/kg]
Pressure [dbars]
0
100
200
300
400
500
600
700
800
900
1000
2.27
2.28
2.29
2.30
2.31
2.32
2.33
2.34
2.35
2.36
O N D J F M A M J J A S O N D J F M A M J J A S O N D J F M A M J J A S O N D
1988
1989
1990
1991

Figure 6.4.4

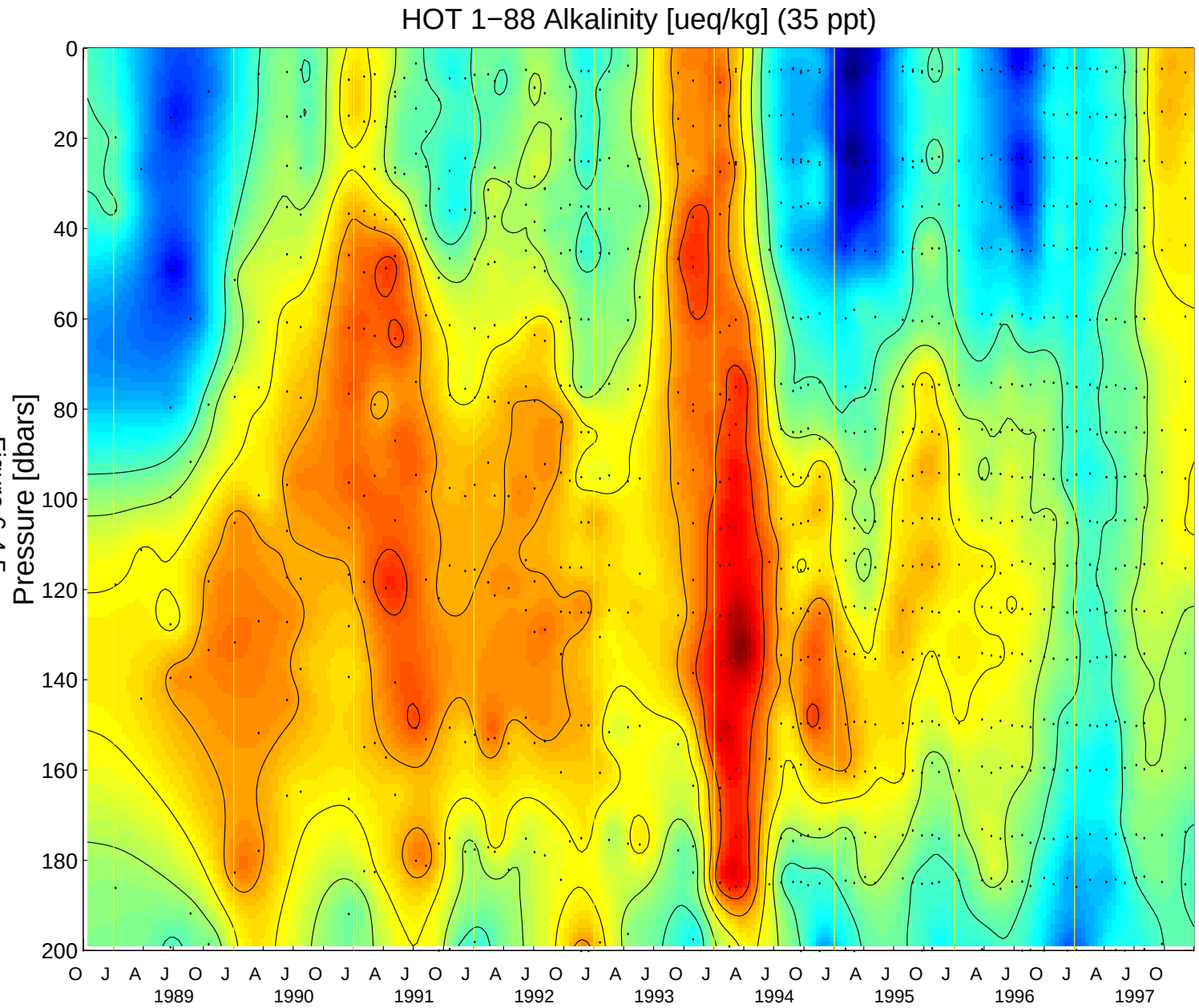
HOT 1−88 Alkalinity [ueq/kg] (35 ppt)
Pressure [dbars]
0
20
40
60
80
100
120
140
160
180
200
O J A J O J A J O J A J O J A J O J A J O J A J O J A J O J A J O J A J O
1989
1990
1991
1992
1993
1994
1995
1996
1997

Figure 6.4.5

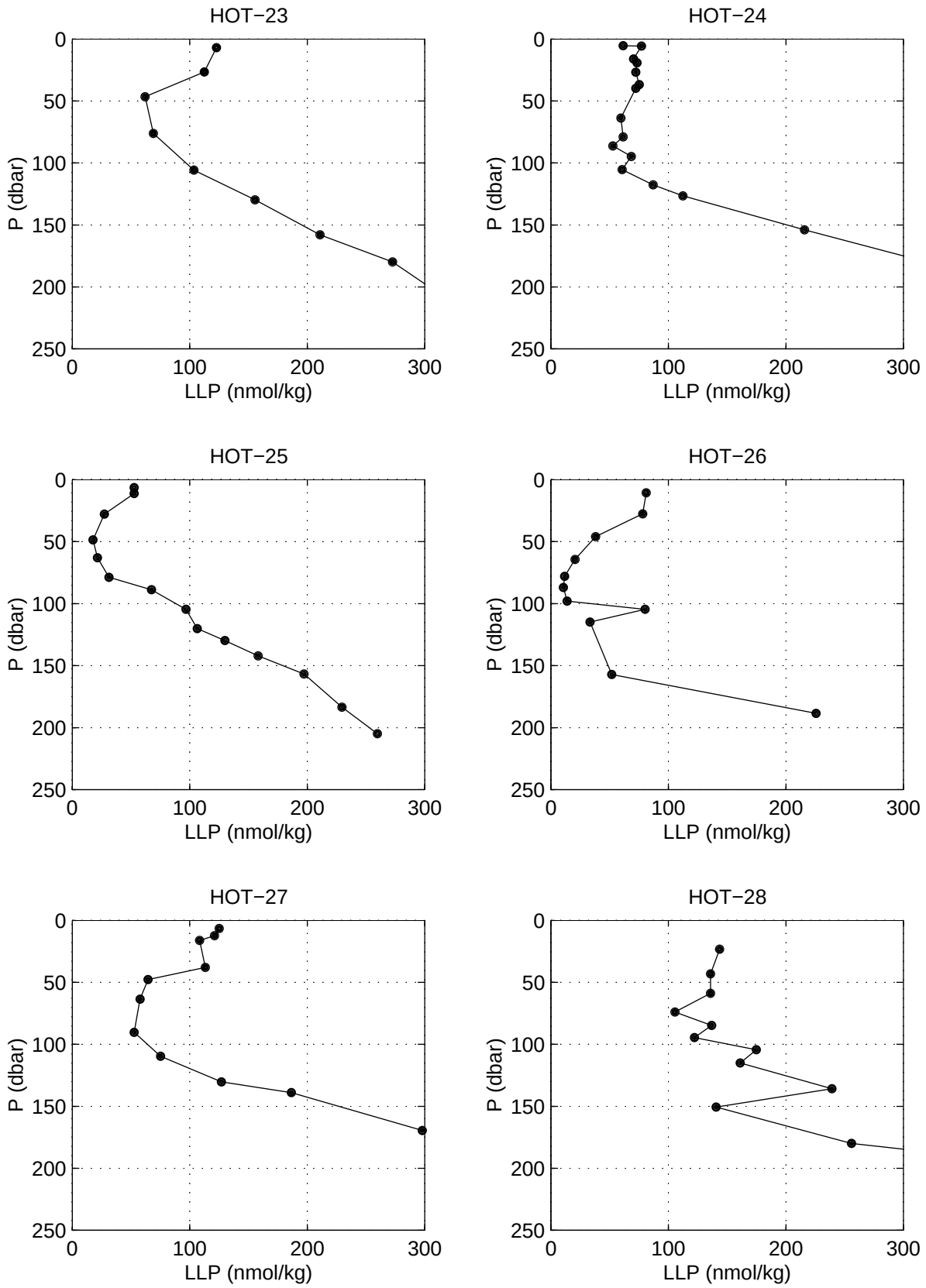
HOT−23
HOT−24
HOT−25
HOT−26
HOT−27
HOT−28
P (dbar)
LLP (nmol/kg)
0
50
100
150
200
250
0
100
200
300

Figure 6.4.6

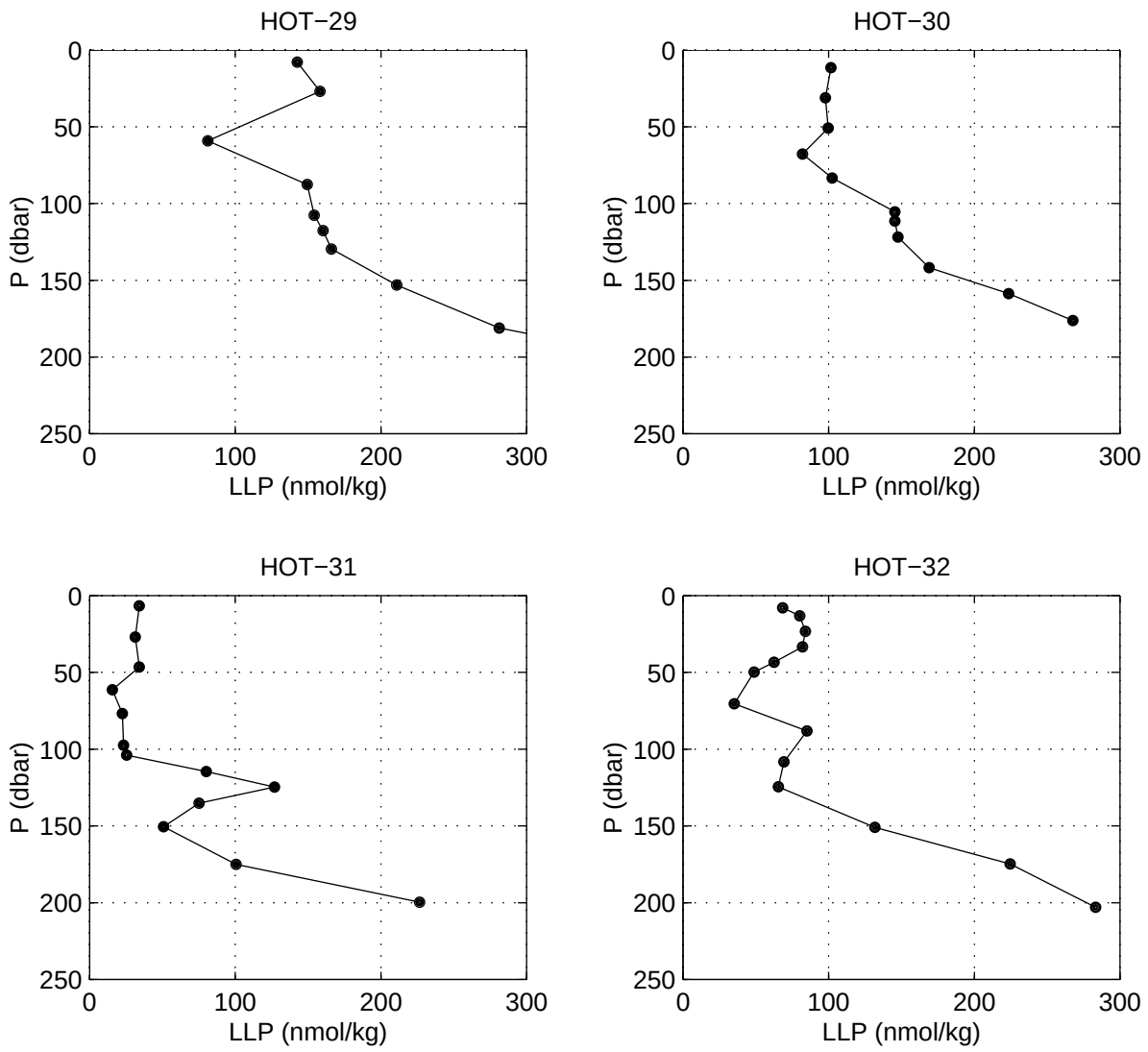

Figure 6.4.6 (continued)

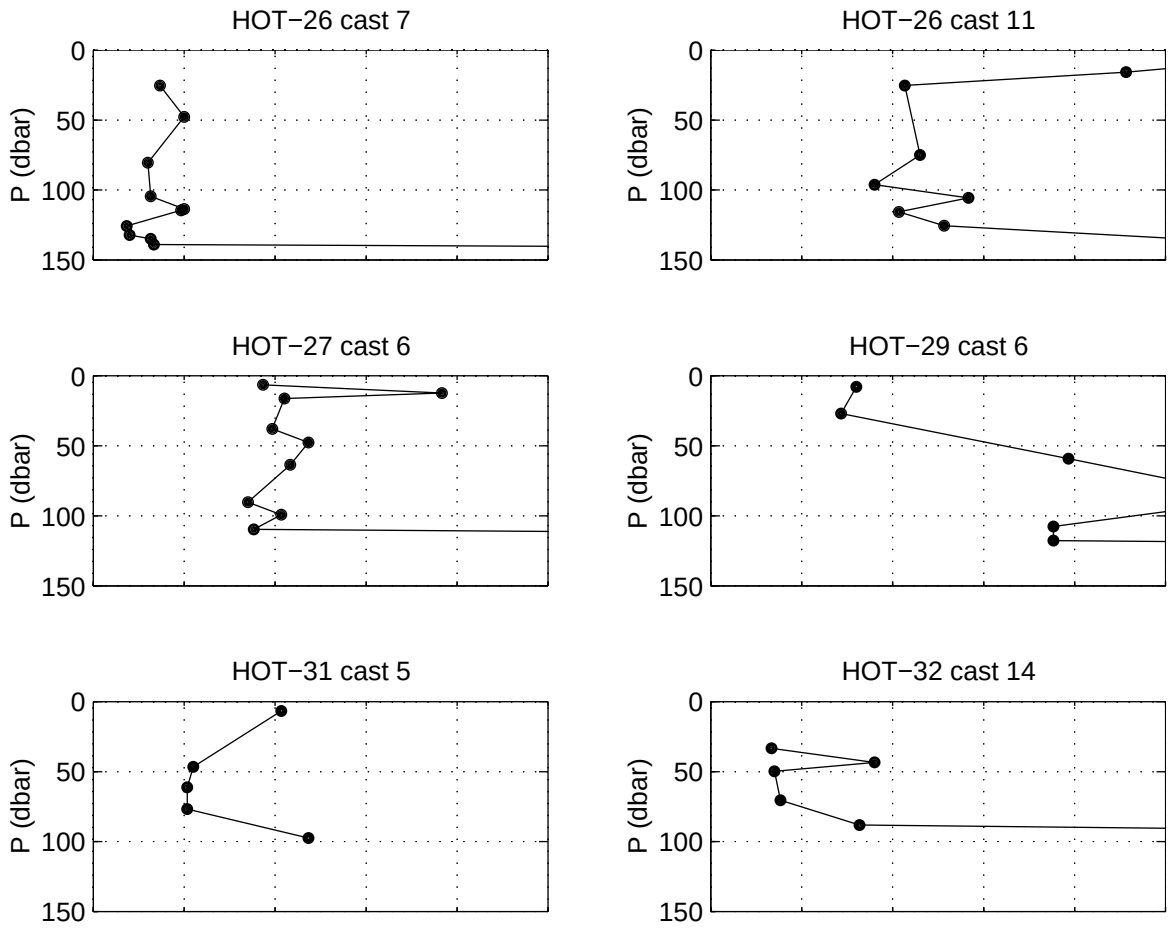
HOT−26 cast 7
HOT−26 cast 11
HOT−27 cast 6
HOT−29 cast 6
HOT−31 cast 5
HOT−32 cast 14
P (dbar)
0
50
100
150

Figure 6.4.7

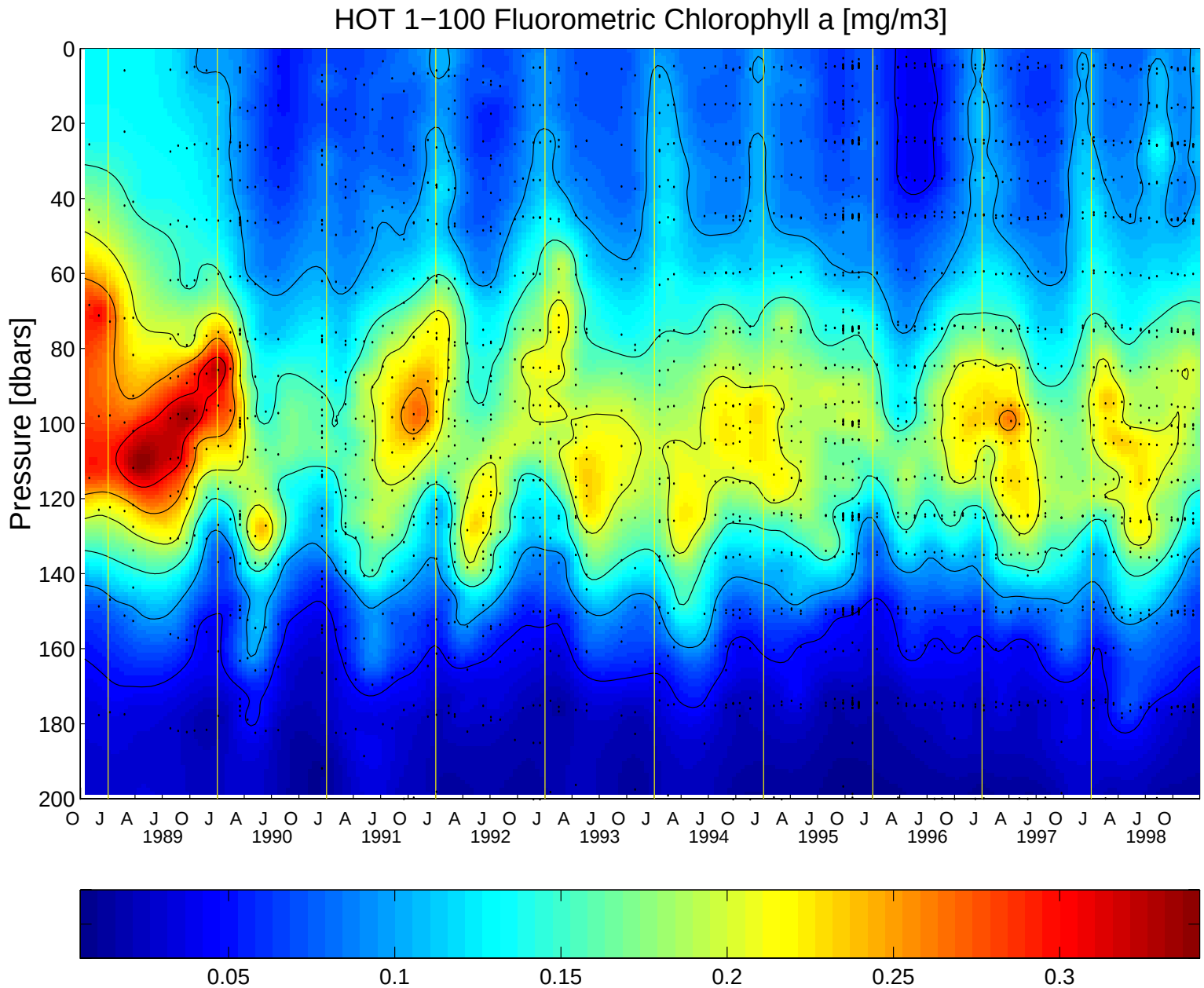
HOT 1−100 Fluorometric Chlorophyll a [mg/m3]
Pressure [dbars]
0
20
40
60
80
100
120
140
160
180
200
O J A J O J A J O J A J O J A J O J A J O J A J O J A J O J A J O J A J O J A J O
1989
1990
1991
1992
1993
1994
1995
1996
1997
1998
0.05
0.1
0.15
0.2
0.25
0.3

Figure 6.4.8

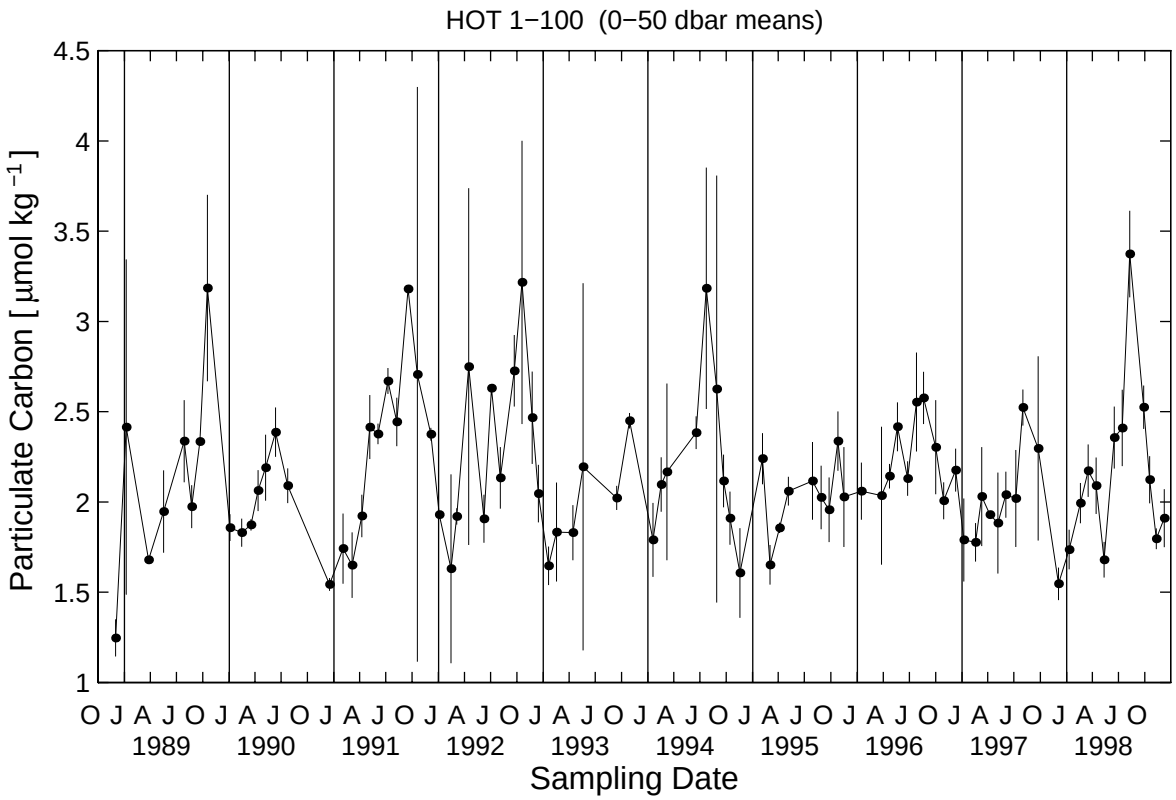
HOT 1−100 (0−50 dbar means)
Particulate Carbon [µmol kg −1]
4.5
4
3.5
3
2.5
2
1.5
1
O J A J O J A J O J A J O J A J O J A J O J A J O J A J O J A J O J A J O J A J O J A J O
1989
1990
1991
1992
1993
1994
1995
1996
1997
1998
Sampling Date

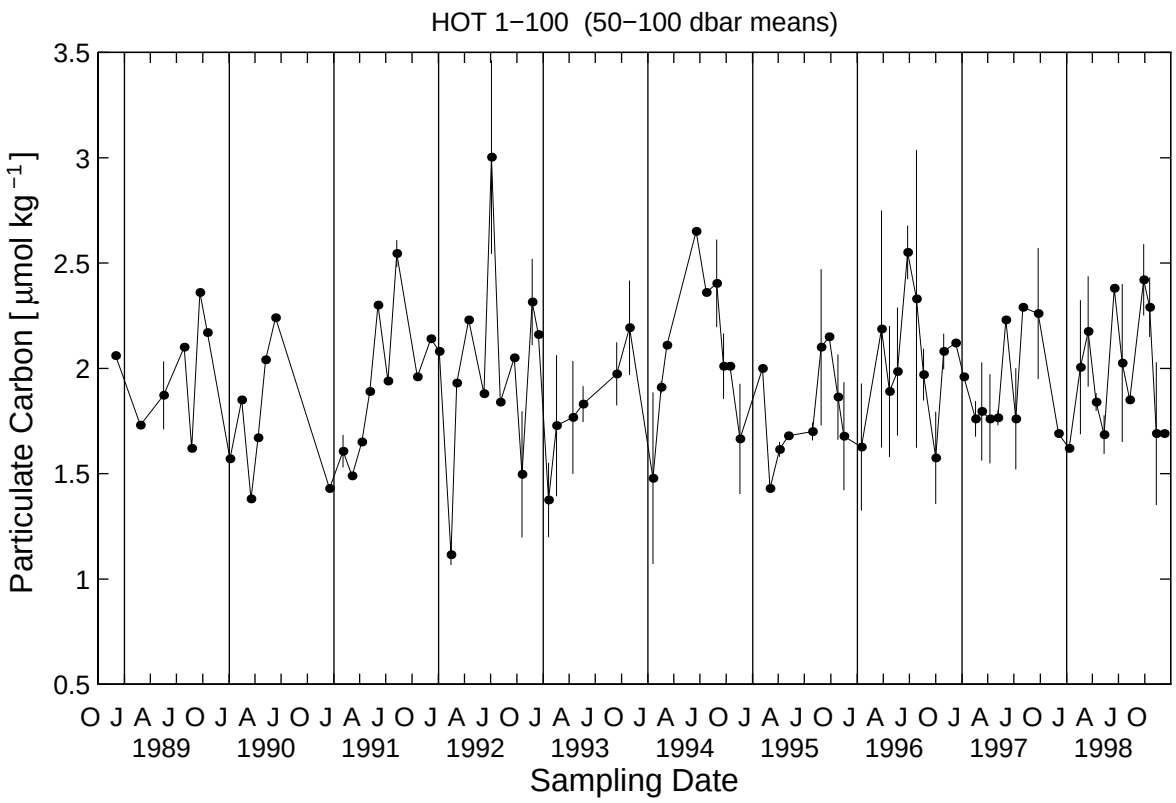
HOT 1−100 (50−100 dbar means)
Particulate Carbon [µmol kg −1]
3.5
3
2.5
2
1.5
1
0.5
O J A J O J A J O J A J O J A J O J A J O J A J O J A J O J A J O J A J O J A J O J A J O J A J O
1989
1990
1991
1992
1993
1994
1995
1996
1997
1998
Sampling Date

Figure 6.4.9

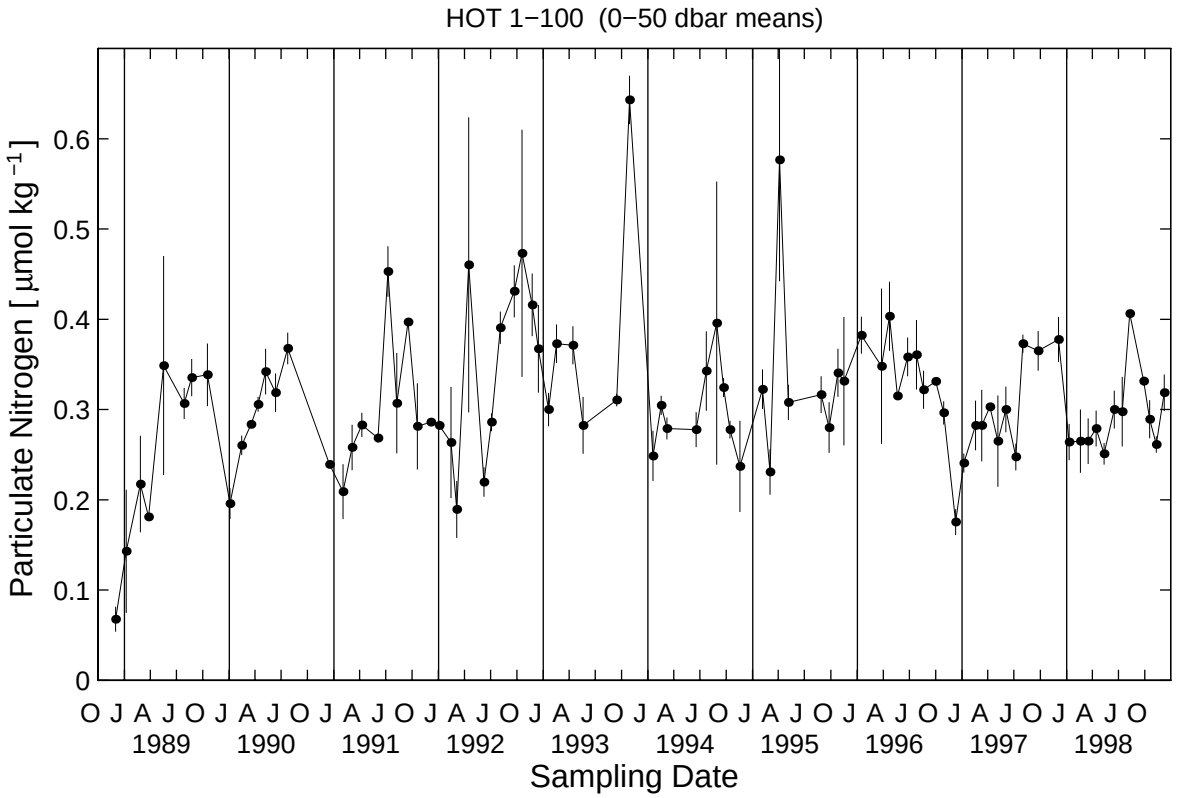
HOT 1−100 (0−50 dbar means)
Particulate Nitrogen [µmol kg −1]
0
0.1
0.2
0.3
0.4
0.5
0.6
O J A J O J A J O J A J O J A J O J A J O J A J O J A J O J A J O J A J O J A J O J A J O
1989
1990
1991
1992
1993
1994
1995
1996
1997
1998
Sampling Date

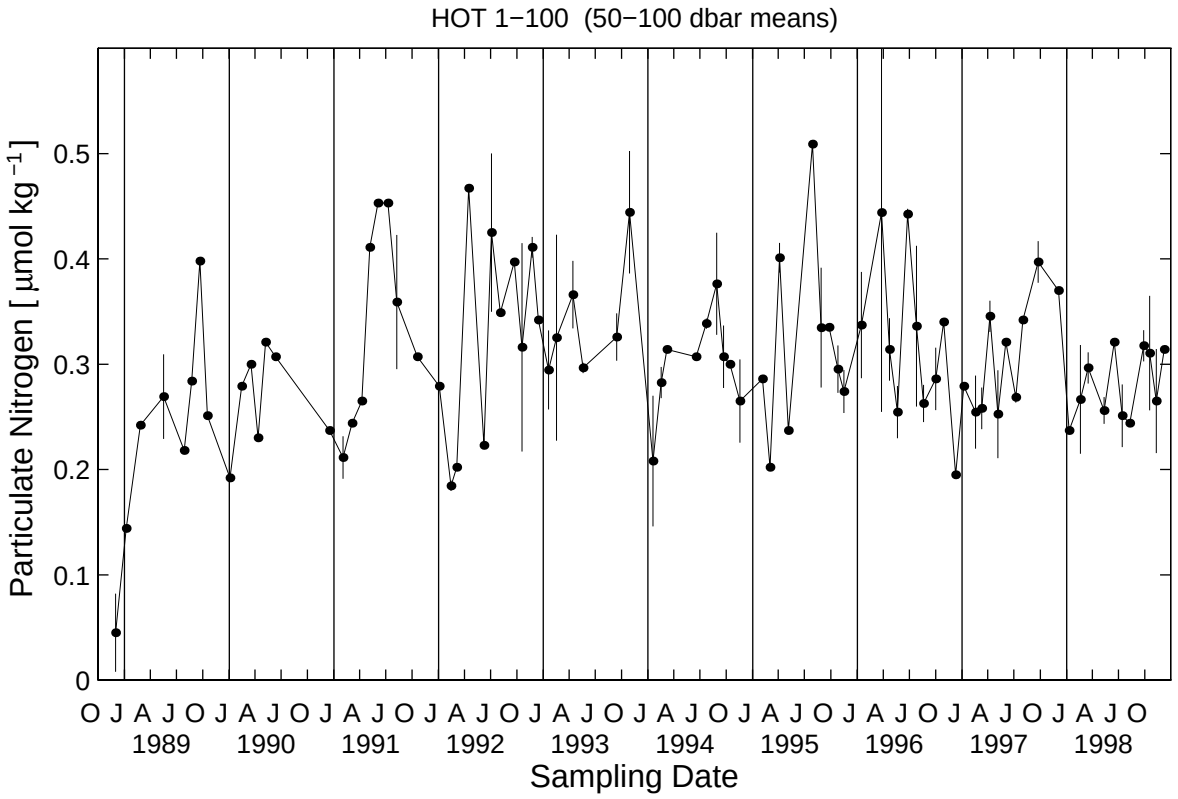
HOT 1−100 (50−100 dbar means)
Particulate Nitrogen [µmol kg −1]
0
0.1
0.2
0.3
0.4
0.5
O J A J O J A J O J A J O J A J O J A J O J A J O J A J O J A J O J A J O J A J O J A J O
1989
1990
1991
1992
1993
1994
1995
1996
1997
1998
Sampling Date

Figure 6.4.10

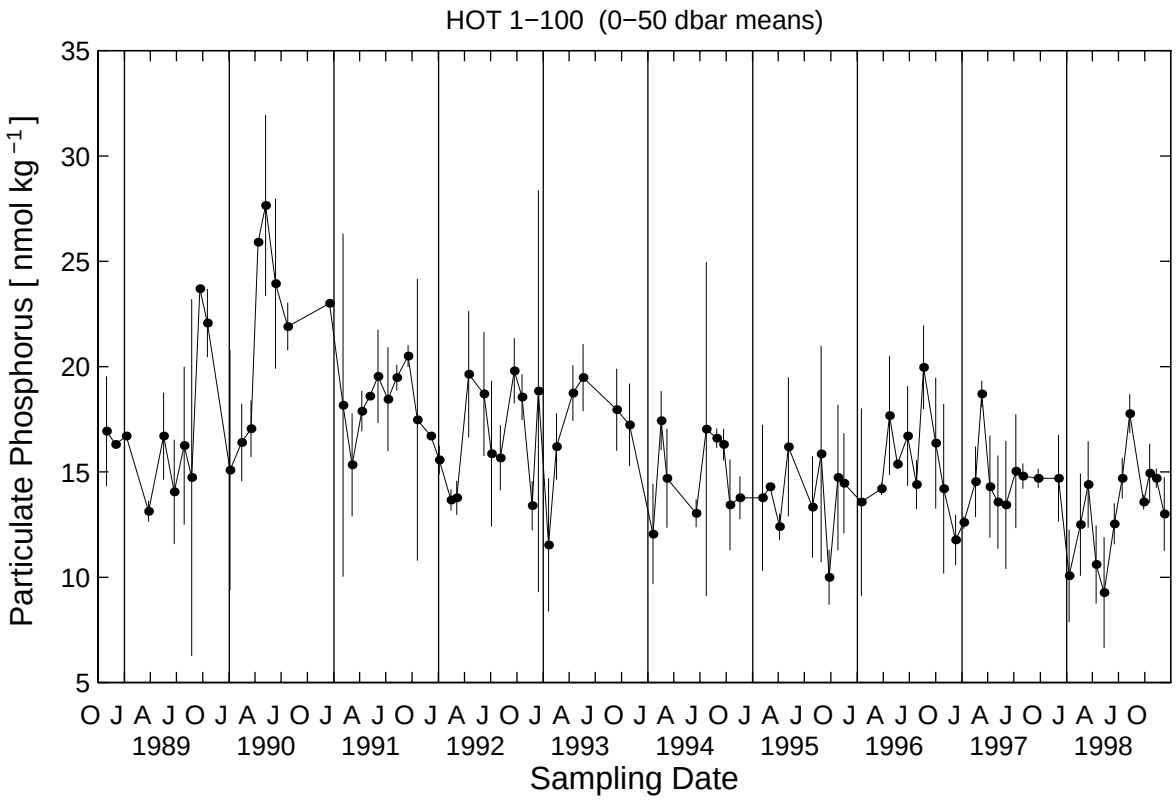
HOT 1−100 (0−50 dbar means)
Particulate Phosphorus [nmol kg −1]
35
30
25
20
15
10
5
O J A J O J A J O J A J O J A J O J A J O J A J O J A J O J A J O J A J O J A J O
1989
1990
1991
1992
1993
1994
1995
1996
1997
1998
Sampling Date

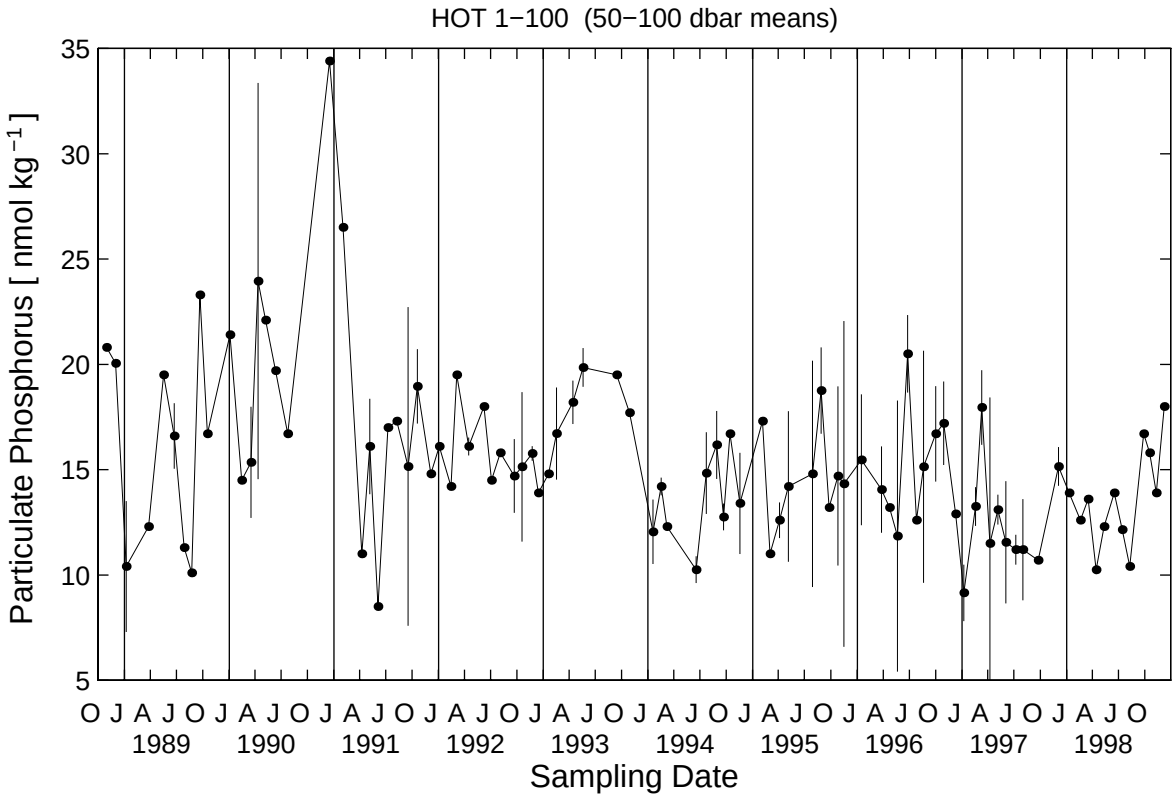
HOT 1−100 (50−100 dbar means)
Particulate Phosphorus [nmol kg −1]
35
30
25
20
15
10
5
O J A J O J A J O J A J O J A J O J A J O J A J O J A J O J A J O J A J O J A J O J A J O J A J O
1989
1990
1991
1992
1993
1994
1995
1996
1997
1998
Sampling Date

Figure 6.4.11

6.5. Primary Production and Particle Flux

Figure 6.5.1: Integrated primary production rates measured on all HOT cruises. Data for both *in situ* and on-deck incubations are presented. On HOT-15 (March 1990) primary production was measured on three consecutive days.

Figure 6.5.2: Carbon flux at 150 m measured on all HOT cruises from 1988 through 1991. Error bars represent the standard deviation of replicate determinations.

Figure 6.5.3: As in Figure 6.5.2 except for nitrogen.

Figure 6.5.4: As in Figure 6.5.2 except for phosphorus.

Figure 6.5.5: As in Figure 6.5.2 except for total mass.

Figure 6.5.6: Contour plot of carbon flux for all cruises from 1988.

Figure 6.5.7: As in Figure 6.5.6 except for nitrogen.

Figure 6.5.8: As in Figure 6.5.6 except for phosphorus.

Figure 6.5.9: As in Figure 6.5.6 except for total mass.

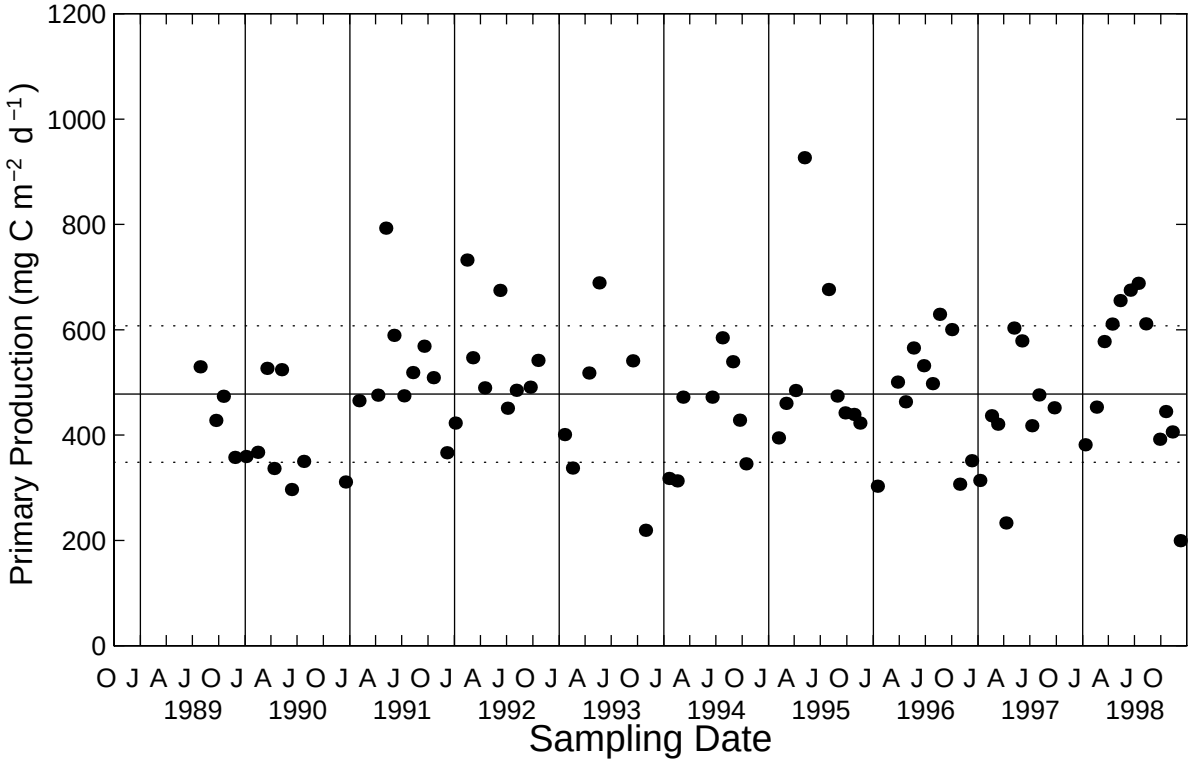
Primary Production (mg C m^{-2} d^{-1})
0
200
400
600
800
1000
1200
O J A J O J A J O J A J O J A J O J A J O J A J O J A J O J A J O J A J O J A J O J A J O J A J O
1989
1990
1991
1992
1993
1994
1995
1996
1997
1998
Sampling Date

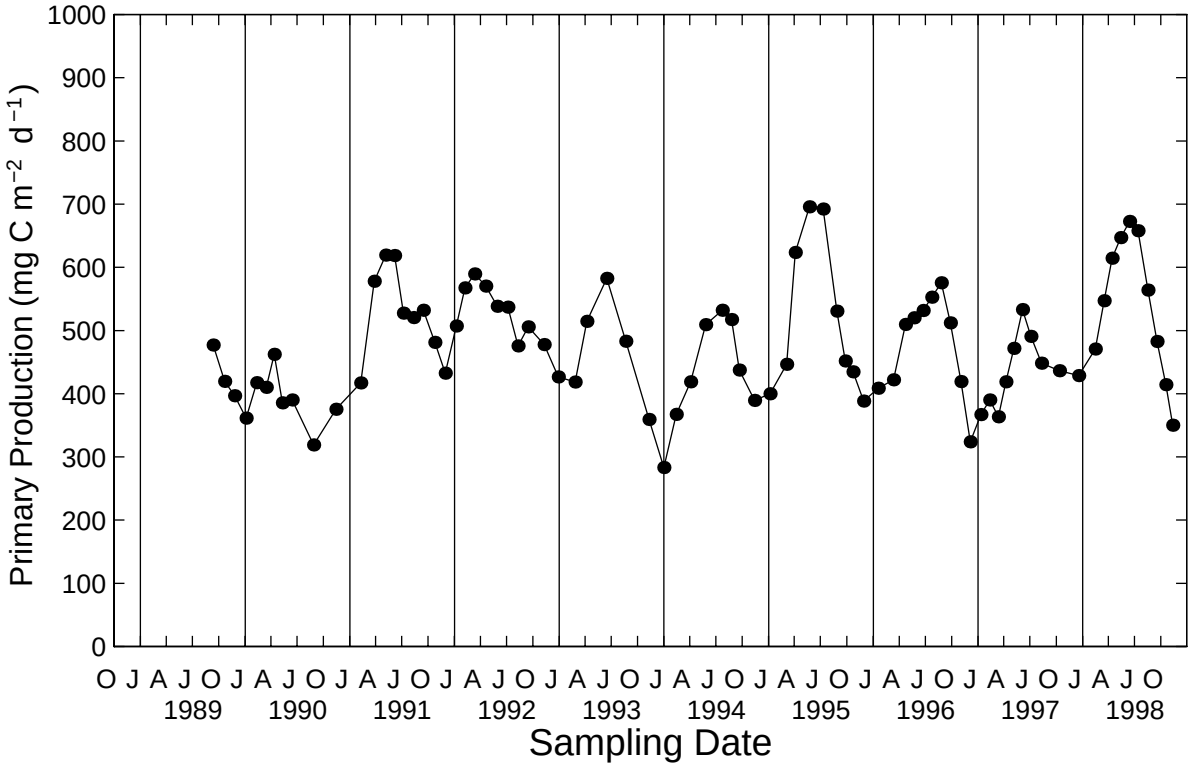
Primary Production (mg C m^{-2} d^{-1})
0
100
200
300
400
500
600
700
800
900
1000
O J A J O J A J O J A J O J A J O J A J O J A J O J A J O J A J O J A J O J A J O J A J O J A J O
1989
1990
1991
1992
1993
1994
1995
1996
1997
1998
Sampling Date

Figure 6.5.1

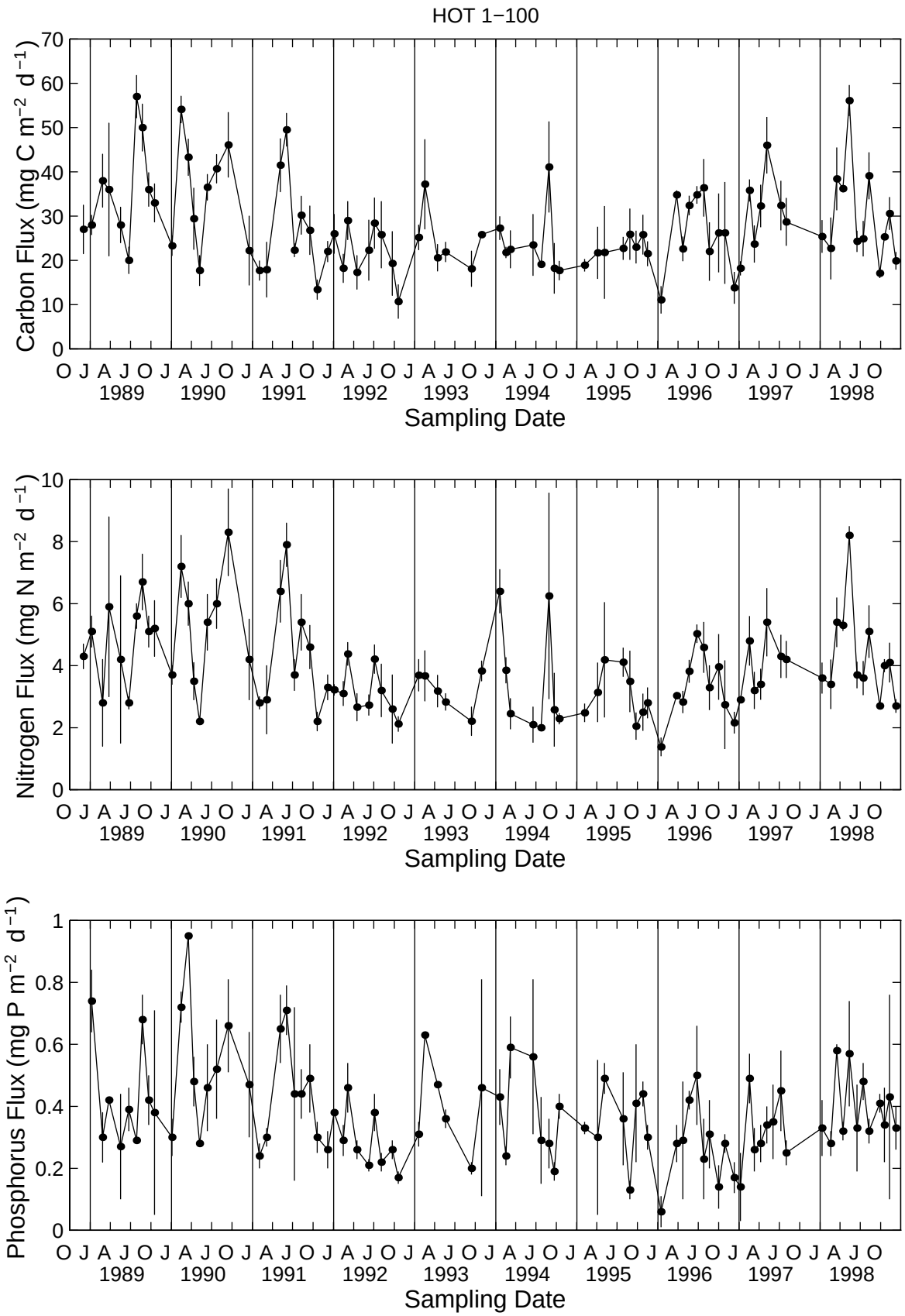

Figure 6.5.2 (upper panel), 6.5.3 (middle panel), 6.5.4 (lower panel)

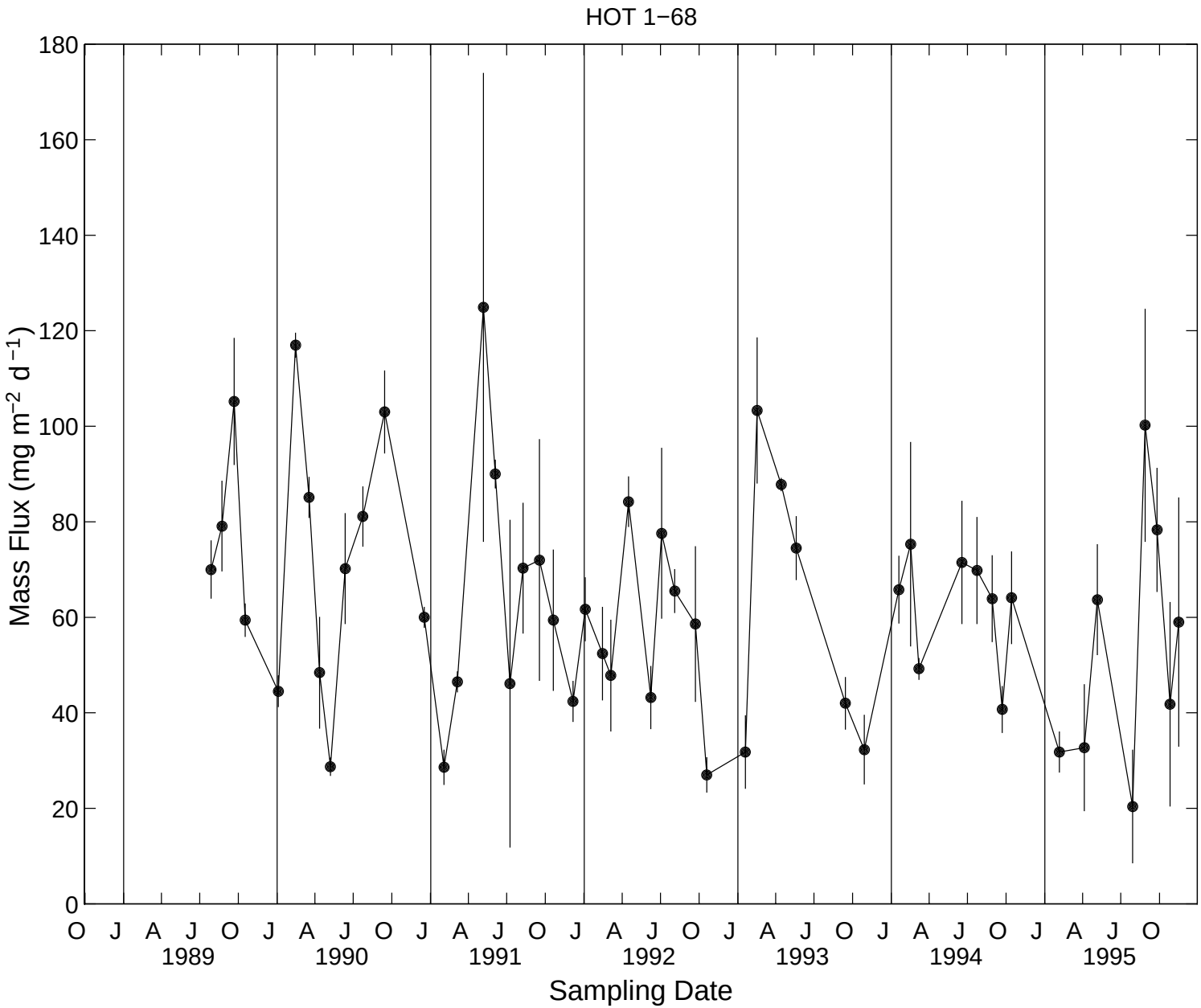
HOT 1−68
Mass Flux (mg m−2 d−1)
0
20
40
60
80
100
120
140
160
180
O J A J O J A J O J A J O J A J O J A J O J A J O J A J O
1989
1990
1991
1992
1993
1994
1995
Sampling Date

Figure 6.5.5

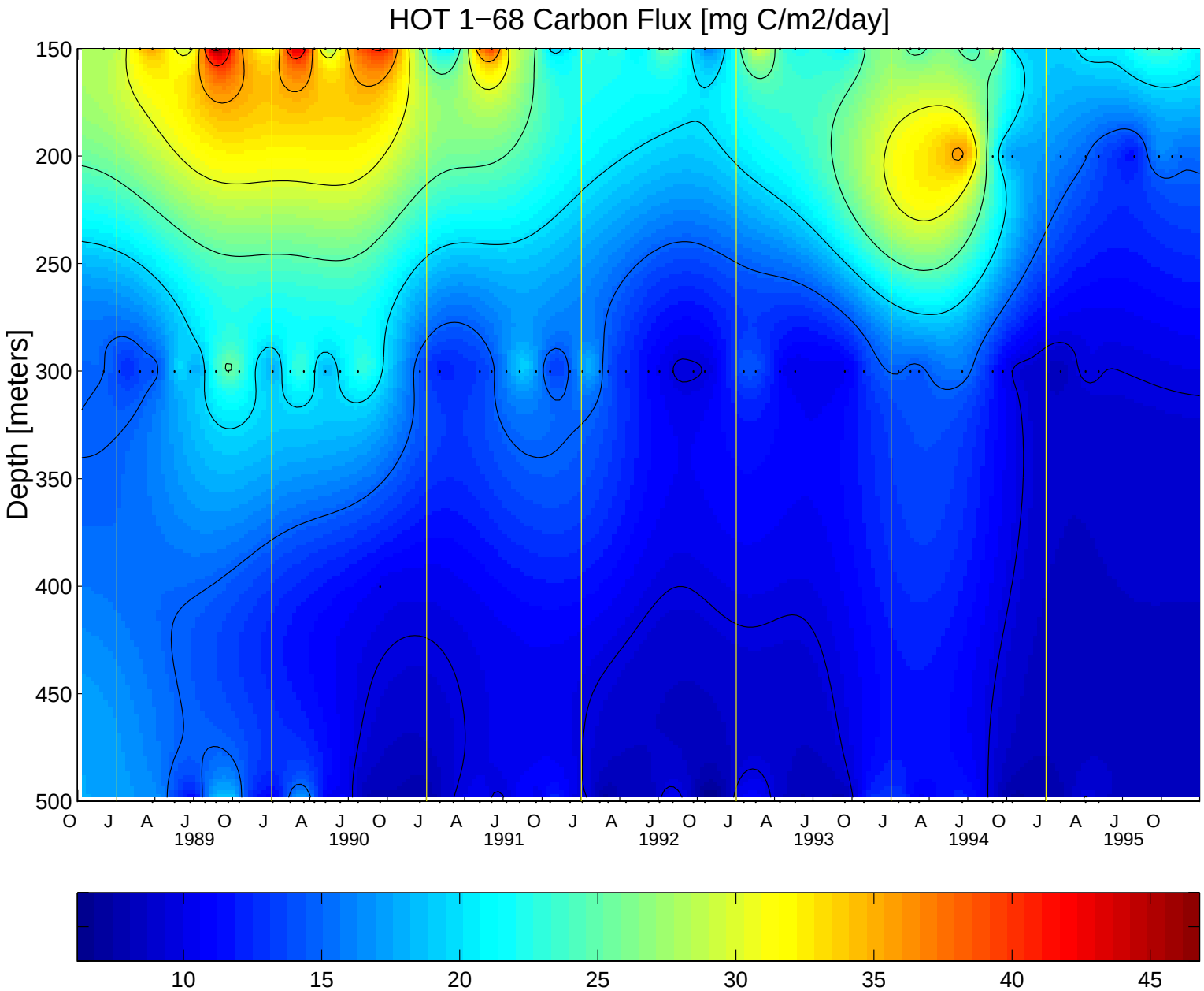
HOT 1−68 Carbon Flux [mg C/m2/day]
Depth [meters]
150
200
250
300
350
400
450
500
O J A J O J A J O J A J O J A J O J A J O J A J O J A J O
1989
1990
1991
1992
1993
1994
1995
10
15
20
25
30
35
40
45

Figure 6.5.6

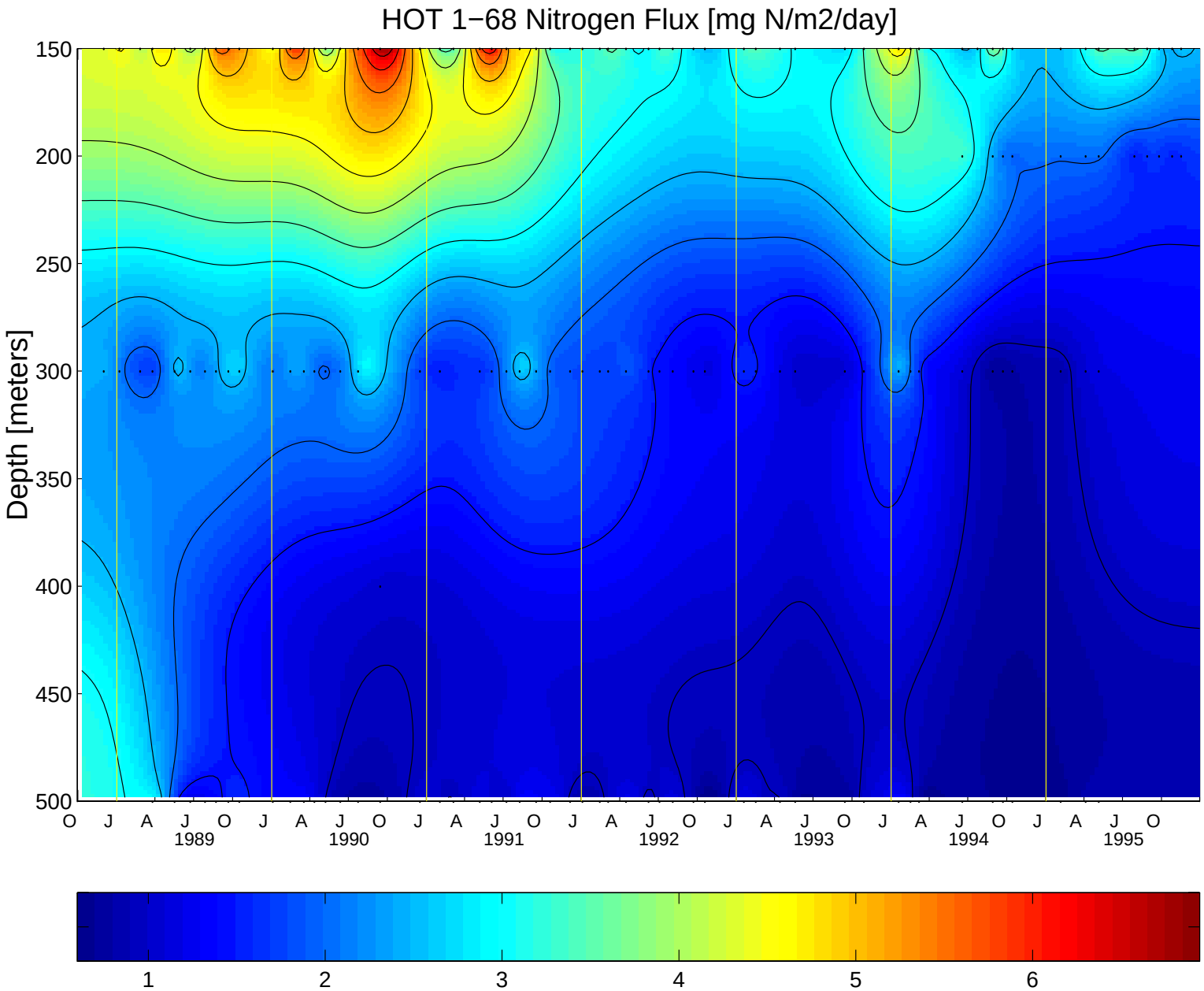
HOT 1−68 Nitrogen Flux [mg N/m2/day]
Depth [meters]
150
200
250
300
350
400
450
500
O J A J O J A J O J A J O J A J O J A J O J A J O J A J O
1989
1990
1991
1992
1993
1994
1995
1
2
3
4
5
6

Figure 6.5.7

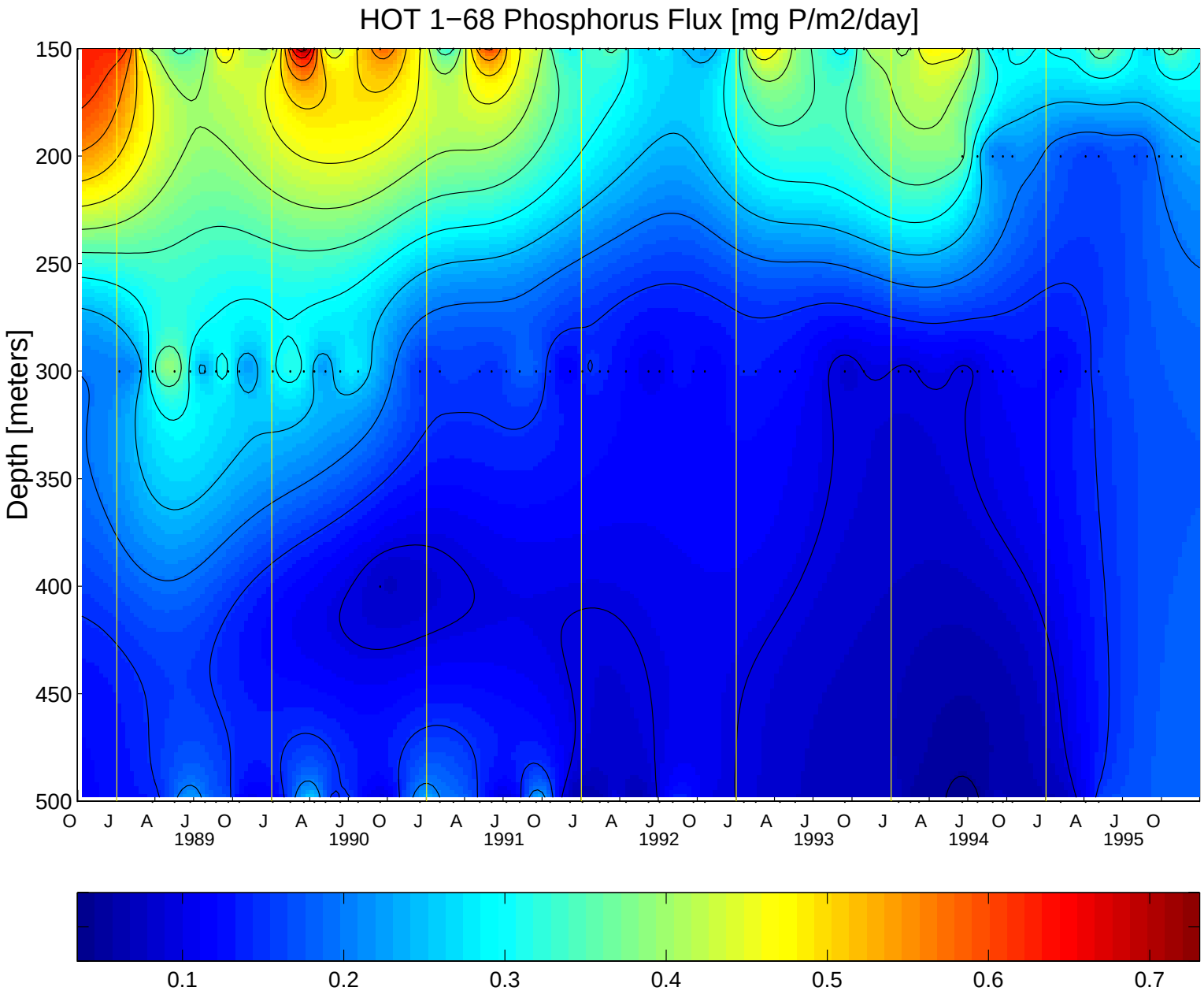
HOT 1−68 Phosphorus Flux [mg P/m2/day]
Depth [meters]
150
200
250
300
350
400
450
500
O J A J O J A J O J A J O J A J O J A J O J A J O J A J O
1989
1990
1991
1992
1993
1994
1995
0.1
0.2
0.3
0.4
0.5
0.6
0.7

Figure 6.5.8

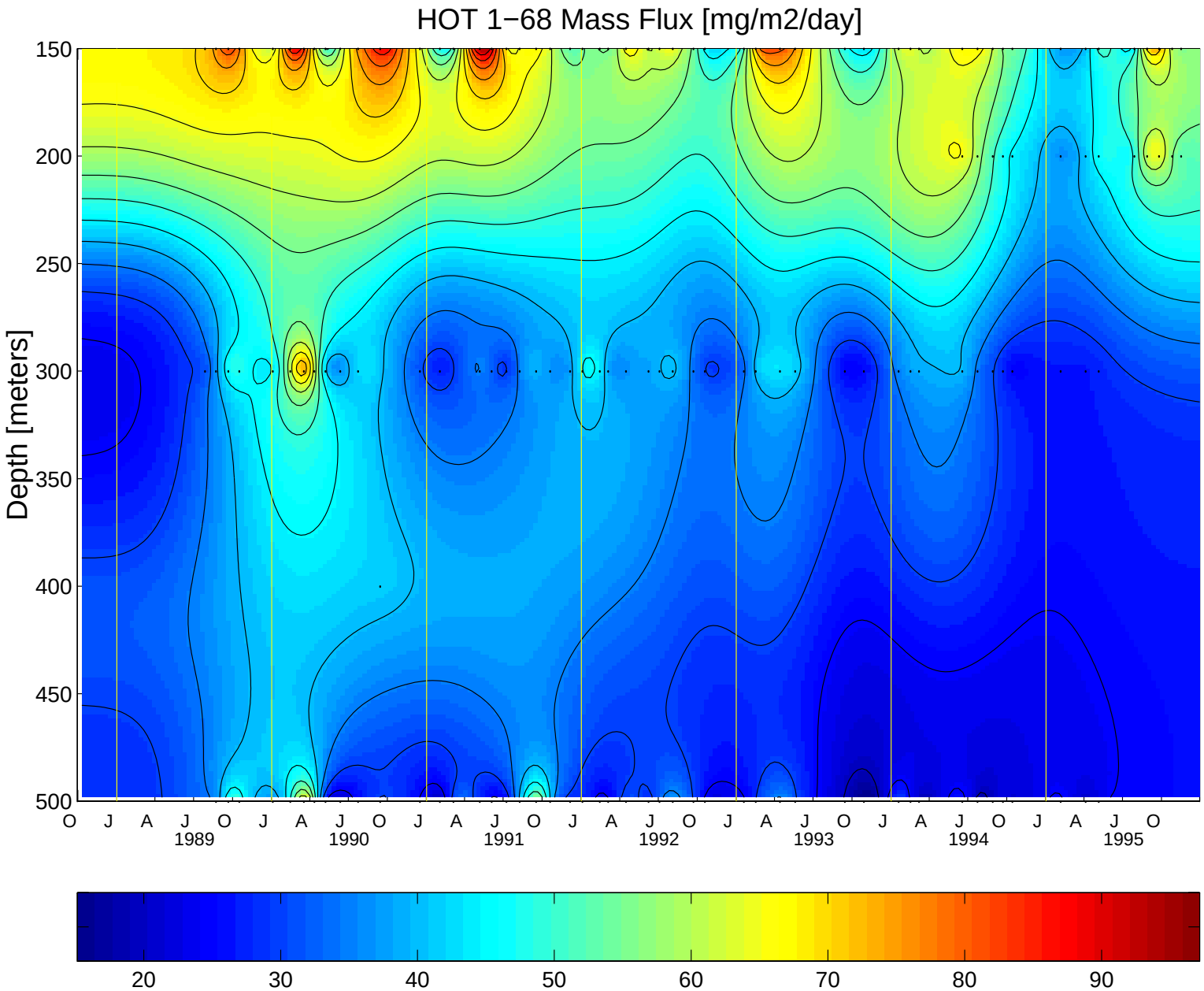
HOT 1−68 Mass Flux [mg/m2/day]
Depth [meters]
150
200
250
300
350
400
450
500
O J A J O J A J O J A J O J A J O J A J O J A J O J A J O
1989
1990
1991
1992
1993
1994
1995
20
30
40
50
60
70
80
90

Figure 6.5.9

6.6. ADCP Measurements

For each cruise with shipboard ADCP, the following figures (6.6.1-10) are provided:

Figures 6.6.1-10: Reference layer velocity (upper panels) and ship's longitude and latitude (lower panels) as functions of time. Time is given in days from the beginning of the year. For example, noon on 1 January is 0.5 decimal days. The reference layer velocity is shown averaged between fixes (steppy curves), and smoothed, as used in the final velocity estimates (smooth curves). Plus signs near the bottom of the reference layer velocity plots indicate ADCP data gaps. The ship's position is shown by asterisks at fixes and by a continuous curve (actually closely-spaced dots) as determined by fixes together with the ADCP data.

Figures 6.6.11a-22a: Velocity fields at Station ALOHA during HOT 23-32. The top panel shows hourly averages at 20-m depth intervals while the ship was at Station ALOHA. The orientation of each stick gives the direction of the current: up is northward, to the right is eastward. The bottom panel shows the results of a least-squares fit of the hourly averages to a mean, trend, semidiurnal and diurnal tides and an inertial cycle. In the first column, the arrow shows the mean current, and the headless stick shows the sum of the mean plus the trend at the end of the station. For each harmonic, the current ellipse is shown in the first column. The orientation of the stick in the second column shows the direction of that harmonic component of the current at the beginning of the station, and the arrowhead at the end of the stick shows the direction of rotation of the current vector around the ellipse. HOT-25 was preceded by a cruise on the R/V ALPHA HELIX to Station ALOHA. ADCP data were obtained on both these cruises and are included in this report. HOT-27 was conducted in two legs.

Figures 6.6.11b-22b: Velocity field on the transits to and from the Station ALOHA. Velocity is shown as a function of latitude, averaged in 10-minute time intervals. Because HOT-25 and HOT-27 were conducted in two segments, ADCP data are available for two legs on this cruise. Equipment problems during HOT-24 and the early part of HOT-27 prevented the collection of ADCP data.

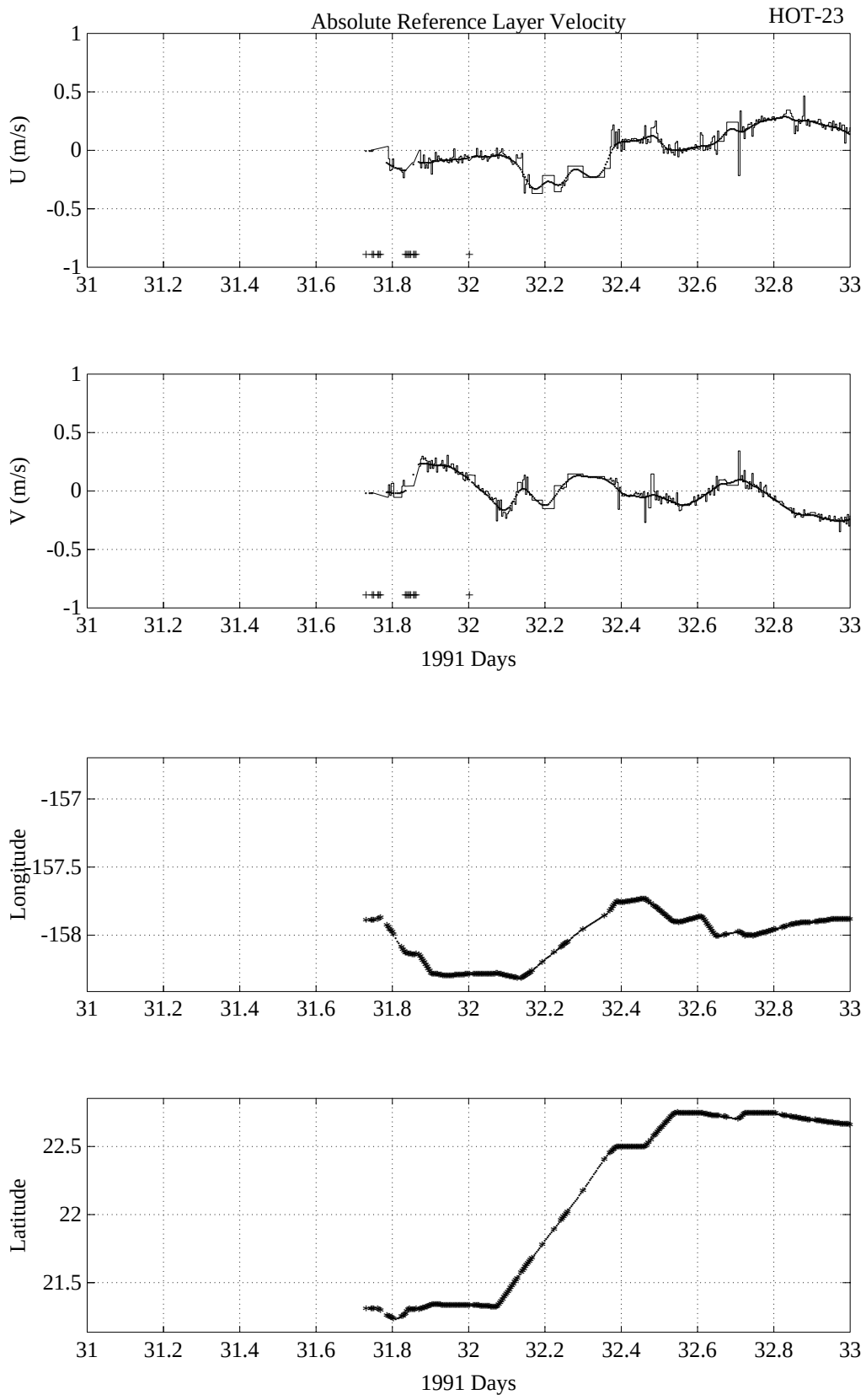
Absolute Reference Layer Velocity
HOT-23
U (m/s)
V (m/s)
1991 Days
Longitude
Latitude
1991 Days

Figure 6.6.1

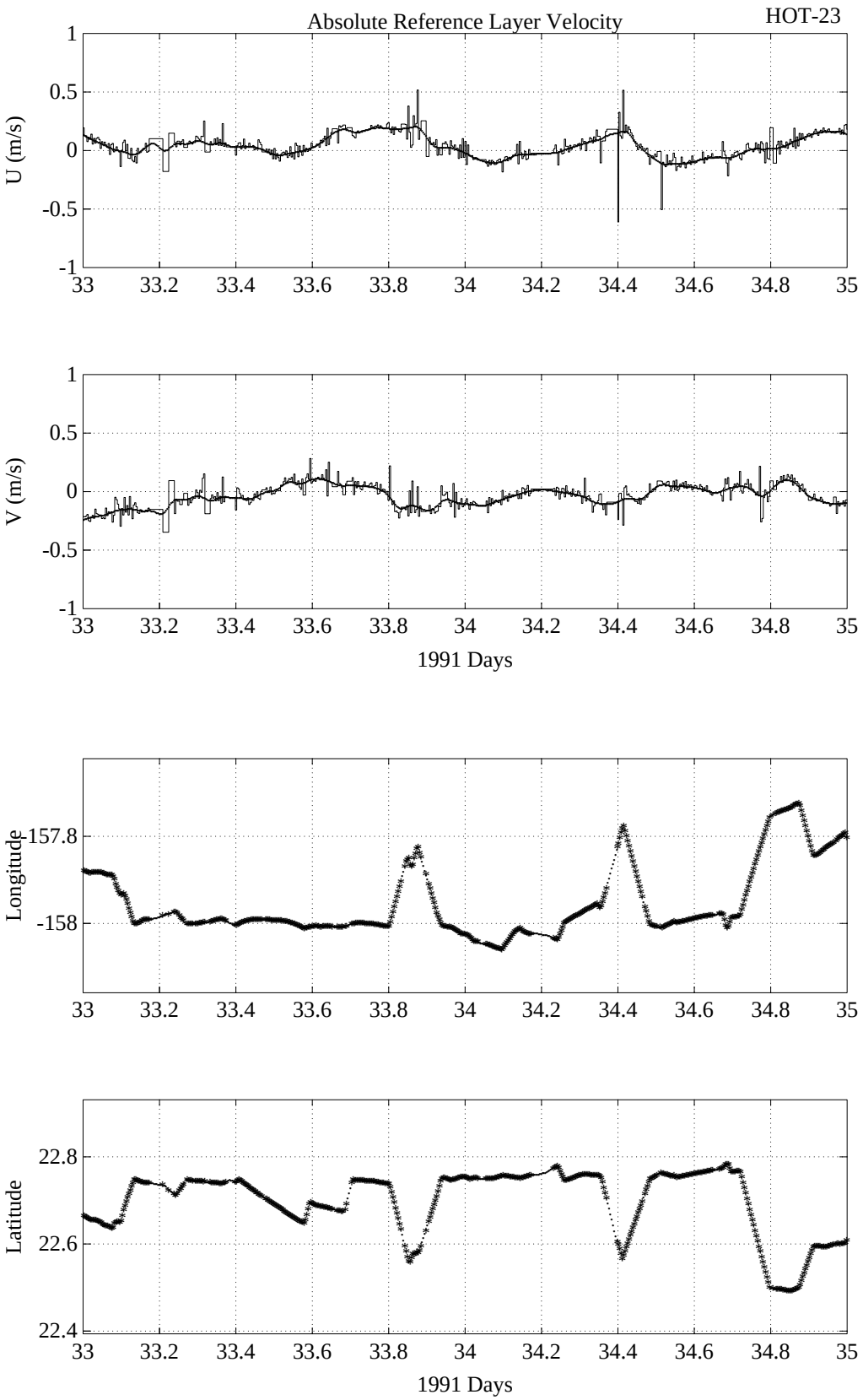

Figure 6.6.1 (continued)

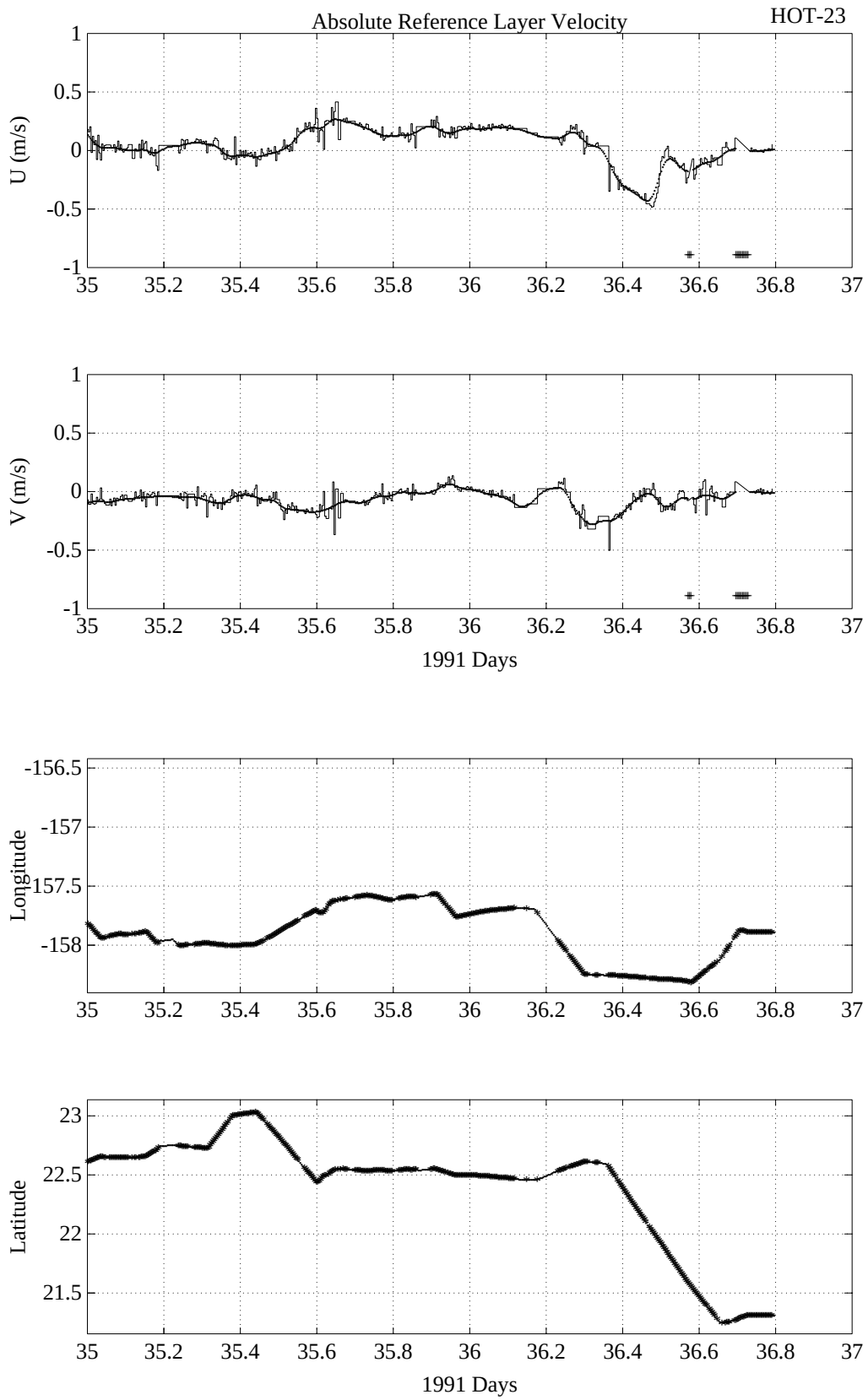

Figure 6.6.1 (continued)

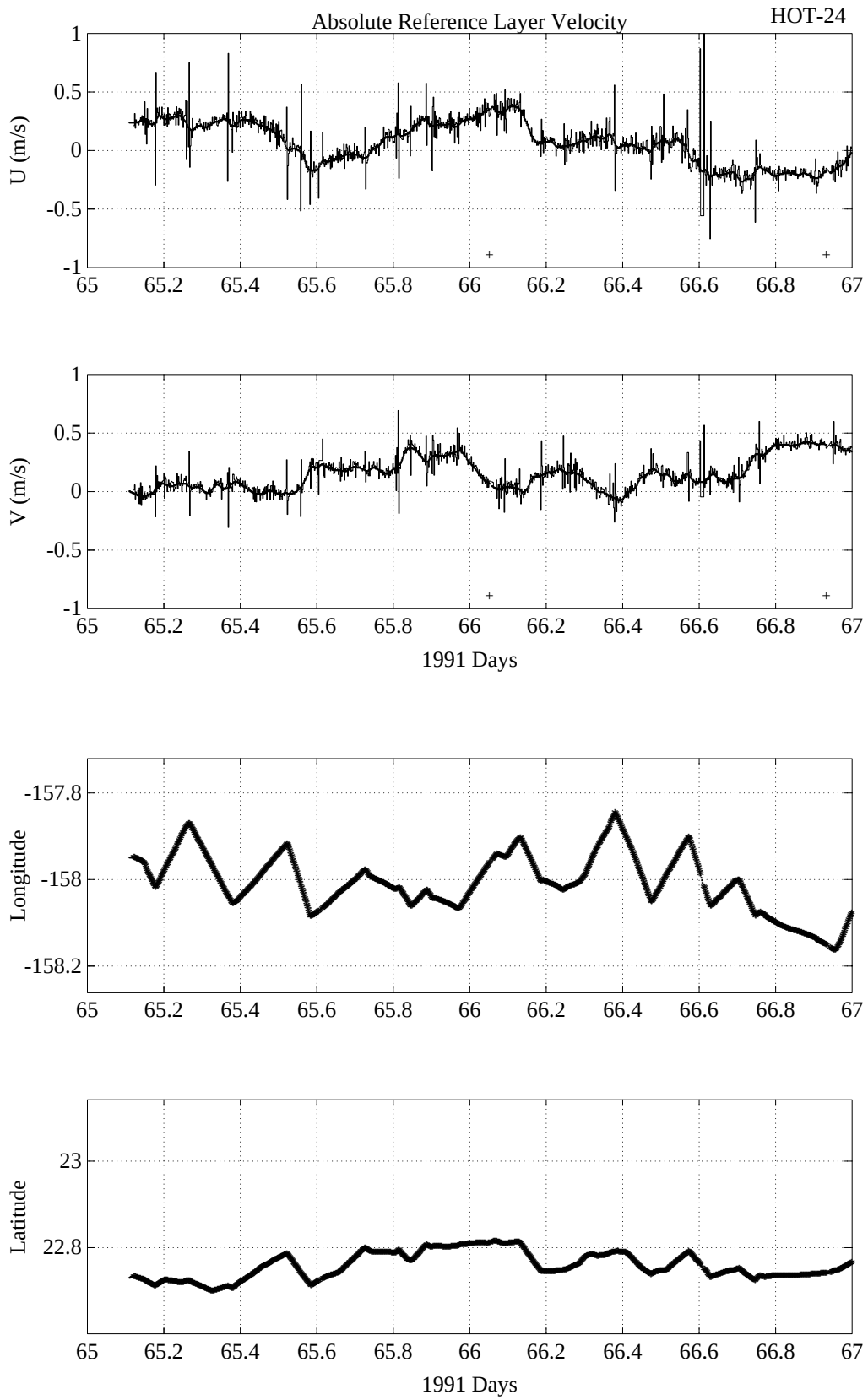
Absolute Reference Layer Velocity
HOT-24
U (m/s)
V (m/s)
1991 Days
Longitude
Latitude
1991 Days

Figure 6.6.2

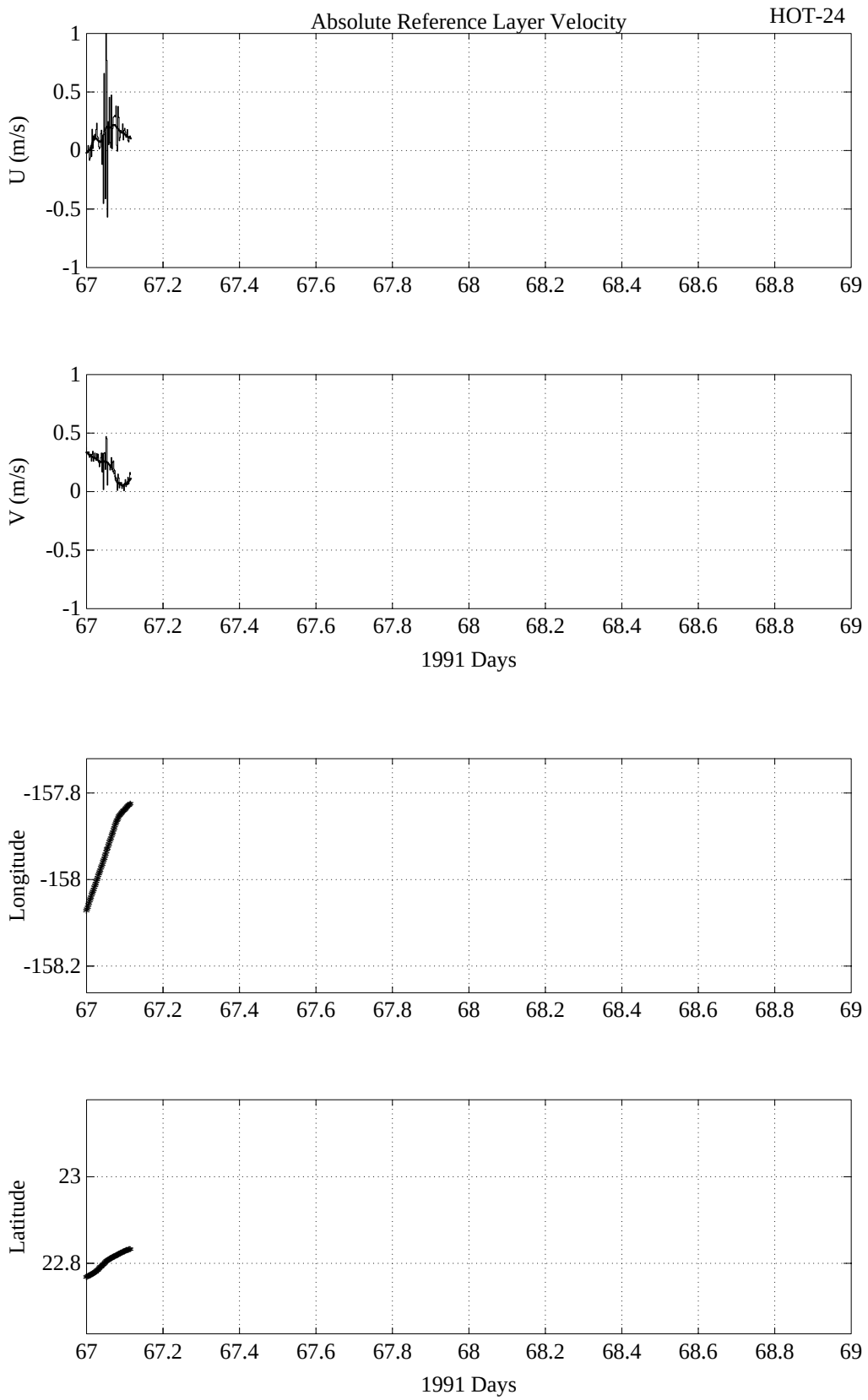

Figure 6.6.2 (continued)

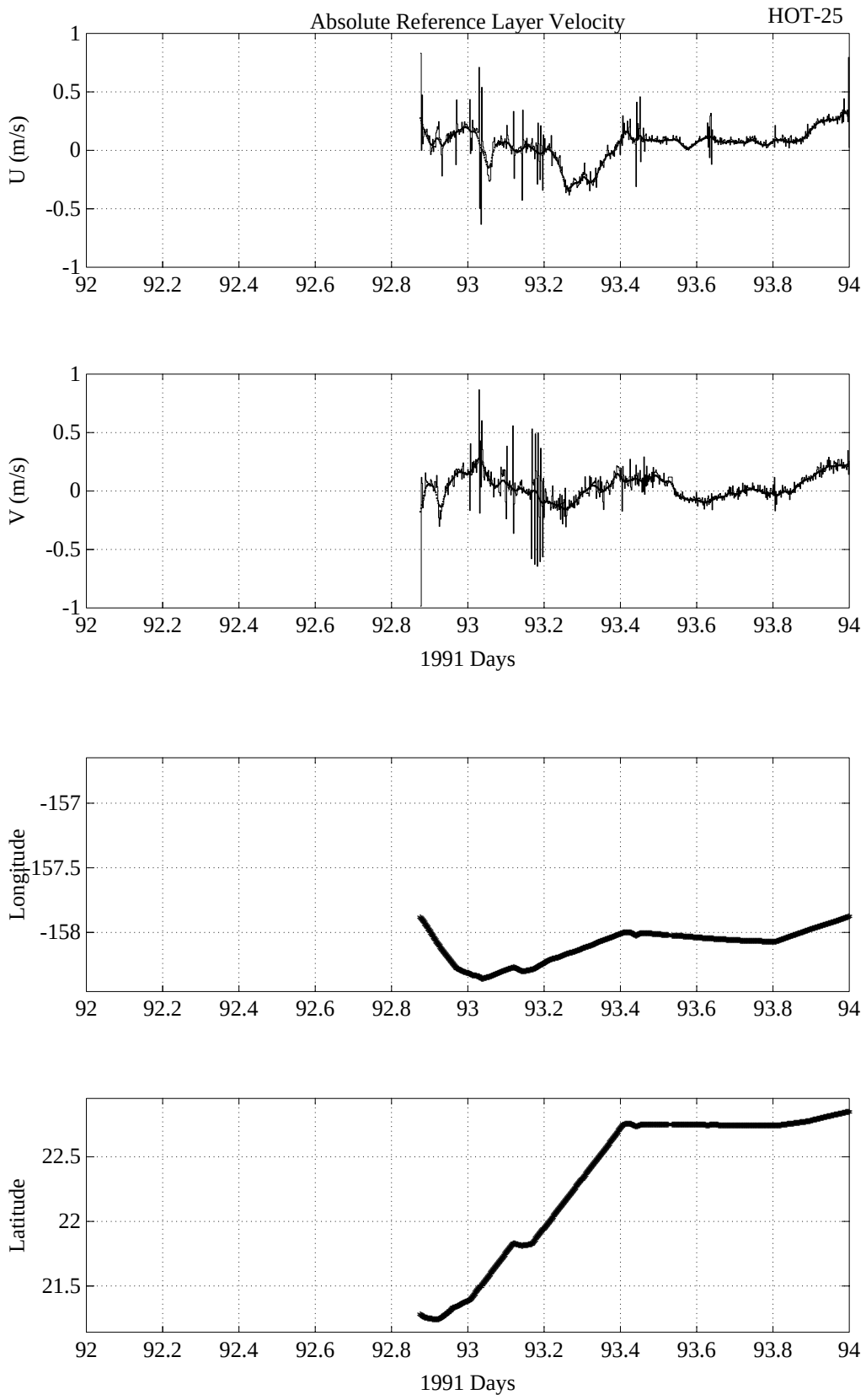
Absolute Reference Layer Velocity
HOT-25
U (m/s)
V (m/s)
1991 Days
Longitude
Latitude
1991 Days

Figure 6.6.3

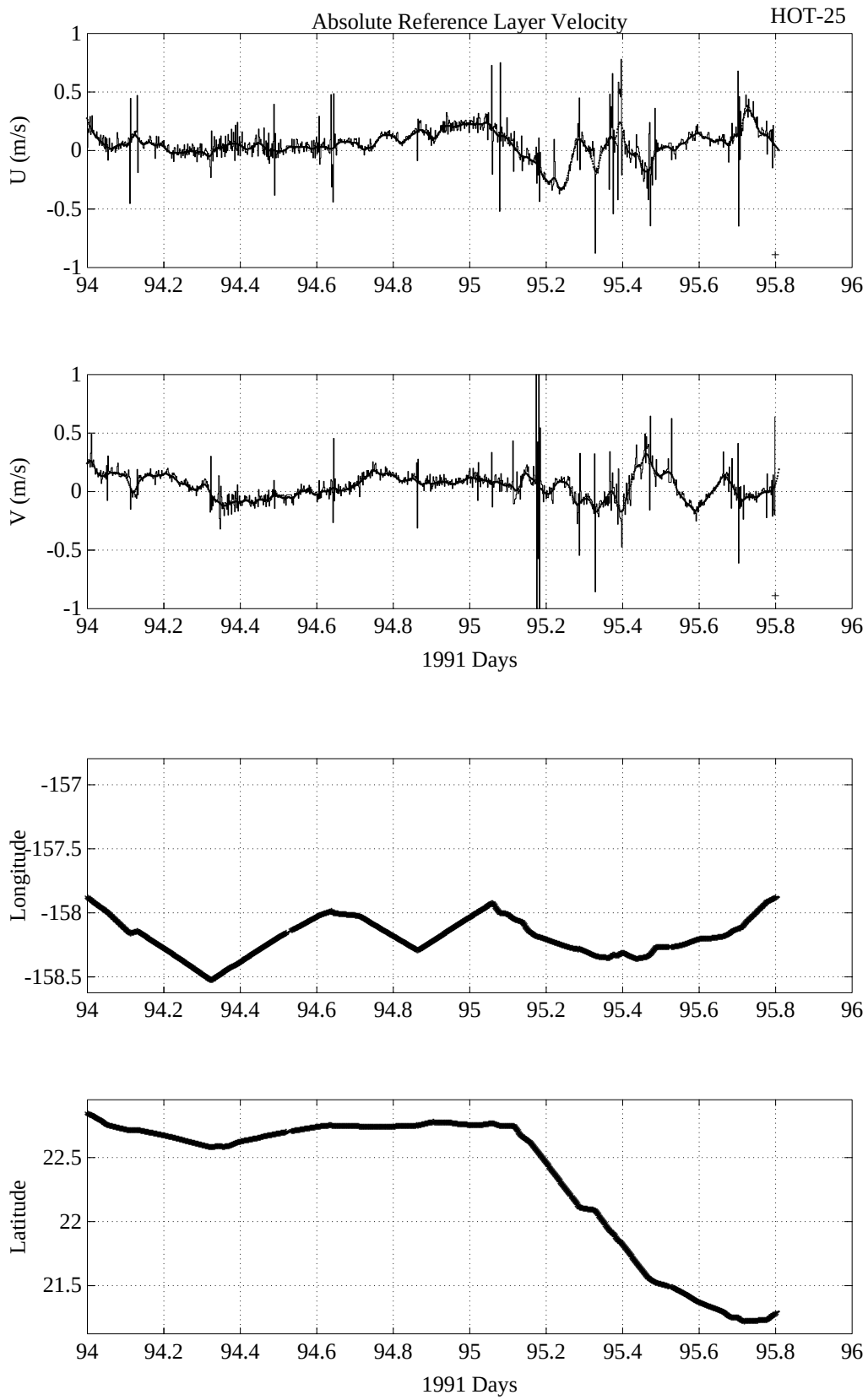

Figure 6.6.3 (continued)

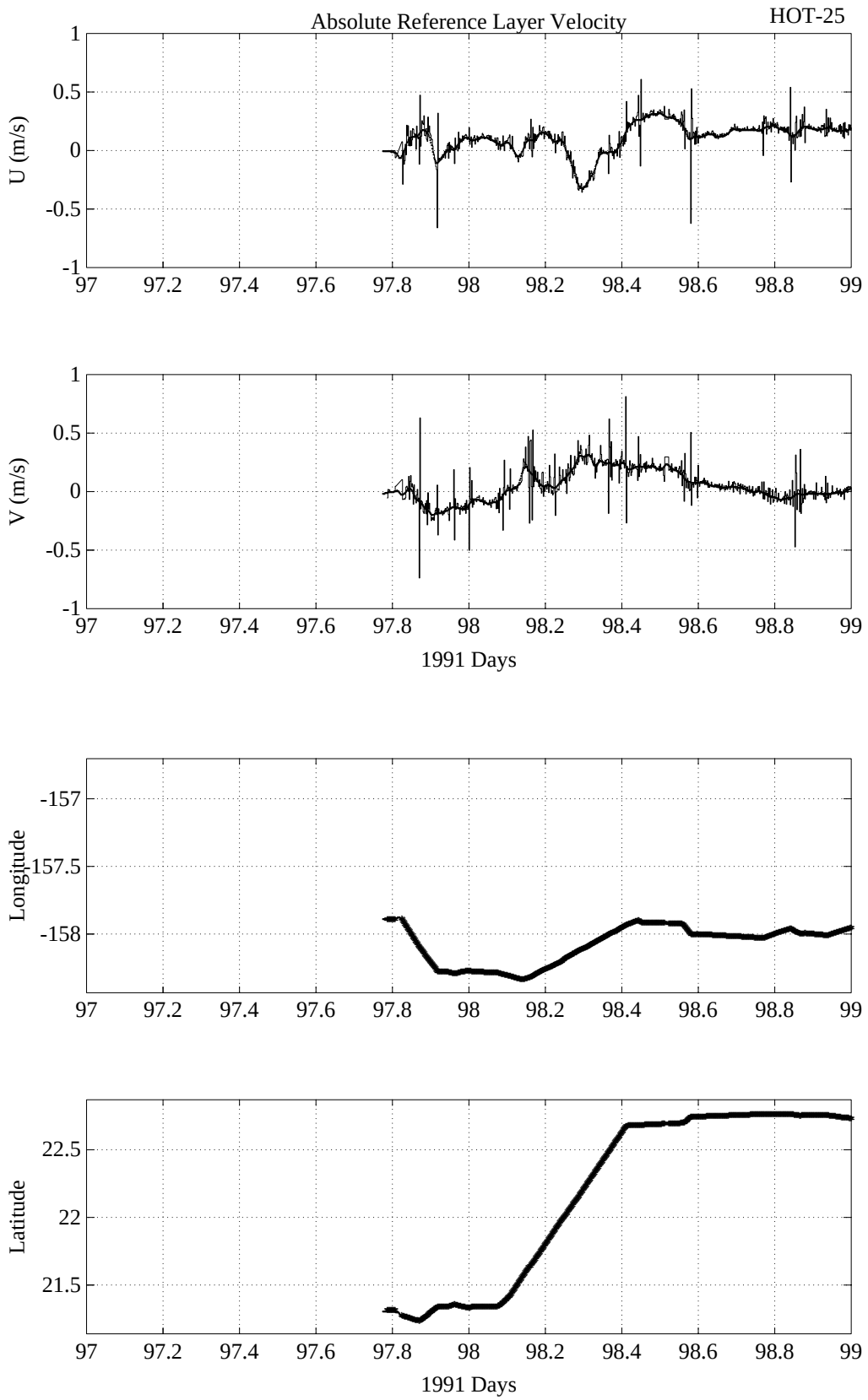

Figure 6.6.3 (continued)

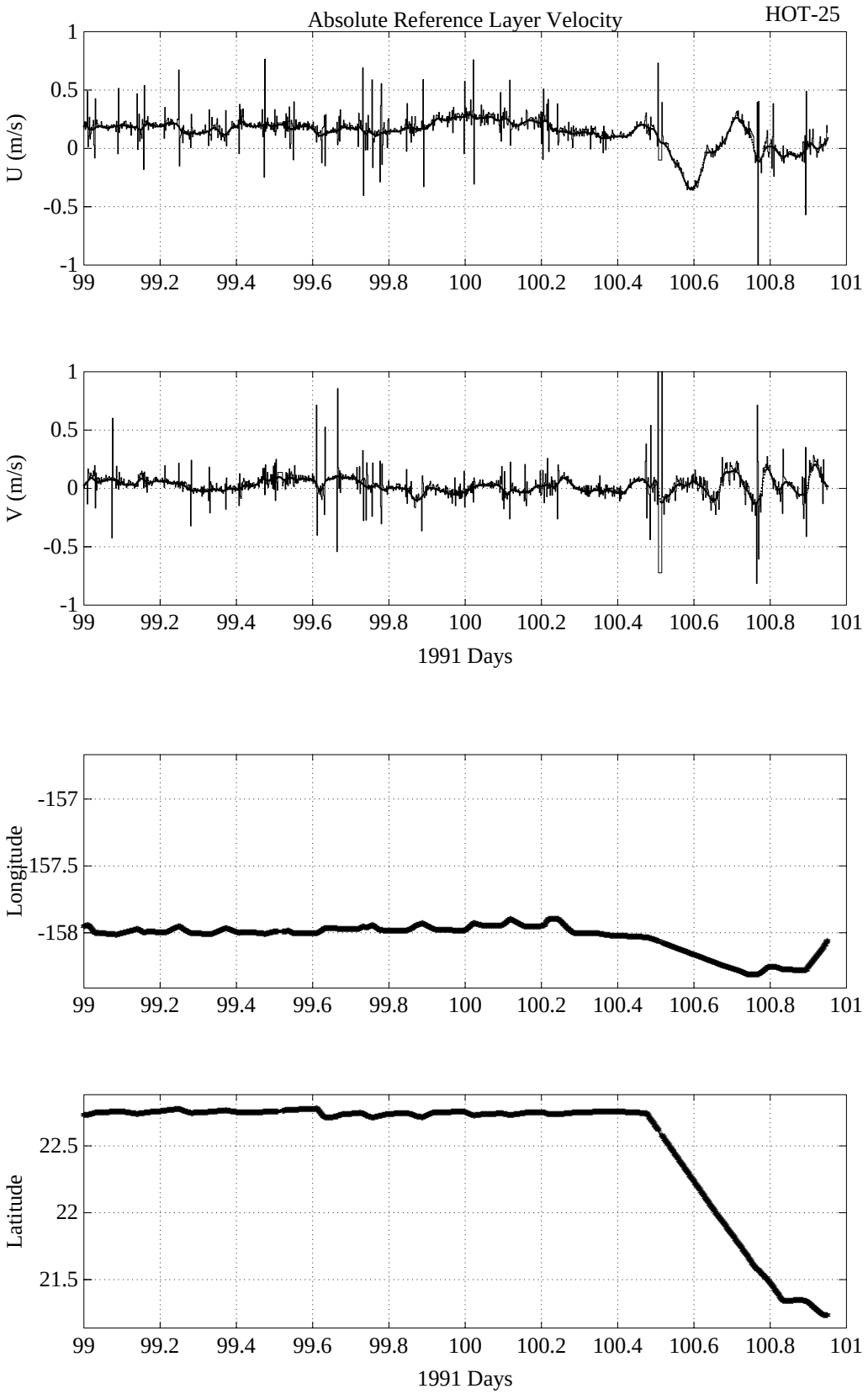

Figure 6.6.3 (continued)

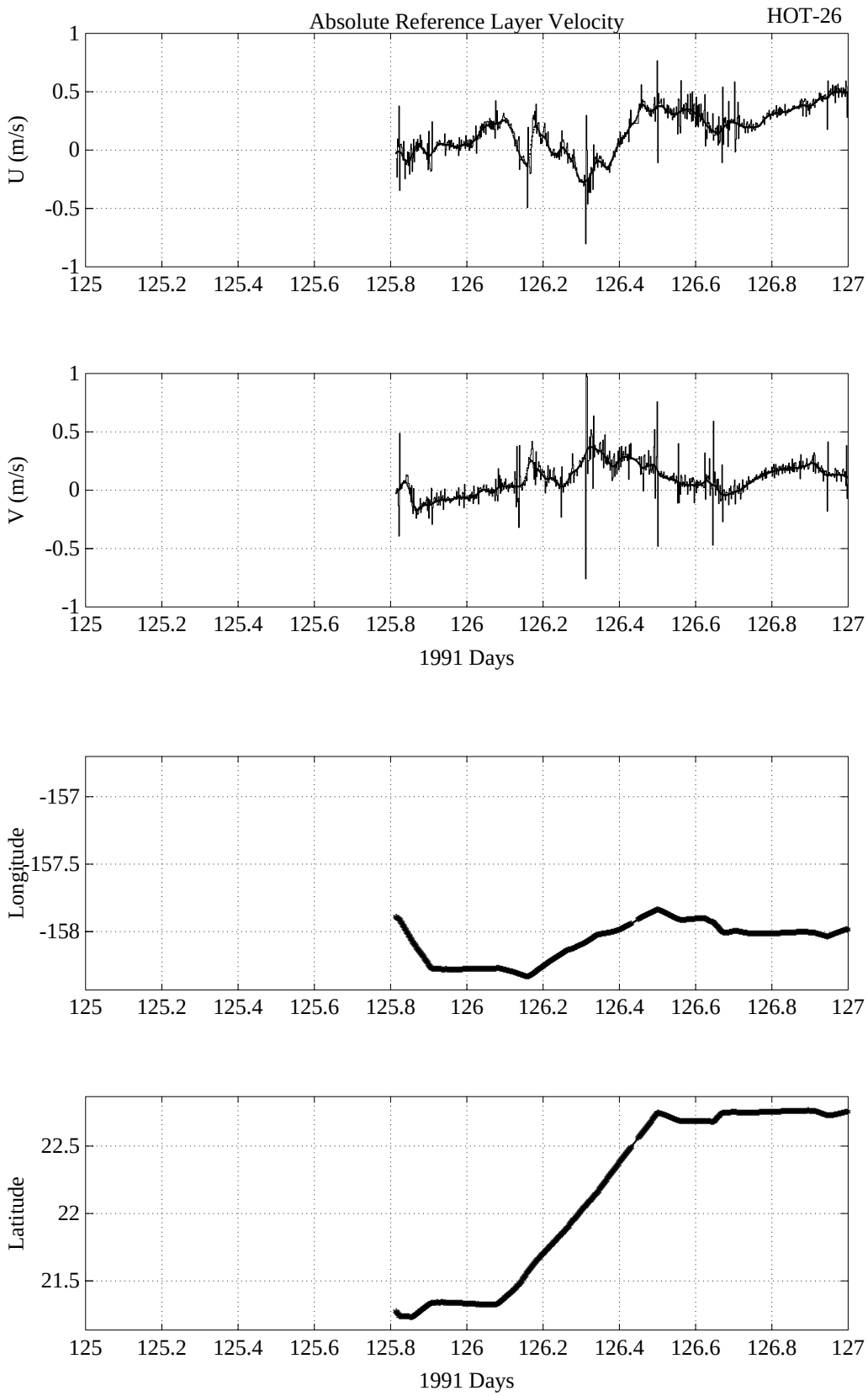
Absolute Reference Layer Velocity
HOT-26
U (m/s)
V (m/s)
1991 Days
Longitude
Latitude
1991 Days

Figure 6.6.4

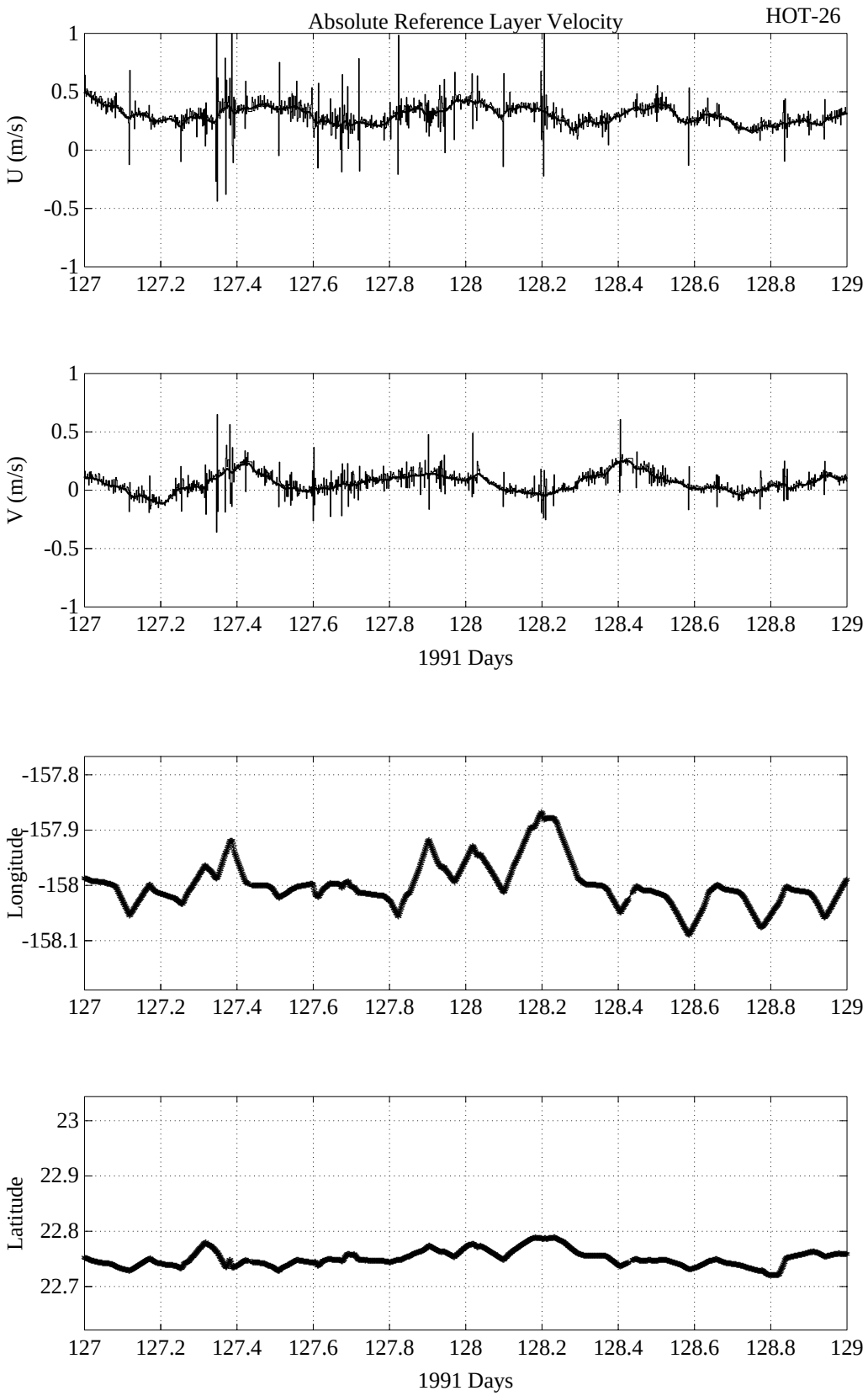

Figure 6.6.4 (continued)

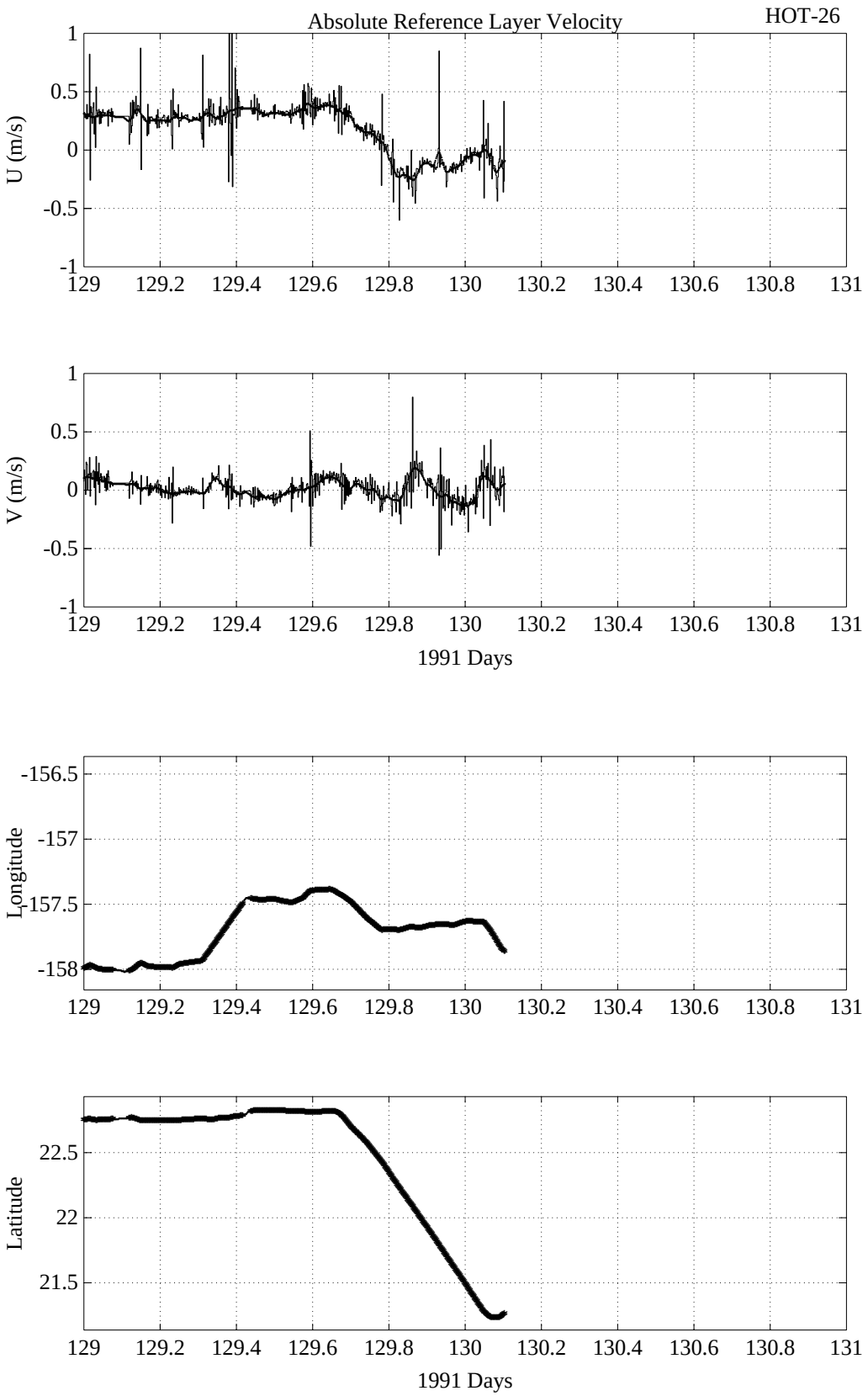

Figure 6.6.4 (continued)

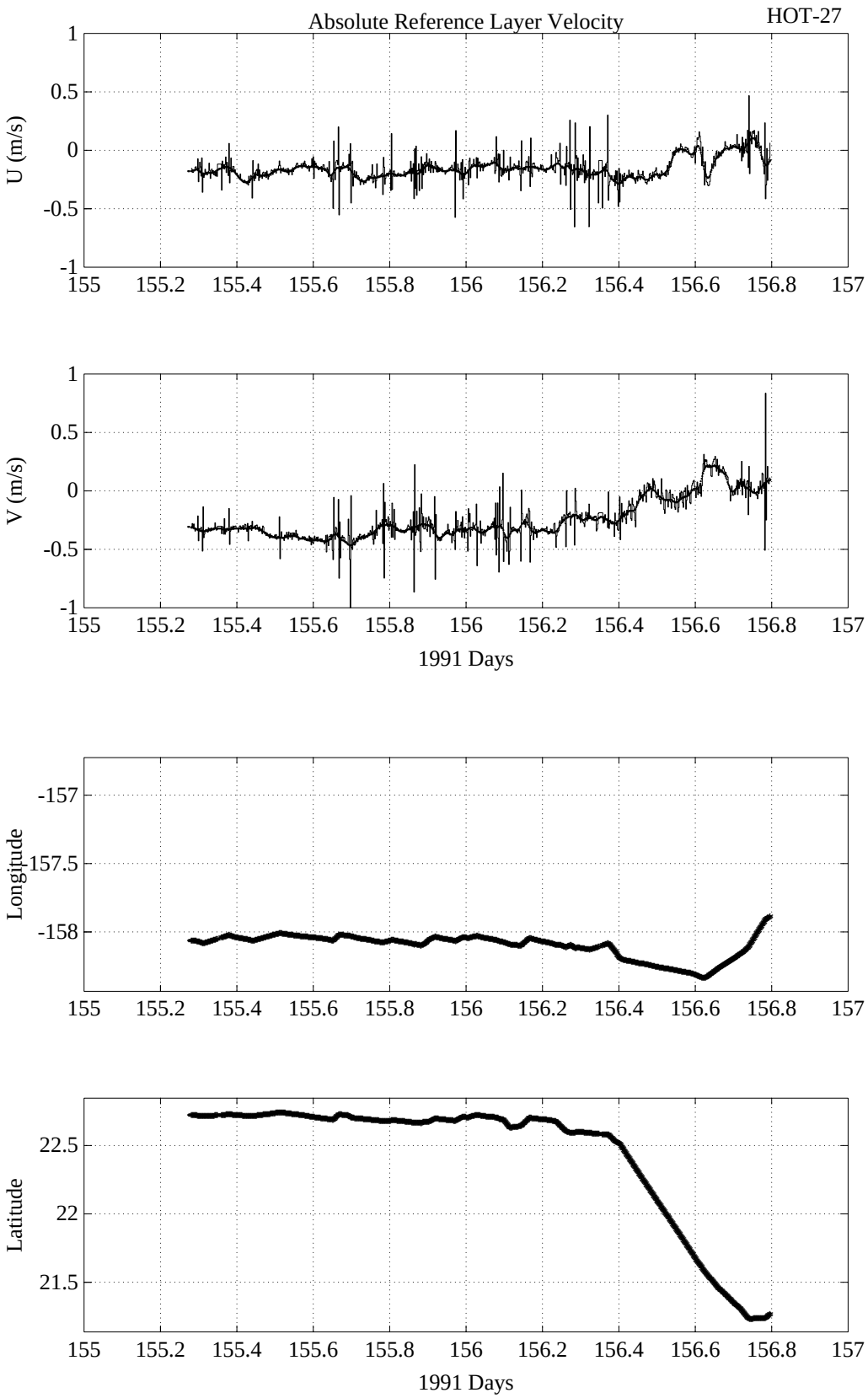
Absolute Reference Layer Velocity
HOT-27
U (m/s)
V (m/s)
1991 Days
Longitude
Latitude
1991 Days

Figure 6.6.5

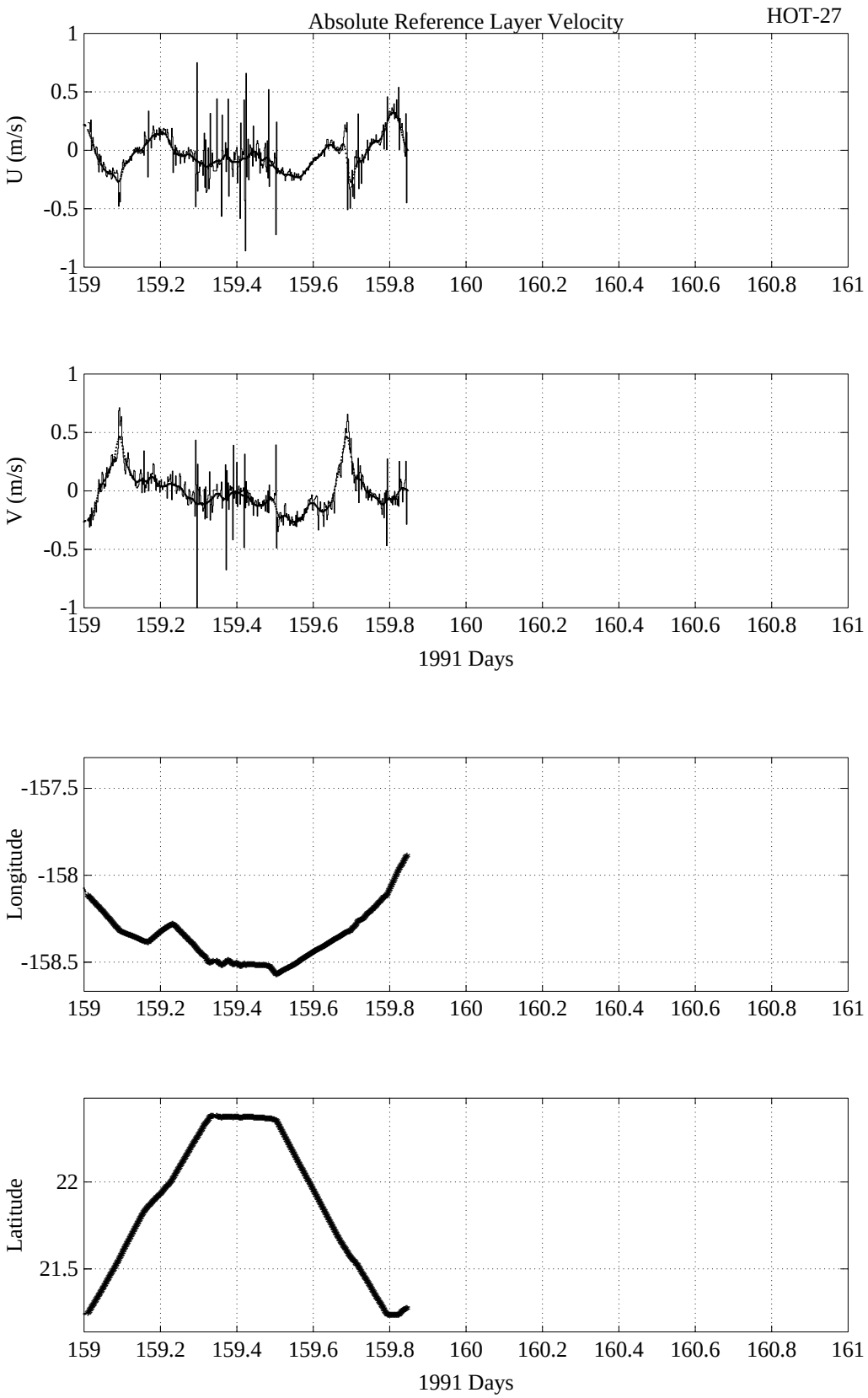

Figure 6.6.5 (continued)

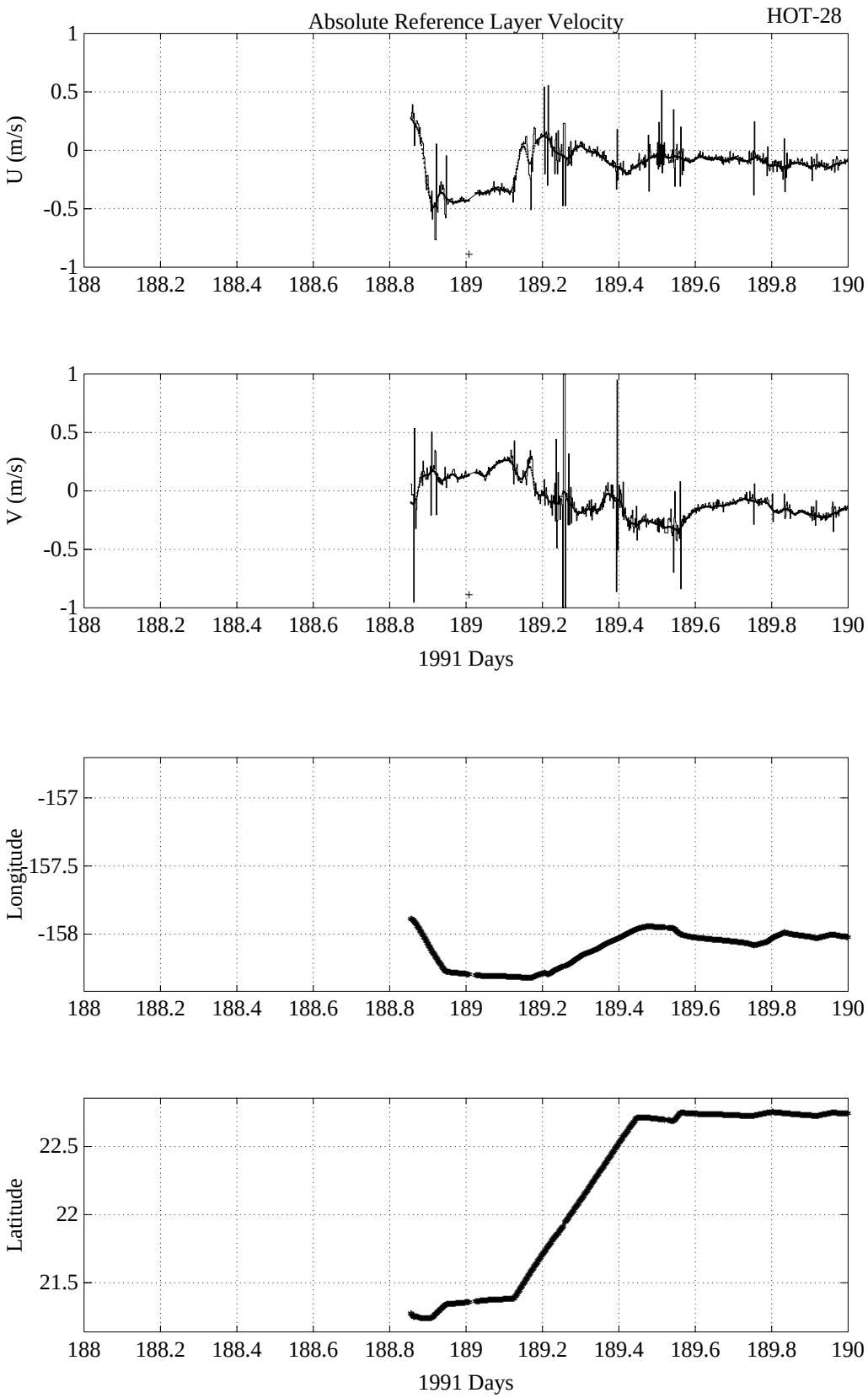
Absolute Reference Layer Velocity
HOT-28
U (m/s)
V (m/s)
1991 Days
Longitude
Latitude
1991 Days

Figure 6.6.6

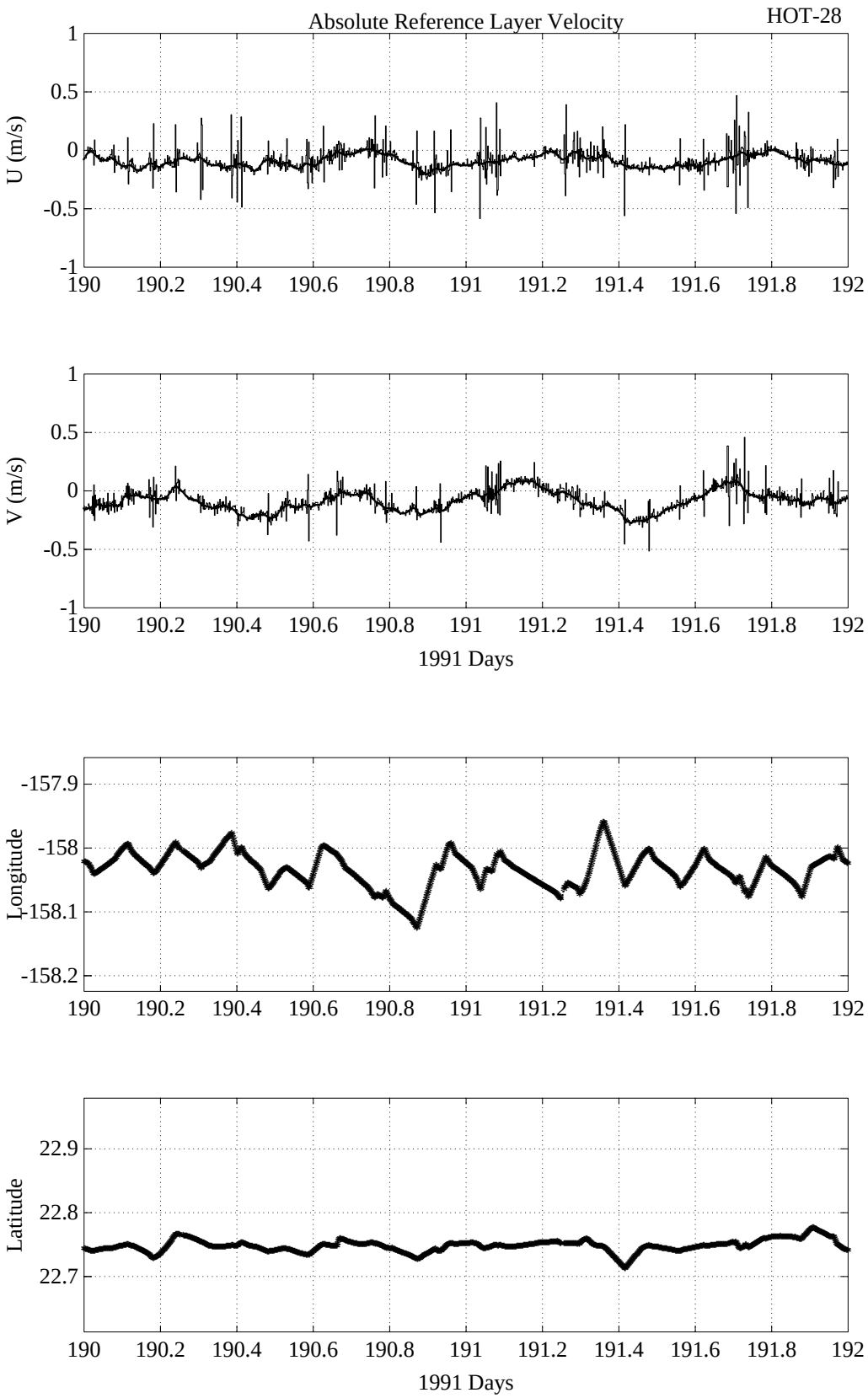

Figure 6.6.6 (continued)

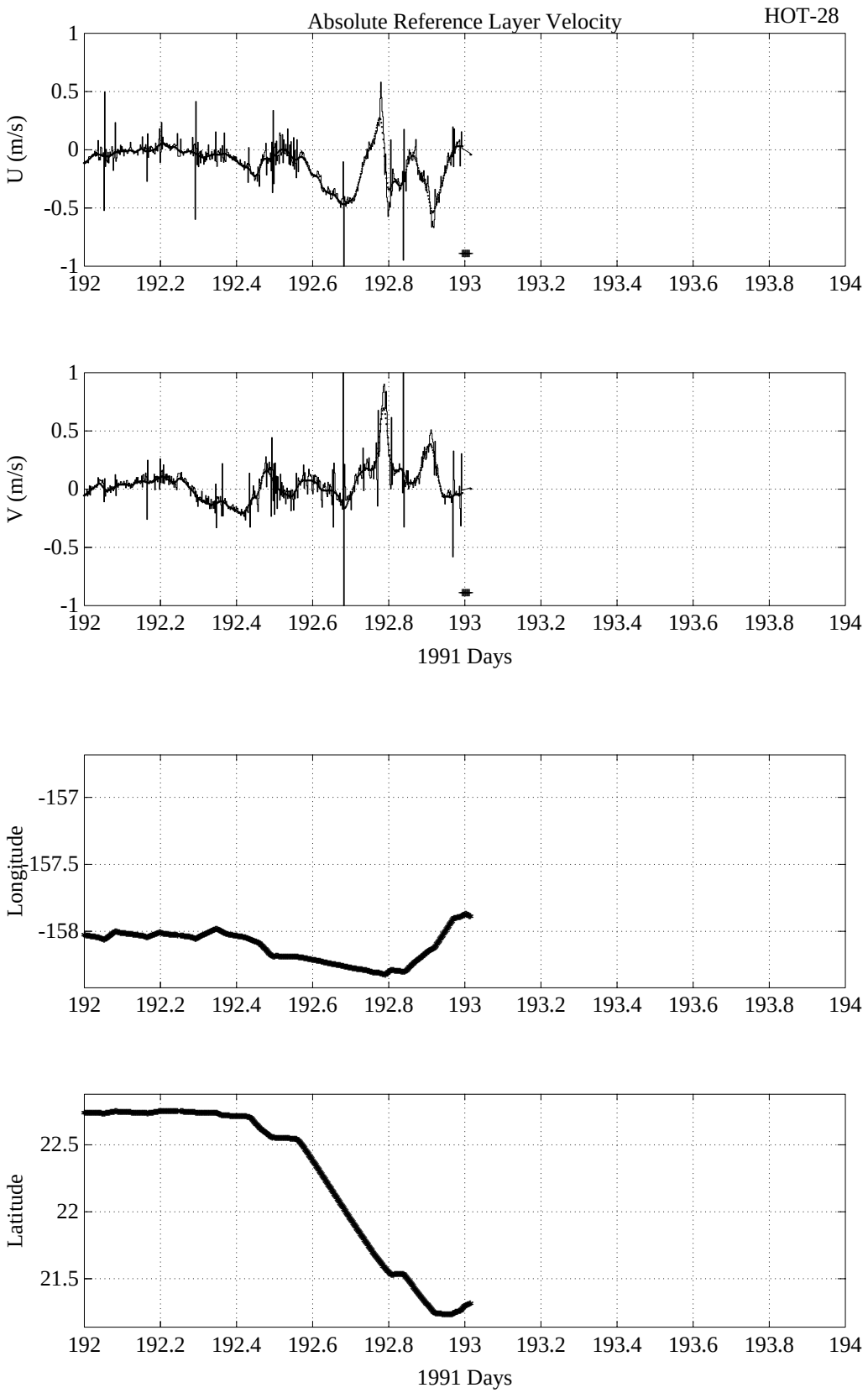

Figure 6.6.6 (continued)

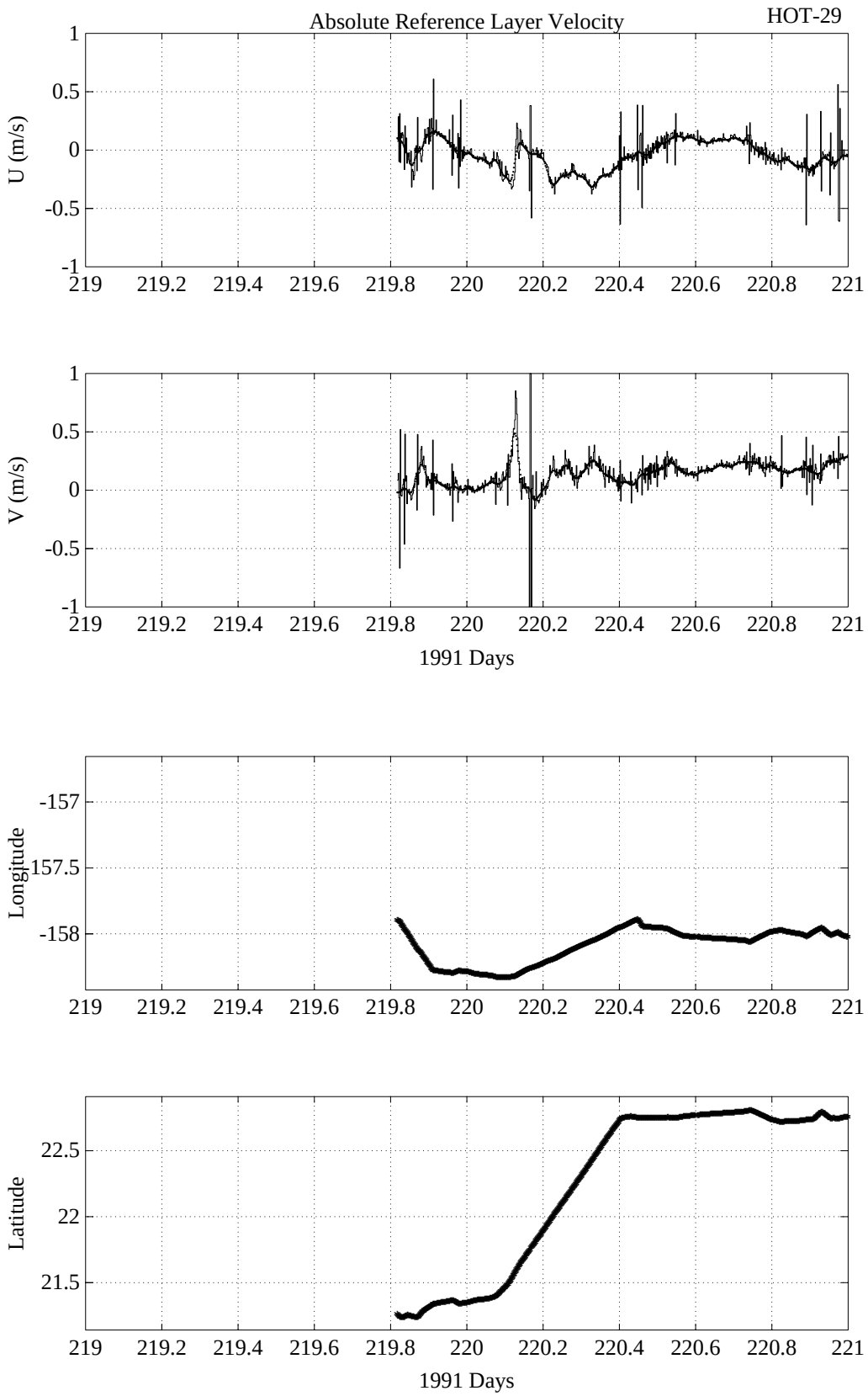
Absolute Reference Layer Velocity
HOT-29
U (m/s)
V (m/s)
1991 Days
Longitude
Latitude
1991 Days

Figure 6.6.7

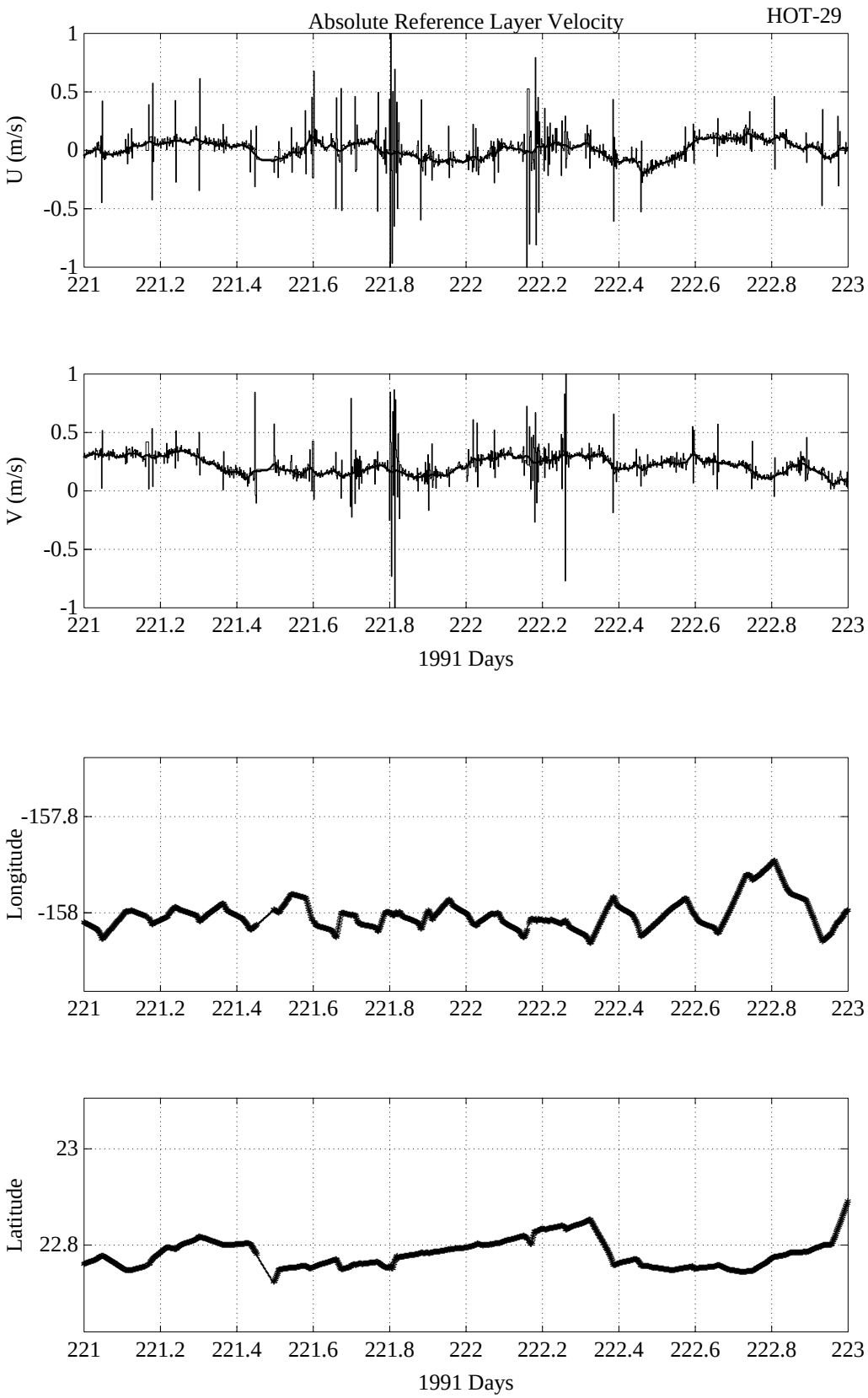

Figure 6.6.7 (continued)

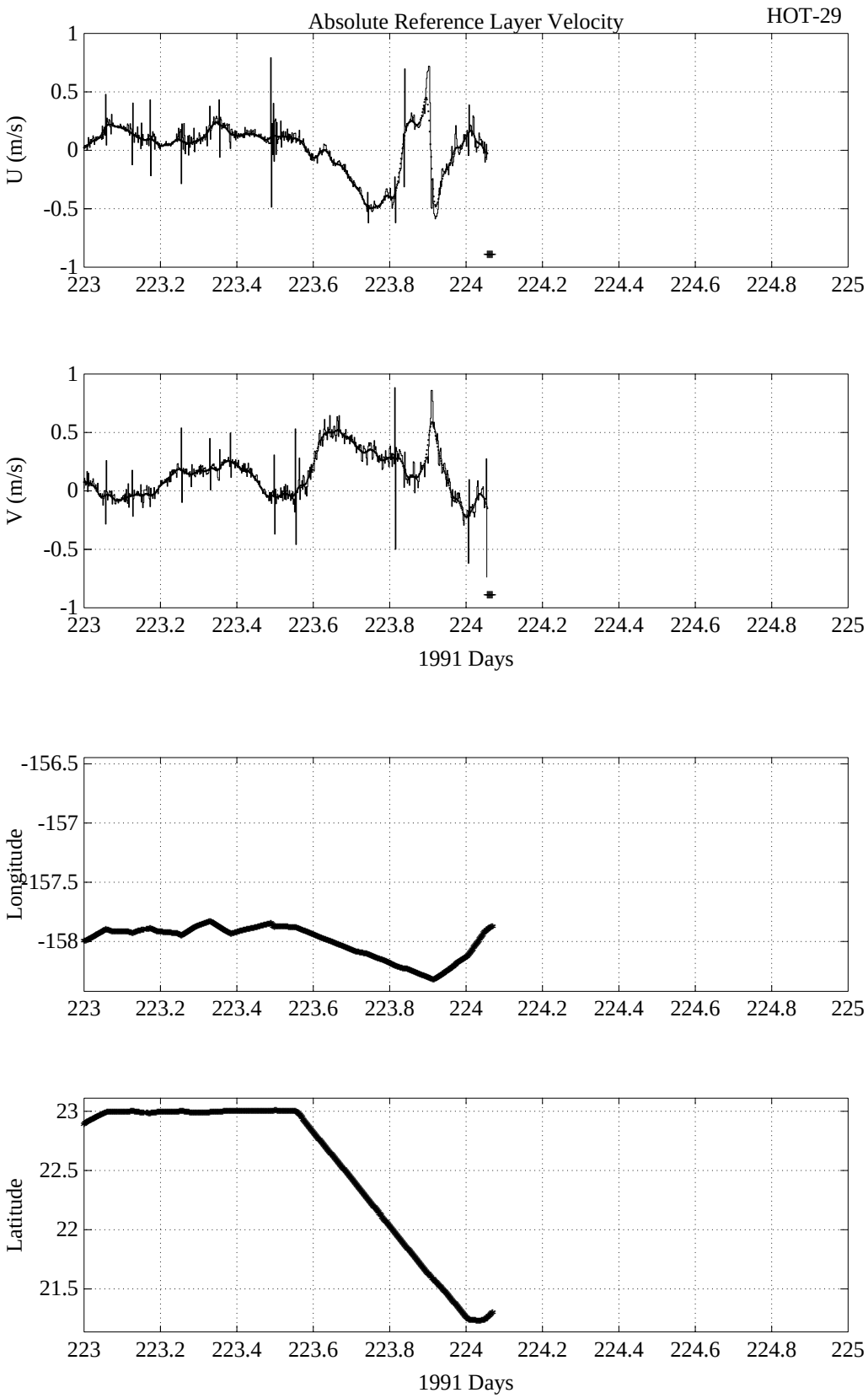

Figure 6.6.7 (continued)

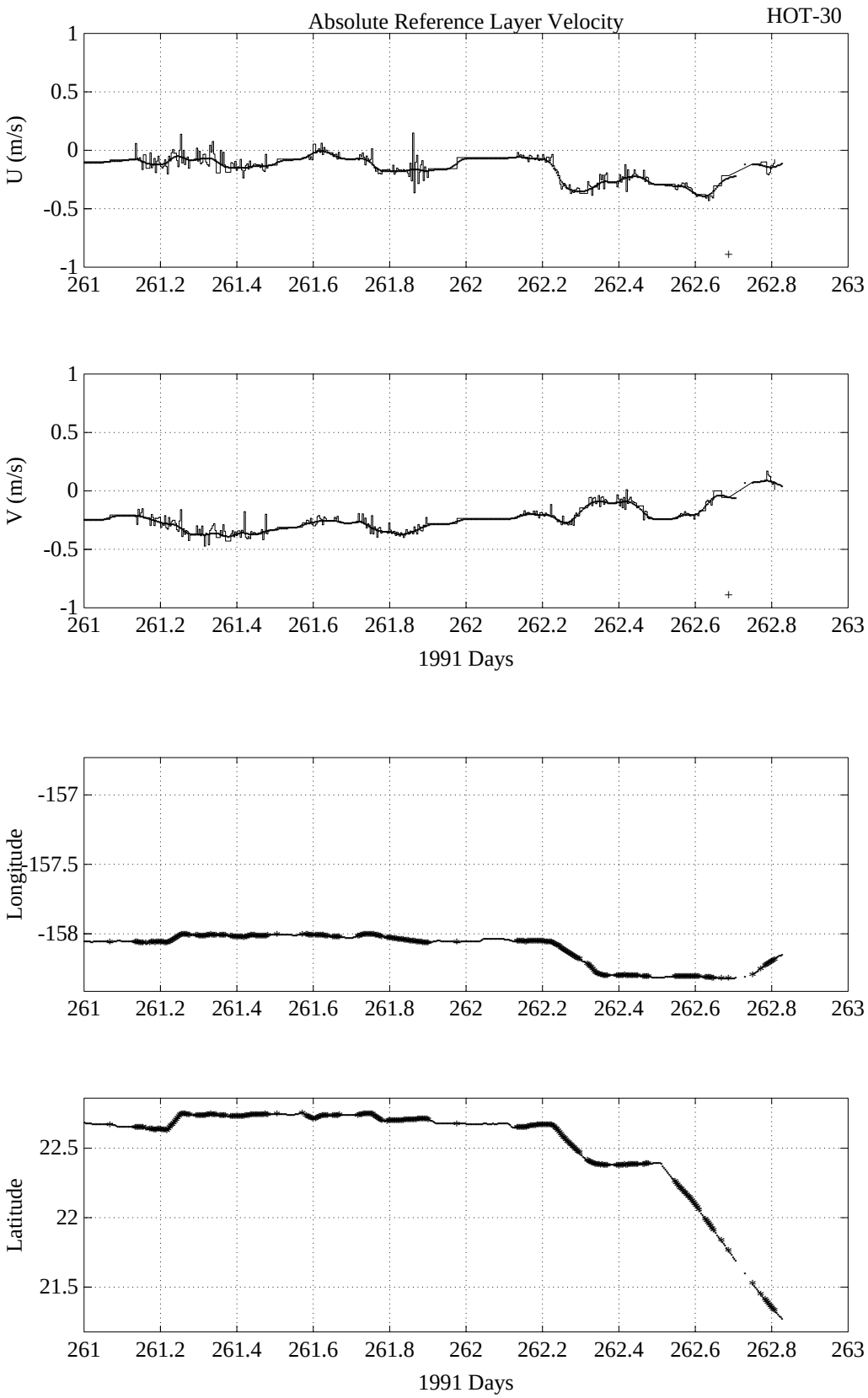
Absolute Reference Layer Velocity
HOT-30
U (m/s)
V (m/s)
Longitude
Latitude
1991 Days
1991 Days

Figure 6.6.8

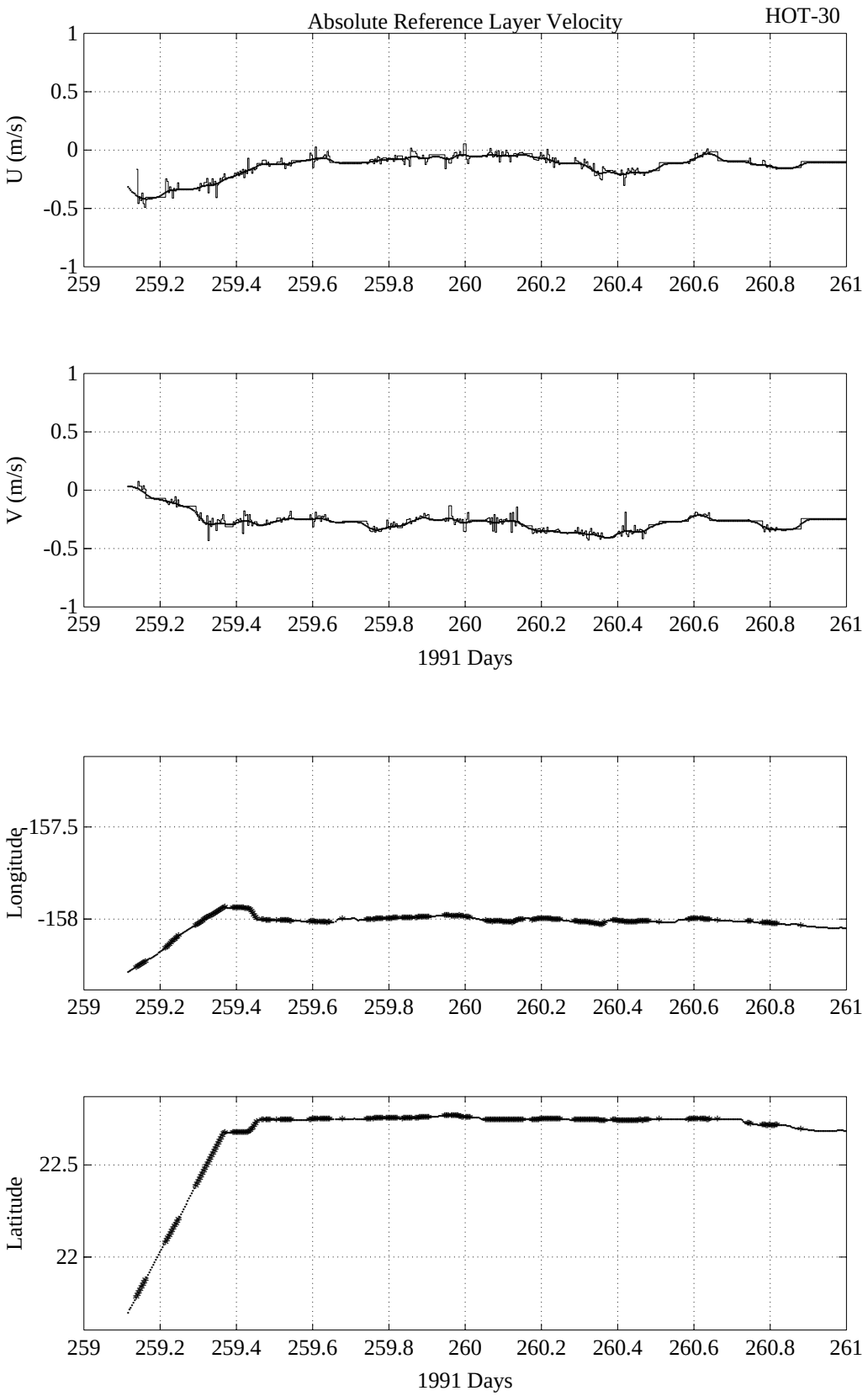

Figure 6.6.8 (continued)

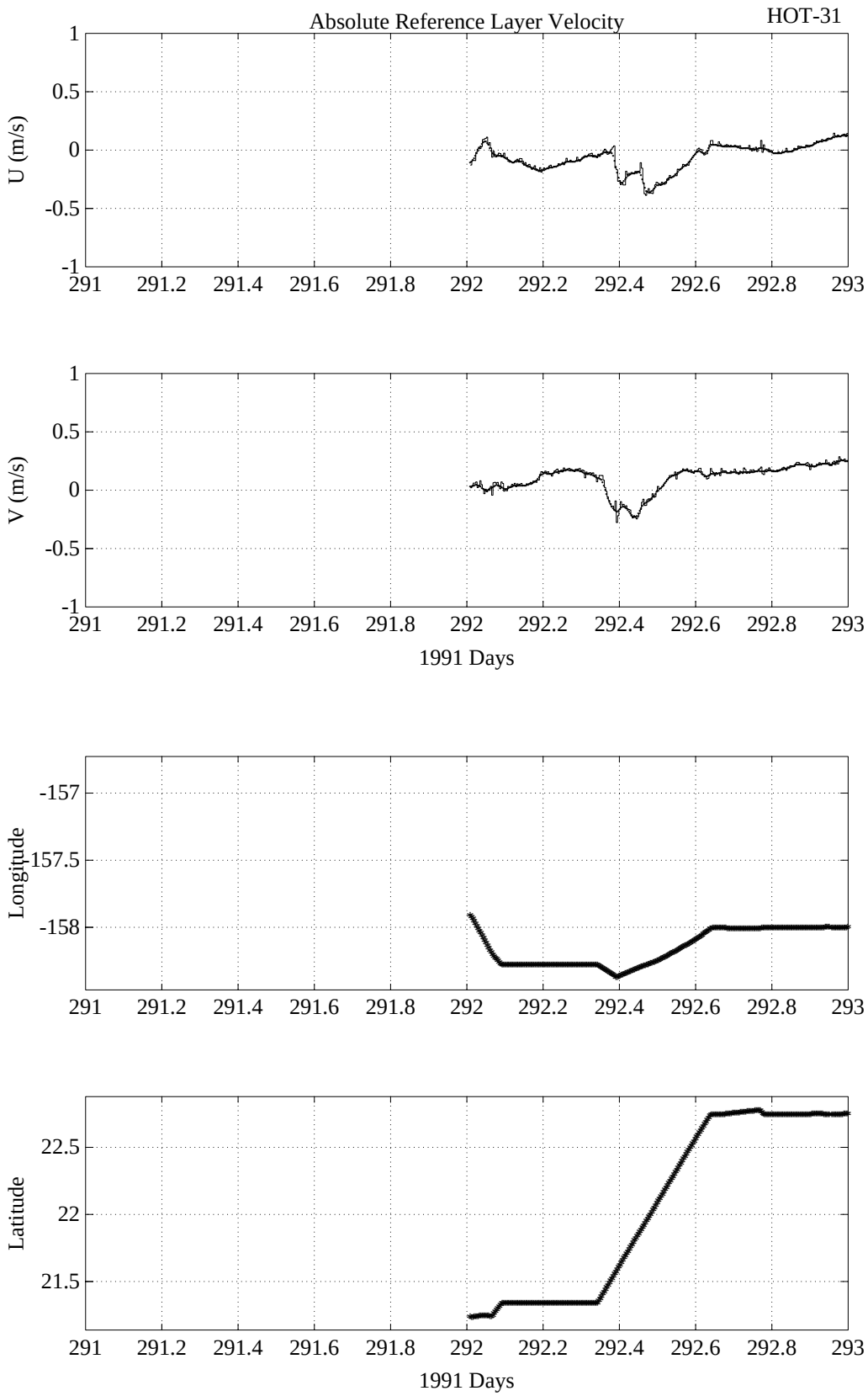
Absolute Reference Layer Velocity
HOT-31
U (m/s)
V (m/s)
Longitude
Latitude
1991 Days
1991 Days

Figure 6.6.9

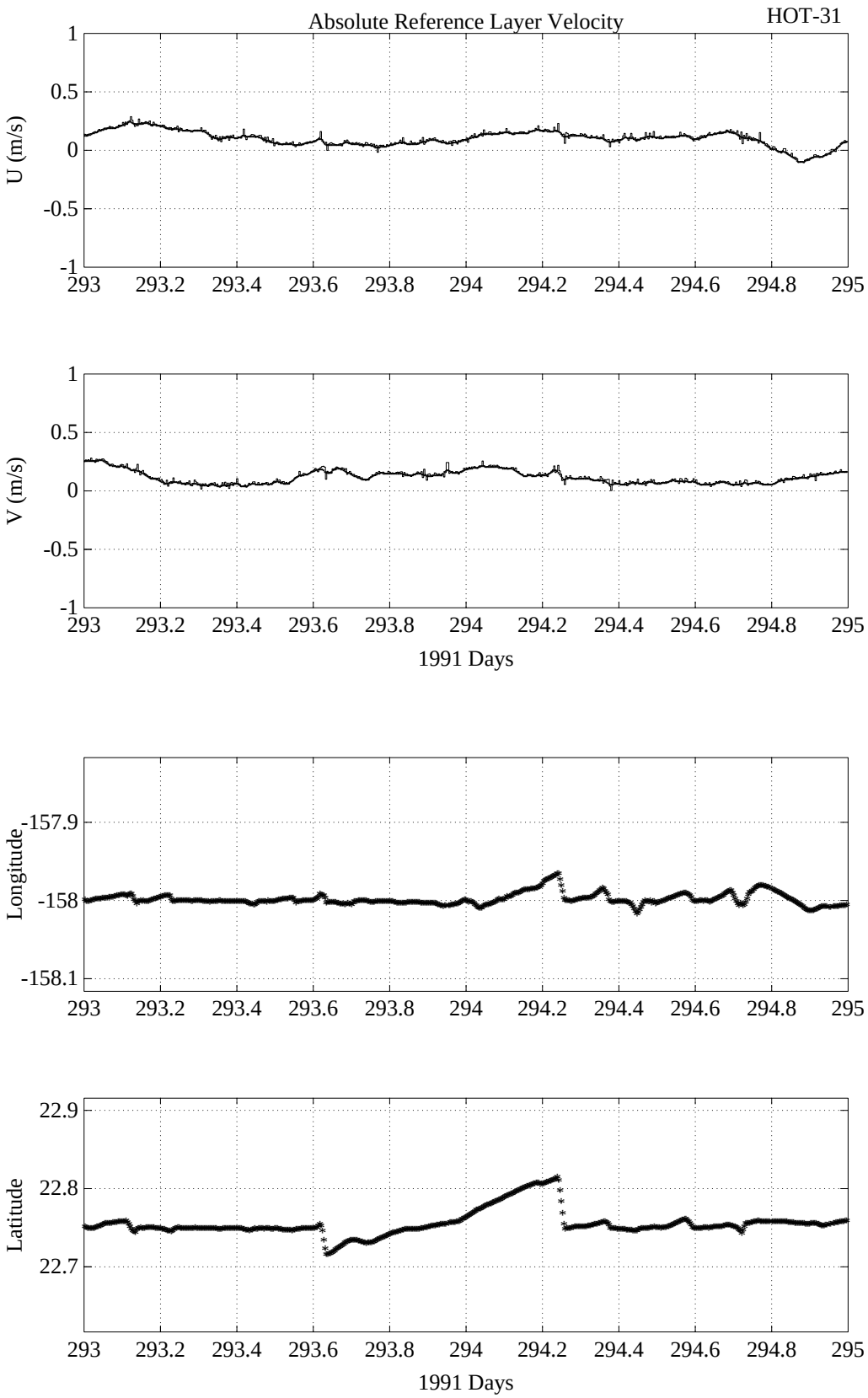

Figure 6.6.9 (continued)

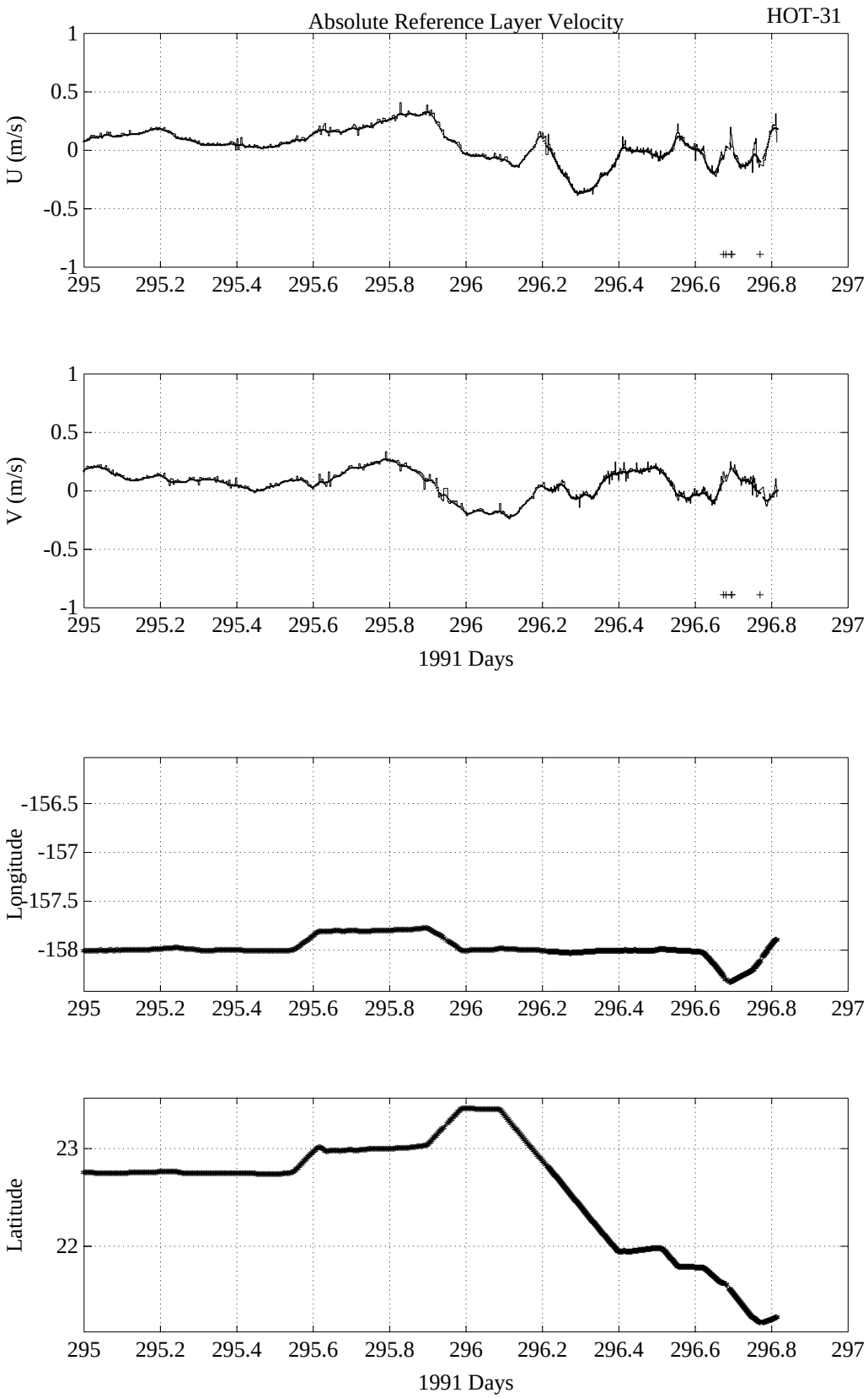

Figure 6.6.9 (continued)

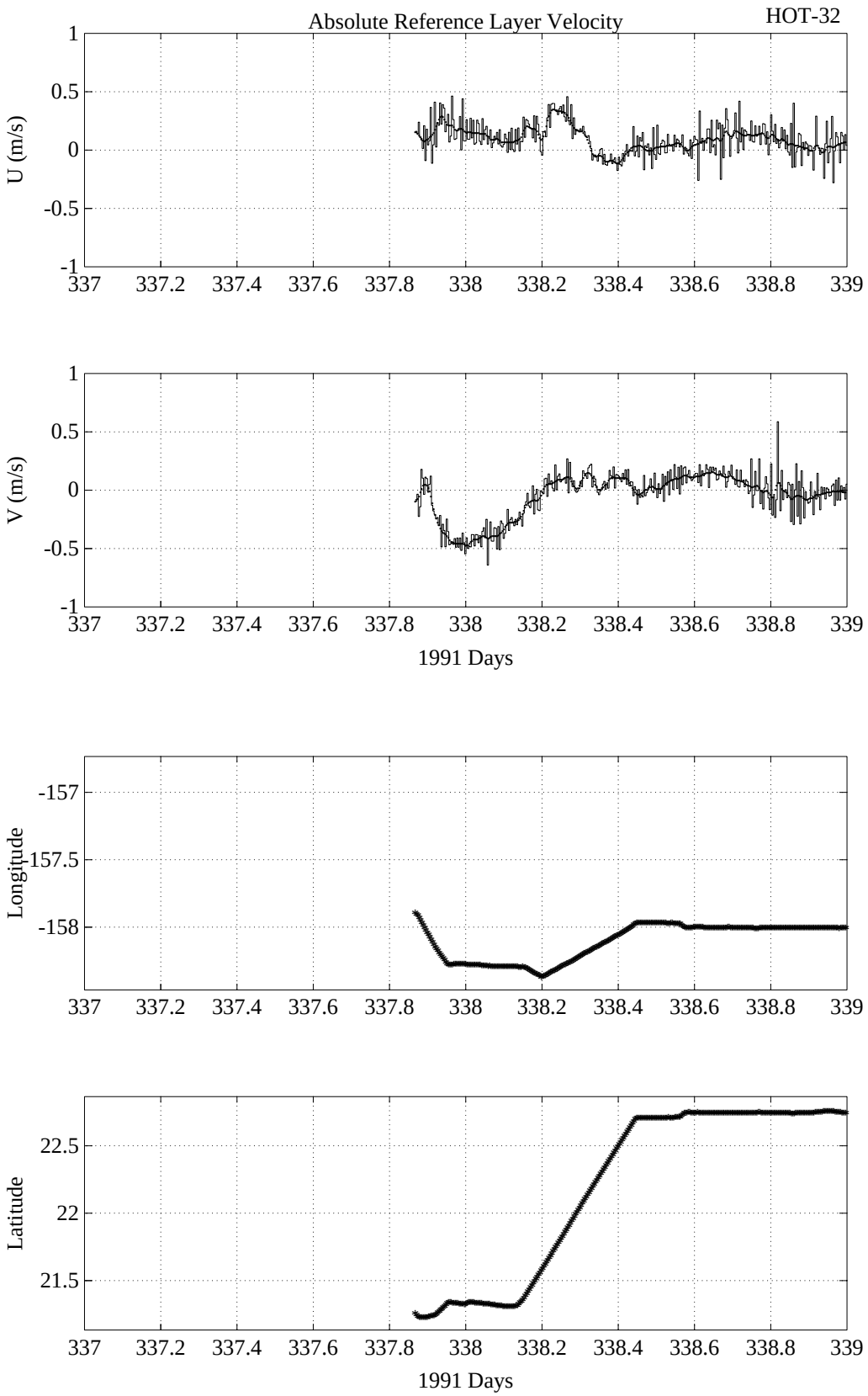
Absolute Reference Layer Velocity
HOT-32
U (m/s)
V (m/s)
Longitude
Latitude
1991 Days
1991 Days

Figure 6.6.10

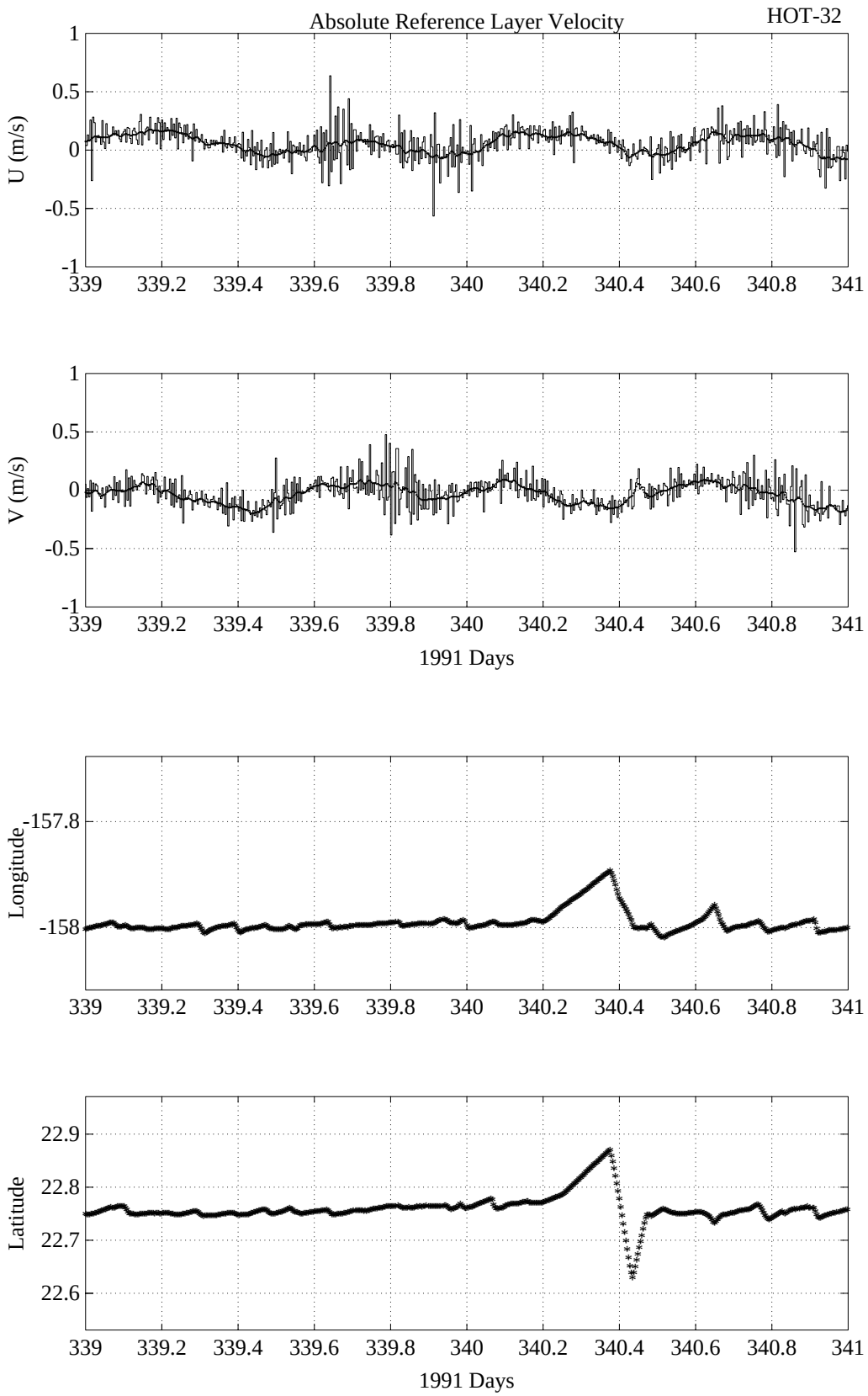

Figure 6.6.10 (continued)

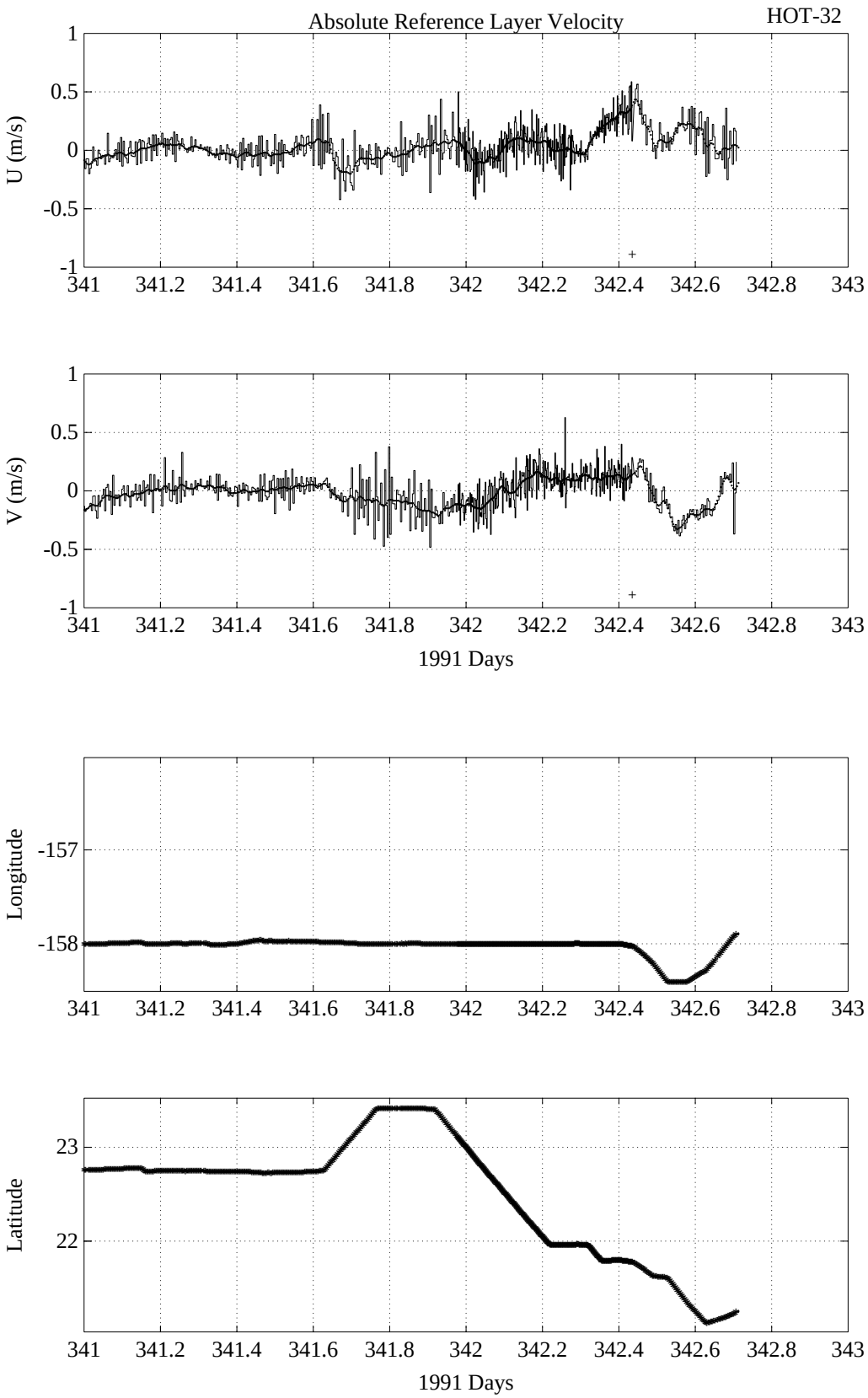

Figure 6.6.10 (continued)

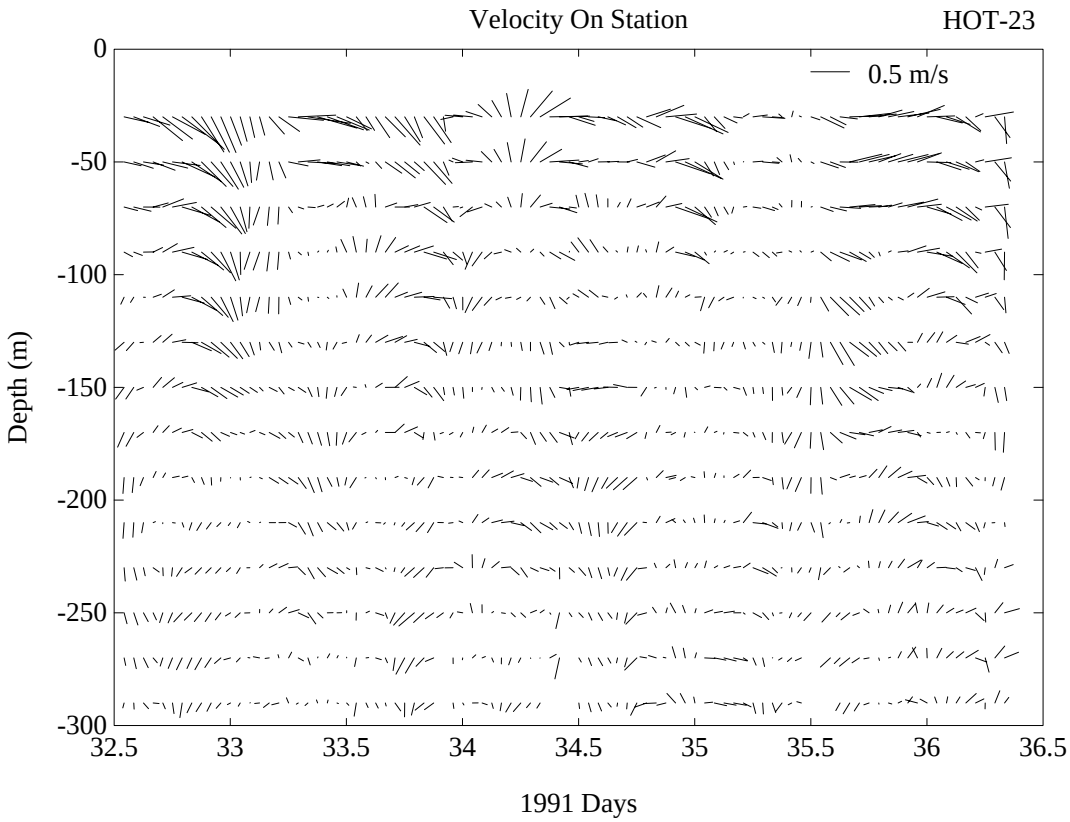

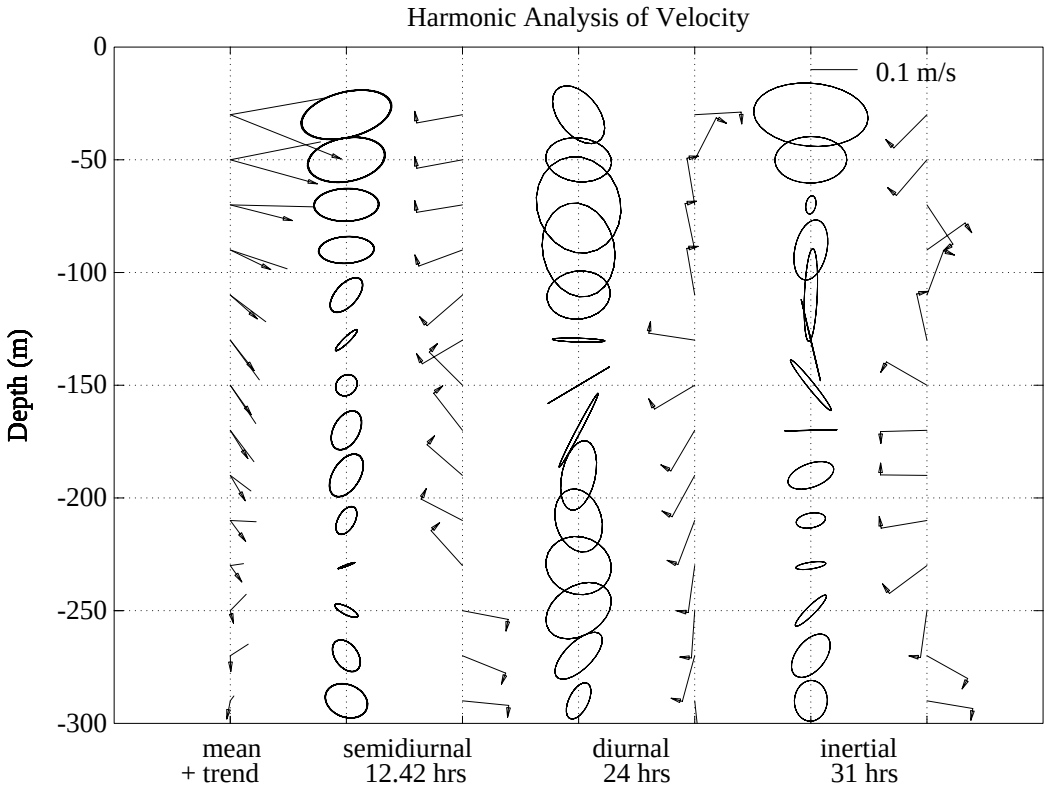

Figure 6.6.11a

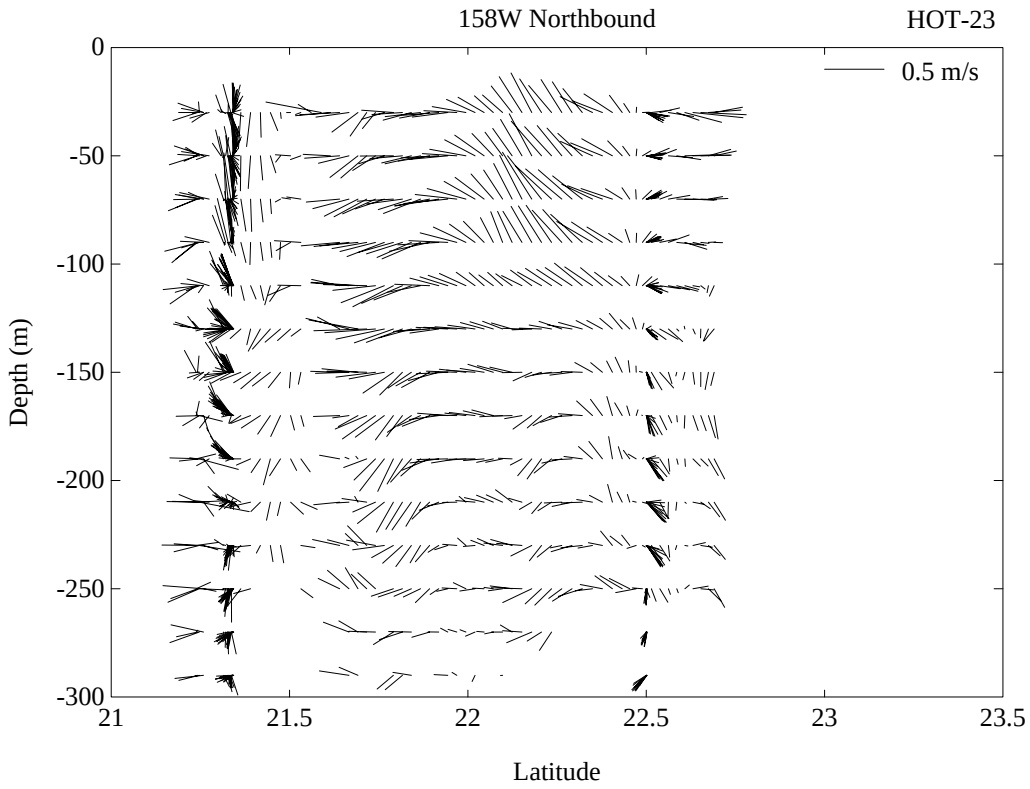

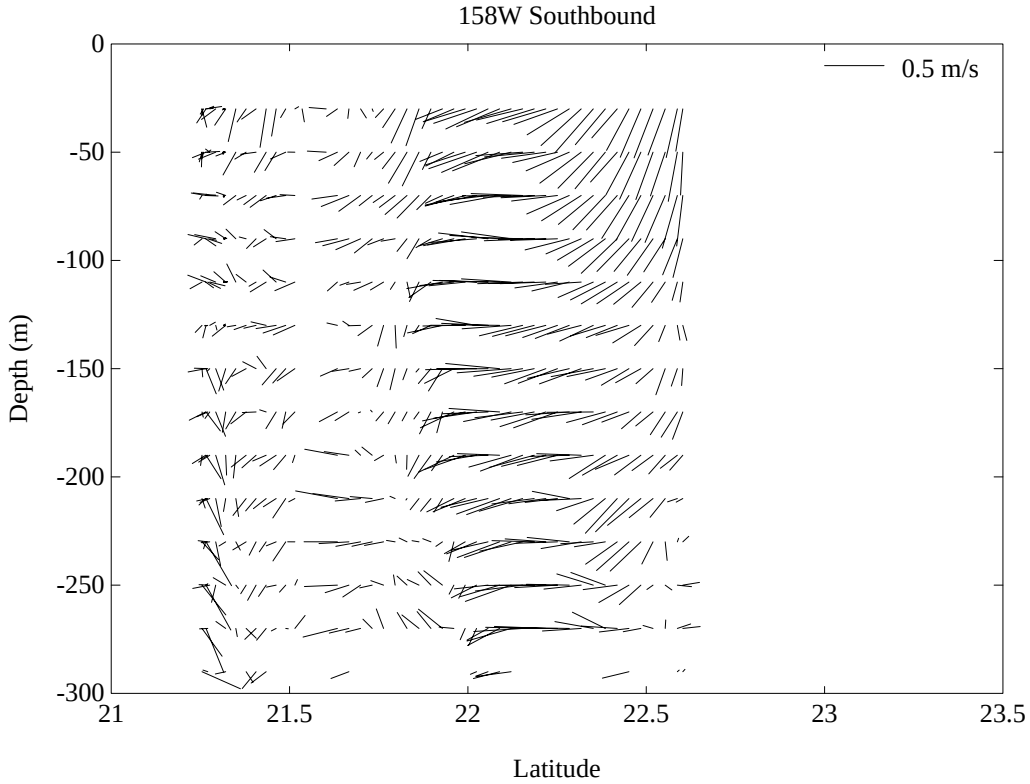

Figure 6.6.11b

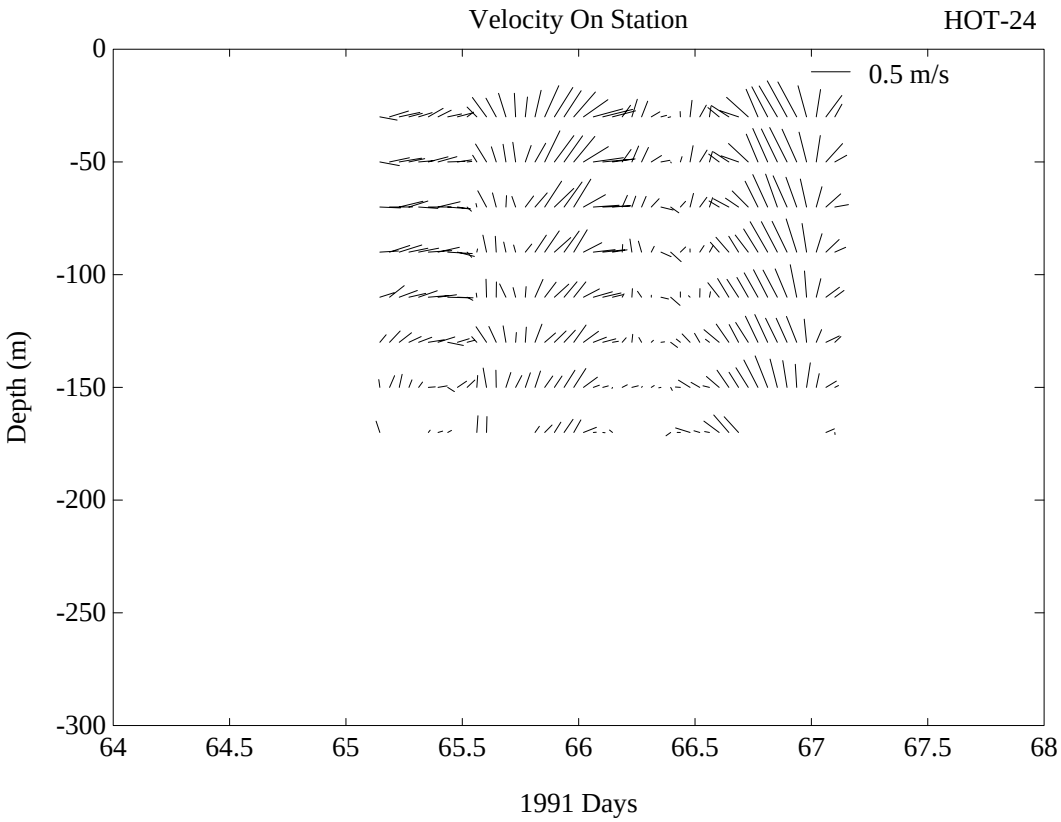

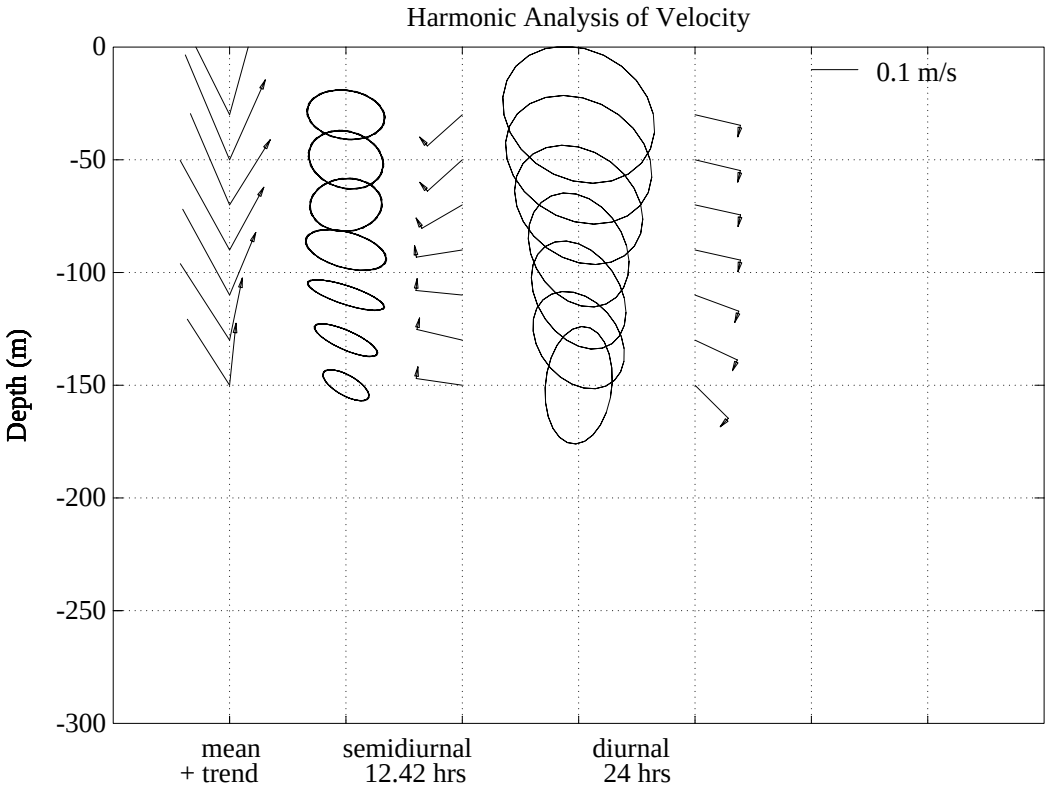

Figure 6.6.12a

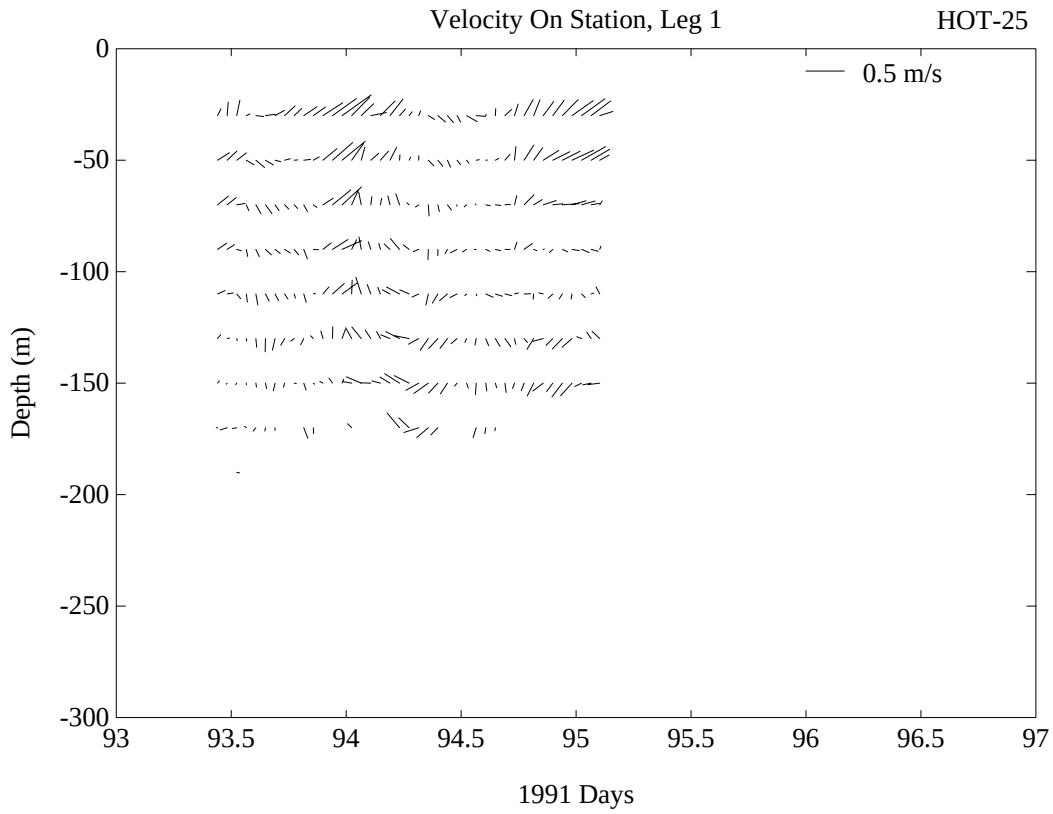

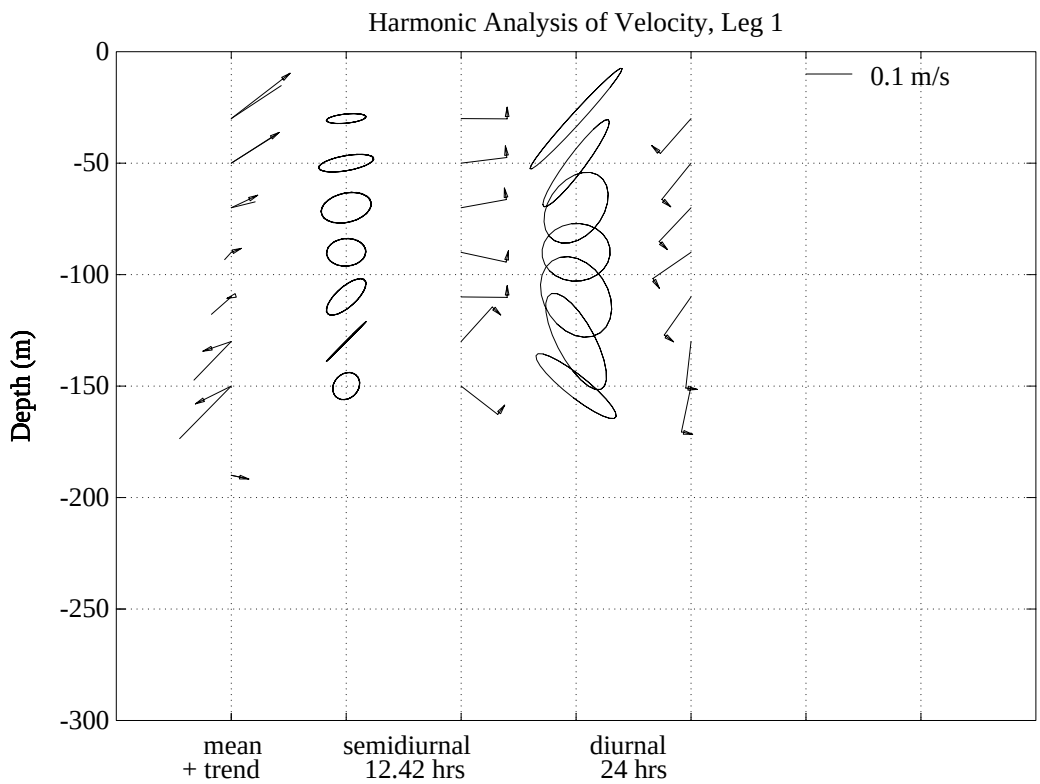

Figure 6.6.13a

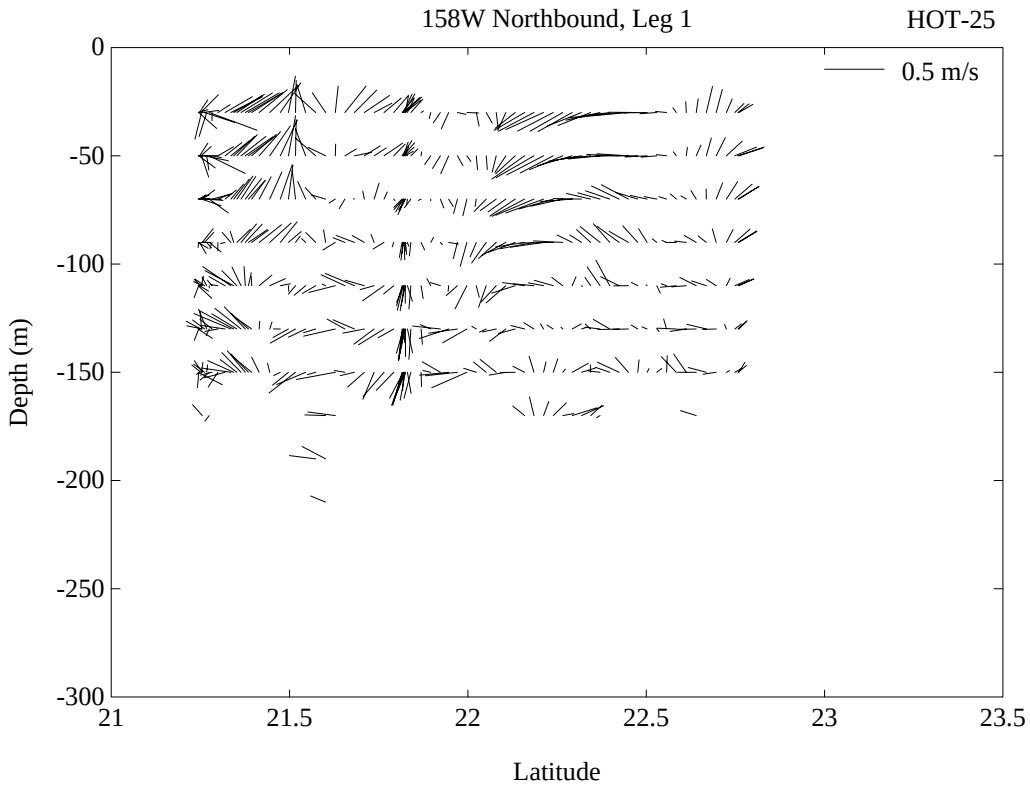

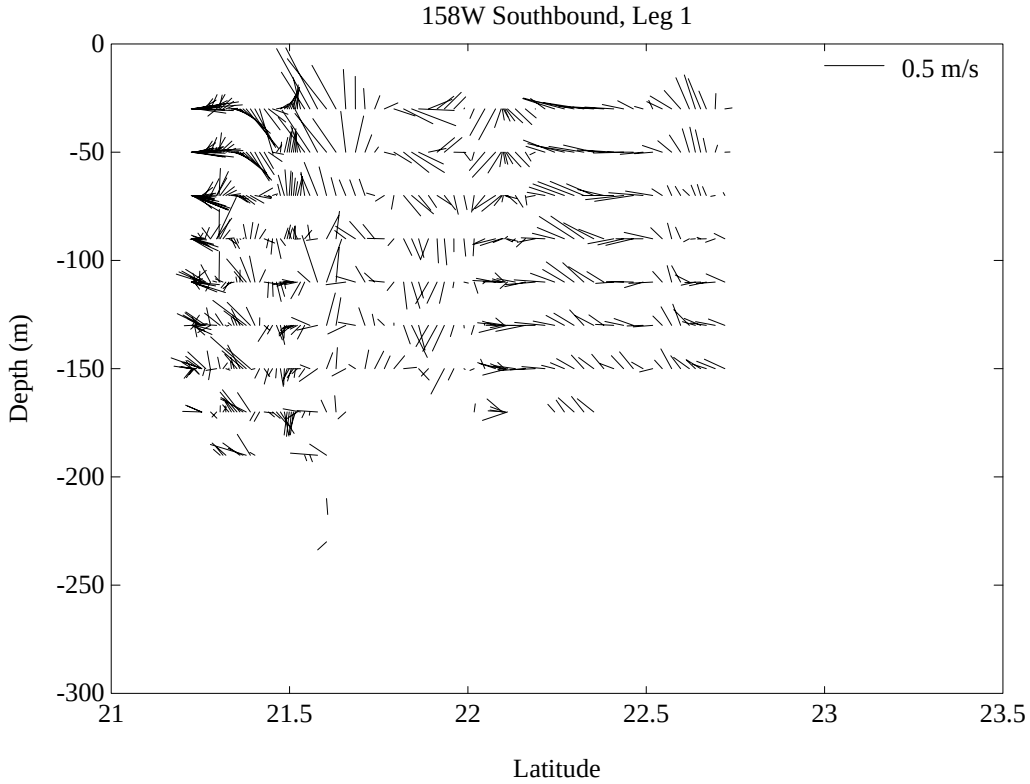

Figure 6.6.13b

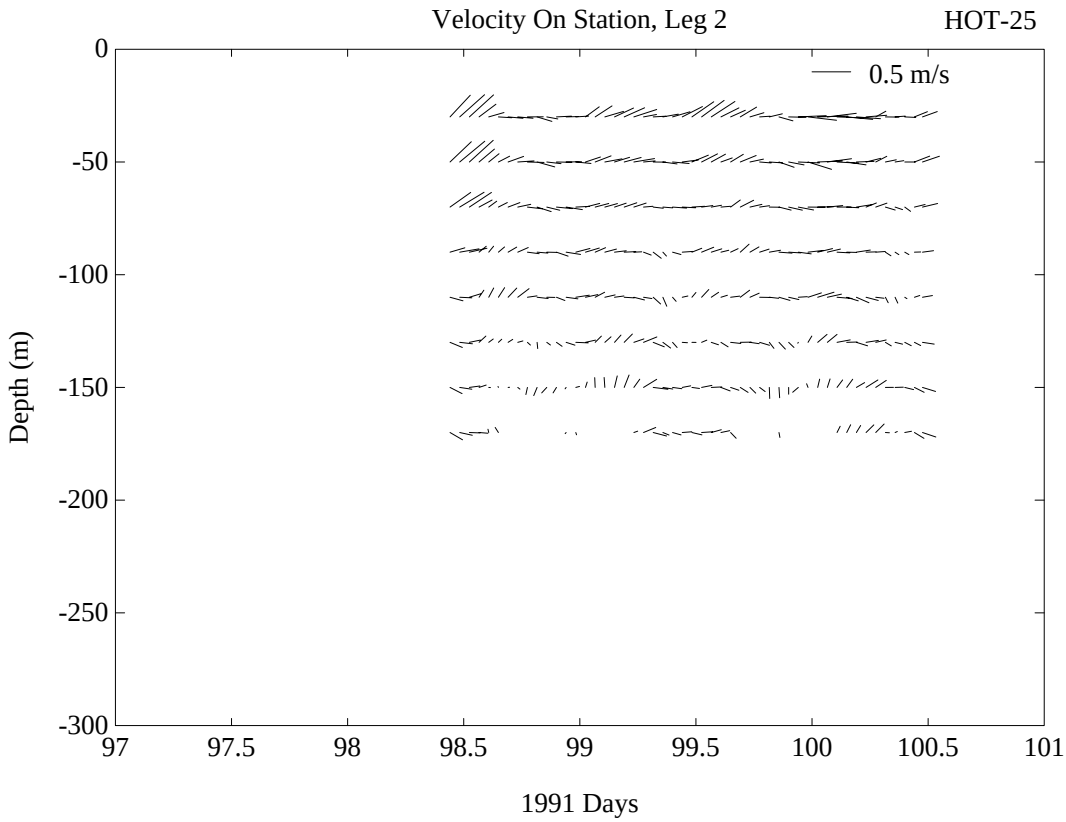

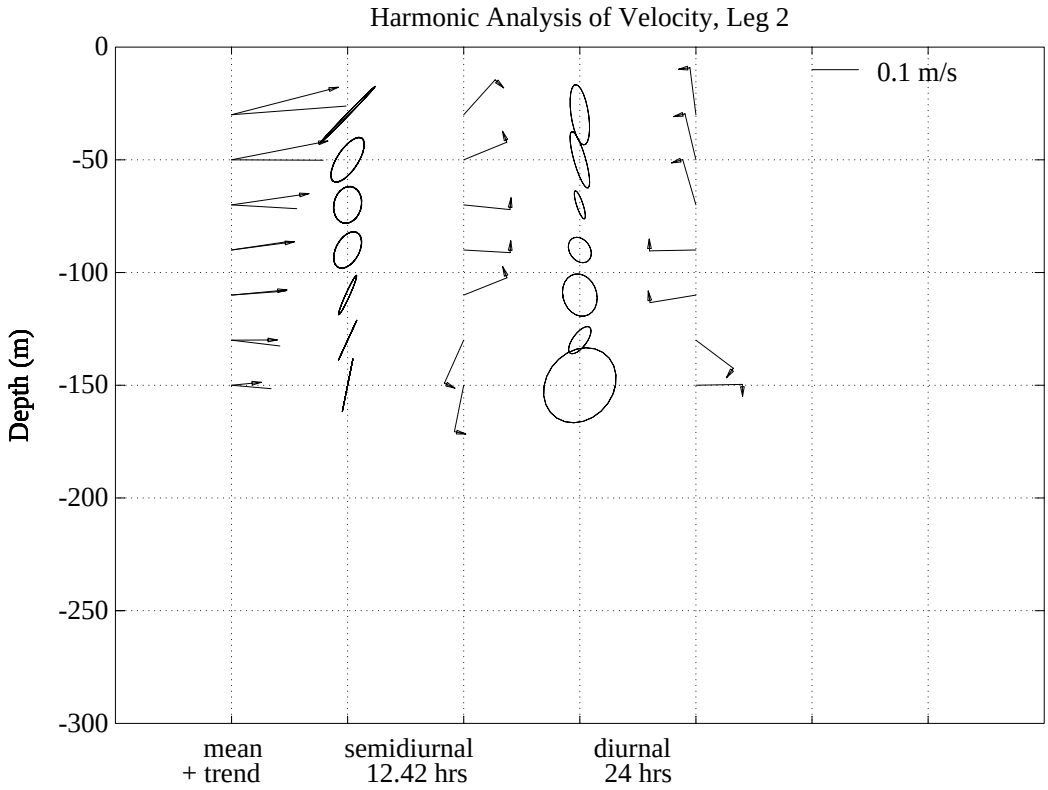

Figure 6.6.14a

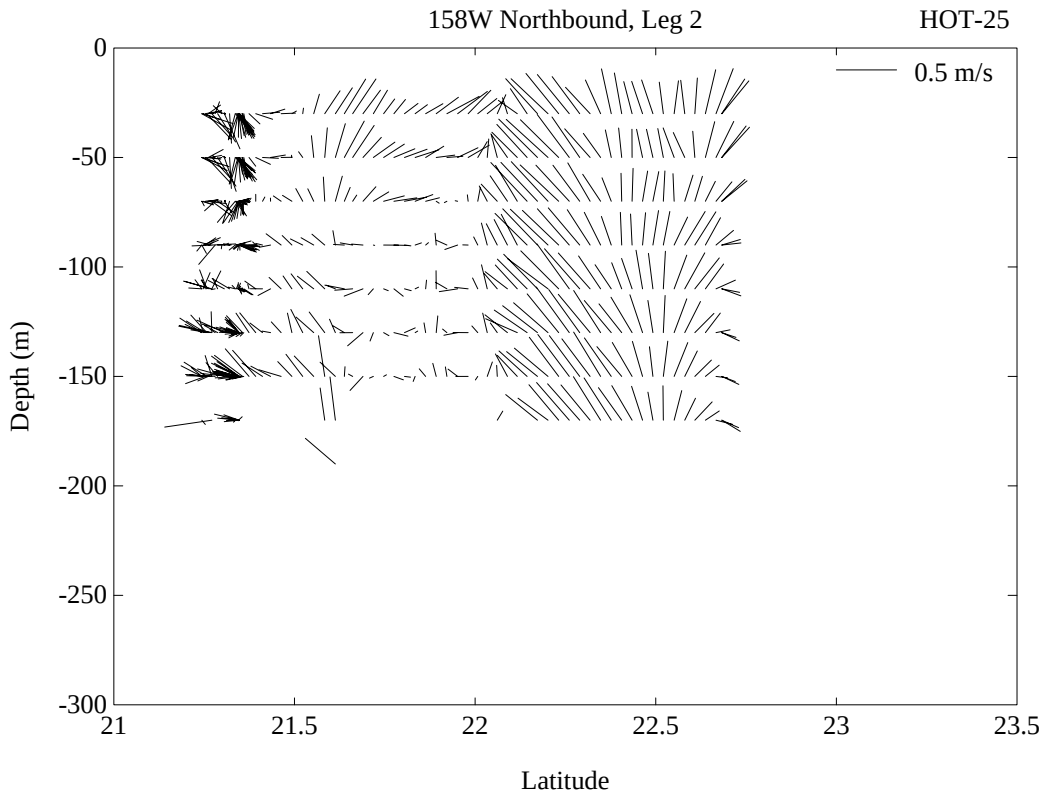

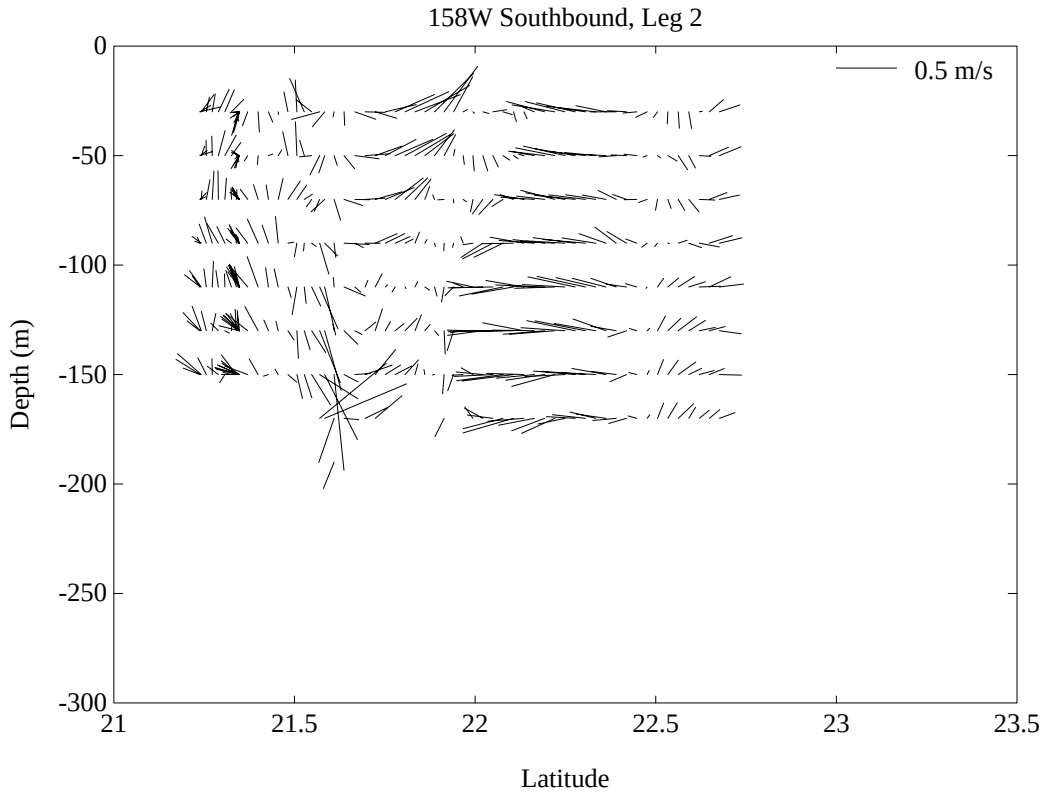

Figure 6.6.14b

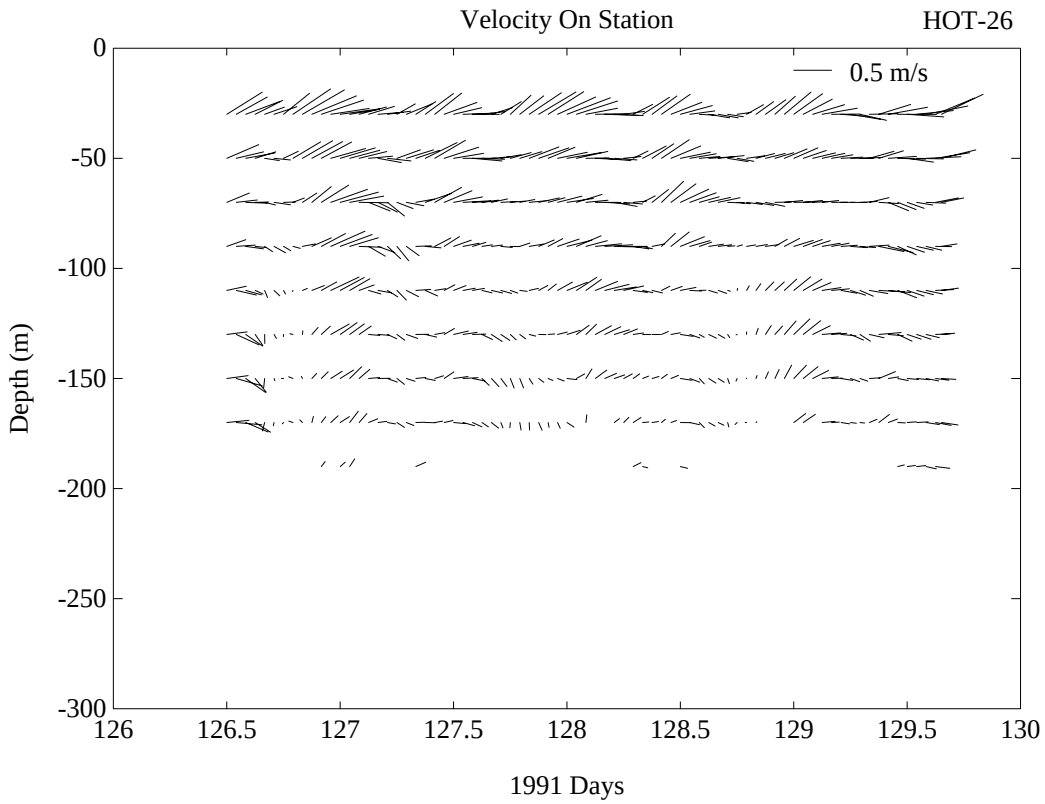

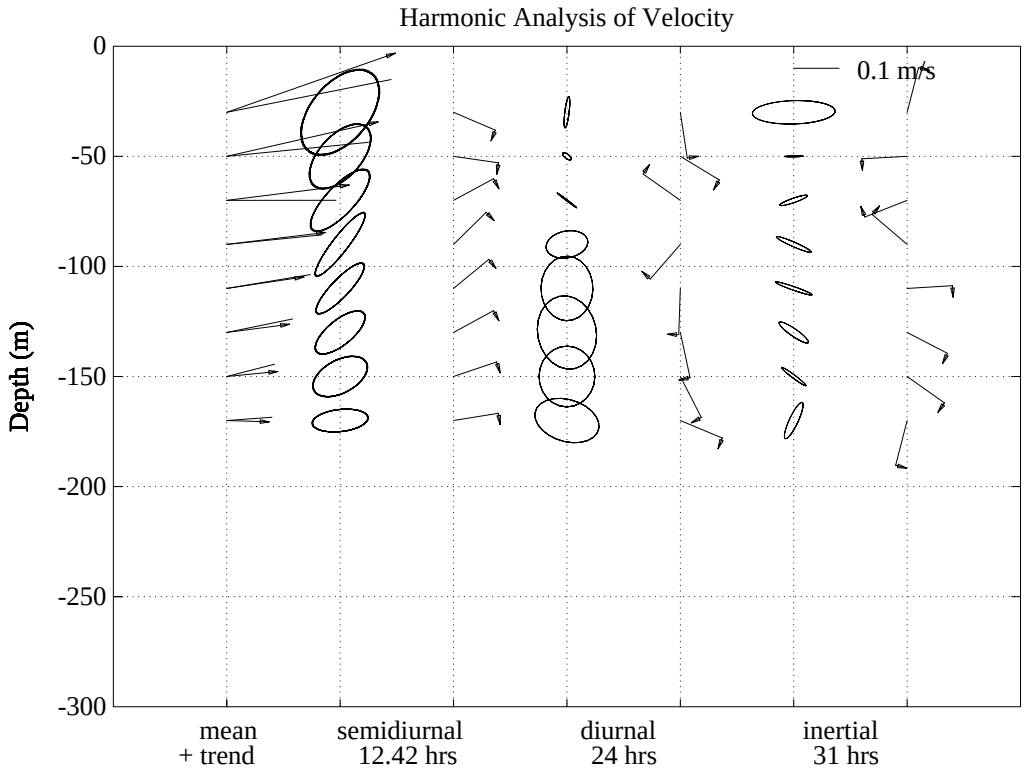

Figure 6.6.15a

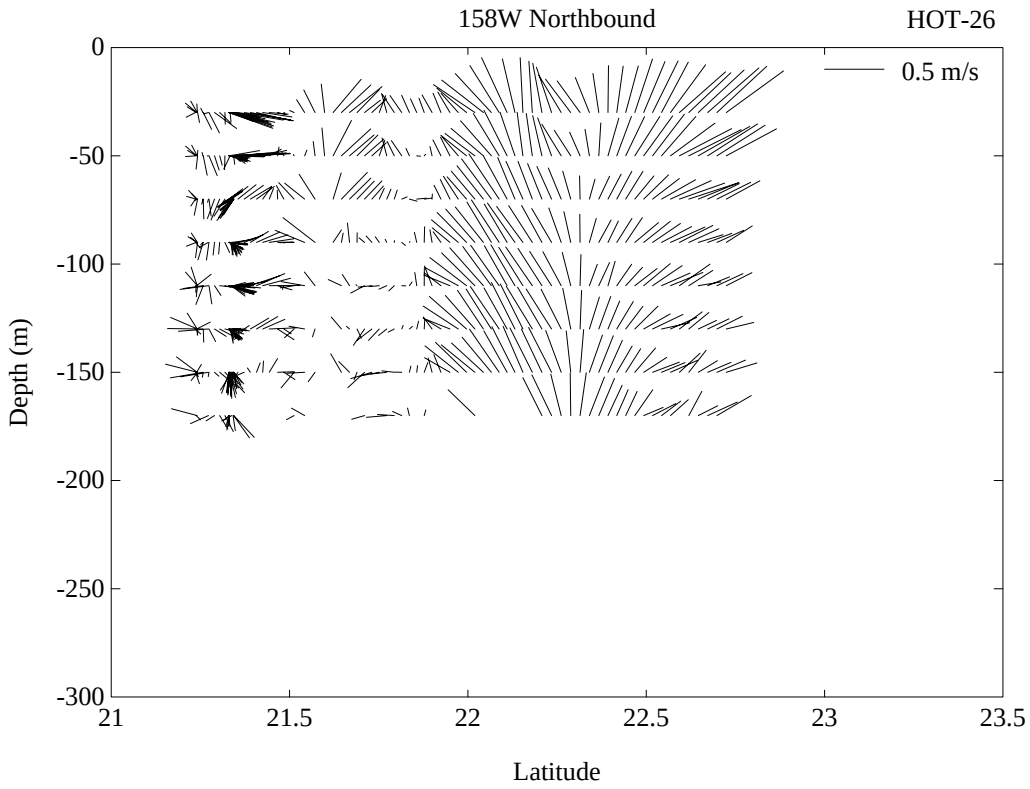

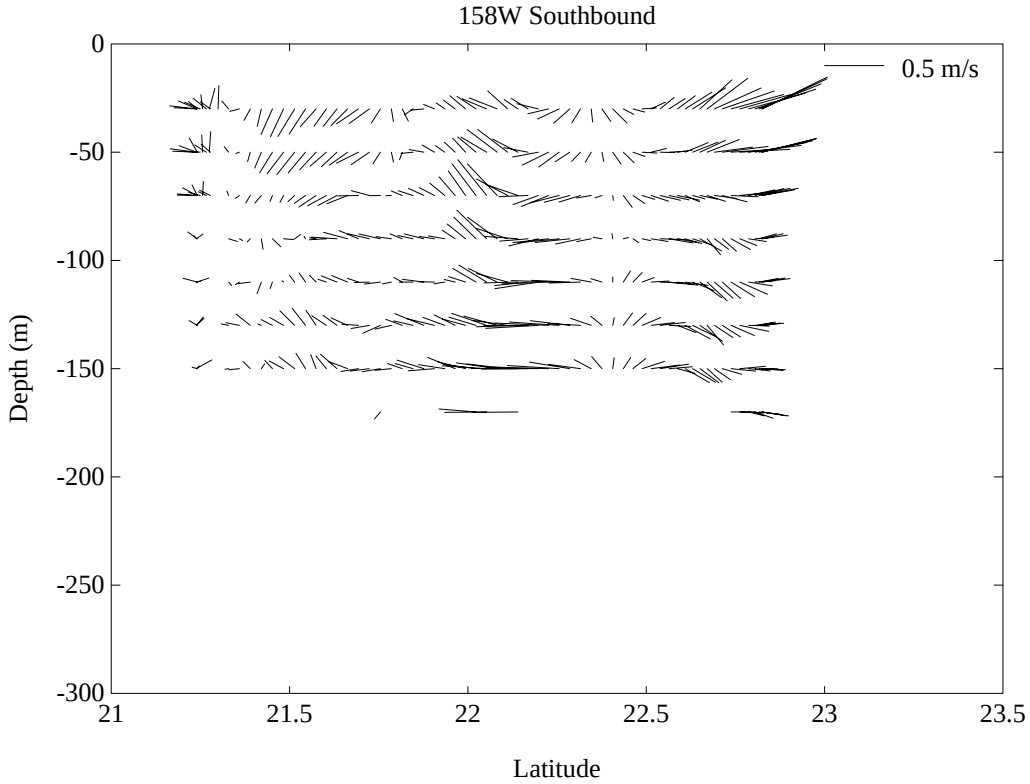

Figure 6.6.15b

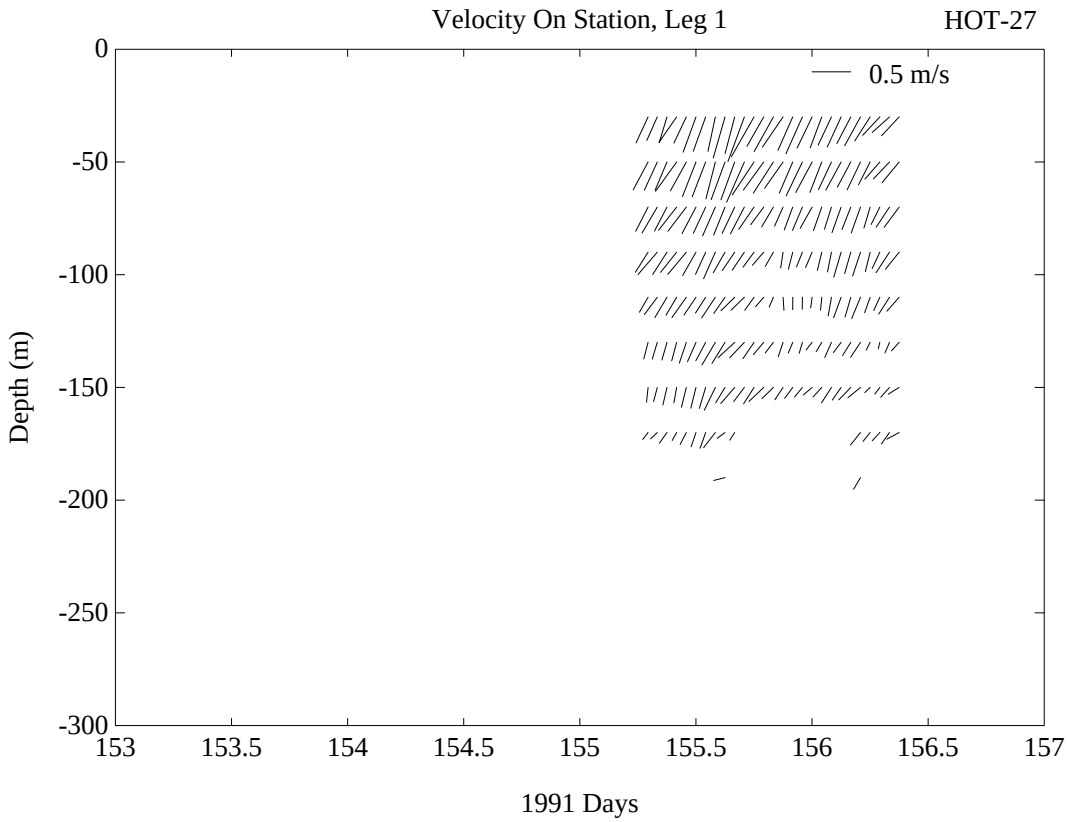

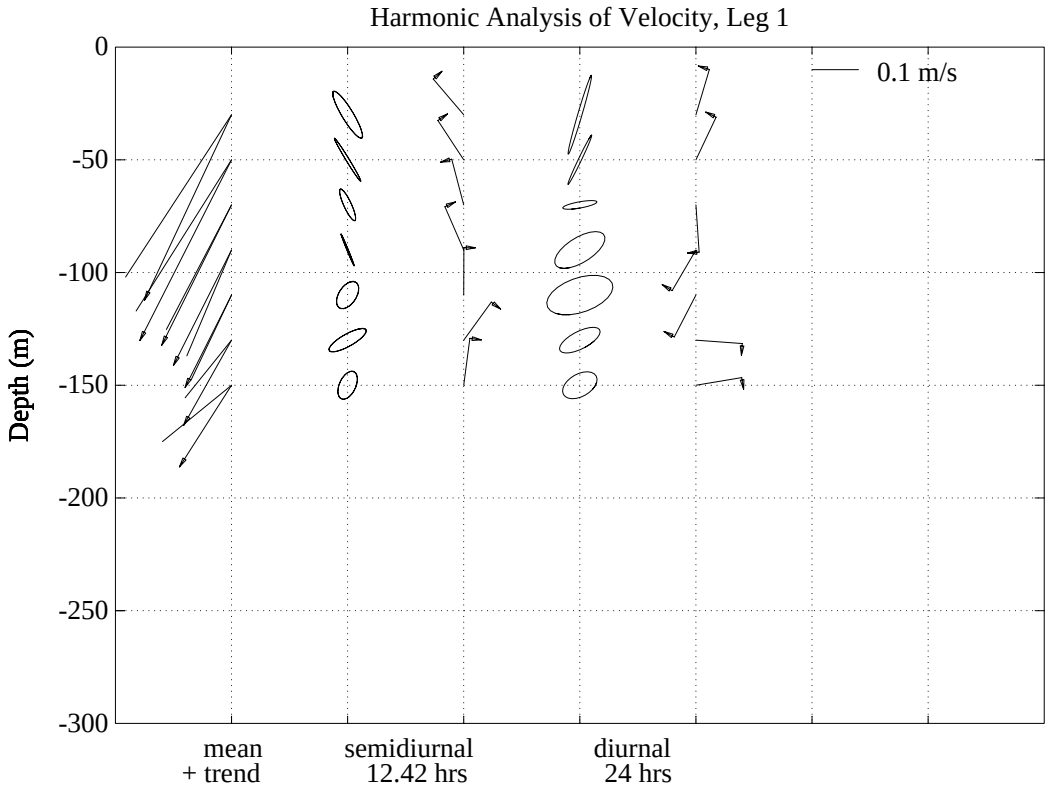

Figure 6.6.16a

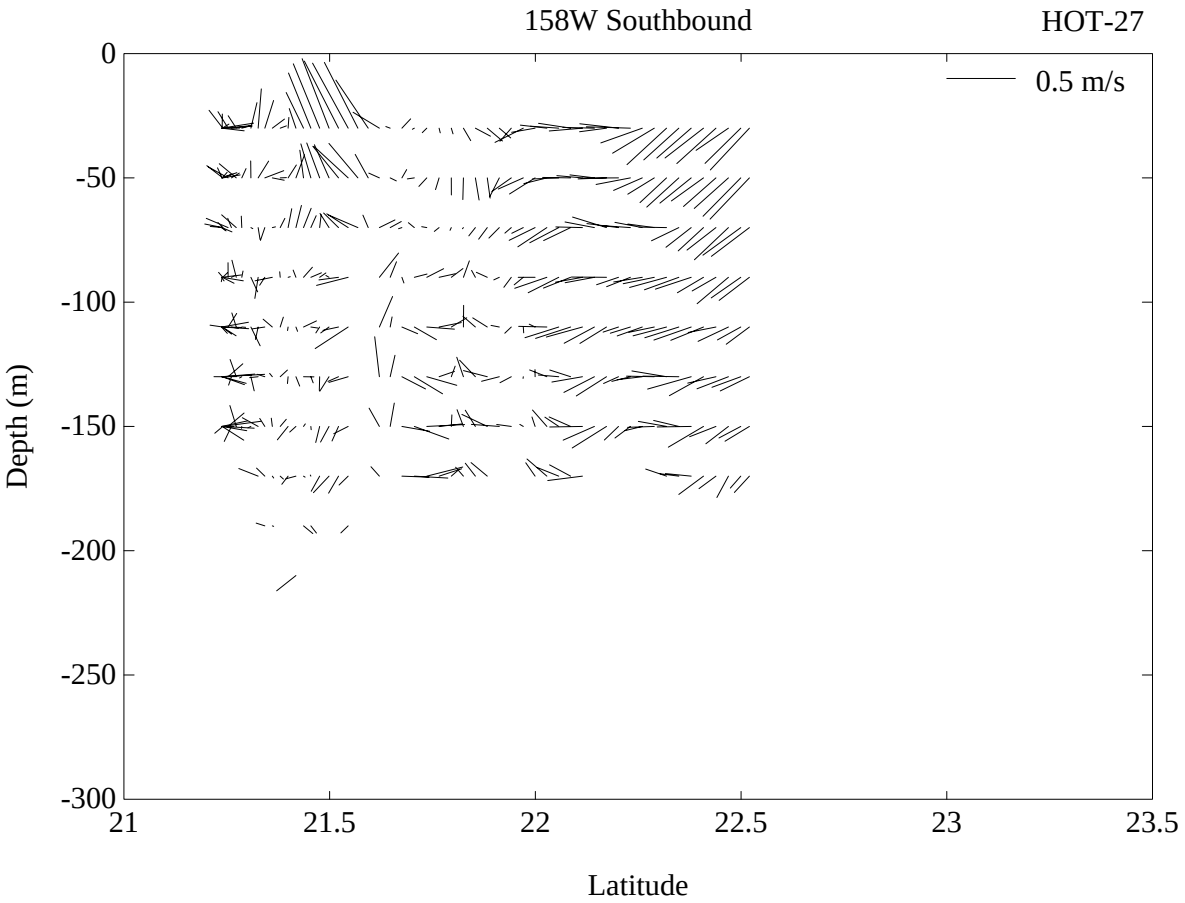

Figure 6.6.16b

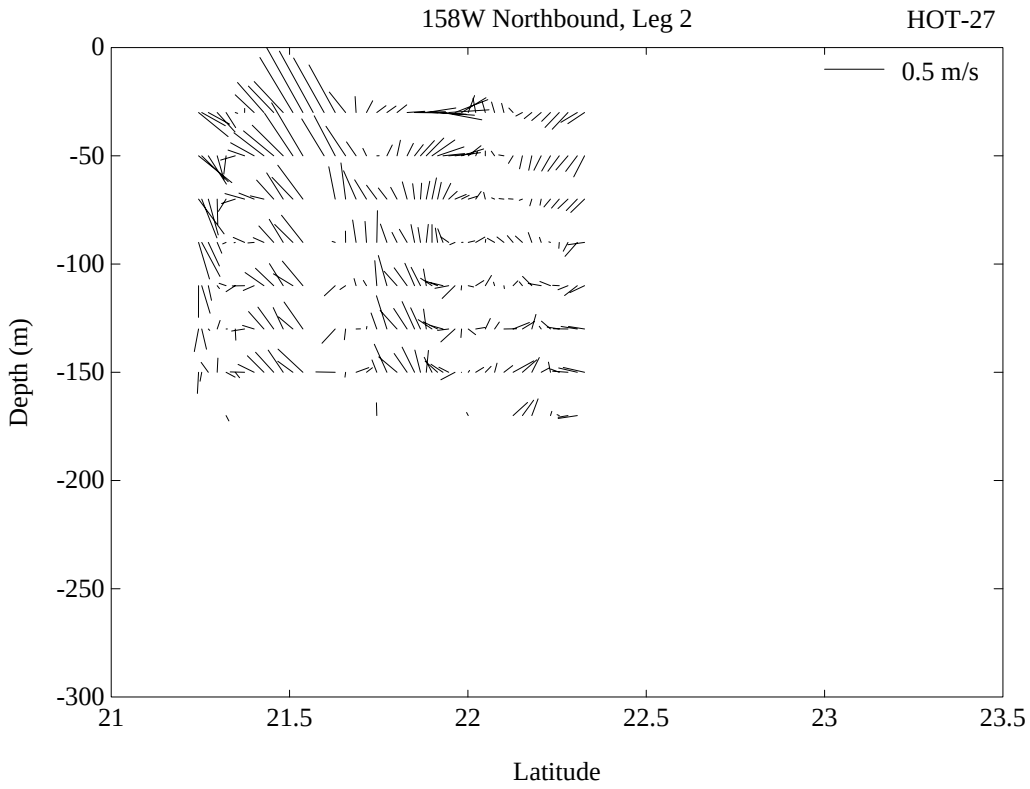

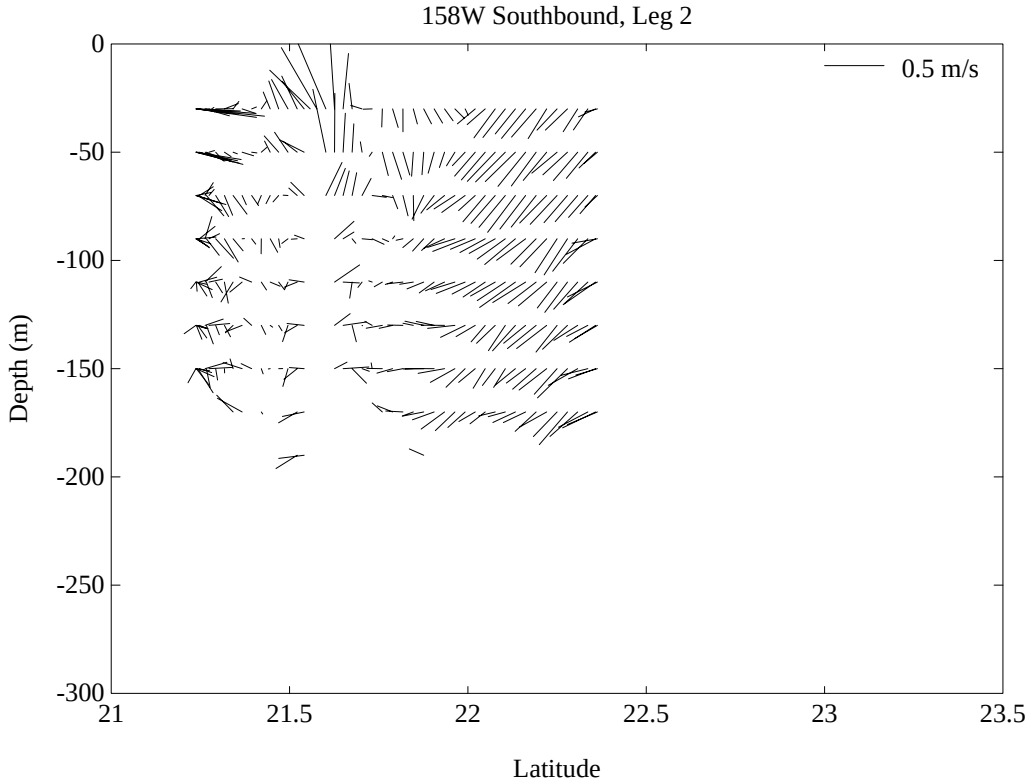

Figure 6.6.17b

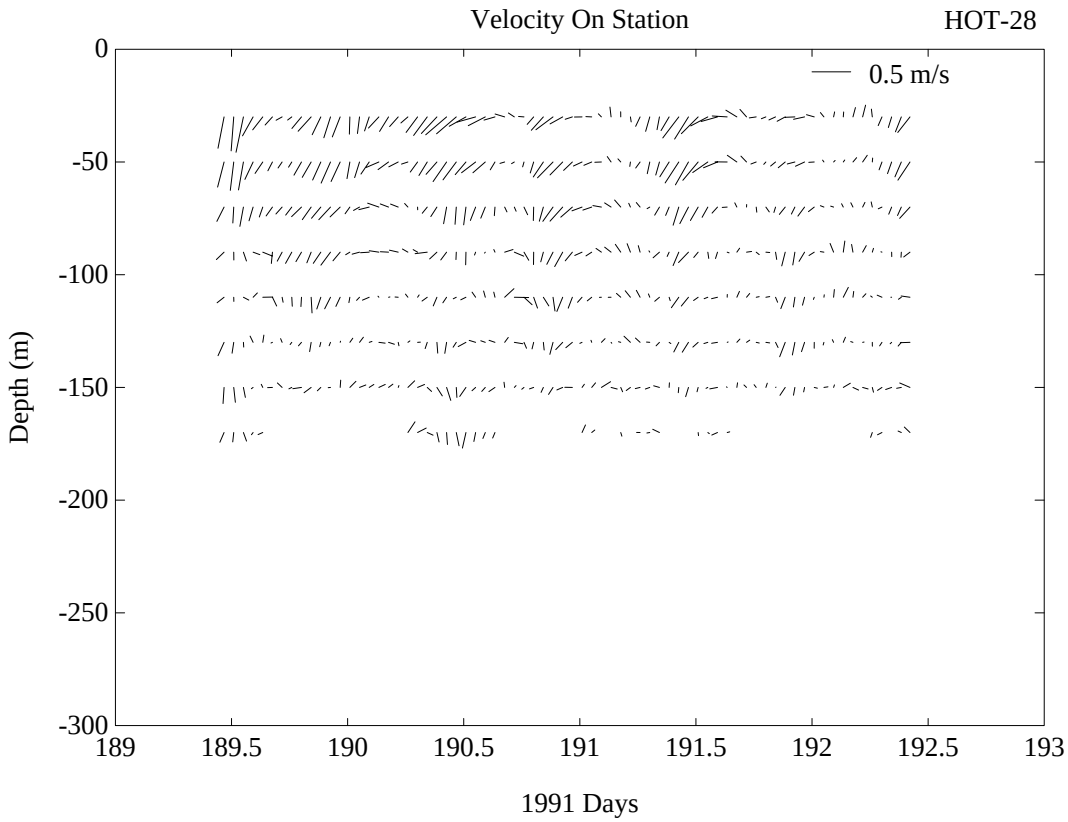

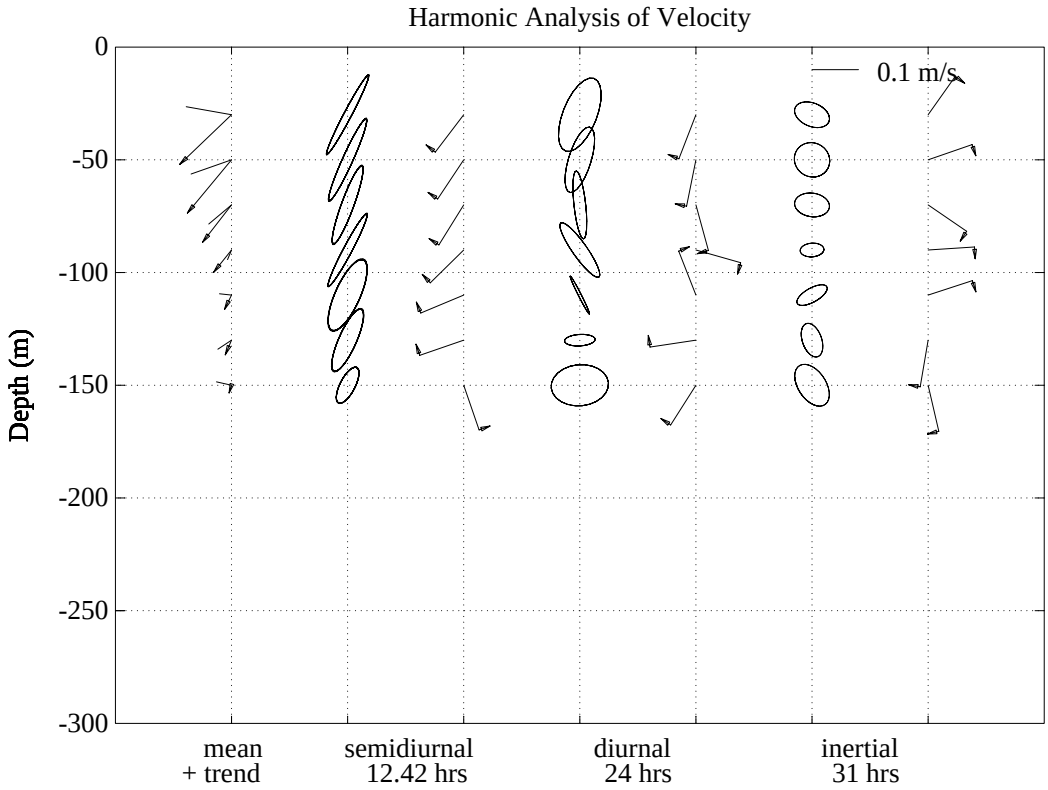

Figure 6.6.18a

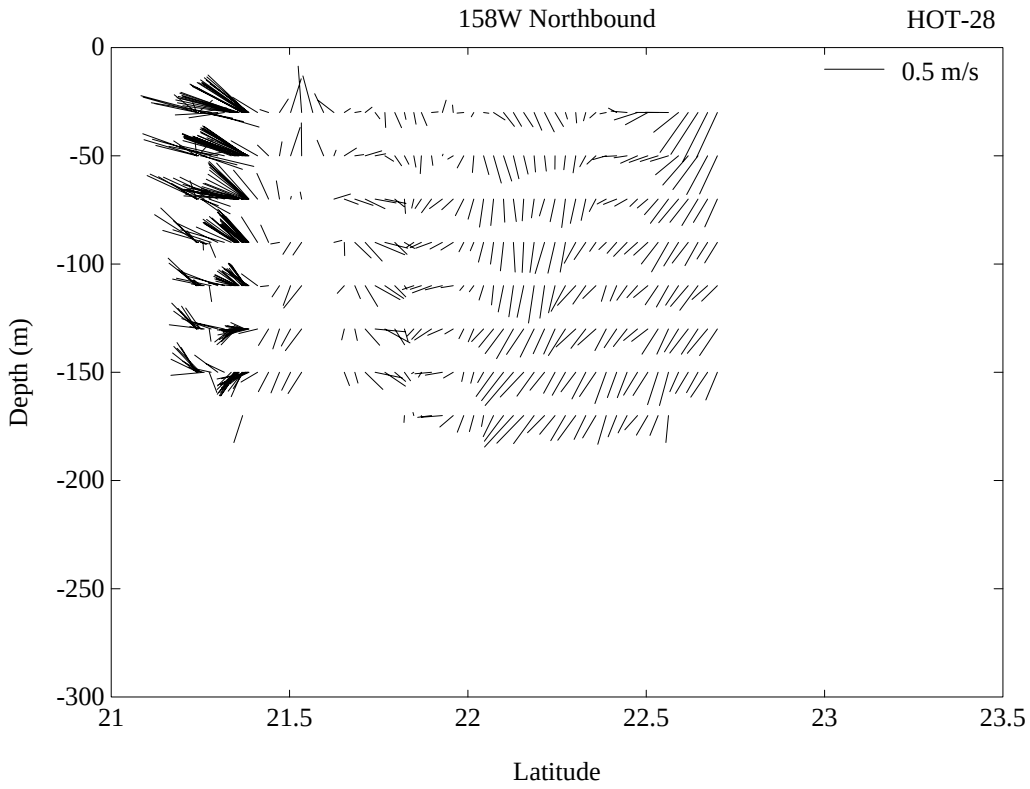

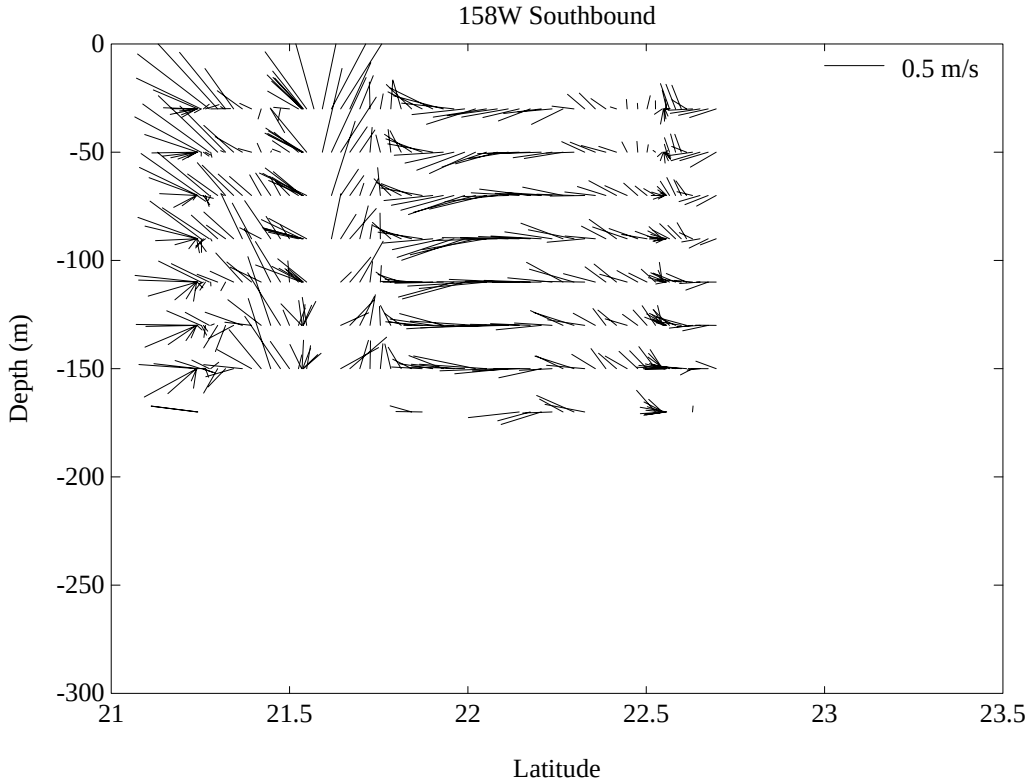

Figure 6.6.18b

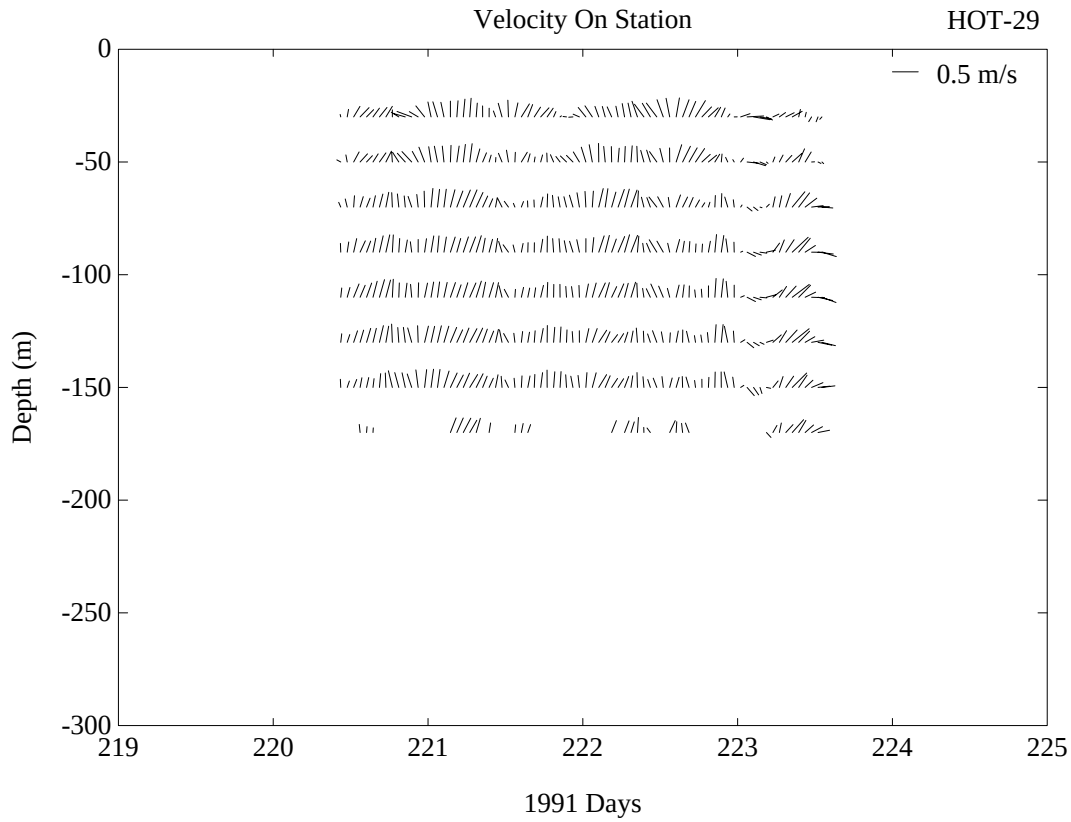

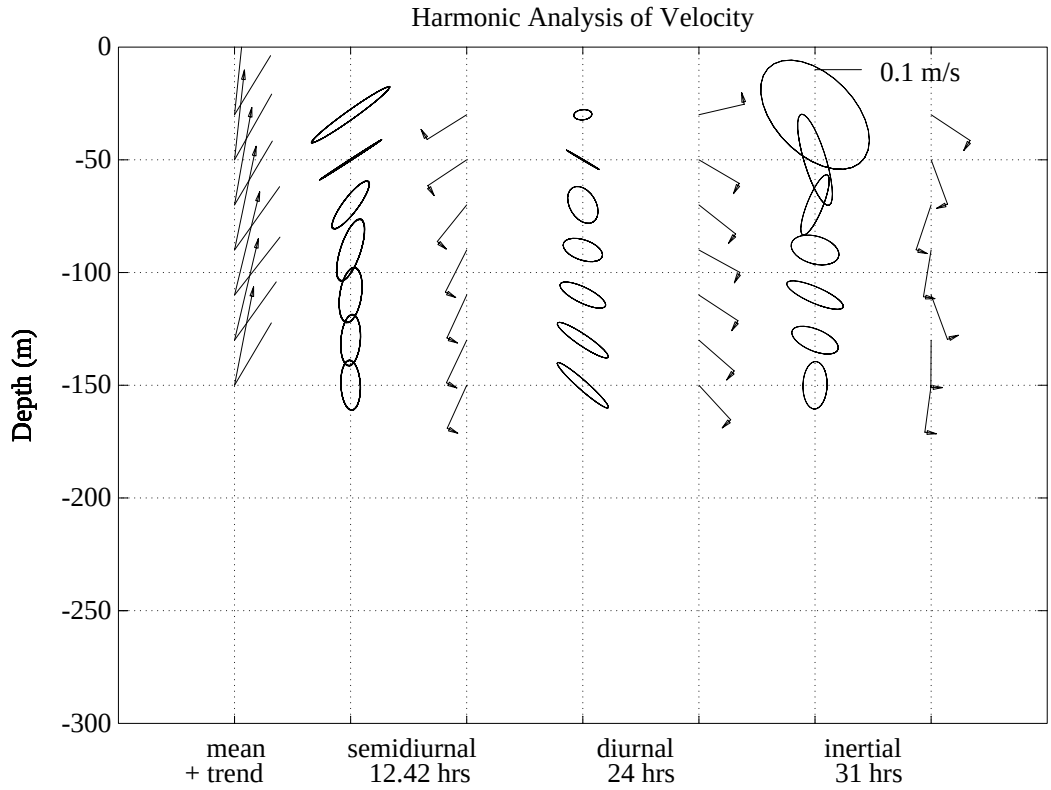

Figure 6.6.19a

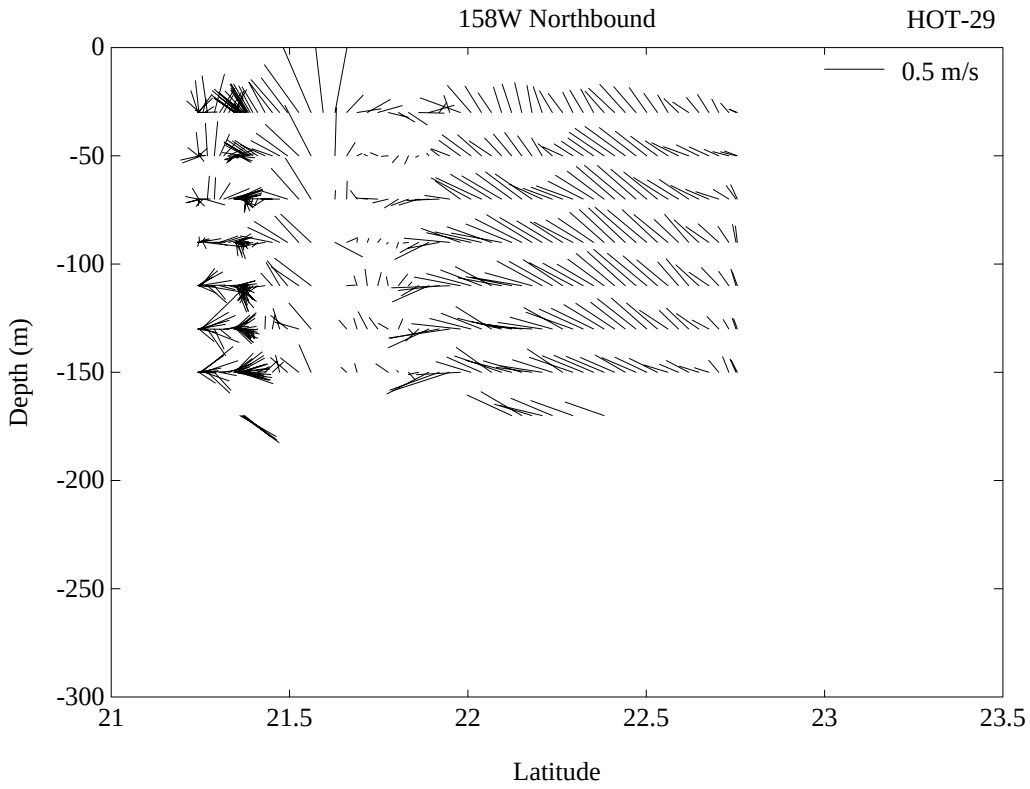

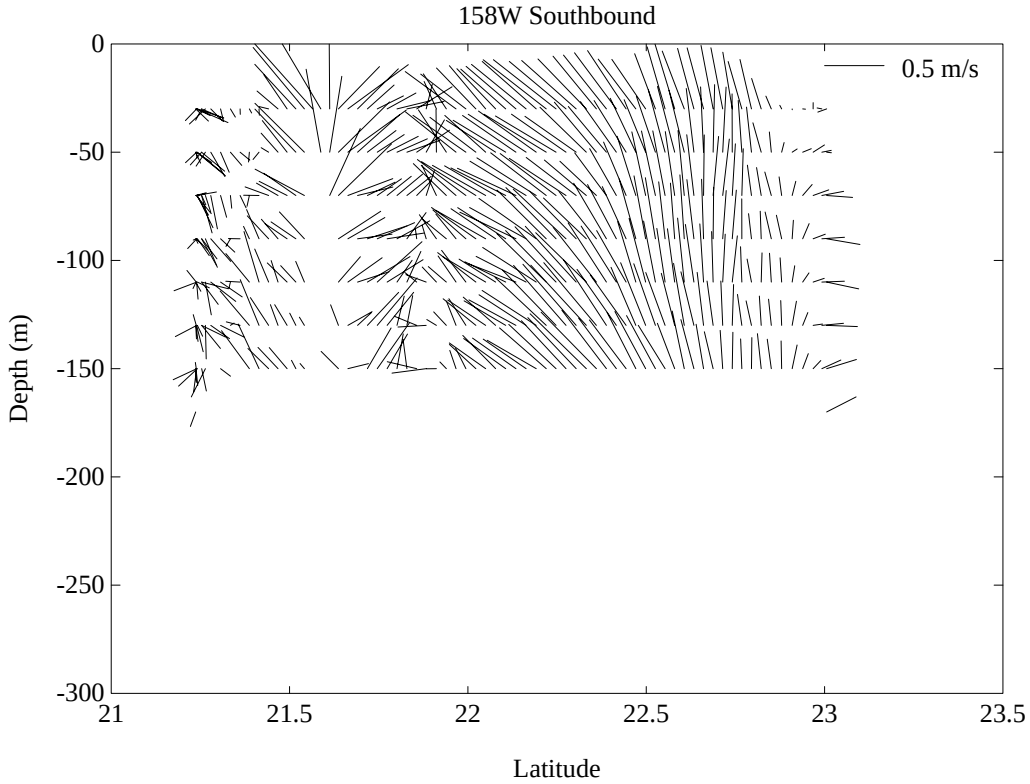

Figure 6.6.19b

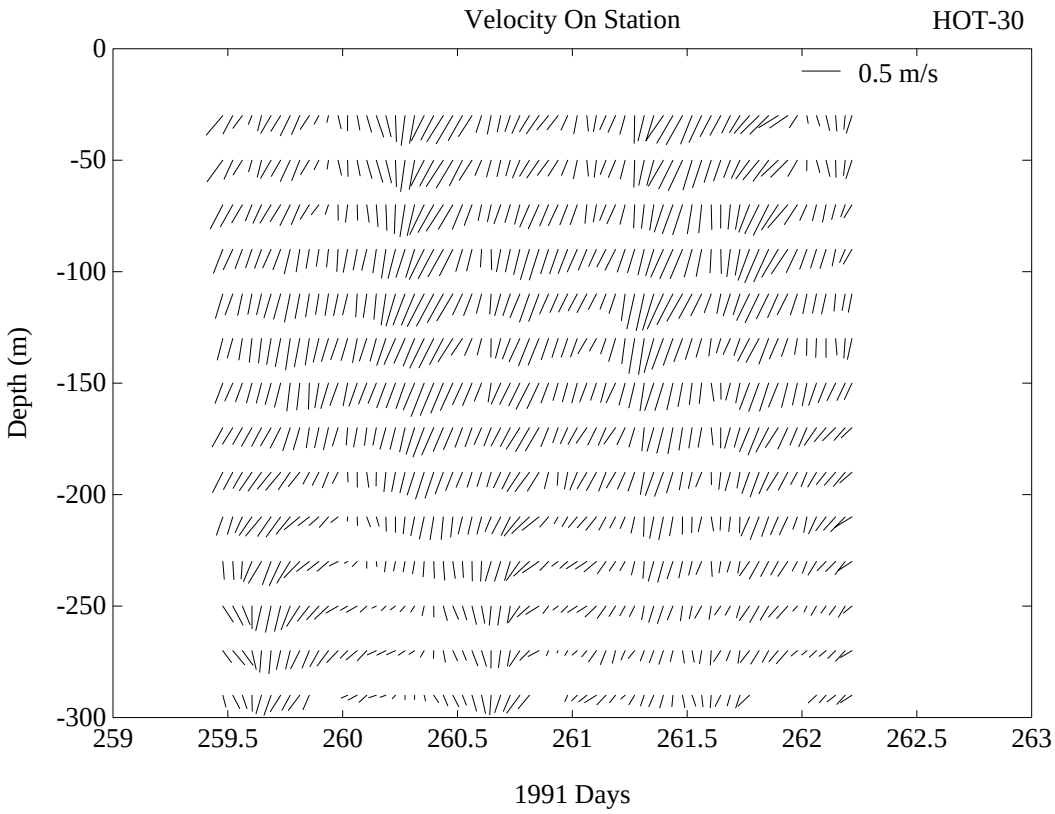

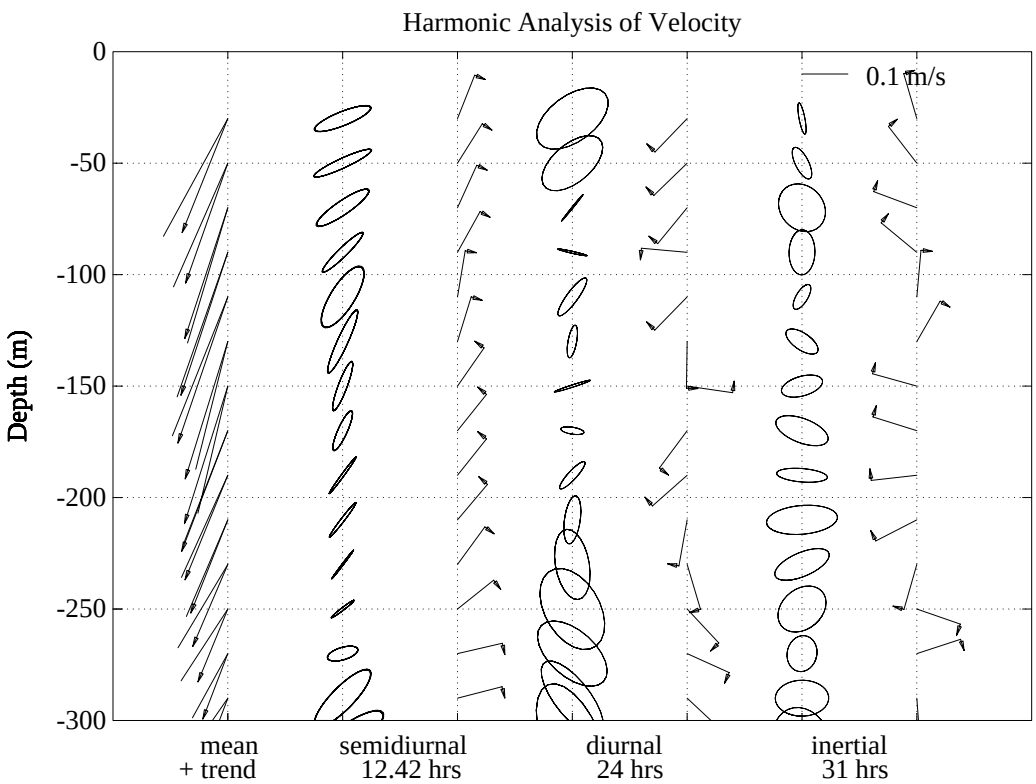

Figure 6.6.20a

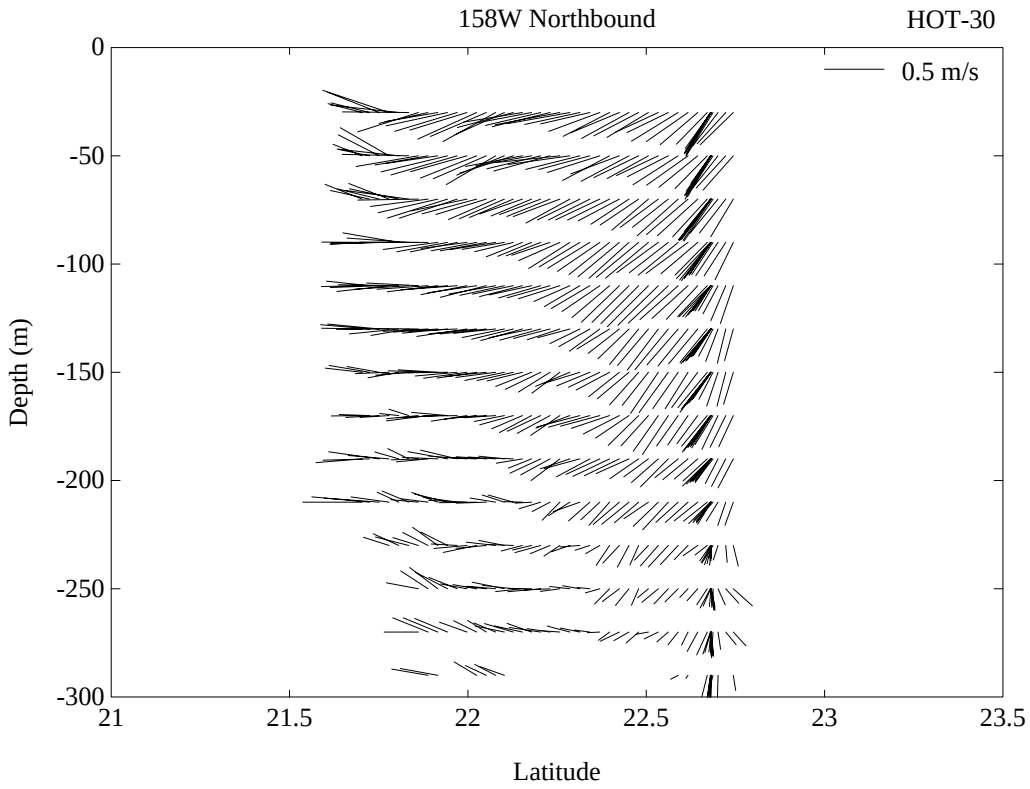

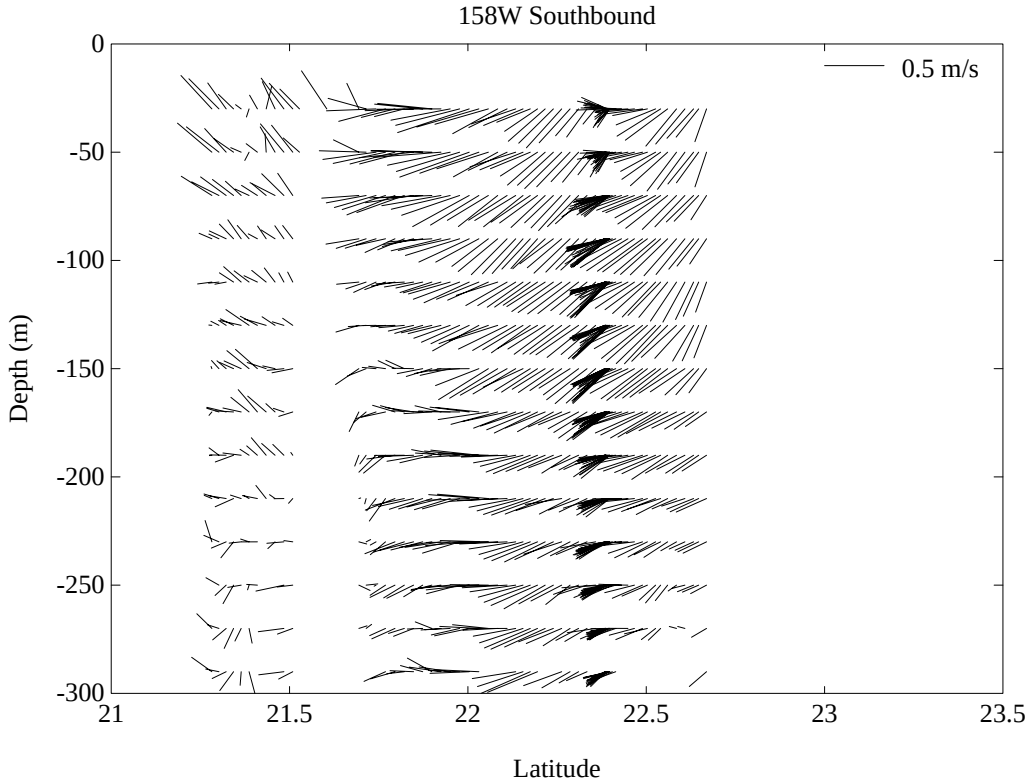

Figure 6.6.20b

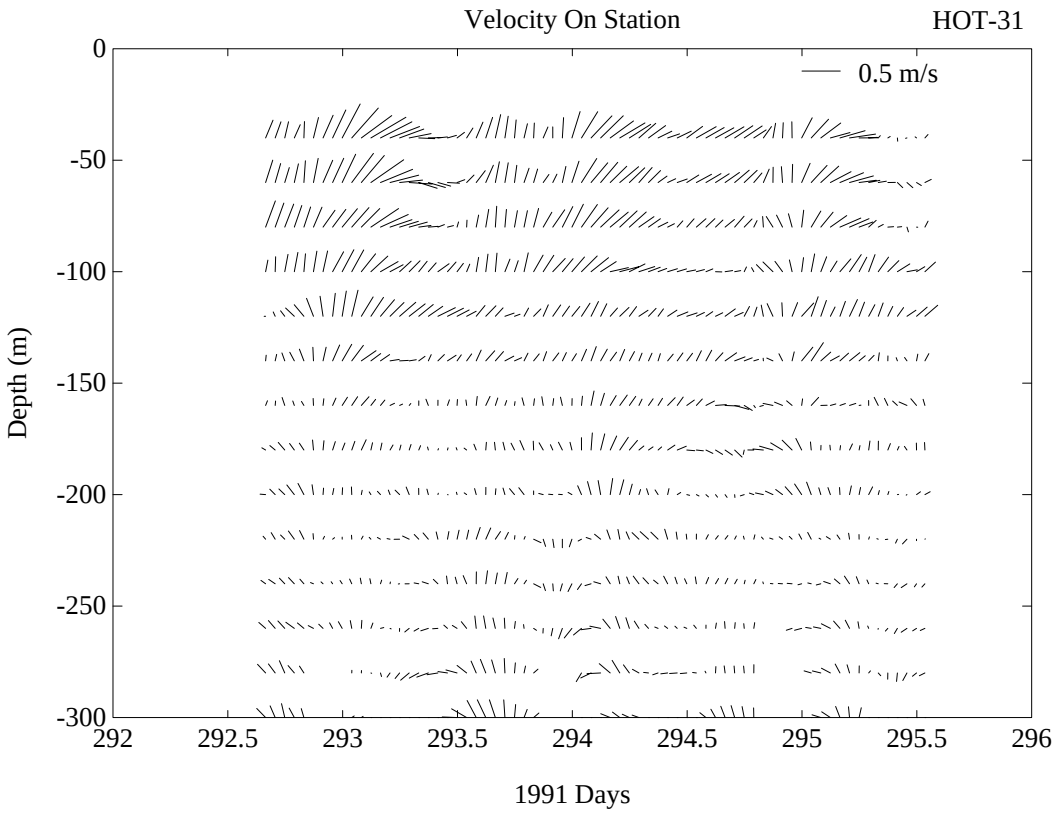

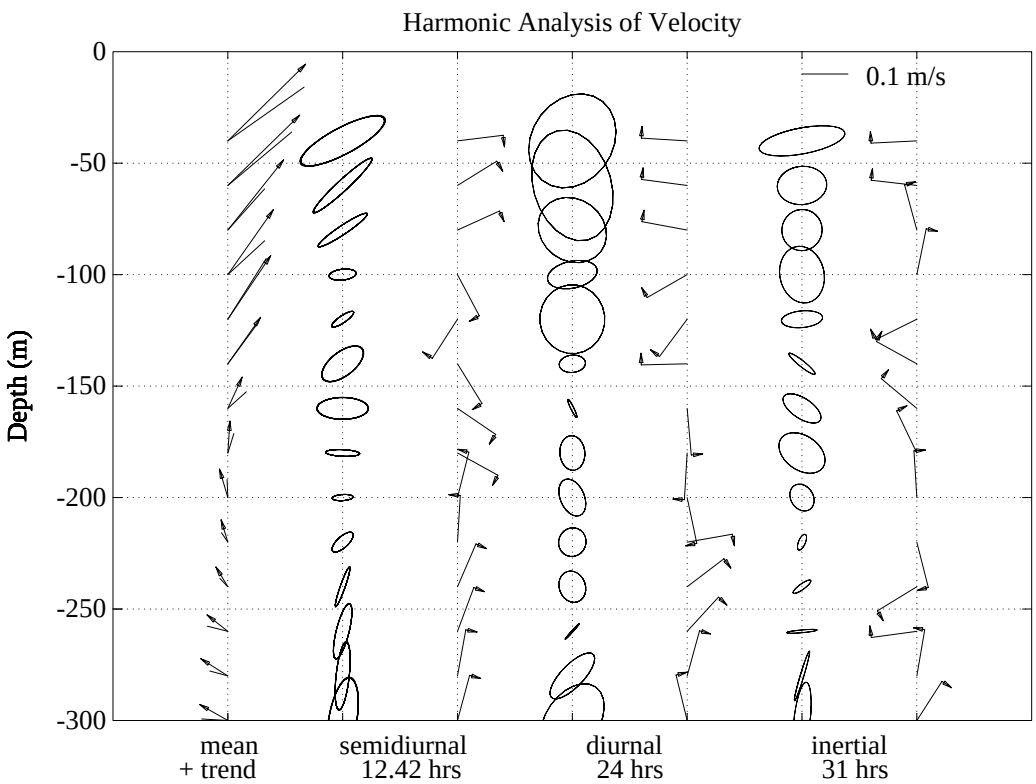

Figure 6.6.21a

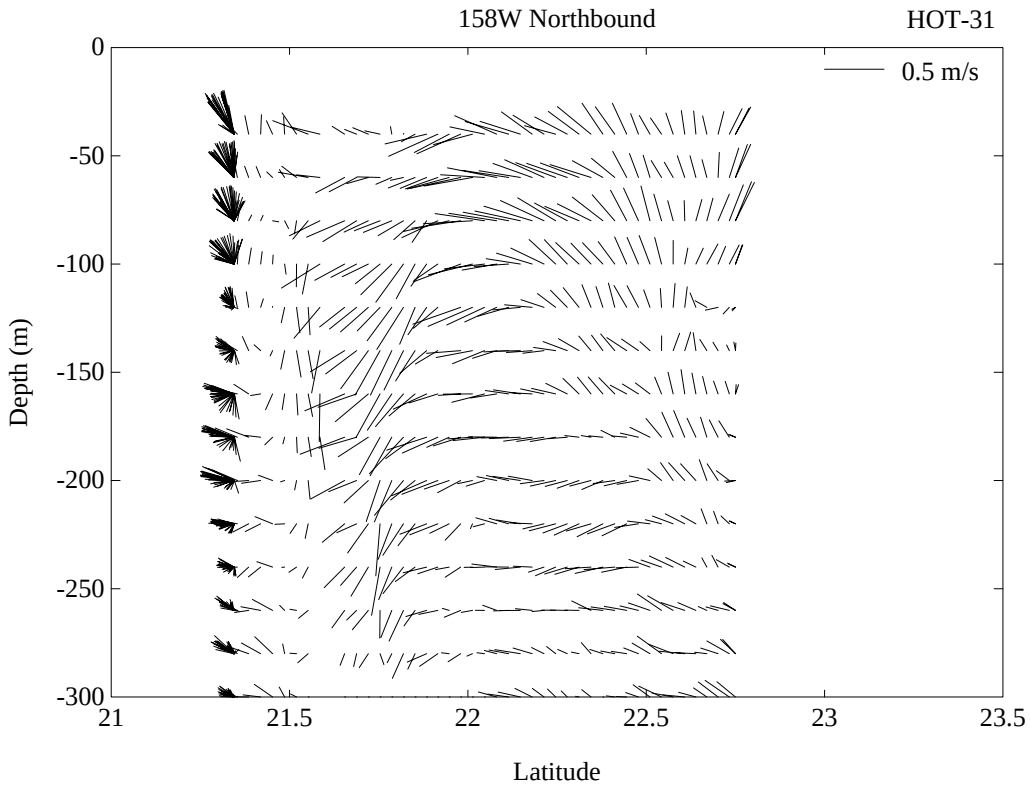

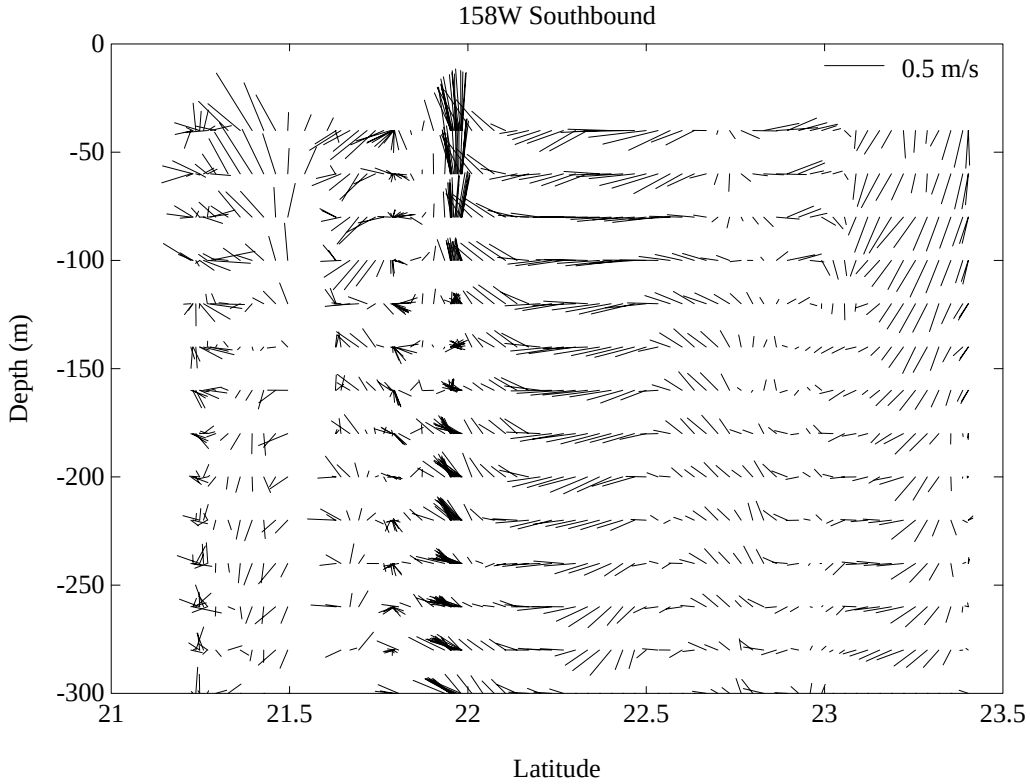

Figure 6.6.21b

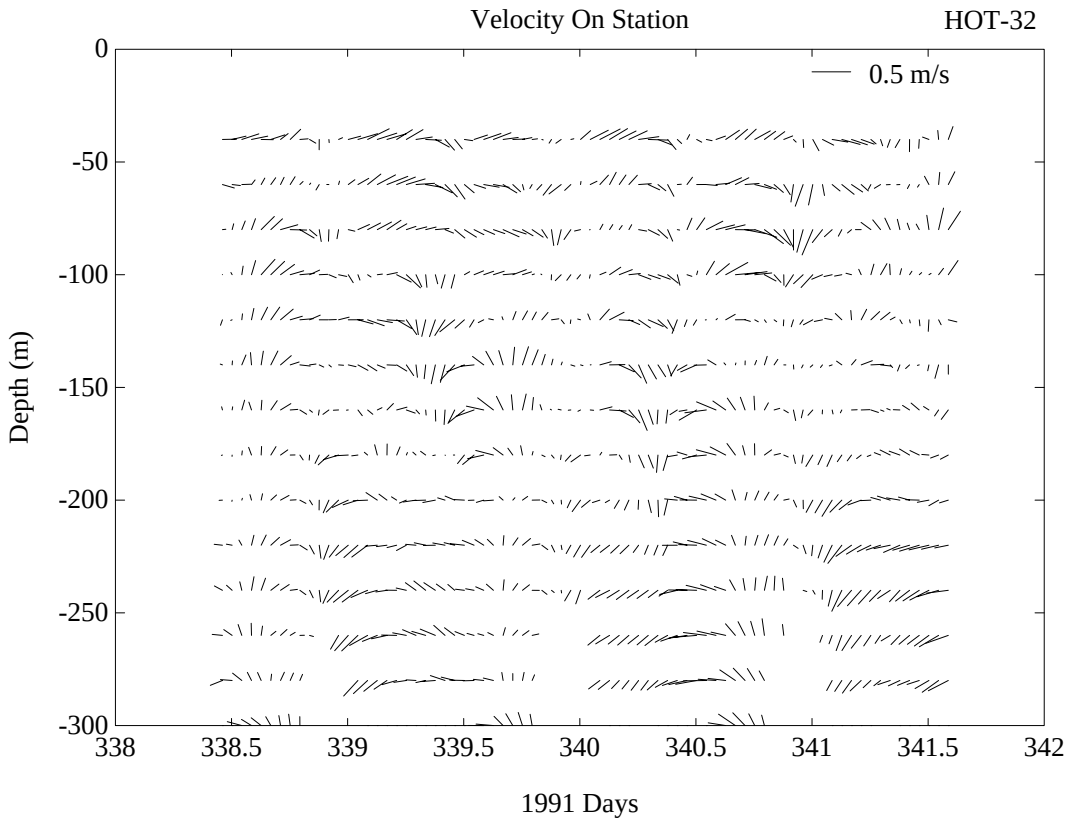

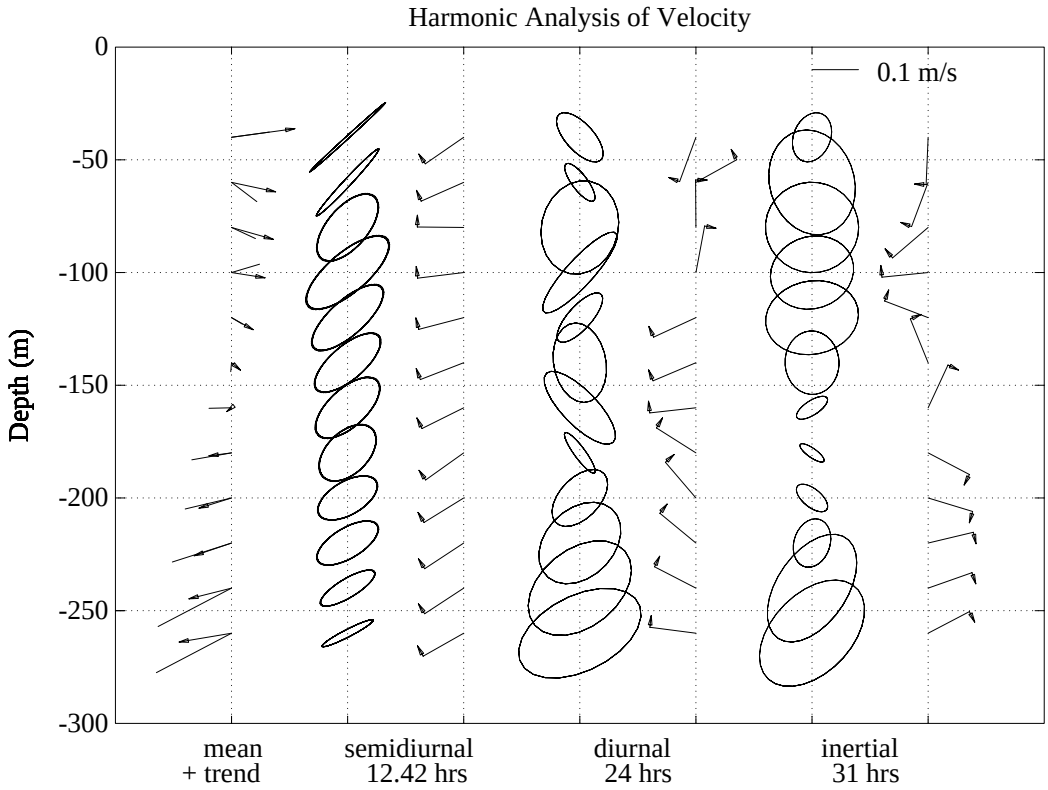

Figure 6.6.22a

6.7. Meteorology

Figure 6.7.1: Upper panel: Atmospheric pressure measured while at Station ALOHA during 1991. Open circles represent individual measurements. Lower panel: Sea surface temperature measured while at Station ALOHA during 1991.

Figure 6.7.2: Upper panel: Dry bulb temperature measured while on station during 1991. Lower panel: Wet bulb air temperature measure while as Station ALOHA during 1991.

Figure 6.7.3: Upper panel: Dry air temperature measured at Station ALOHA during 1991. Dry-wet air temperature measured at Station ALOHA during 1991.

Figure 6.7.4: True winds measured at Station ALOHA on HOT-23 and at NDBC Buoy 51001 during HOT-23. Upper panel: True winds measured at Station ALOHA. Lower panel: True winds collected by NDBC Buoy 51001.

Figure 6.7.5: As in Figure 6.7.4, except for HOT-24.

Figure 6.7.6: As in Figure 6.7.4, except for HOT-25.

Figure 6.7.7: As in Figure 6.7.4, except for HOT-26.

Figure 6.7.8: As in Figure 6.7.4, except for HOT-27.

Figure 6.7.9: As in Figure 6.7.4, except for HOT-28.

Figure 6.7.10: As in Figure 6.7.4, except for HOT-29.

Figure 6.7.11: As in Figure 6.7.4, except for HOT-30.

Figure 6.7.12: As in Figure 6.7.4, except for HOT-31. Wind data was not available from the buoy on HOT-31.

Figure 6.7.13: As in Figure 6.7.4, except for HOT-32. Wind data was not available from the buoy on HOT-32.

Figure 6.7.14: Air temperature measured at Station ALOHA and NDBC buoy 51001. Upper panel: Air temperature measured at both the buoy and at Station ALOHA plotted against Julian day from 1 January 1990. Lower panel: Scatter plot of these data.

Figure 6.7.15: Sea surface temperature at Station ALOHA and the NDBC buoy. Upper and lower

panels as described in Figure 6.7.14.

Figure 6.7.16: Atmospheric pressure at Station ALOHA and the NDBC buoy. Upper and lower panels as described in Figure 6.7.14.

Figure 6.7.17: Wind speed at Station ALOHA and the NDBC buoy. Upper and lower panels as described in Figure 6.7.14.

Figure 6.7.18: Wind direction and wind speed at Station ALOHA and the NDBC buoy. Upper panel: Wind direction at both Station ALOHA and NDBC buoy 51001 plotted against Julian day from 1 January 1990. Lower panel: Wind speed at both Station ALOHA and the NDBC buoy plotted against Julian day from 1 January 1990.

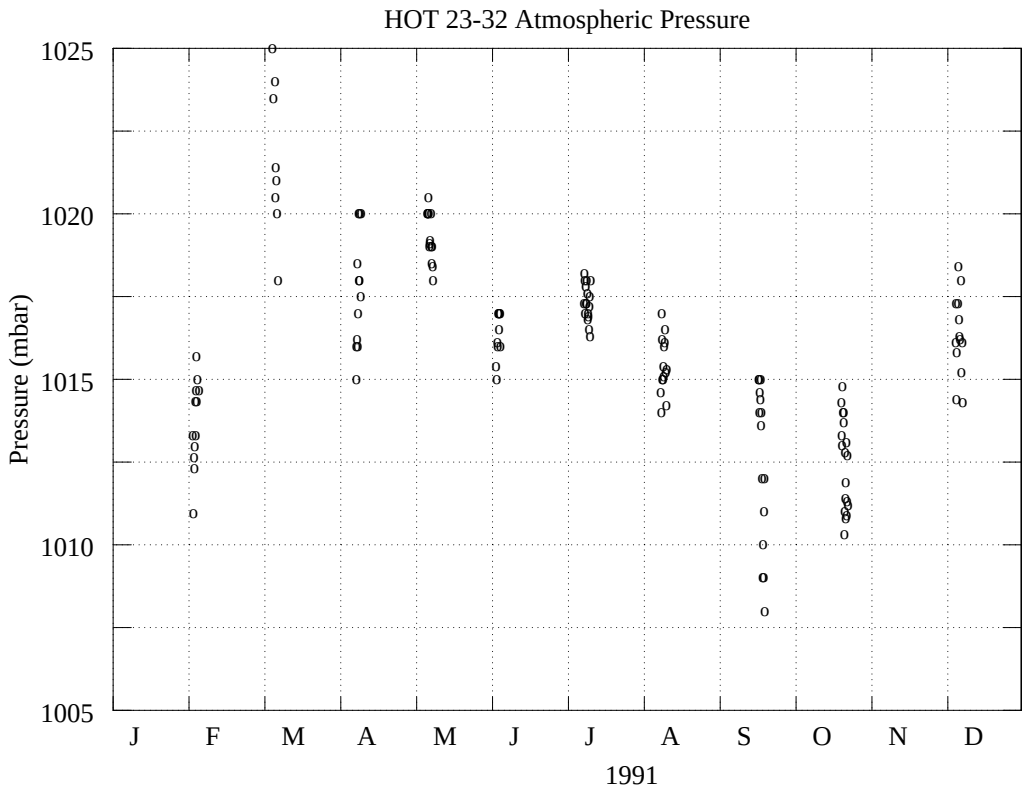
HOT 23-32 Atmospheric Pressure
Pressure (mbar)
1025
1020
1015
1010
1005
J F M A M J J A S O N D
1991

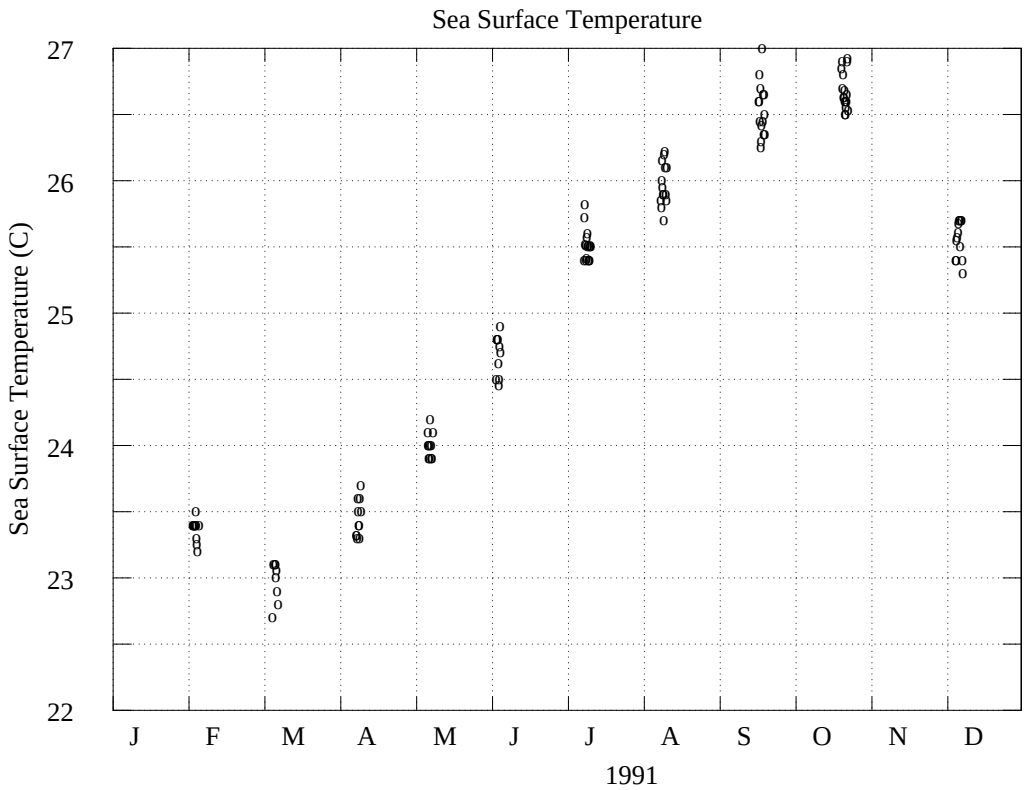
Sea Surface Temperature
Sea Surface Temperature (C)
27
26
25
24
23
22
J F M A M J J A S O N D
1991

Figure 6.7.1

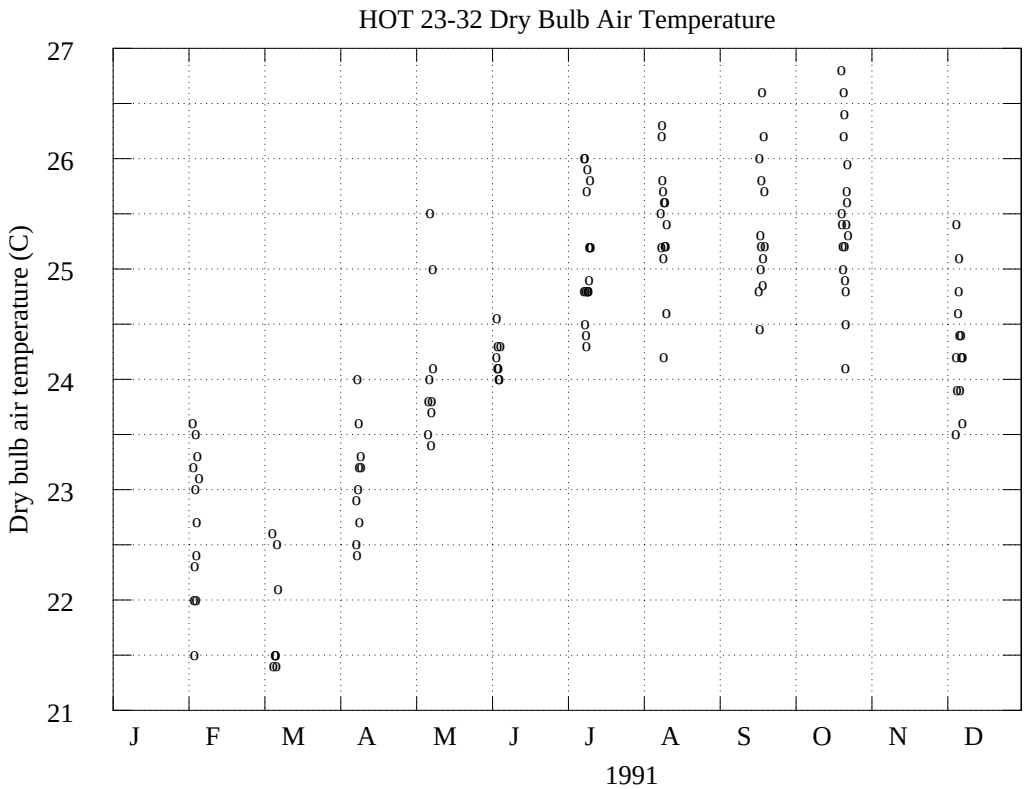
HOT 23-32 Dry Bulb Air Temperature
Dry bulb air temperature (C)
27
26
25
24
23
22
21
J F M A M J J A S O N D
1991

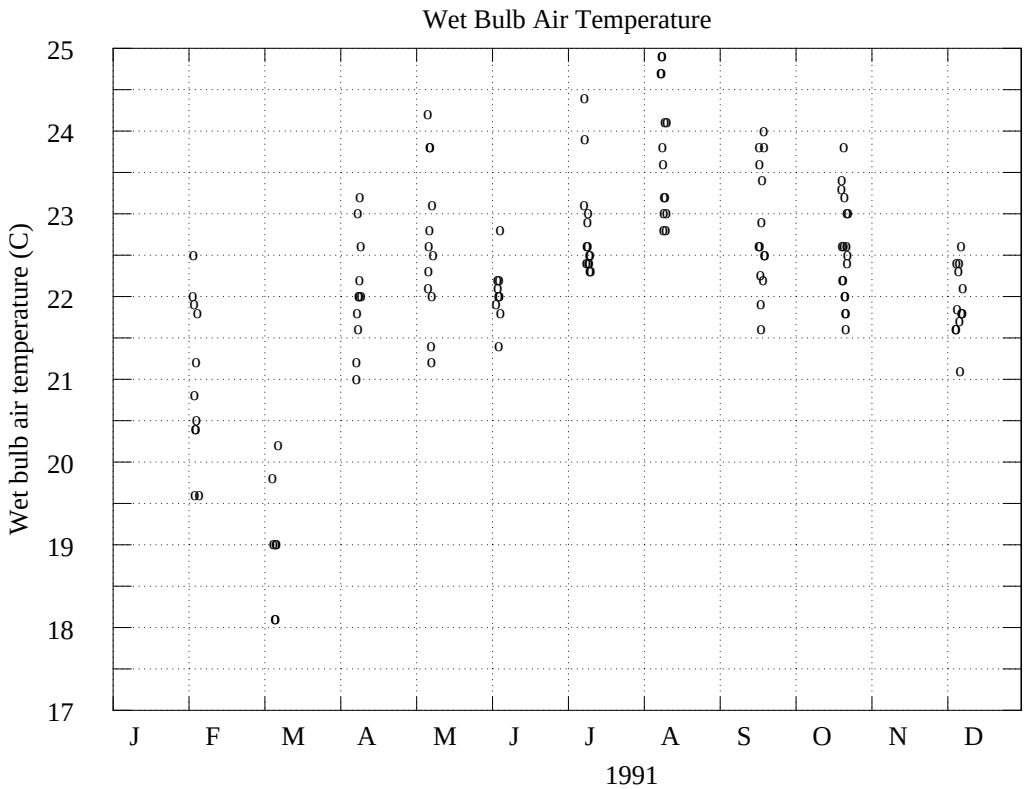
Wet Bulb Air Temperature
Wet bulb air temperature (C)
25
24
23
22
21
20
19
18
17
J F M A M J J A S O N D
1991

Figure 6.7.2

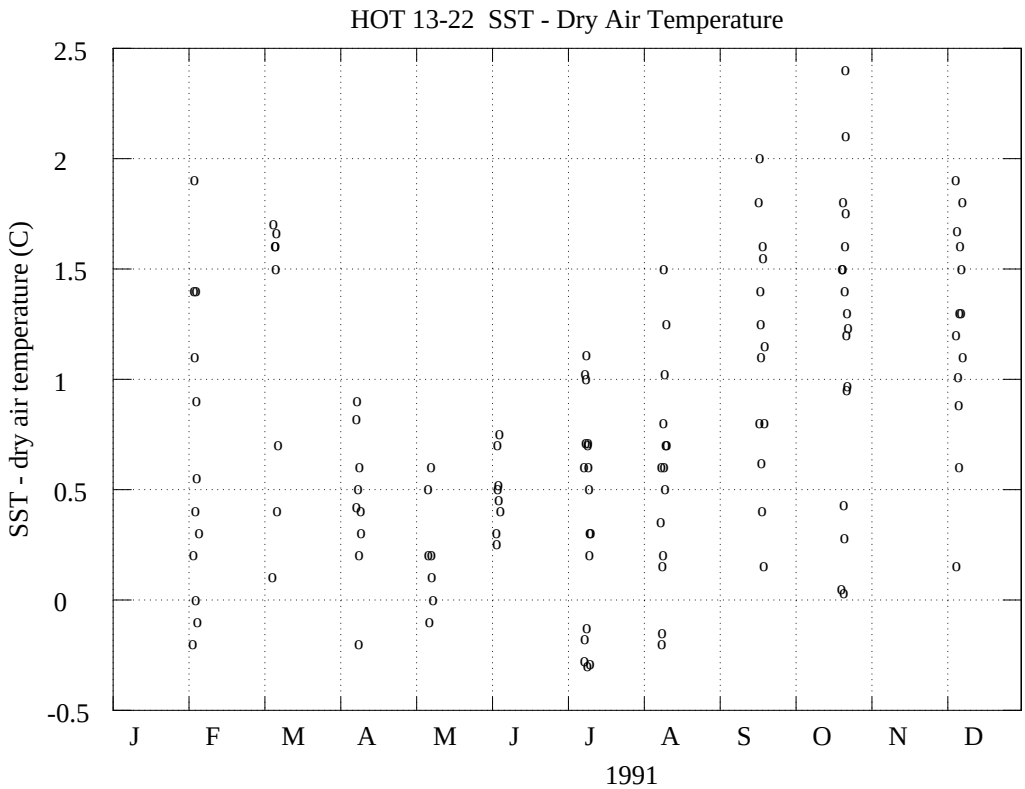
HOT 13-22 SST - Dry Air Temperature
SST - dry air temperature (C)
2.5
2
1.5
1
0.5
0
-0.5
J F M A M J J A S O N D
1991

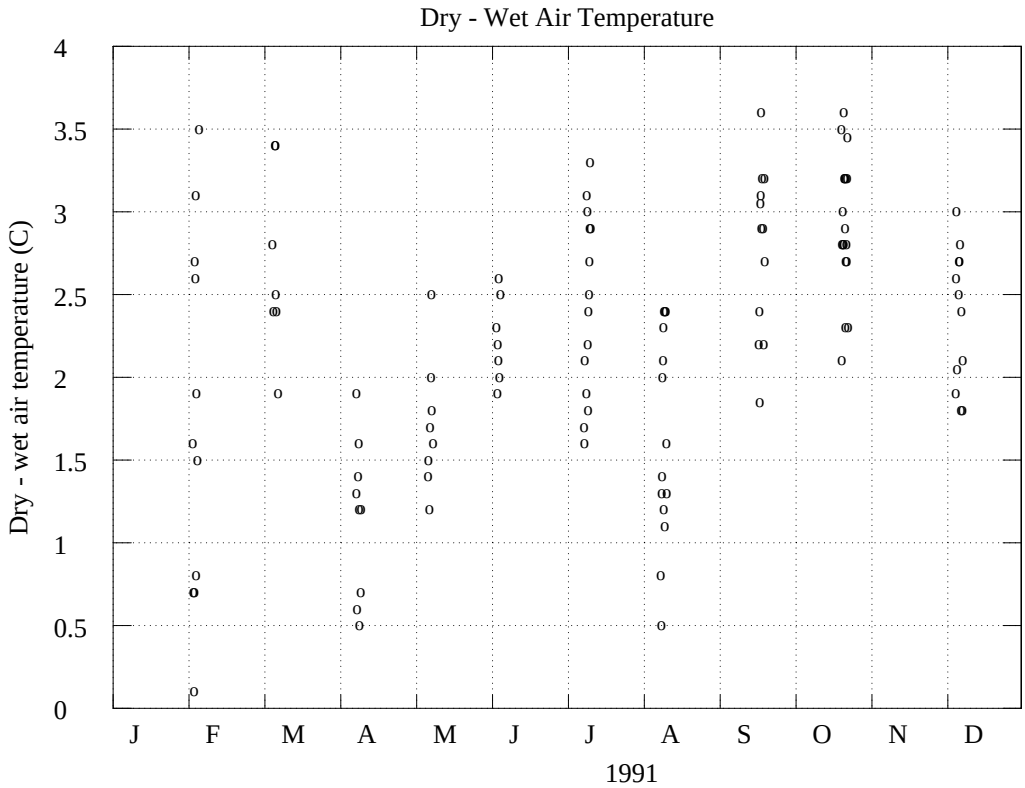
Dry - Wet Air Temperature
Dry - wet air temperature (C)
4
3.5
3
2.5
2
1.5
1
0.5
0
J F M A M J J A S O N D
1991

Figure 6.7.3

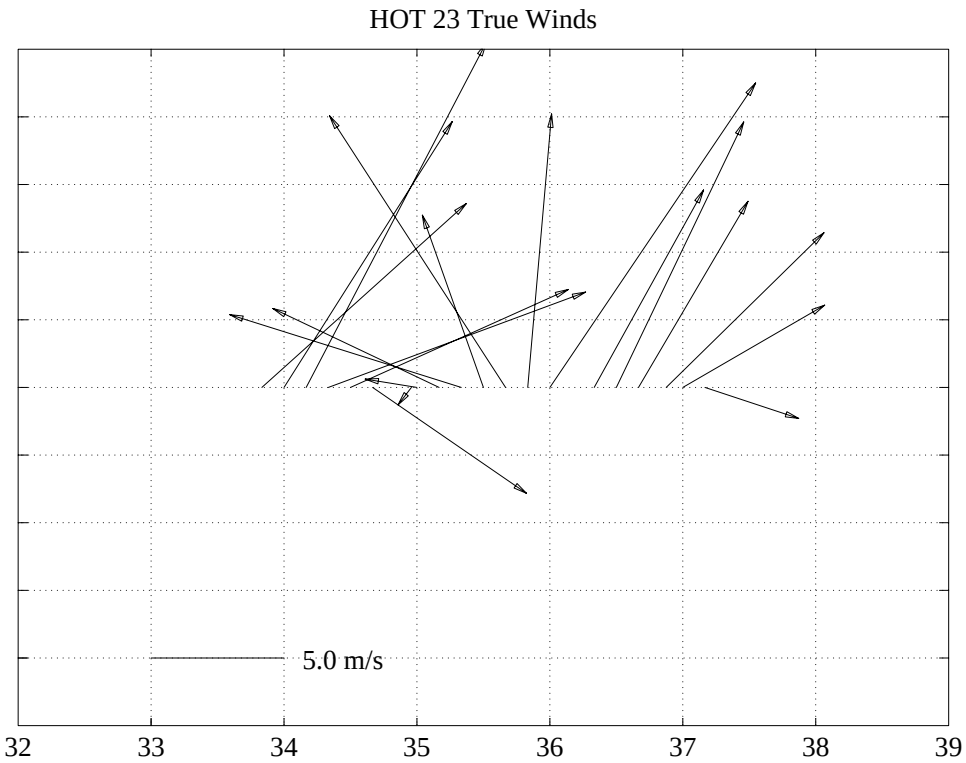

Julian days from January, 1, 1991

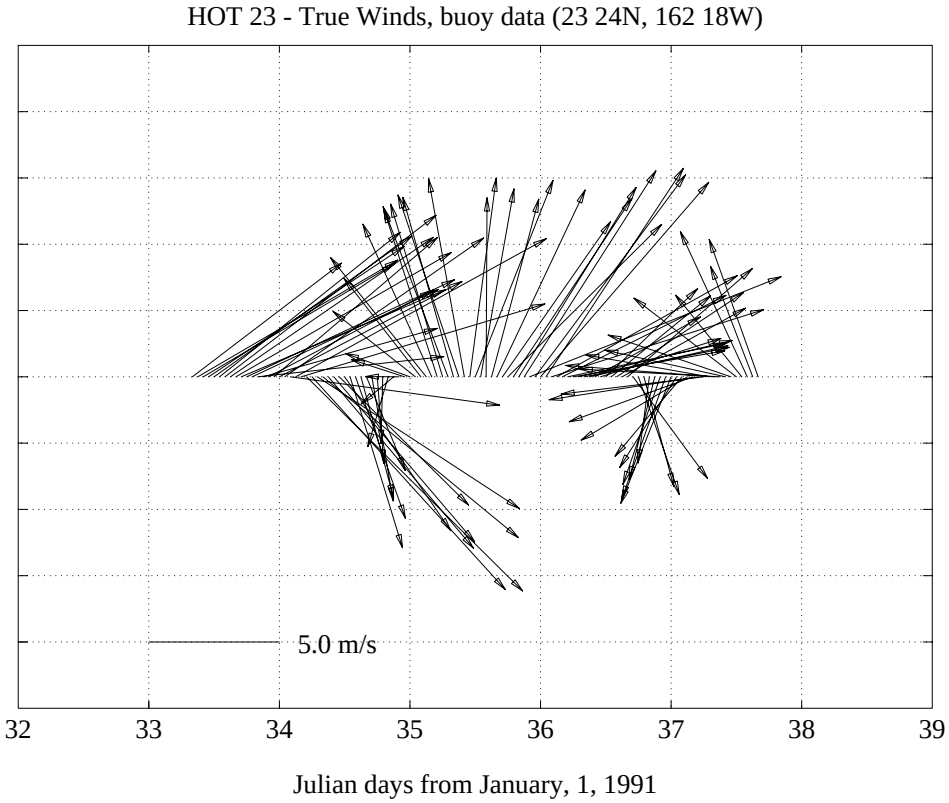

Julian days from January, 1, 1991

Figure 6.7.4

HOT 24 True Winds

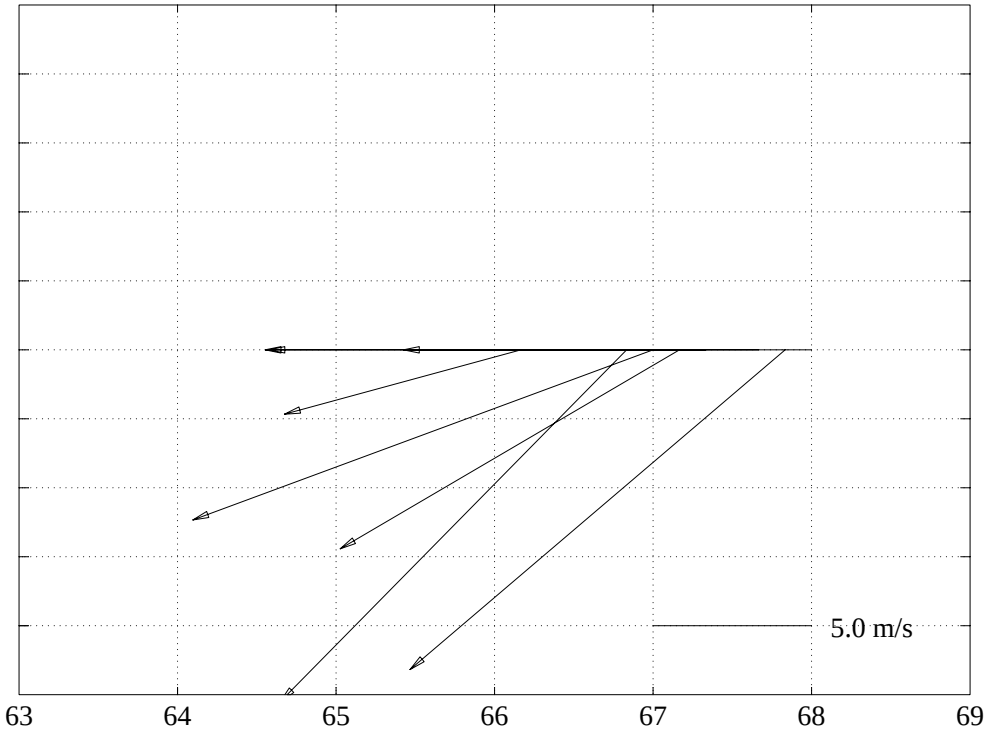

Julian days from January, 1991

HOT 24 - True Winds, buoy data (23 24N, 162 18W)

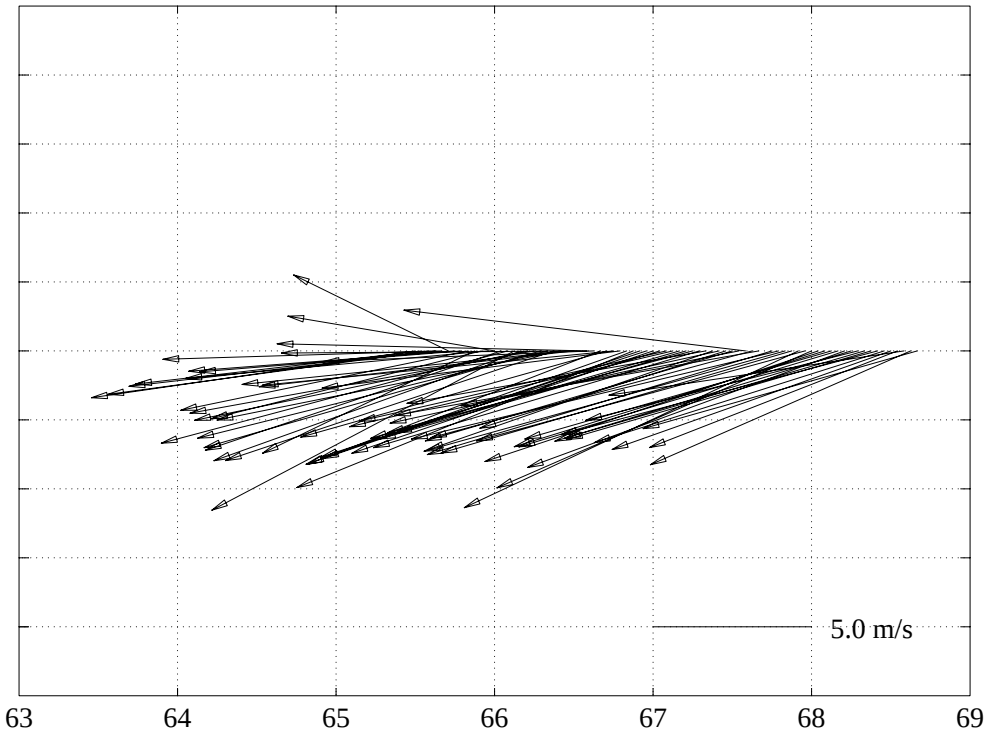

Julian days from January, 1991

Figure 6.7.5

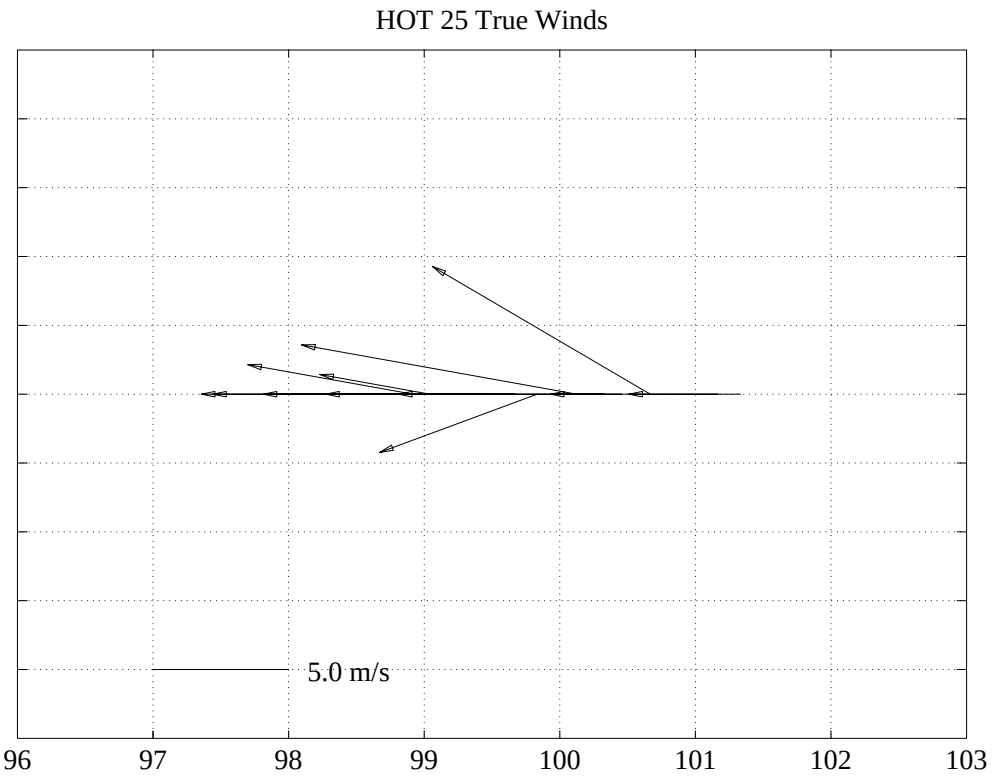

Julian days from January, 1, 1991

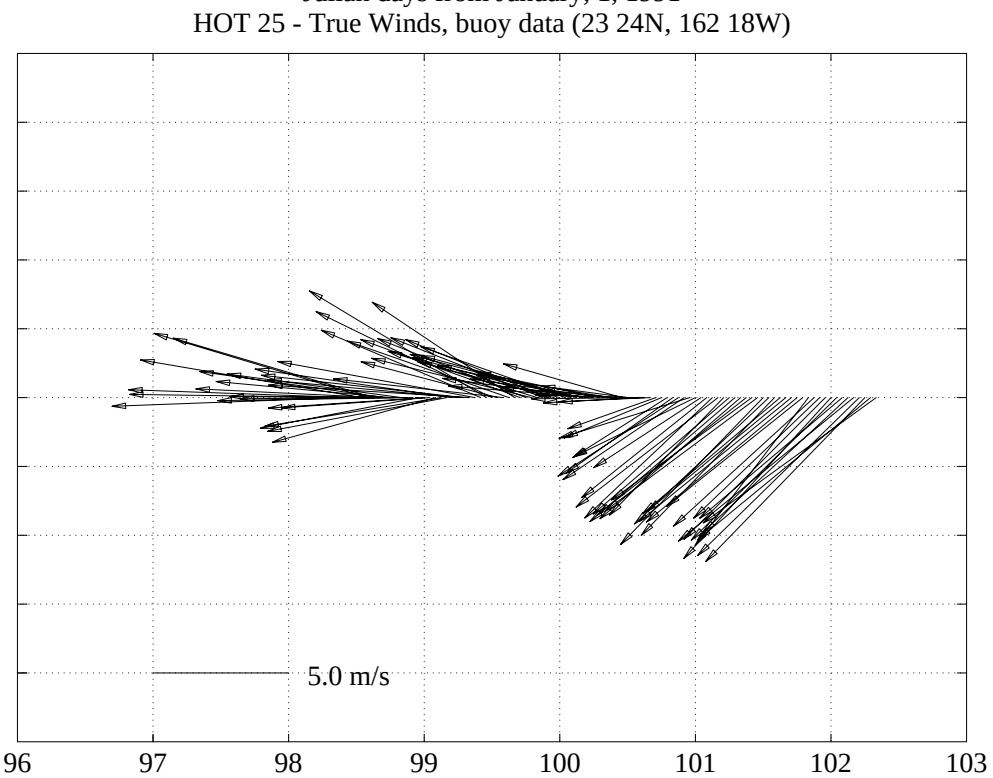

Julian days from January, 1, 1991

Figure 6.7.6

HOT 26 True Winds

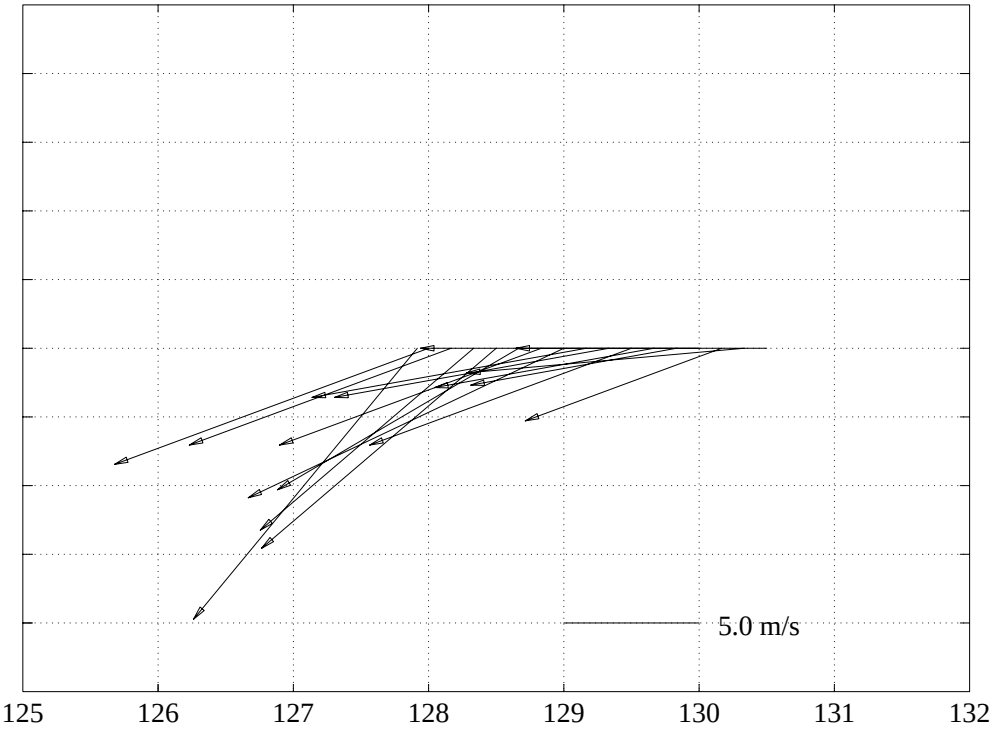

Julian days from January, 1, 1991

HOT 26 - True Winds, buoy data (23 24N, 162 18W)

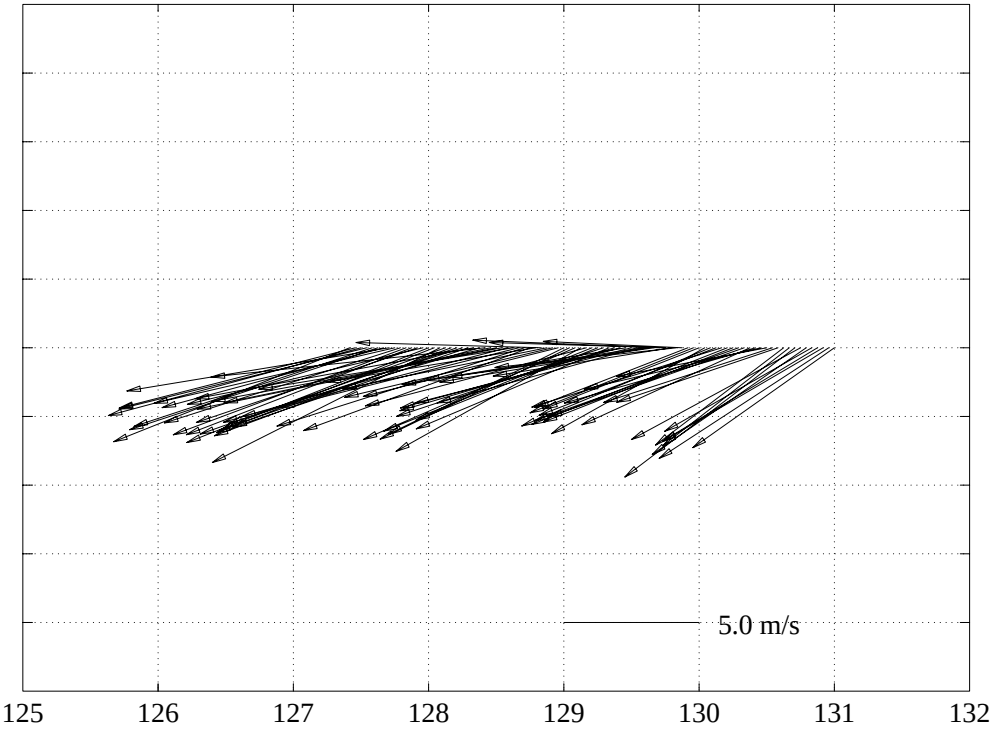

Julian days from January, 1, 1991

Figure 6.7.7

HOT 27 True Winds

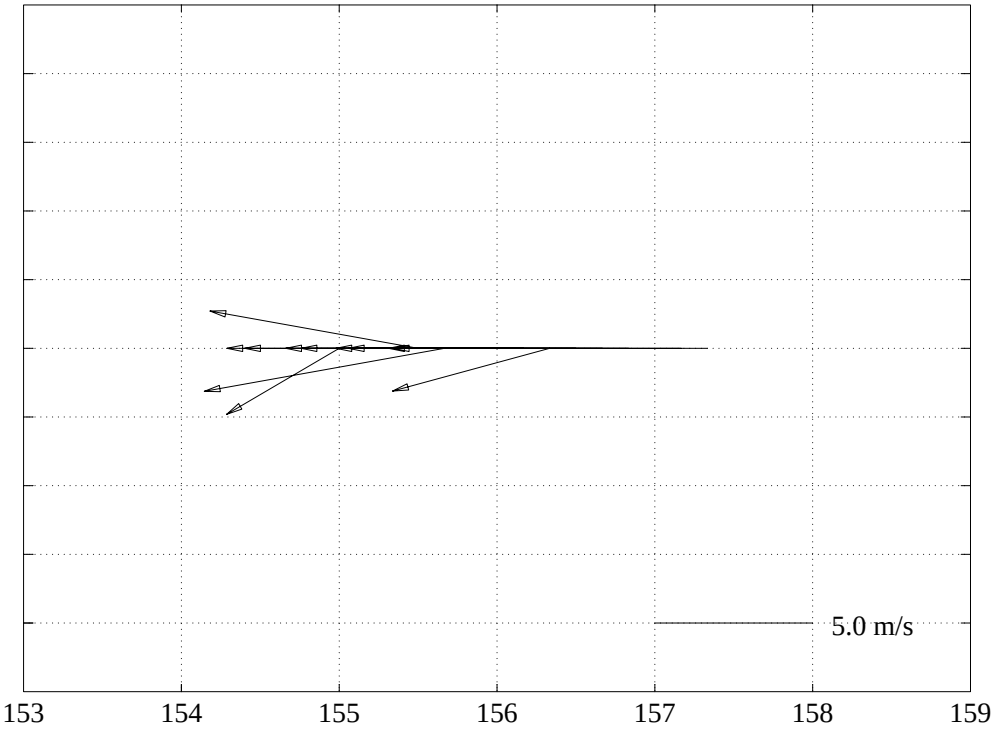

Julian days from January, 1, 1991

HOT 27 - True Winds, buoy data (23 24N, 162 18W)

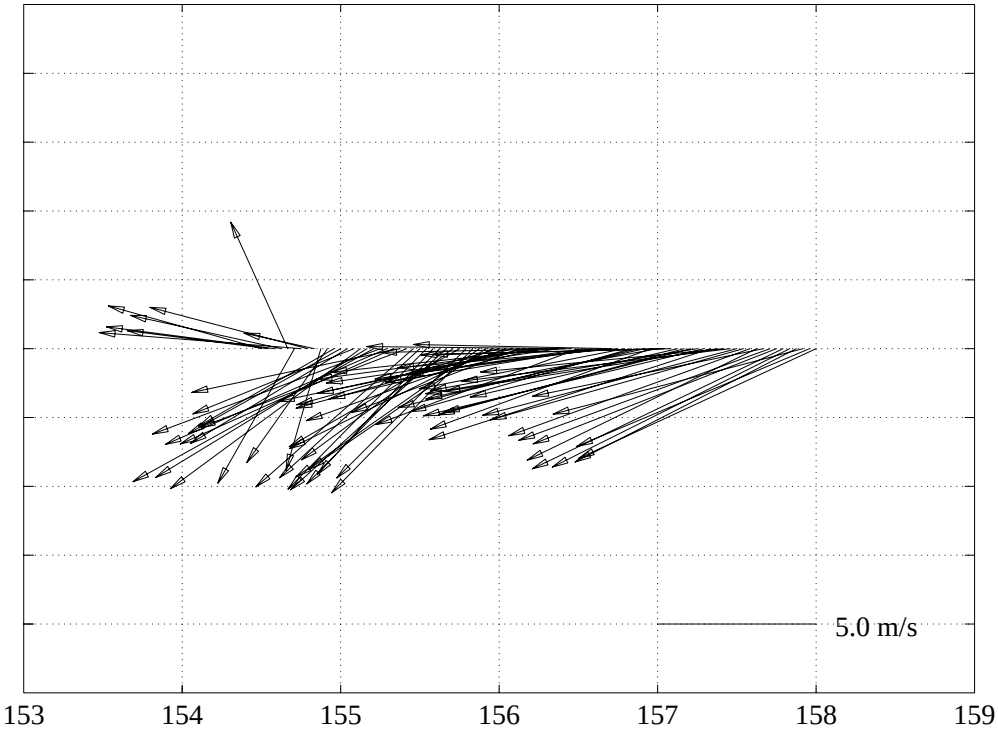

Julian days from January, 1, 1991

Figure 6.7.8

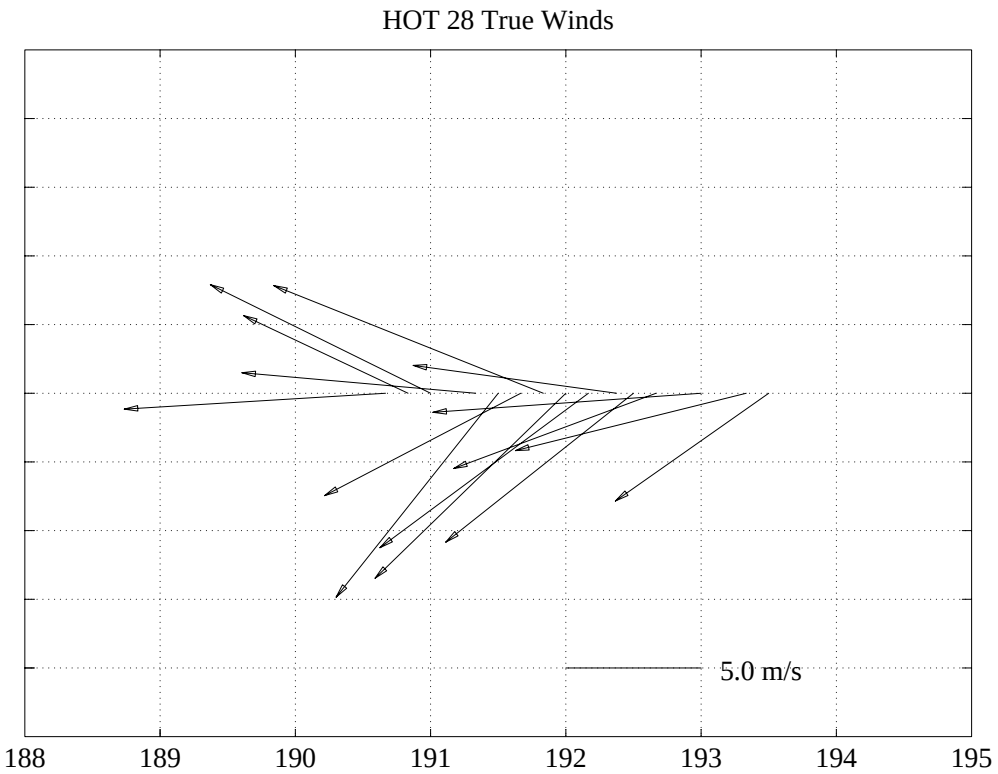
HOT 28 True Winds
5.0 m/s
188
189
190
191
192
193
194
195
Julian days from January, 1, 1991

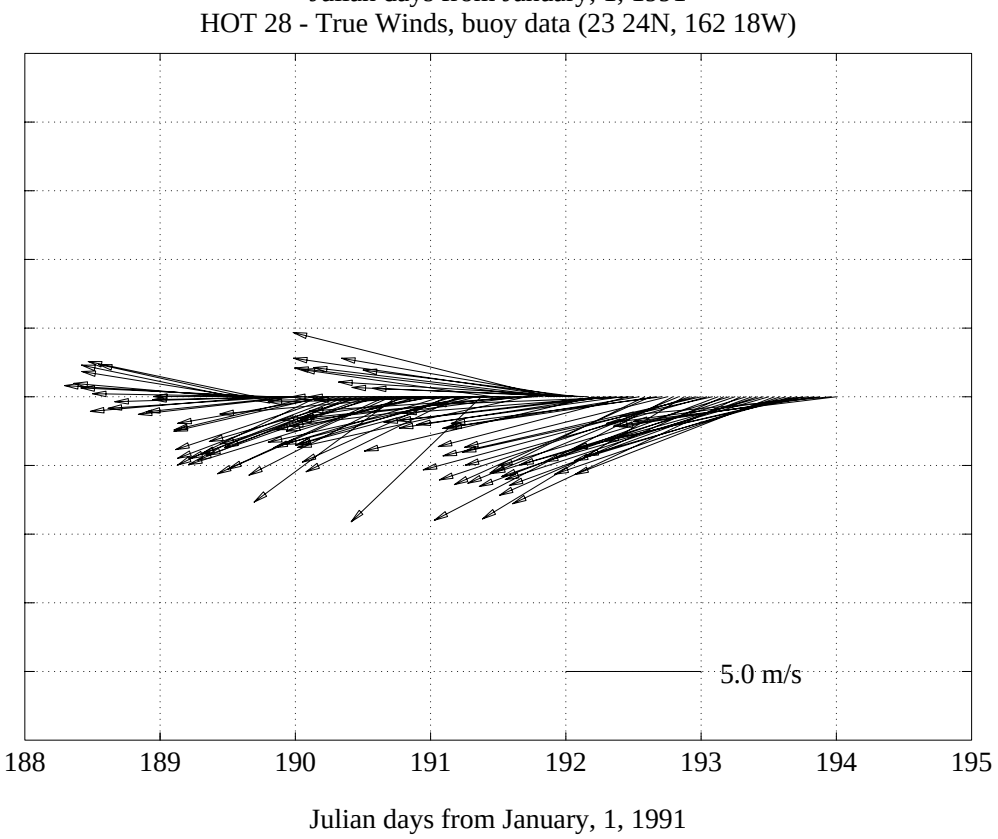
HOT 28 - True Winds, buoy data (23 24N, 162 18W)
5.0 m/s
188
189
190
191
192
193
194
195
Julian days from January, 1, 1991

Figure 6.7.9

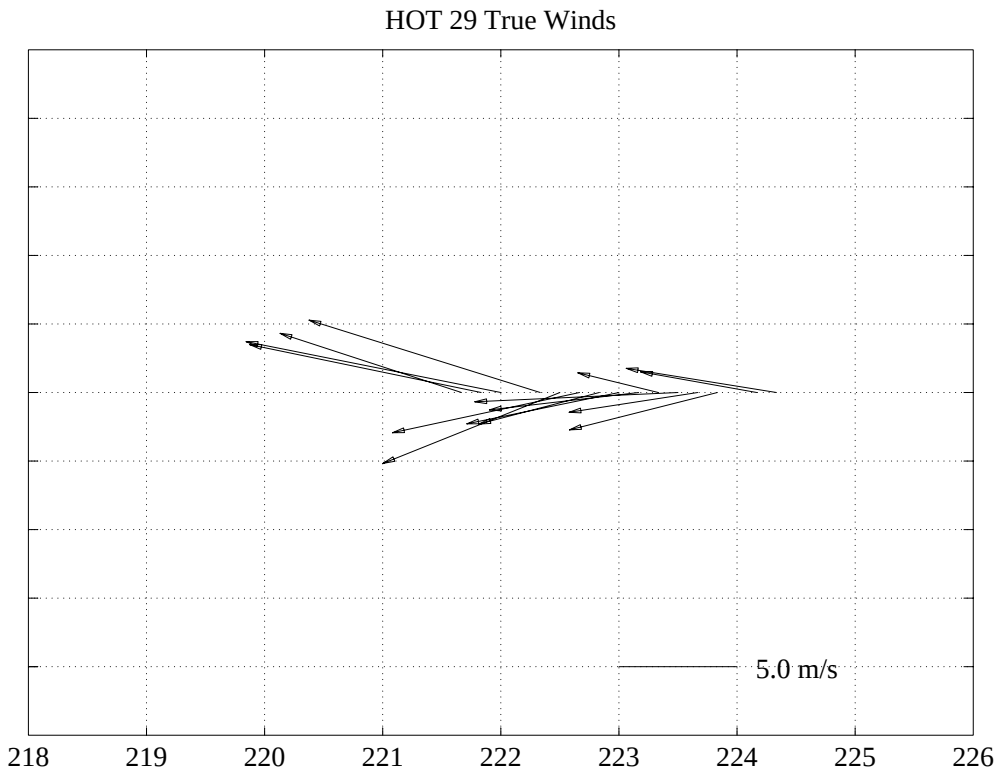
HOT 29 True Winds
5.0 m/s
218
219
220
221
222
223
224
225
226
Julian days from January, 1, 1991


HOT 29 - True Winds, buoy data (23 24N, 162 18W)
5.0 m/s
218
219
220
221
222
223
224
225
226
Julian days from January, 1, 1991

Figure 6.7.10

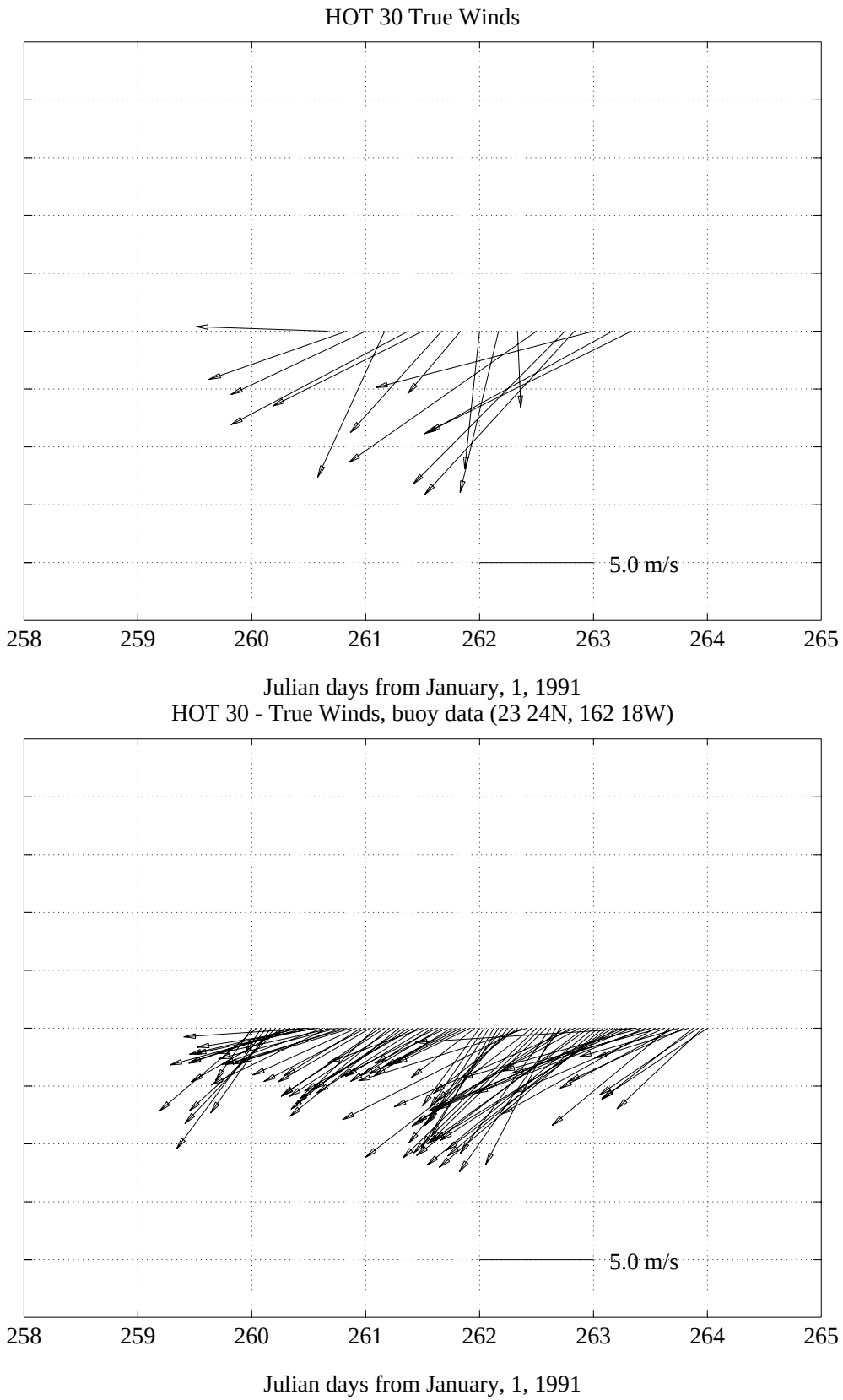
HOT 30 True Winds
5.0 m/s
258
259
260
261
262
263
264
265
Julian days from January, 1, 1991
HOT 30 - True Winds, buoy data (23 24N, 162 18W)
5.0 m/s
258
259
260
261
262
263
264
265
Julian days from January, 1, 1991

Figure 6.7.11


HOT 31 True Winds
5.0 m/s
292
293
294
295
296
297
298
299
Julian days from January, 1, 1991

Figure 6.7.12

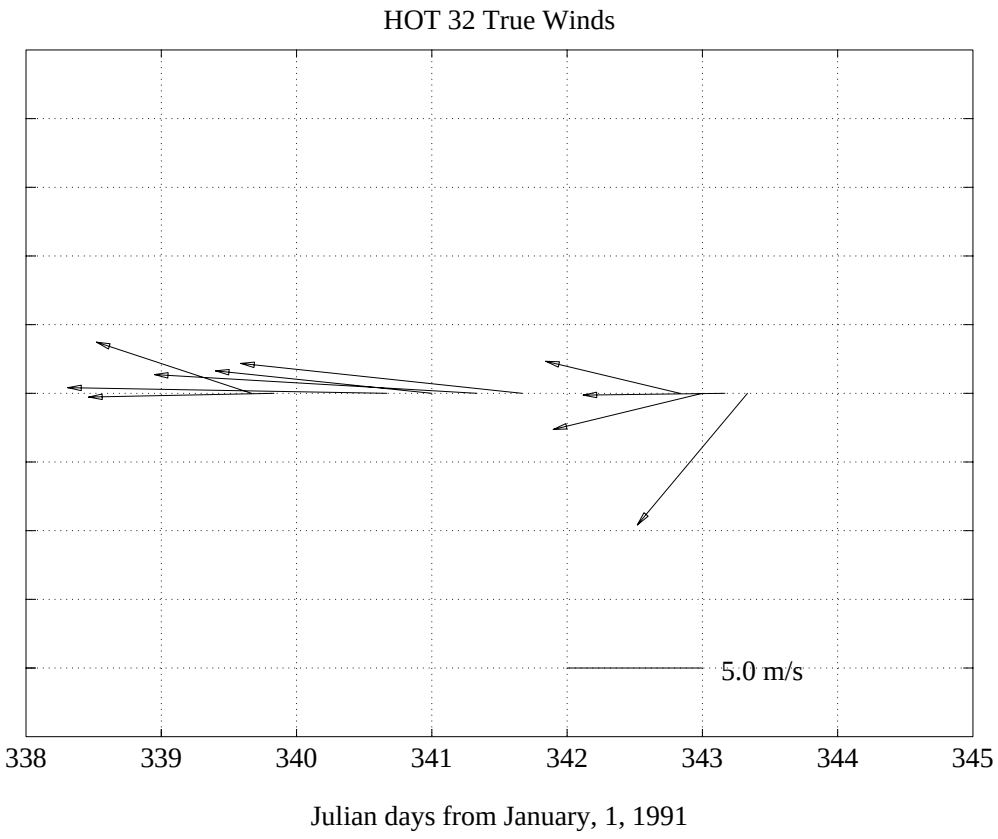
HOT 32 True Winds
5.0 m/s
338
339
340
341
342
343
344
345
Julian days from January, 1, 1991

Figure 6.7.13

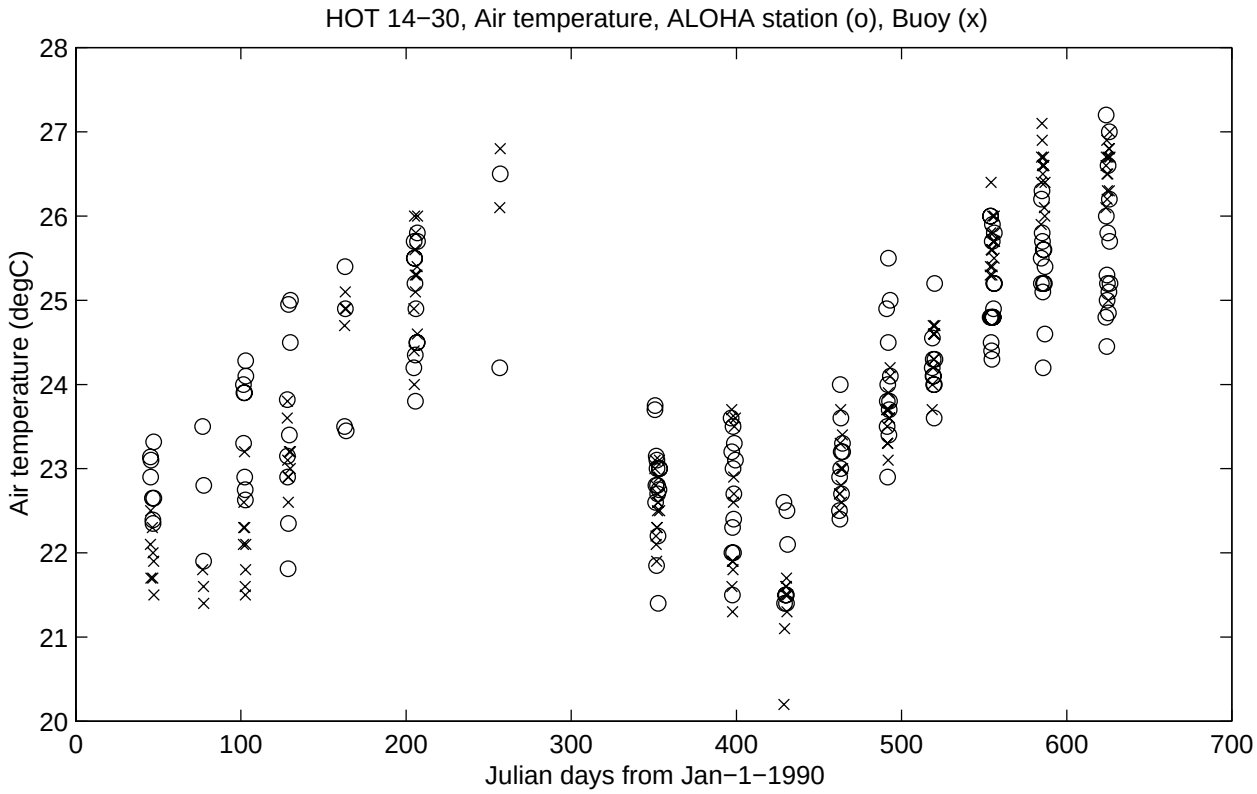
HOT 14−30, Air temperature, ALOHA station (o), Buoy (x)
Air temperature (degC)
Julian days from Jan−1−1990
28
27
26
25
24
23
22
21
20
0
100
200
300
400
500
600
700

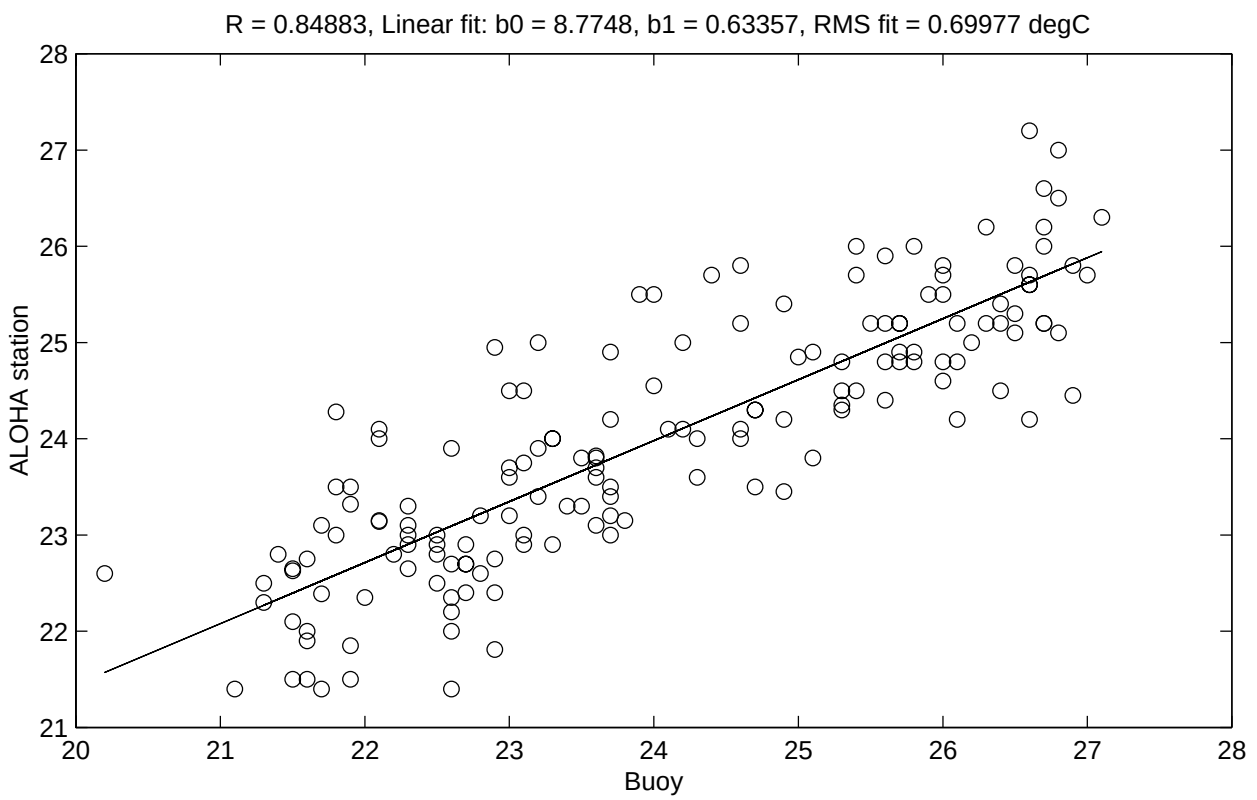
R = 0.84883, Linear fit: b0 = 8.7748, b1 = 0.63357, RMS fit = 0.69977 degC
ALOHA station
Buoy
28
27
26
25
24
23
22
21
20
21
22
23
24
25
26
27
28

Figure 6.7.14

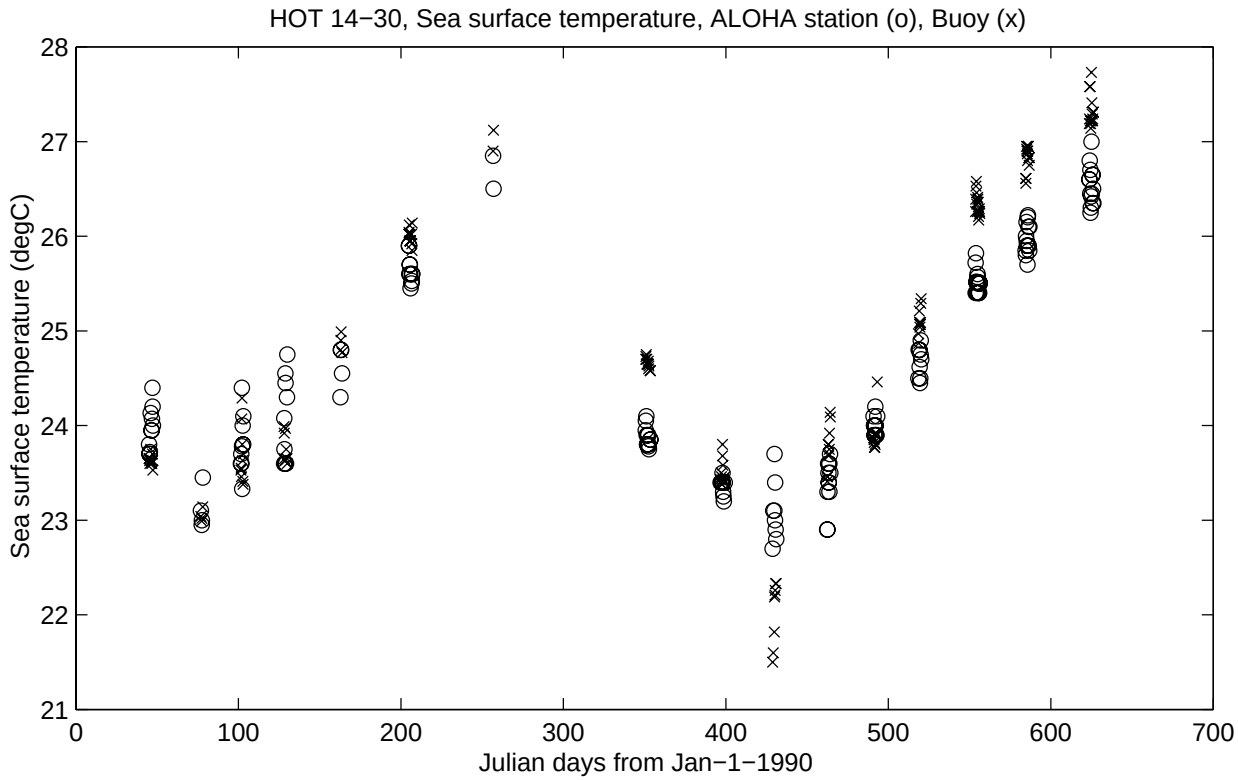
HOT 14−30, Sea surface temperature, ALOHA station (o), Buoy (x)
Sea surface temperature (degC)
Julian days from Jan−1−1990
28
27
26
25
24
23
22
21
0
100
200
300
400
500
600
700

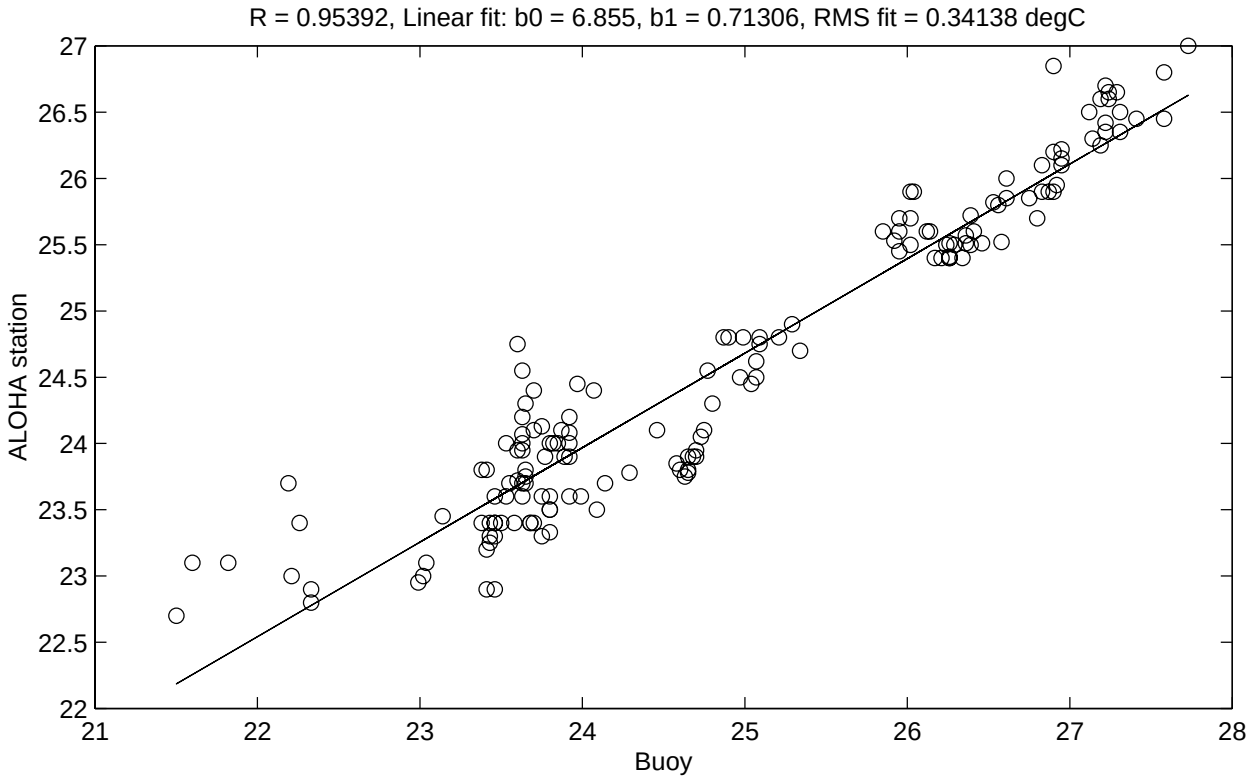
R = 0.95392, Linear fit: b0 = 6.855, b1 = 0.71306, RMS fit = 0.34138 degC
ALOHA station
Buoy
27
26.5
26
25.5
25
24.5
24
23.5
23
22.5
22
21
22
23
24
25
26
27
28

Figure 6.7.15

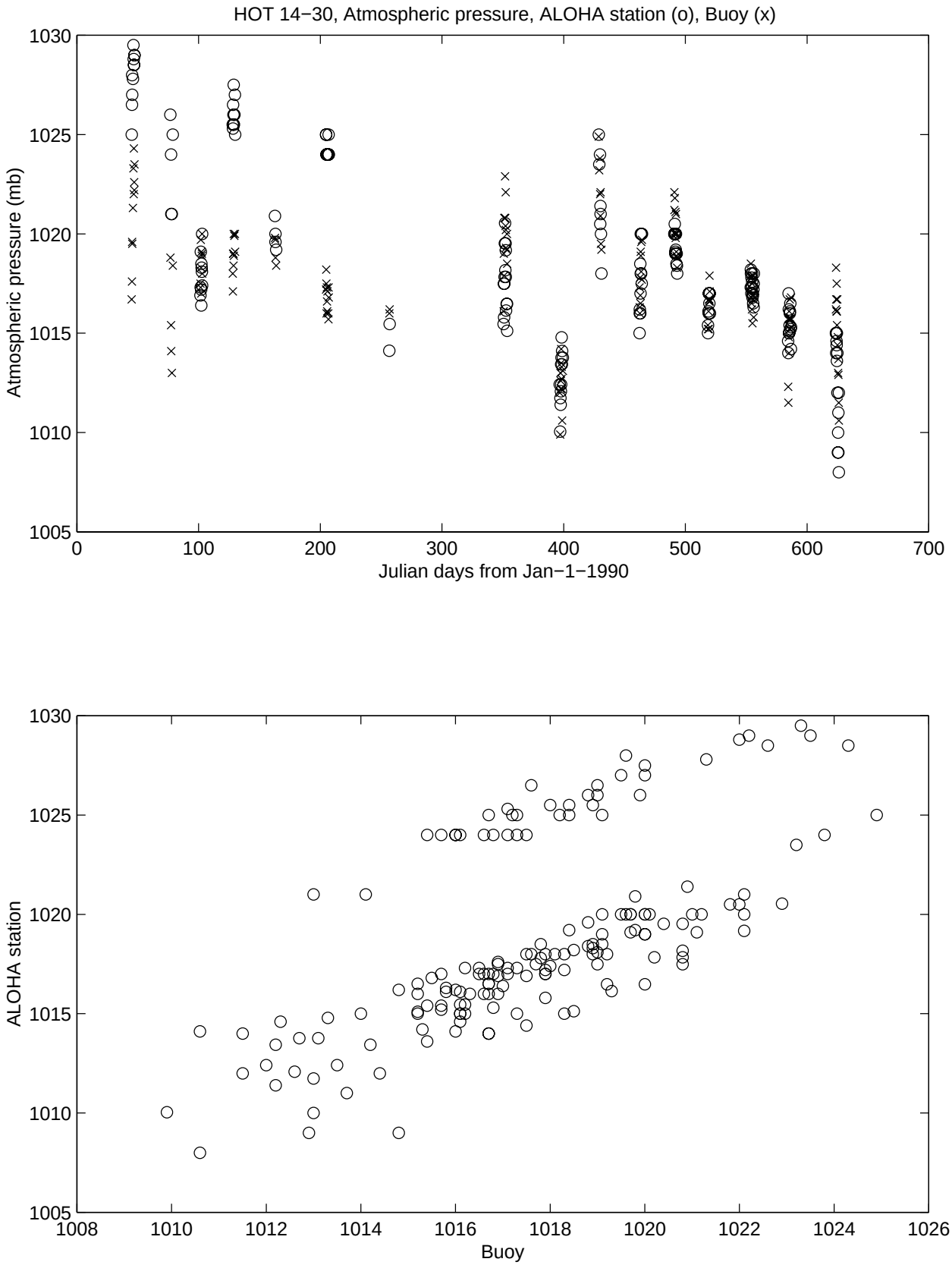
HOT 14−30, Atmospheric pressure, ALOHA station (o), Buoy (x)
Atmospheric pressure (mb)
Julian days from Jan−1−1990
1030
1025
1020
1015
1010
1005
0
100
200
300
400
500
600
700
ALOHA station
Buoy
1008
1010
1012
1014
1016
1018
1020
1022
1024
1026

Figure 6.7.16

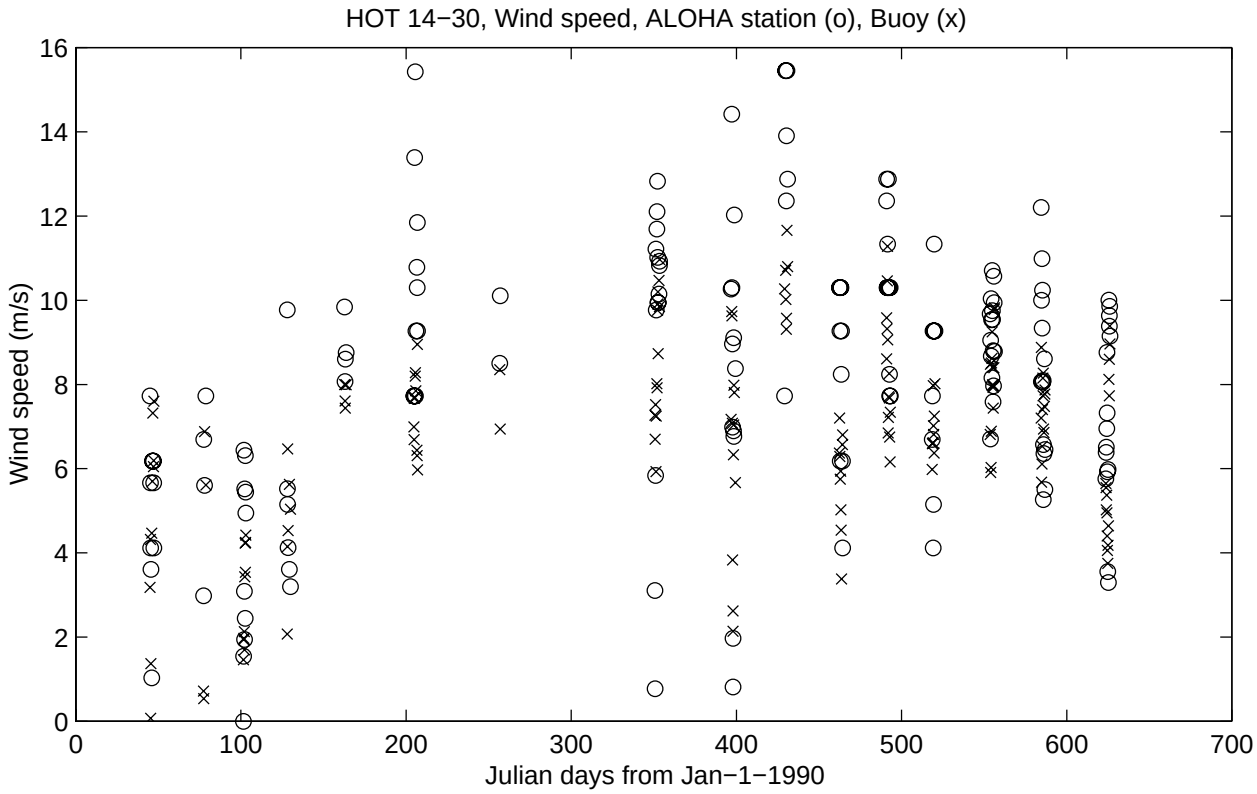
HOT 14−30, Wind speed, ALOHA station (o), Buoy (x)
Wind speed (m/s)
Julian days from Jan−1−1990
0
2
4
6
8
10
12
14
16
0
100
200
300
400
500
600
700

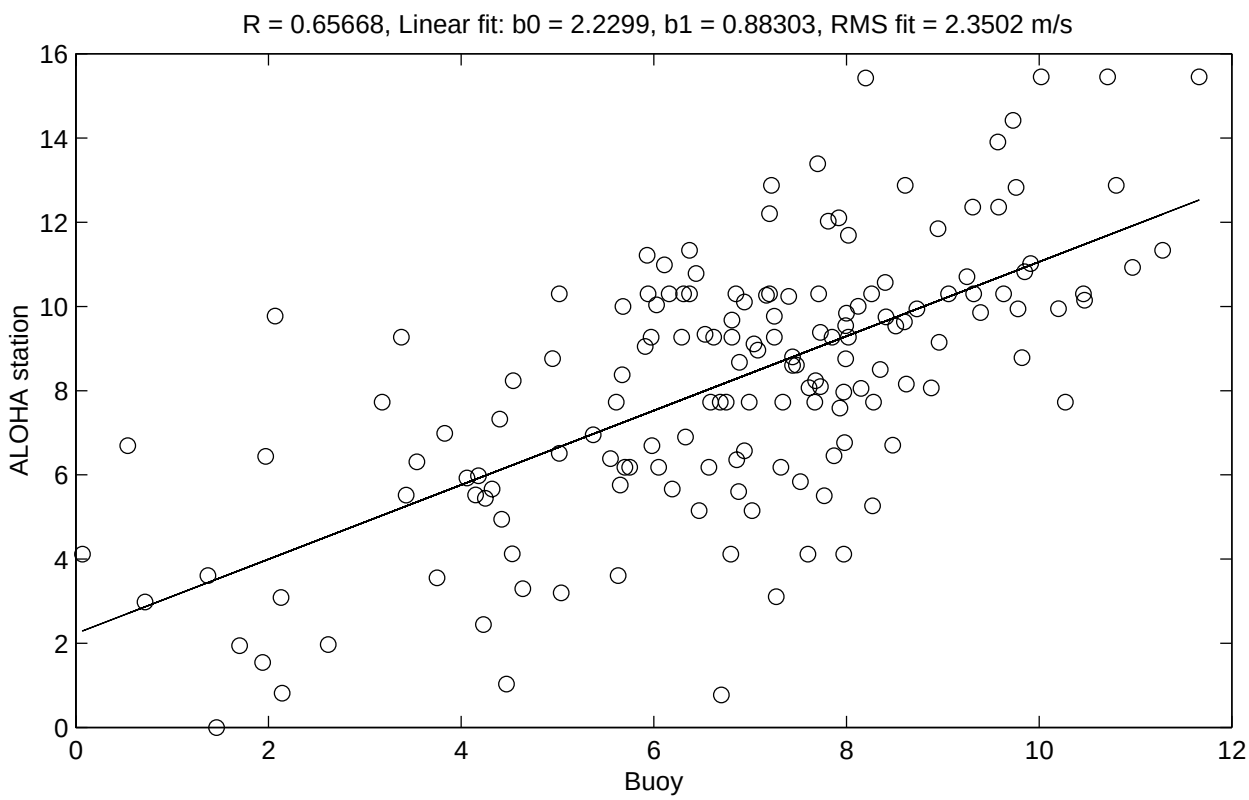
R = 0.65668, Linear fit: b0 = 2.2299, b1 = 0.88303, RMS fit = 2.3502 m/s
ALOHA station
Buoy
0
2
4
6
8
10
12
14
16
0
2
4
6
8
10
12

Figure 6.7.17

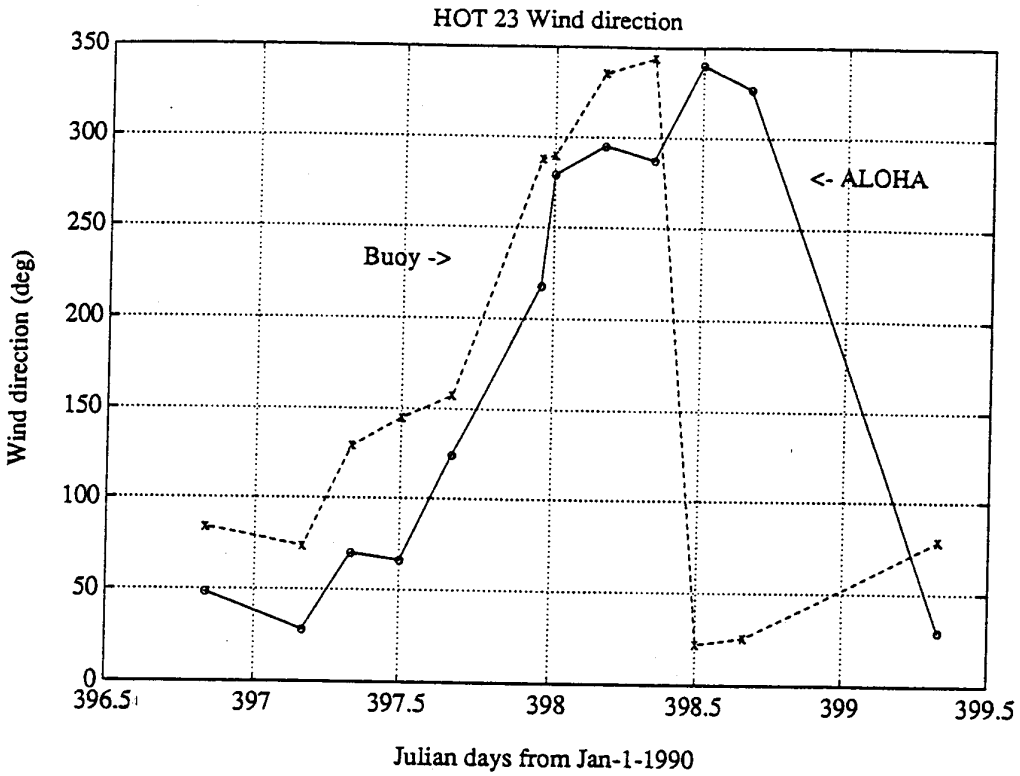
HOT 23 Wind direction
Wind direction (deg)
350
300
250
200
150
100
50
0
396.5
397
397.5
398
398.5
399
399.5
Julian days from Jan-1-1990
<- ALOHA
Buoy ->

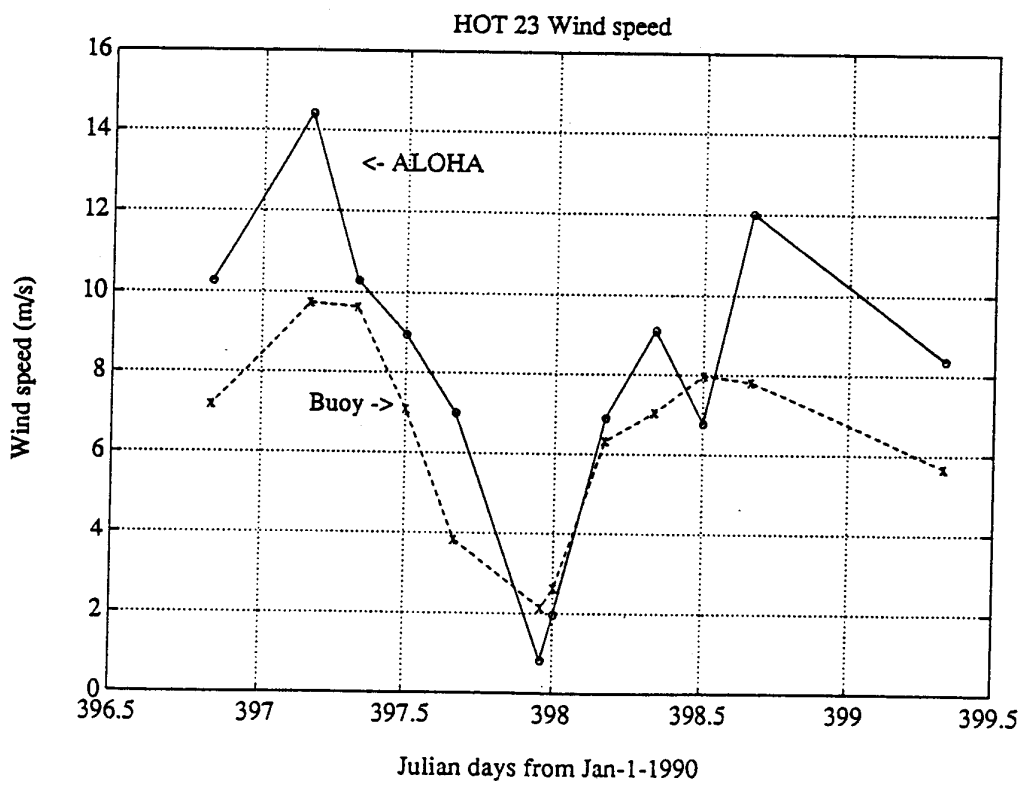
HOT 23 Wind speed
Wind speed (m/s)
16
14
12
10
8
6
4
2
0
396.5
397
397.5
398
398.5
399
399.5
Julian days from Jan-1-1990
<- ALOHA
Buoy ->

Figure 6.7.18

6.8. CTD Station Locations and Sediment Trap Drift Tracks

Figure 6.8.1: (Right panel) CTD station locations on HOT-23. CTD stations represented by open circles relative to Station ALOHA. Solid lines connect casts taken in sequence and numbers show location of first and last casts. Dashed line shows area nominally defined as Station ALOHA. (Left panel) Drift track for the sediment trap array during the 72-hour deployment period.

Figure 6.8.2: As in Figure 6.8.1, except for HOT-24.

Figure 6.8.3: As in Figure 6.8.1, except for HOT-25.

Figure 6.8.4: As in Figure 6.8.1, except for HOT-26.

Figure 6.8.5: As in Figure 6.8.1, except for HOT-27.

Figure 6.8.6: As in Figure 6.8.1, except for HOT-28.

Figure 6.8.7: As in Figure 6.8.1, except for HOT-29.

Figure 6.8.8: As in Figure 6.8.1, except for HOT-30.

Figure 6.8.9: As in Figure 6.8.1, except for HOT-31.

Figure 6.8.10: As in Figure 6.8.1, except for HOT-32.

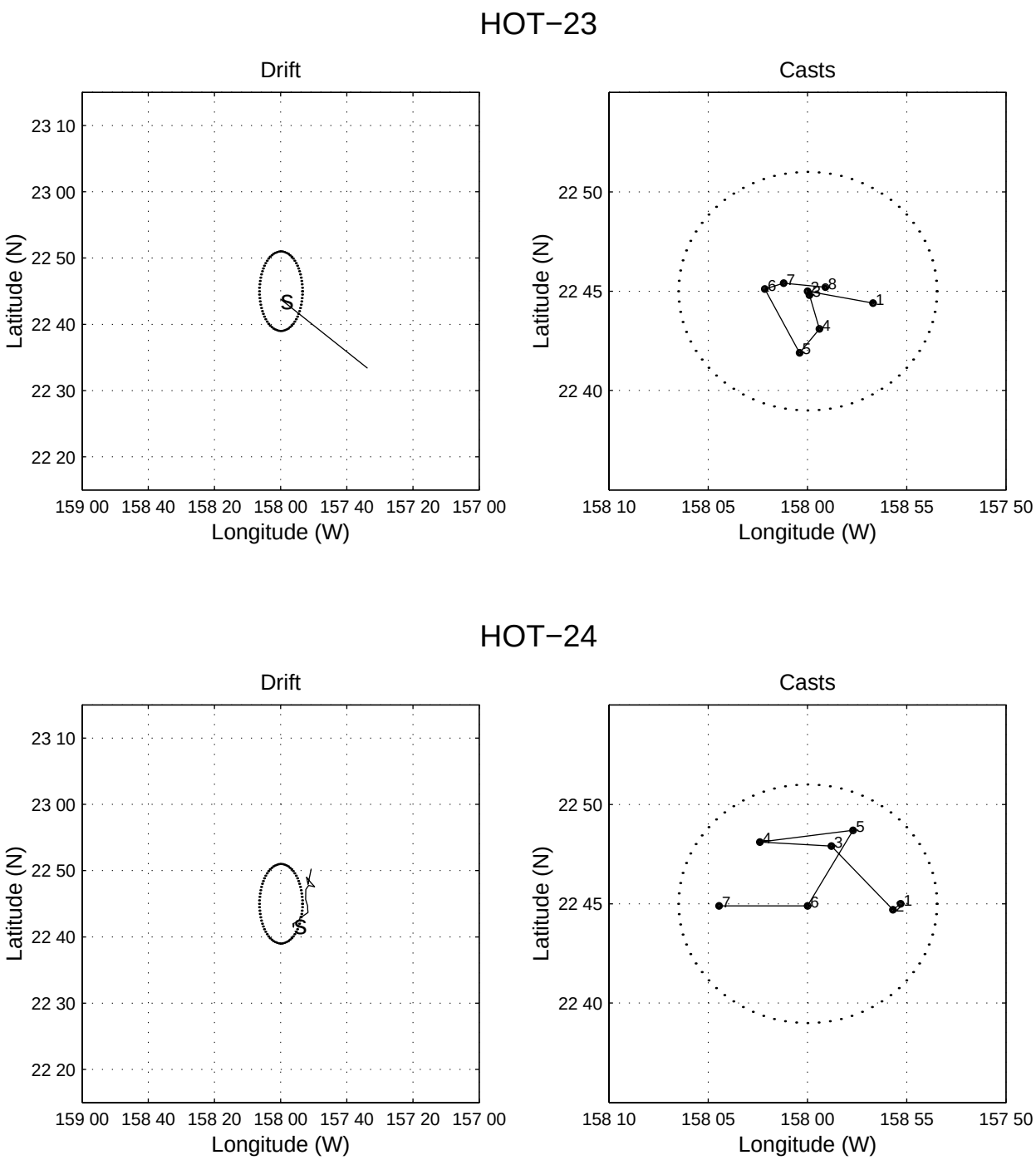
HOT−23
Drift
Casts
Latitude (N)
Longitude (W)
23 10
23 00
22 50
22 40
22 30
22 20
159 00
158 40
158 20
158 00
157 40
157 20
157 00
S
22 45
158 10
158 05
158 55
157 50
1
2
3
4
5
6
7
8
HOT−24
Drift
Casts
S

Figure 6.8.1-2

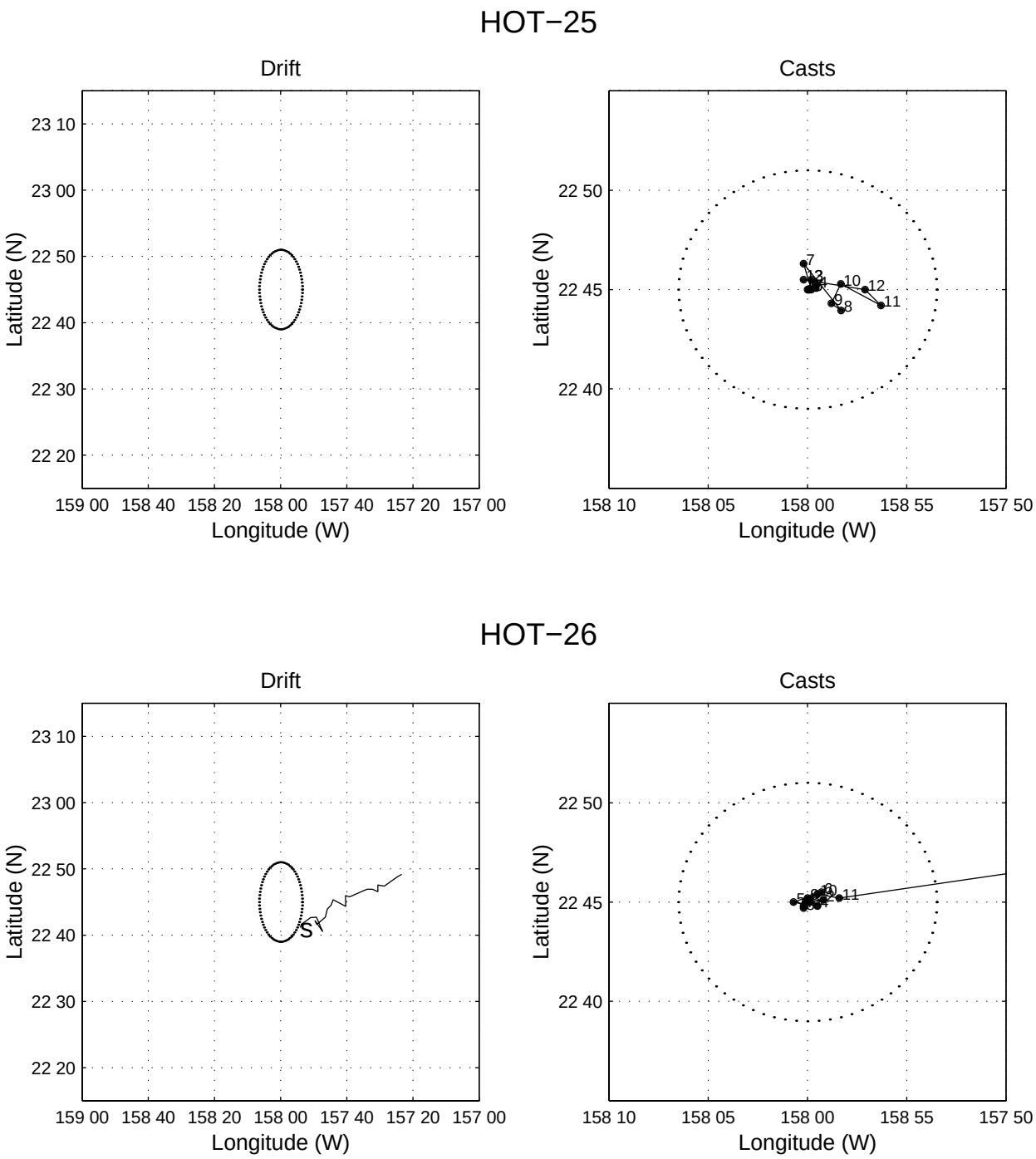
HOT−25
Drift
Casts
Latitude (N)
Longitude (W)
23 10
23 00
22 50
22 40
22 30
22 20
159 00
158 40
158 20
158 00
157 40
157 20
157 00
22 45
158 10
158 05
158 55
157 50
7
10
12
11
9
8
HOT−26
S

Figure 6.8.3-4

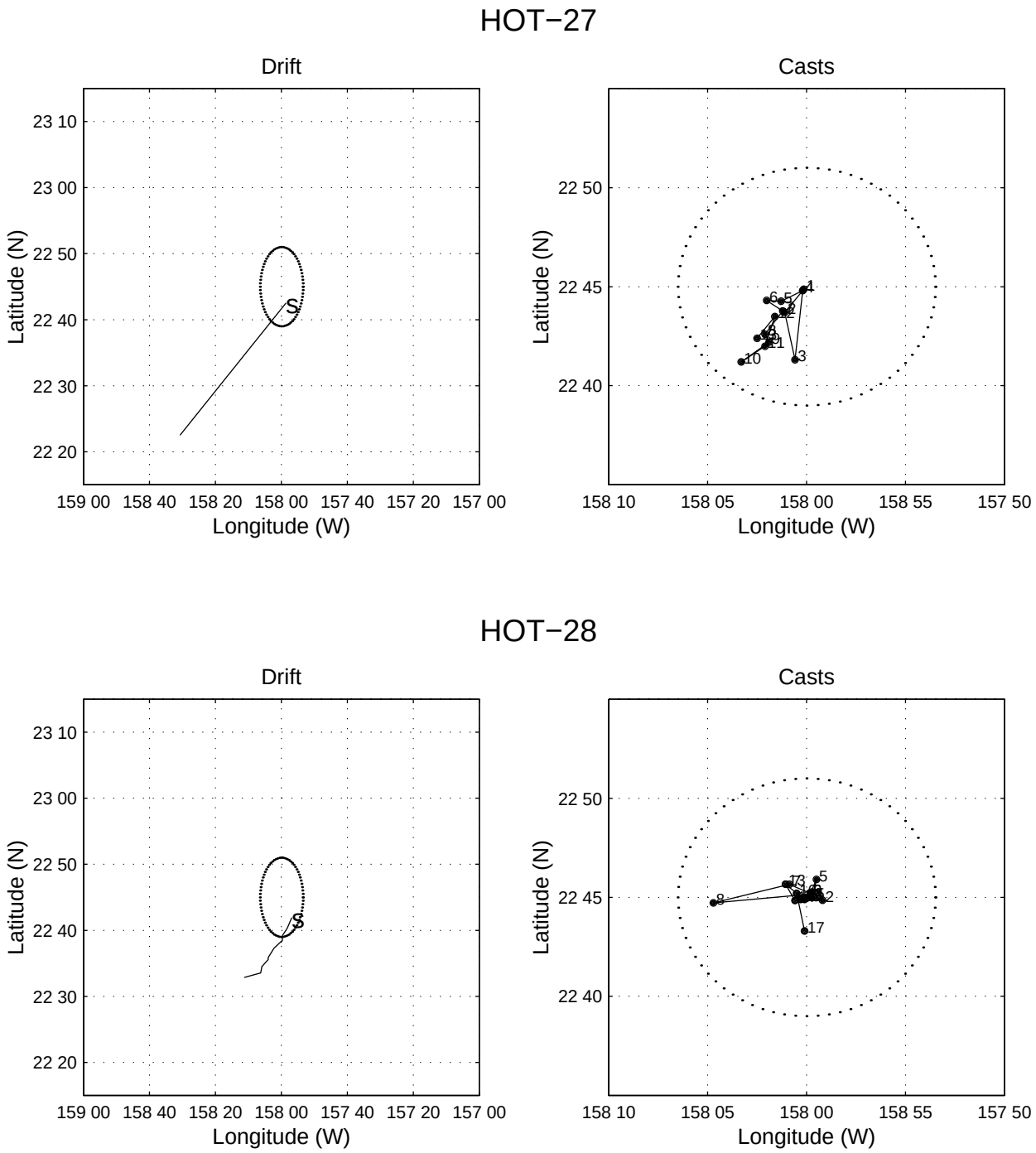
HOT−27
Drift
Casts
Latitude (N)
Longitude (W)
23 10
23 00
22 50
22 40
22 30
22 20
159 00
158 40
158 20
158 00
157 40
157 20
157 00
S
22 45
158 10
158 05
158 55
157 50
HOT−28

Figure 6.8.5-6

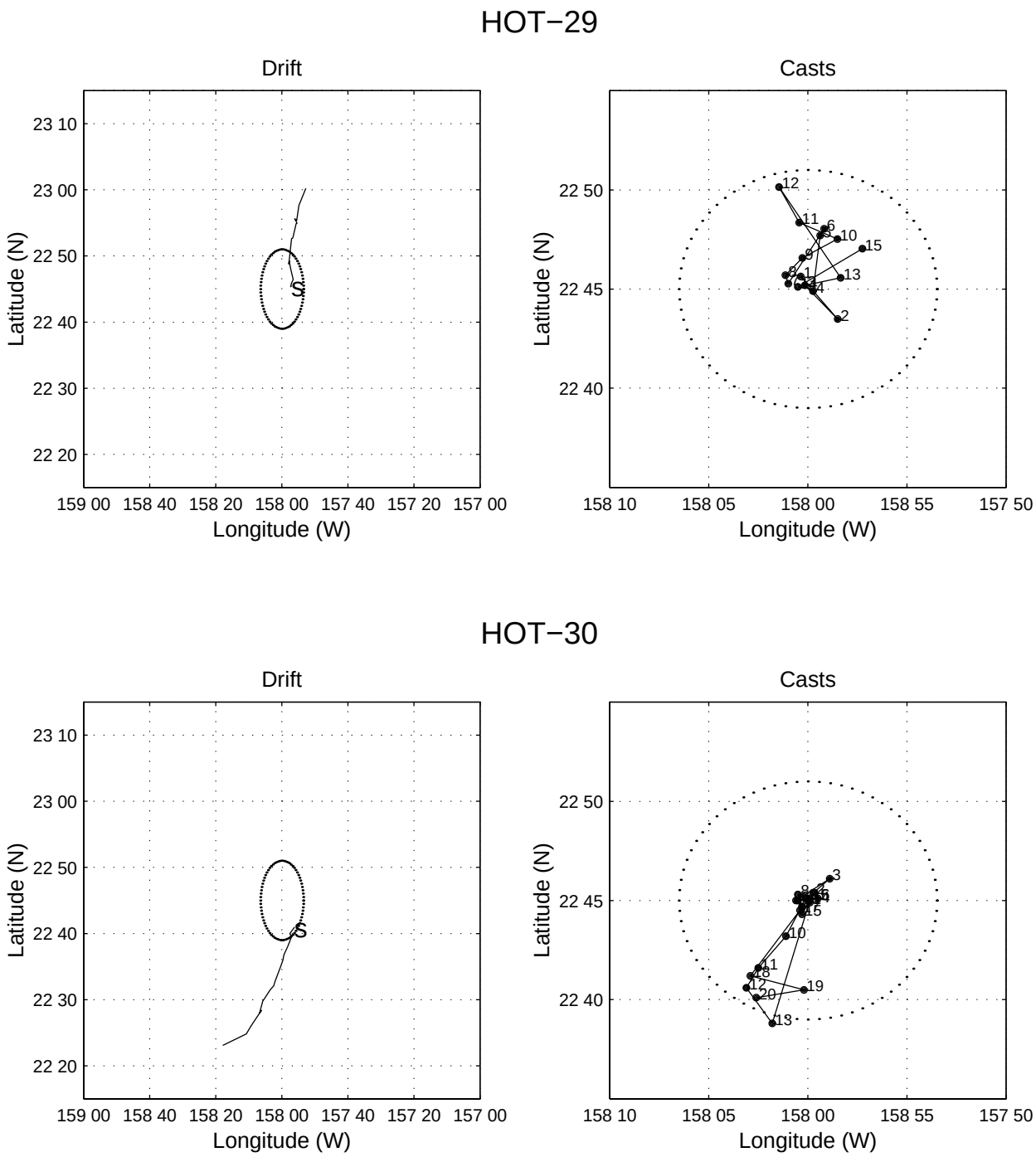
HOT−29
Drift
Casts
Latitude (N)
Longitude (W)
23 10
23 00
22 50
22 40
22 30
22 20
159 00
158 40
158 20
158 00
157 40
157 20
157 00
22 45
158 10
158 05
158 55
157 50
HOT−30

Figure 6.8.7-8

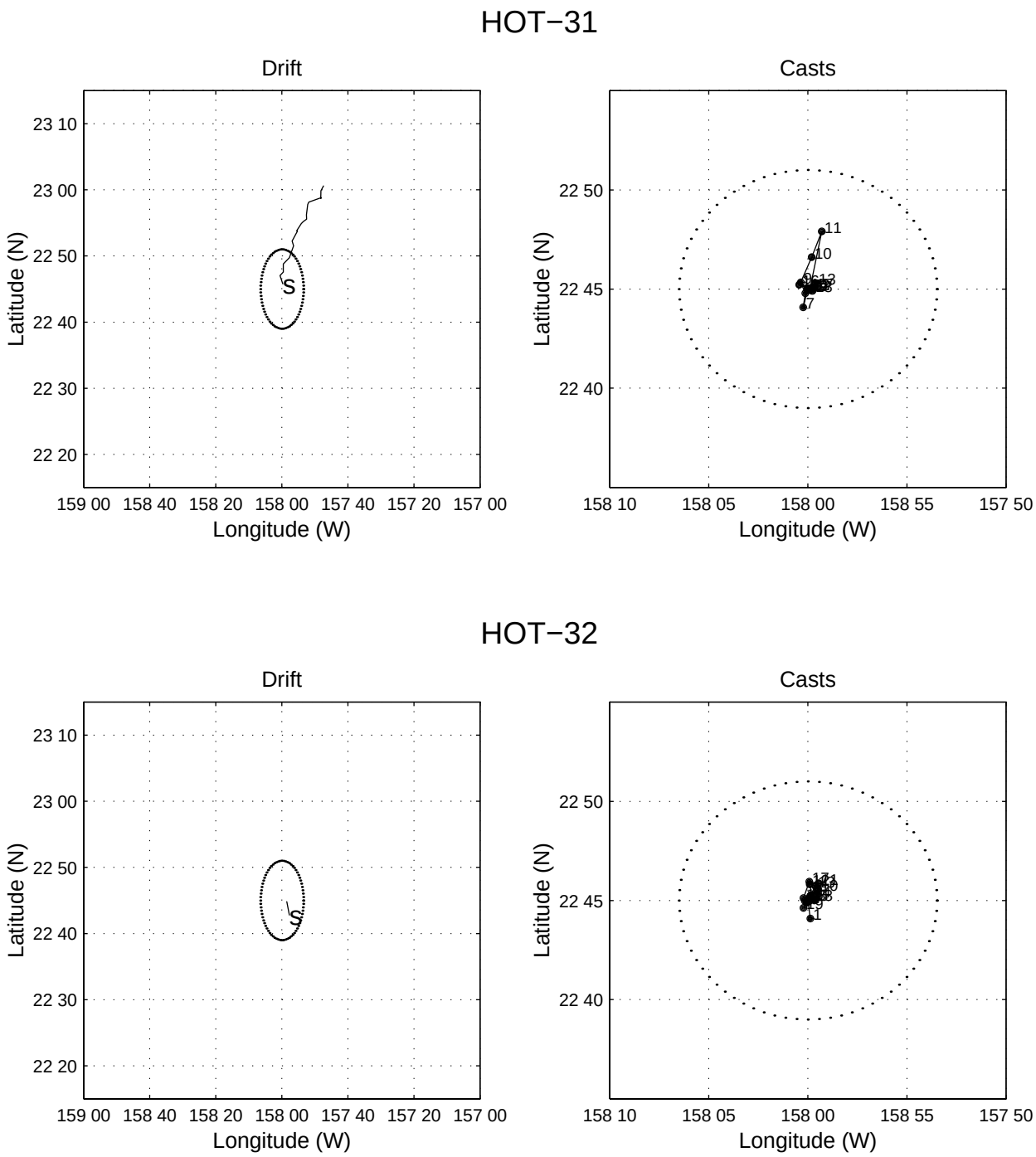

Figure 6.8.9-10

7. Hawaii Ocean Time-series Publications
Invited Presentations and Published Abstracts

1988 Karl, D. NSF-sponsored symposium on Dissertations in Chemical Oceanography, "Research opportunities in Hawaiian waters", Honolulu, Hawaii, November 1988.

1988 Karl, D. NSF/GOFS-sponsored workshop on sediment traps, "Determination of total C, N, P flux" and "Screens: A potential solution to the problem of swimmers", Gulf Coast Research Laboratory, Mississippi, November 1988.

1989 Winn, C. D., S. Chiswell, D. M. Karl and R. Lukas. Long time-series research in the Central Pacific Ocean. The Oceanography Society 1st Annual Meeting, Monterey, California.

1990 Chiswell, S. M. and R. Lukas. The Hawaii Ocean Time-series (HOT). EOS, *Transactions of the American Geophysical Union* 71, 1397.

1990 Karl, D. "JGOFS time-series programs," San Francisco, California, December 1990.

1990 Karl, D., R. Letelier, D. Bird, D. Hebel, C. Sabine and C. Winn. An Oscillatoria bloom in the oligotrophic North Pacific Ocean near the GOFS station ALOHA. *EOS, Transactions of the American Geophysical Union* 71, 177-178.

1990 Winn, C. D., D. Hebel, R. Letelier, D. Bird and D. Karl. Variability in biogeochemical fluxes in the oligotrophic central Pacific: Results of the Hawaii Ocean Time-Series Program. *EOS, Transactions of the American Geophysical Union* 71, 190.

1991 Karl, D. "The Hawaii Ocean Time-series program: Carbon production and particle flux", The Oceanography Society 2nd Annual Meeting, St. Petersburg, Florida, March 1991.

1991 Karl, D. NATO symposium on Biology and Ecology of Diazotrophic Marine Organisms, "*Trichodesmium* blooms and new nitrogen in the North Pacific gyre", Bamberg, Germany, May 1991.

1991 Letelier, R., D. Karl, R. Bidigare, J. Christian, J. Dore, D. Hebel and C. Winn. Temporal variability of phytoplankton pigments at the U.S.-JGOFS station ALOHA (22°45'N, 158°W). *EOS, Transactions of the American Geophysical Union* 72, 74.

1991 Winn, C., C. Sabine, D. Hebel, F. Mackenzie and D. M. Karl. Inorganic carbon system dynamics in the central Pacific Ocean: Results of the Hawaii Ocean Time-series program. *EOS, Transactions of the American Geophysical Union* 72, 70.

1992 Anbar, A. D. Rhenium in seawater: Confirmation of generally conservative behavior. *EOS, Transactions of the American Geophysical Union* 73, 278.

1992 Bidigare, R. R., L. Campbell, M. Ondrusek, R. Letelier and D. Vaulot. Characterization of picophytoplankton at Station ALOHA (22°45'N, 158°W) using HPLC, flow cytometry and immunofluorescence techniques. PACON 1992 Meeting, 1-5 June 1992.

1992 Karl, D. NSF-sponsored GLOBEC scientific steering committee meeting, "Hawaii Ocean

Time-series (HOT) program: A GLOBEC 'Blue Water' initiative", Honolulu, Hawaii, March 1992.

1992 Karl, D. IGBP International Symposium on Global Change, "Oceanic ecosystem variability: Initial results from the JGOFS Hawaii Ocean Time-series (HOT) experiment", Tokyo, Japan, March 1992.

1992 Karl, D. Conoco HOT Topics Seminar Series, "The U.S.-JGOFS Hawaii Ocean Time-Series (HOT) Program: Biogeochemical Vignettes from the Oligotrophic North Pacific Ocean" and "Temporal Variability in Bioelement Flux at Station ALOHA (22°45'N, 158°W)", Woods Hole, Massachusetts, May 1992.

1992 Karl, D., C. Winn, D. Hebel, R. Letelier, J. Dore and J. Christian. The U.S.-JGOFS Hawaii Ocean Time-Series (HOT) program. American Society for Limnology and Oceanography Aquatic Sciences Meeting, Santa Fe, NM, February 1992.

1992 Campbell, L., R. R. Bidigare, R. Letelier, M. Ondrusek, S. Hall, B. Tsai and C. Winn. Phytoplankton population structure at the Hawaii Ocean Time-series station. American Society for Limnology and Oceanography Aquatic Sciences Meeting, Santa Fe, NM, February 1992.

1992 Lukas, R. Water mass variability observed in the Hawaii Ocean Time Series. *EOS, Transactions of the American Geophysical Union* 72, 70.

1992 Schudlich, R. and S. R. Emerson. Modelling dissolved gases in the subtropical upper ocean: JGOFS/WOCE Hawaiian Ocean Time-series. *EOS, Transactions of the American Geophysical Union* 73, 287.

1992 Tupas, L. M., B. N. Popp and D. M. Karl. Dissolved organic carbon in oligotrophic waters: Experiments on sample preservation, storage and analysis. *EOS, Transactions of the American Geophysical Union* 73, 287

1992 Winn, C. D., D. Hebel, R. Letelier, J. Christian, J. Dore, R. Lukas and D. M. Karl. Long time-series measurements in the central North Pacific: Results of the Hawaii Ocean Time-series program. PACON conference, Kona, Hawaii, June 1992.

Newsletters

1991 Lukas, R. and S. Chiswell. Submesoscale water mass variations in the salinity minimum of the North Pacific. *WOCE Notes*, 3(1), 6-8.

1992 Chiswell, S. Inverted echo sounders at the WOCE deep-water station. WOCE Notes, 4(4), 1-6.

1992 Firing, E. and P. Hacker. ADCP results from WHP P16/P17. WOCE Notes, 4(3), 6- 12.

plus a periodic column entitled "HOT Stuff", written by D. Karl, which appears in the U.S. JGOFS Program newsletter

Invited Book Chapters and Refereed Publications

1990 Giovannoni, S. J., E. F. DeLong, T. M. Schmidt and N. R. Pace. Tangential flow filtration and preliminary phylogenetic analysis of marine picoplankton. *Applied and Environmental Microbiology*, 56, 2572-2575.

1990 Collins, D. J., W. J. Rhea and A. van Tran. Bio-optical profile data report: HOT-3. National Aeronautics and Space Administration JPL Publ. #90-36.

1990 Firing, E. and R. L. Gordon. Deep ocean acoustic Doppler current profiling. In: G. F. Appell and T. B. Curtin (eds.), *Proceedings of the Fourth IEEE Working Conference on Current Measurements,* pp. 192-201. IEEE, New York.

1991 Karl, D. M., W. G. Harrison, J. Dore et al. Chapter 3. Major bioelements workshop report. In: D. C. Hurd and D. W. Spencer (eds.), *Marine Particles: Analysis and Characterization*, pp. 33-42. American Geophysical Union, Geophysical Monograph 63.

1991 Karl, D. M., J. E. Dore, D. V. Hebel and C. Winn. Procedures for particulate carbon, nitrogen, phosphorus and total mass analyses used in the US-JGOFS Hawaii Ocean Time-Series Program. In: D. Spencer and D. Hurd (eds.), *Marine Particles: Analysis and Characterization*, pp. 71-77. American Geophysical Union, Geophysical Monograph 63.

1991 Karl, D. M. and C. D. Winn. A sea of change: Monitoring the oceans' carbon cycle. *Environmental Science & Technology* 25, 1976-1981.

1991 Sabine, C. L. and F. T. Mackenzie. Oceanic sinks for anthropogenic CO_2. International *Journal of Energy, Environment, Economics* 1, 119-127.

1991 Schmidt, T. M., E. F. DeLong and N. R. Pace. Analysis of a marine picoplankton community by 16S rRNA gene cloning and sequencing. *Journal of Bacteriology*, 173, 4371-4378.

1991 Chiswell, S. M. Dynamic response of CTD pressure sensors to temperature. *Journal of Atmospheric and Oceanic Technology*, 8, 659-668.

1992 Karl, D. M., R. Letelier, D. V. Hebel, D. F. Bird and C. D. Winn. *Trichodesmium* blooms and new nitrogen in the North Pacific gyre. In: E. J. Carpenter et al. (eds.), *Marine Pelagic Cyanobacteria: Trichodesmium and Other Diazotrophs*, pp. 219-237. Kluwer Academic Publishers, Netherlands.

1992 Karl, D. M. and G. Tien. MAGIC: A sensitive and precise method for measuring dissolved phosphorus in aquatic environments. *Limnology and Oceanography*, 37, 105-116.

1992 Chen, R. F. and J. L. Bada. The fluorescence of dissolved organic matter in seawater. *Marine Chemistry*, 37, 191-221.

1992 Quay, P.D., B. Tilbrook and C. S. Wong. Oceanic uptake of fossil fuel CO_2: Carbon-13 evidence. *Science*, 256, 74-78.

1992 Karl, D. M. The oceanic carbon cycle: Primary production and carbon flux in the oligotrophic North Pacific Ocean. *Proceedings of the IGBP Symposium on Global Change*, Tokyo, Japan, in press.

1993 Anbar, A. D., R. A. Creaser, D. A. Papanastassiou and G. J. Wasserburg. Rhenium in seawater: Confirmation of generally conservative behavior. *Geochimica et Cosmochimica Acta*, 56, 4099-4103.

1993 Karl, D. M., G. Tien, J. Dore and C. D. Winn. Total dissolved nitrogen and phosphorus concentrations at US-JGOFS Station ALOHA: Redfield reconciliation. *Marine Chemistry*, 41, 203-208.

1993 Karl, D. M. Total microbial biomass estimation derived from the measurement of particulate adenosine-5'-triphosphate. In: P. F. Kemp, B. F. Sherr, E. B. Sherr and J. J. Cole (eds.), *Current Methods in Aquatic Microbial Ecology*, in press.

1993 Winn, C. D., R. Lukas, D. Hebel, C. Carrillo, R. Letelier and D. M. Karl. Time- series measurements in the oligotrophic ocean: Resolving variability in the North Pacific subtropical gyre. In: Proceedings of the *Pacific Congress on Marine Science and Technology*, in press.

1993 Atkinson, M. A., F. Thomas, R. Lukas and C. Winn. New calibration equations for amperometric membrane oxygen sensors. *Deep-Sea Research*, in press.

1993 Letelier, R. M., R. R. Bidigare, D. V. Hebel, C. D. Winn and D. M. Karl. Temporal variability study of the phytoplankton community structure at the US-JGOFS Time-series Station ALOHA (22°45'N, 158°00'W) based on pigment analyses. *Limnology and Oceanography*, in press.

1993 Campbell, L. and D. Vaulot. Photosynthetic picoplankton community structure in the subtropical North Pacific Ocean near Hawaii (station ALOHA). *Deep-Sea Research*, in press.

1993 Selph, K. E., D. M. Karl, M. R. Landry. Quantification of Chemiluminescent DNA probes using liquid scintillation counting. *Analytical Biochemistry*, in press.

1993 Thomas, F. I. M. and M. J. Atkinson. Field calibration of a potentiostatic micro-hole oxygen sensor. *Deep-Sea Research*, submitted.

1993 Atkinson, M. A., F. Thomas, E. Terrill, K. Morita and C. Liu. A potentiostatic oxygen sensor for oceanic CTDs. Submitted.

1993 Baines, S. B., M. L. Pace and D. M. Karl. Why does the relationship between sinking flux and planktonic primary production differ between lakes and oceans? Submitted to *Limnology and Oceanography*.

1993 Tupas, L. M., B. N. Popp and D. M. Karl. Dissolved organic carbon in oligotrophic waters: Experiments on sample preservation, storage and analysis. *Marine Chemistry*, submitted.

Theses and Dissertations

1992 Sabine, C. L. Geochemistry of particulate and dissolved inorganic carbon in the central North Pacific. Ph.D. Dissertation, May 1992

Data Reports

1990 Karl, D. M., C. D. Winn, D. V. W. Hebel and R. Letelier. Hawaii Ocean Time-series Program Field and Laboratory Protocols, September 1990. School of Ocean and Earth Science and Technology, Univ. of Hawaii, Honolulu, HI, 72 pp.

1990 Chiswell, S., E. Firing, D. Karl, R. Lukas and C. Winn. Hawaii Ocean Time-series Program Data Report 1, 1988-1989. SOEST Tech. Rept. #1, School of Ocean and Earth Science and Technology, Univ. of Hawaii, Honolulu, HI, 269 pp.

1992 Winn, C., S. Chiswell, E. Firing, D. Karl and R. Lukas. Hawaii Ocean Time-series Program Data Report 2, 1990. SOEST Tech. Rept. 92-1, School of Ocean and Earth Science and Technology, Univ. of Hawaii, Honolulu, HI, 175 pp.

8. Data Availability and Distribution

Data collected by the HOT program are made available to the oceanographic community as soon after processing as possible. In order to save paper and to provide easy access to our data for prospective users, we have provided summaries of our CTD and water column chemistry data on the enclosed IBM PC 3.5" high-density floppy diskette. CTD data at NODC standard pressures for temperature, potential temperature, salinity, oxygen and potential density are provided in ASCII files; water column chemistry data are provided in Lotus 1-2-3™ files. The pressure and temperature reported for each water column sample are derived from CTD temperature and pressure readings at the time of bottle trip. Densities are calculated from calibrated CTD temperature, pressure and salinity values. These densities are used, where appropriate, to express chemical concentrations on a per kilogram basis. With the exception of the results of replicate analysis, all water column chemical data collected during 1990 are given in these data sets.

These data included in the Lotus 1-2-3™ files have been quality controlled and the flags associated with each value indicate our estimate of the quality of each value. The text file `readme.txt` gives a description of data formats and quality flags.

A more complete data set, containing data collected in both year 1 and year 2 of the HOT program, as well as 2 dbar averaged CTD data, are available from two sources. The first is through NODC in the normal manner. The second source is via the world-wide Internet system. The data reside in a data base on a workstation at the University of Hawaii, and may be accessed using anonymous ftp on Internet.

In order to maximize ease of access, the data are in ASCII files. File names are chosen so that they may be copied to DOS machines without ambiguity. (DOS users should be aware that Unix is case-sensitive, and Unix extensions may be longer than 3 characters.)

The data are in a subdirectory called /pub/hot. More information about the data base is given in several files called `Readme.*` at this level. The file Readme.first gives general information on the data base; we encourage users to read it first.

The following is an example of how to use ftp to obtain HOT data. The user's command are denoted by `underlined` text, while the computer's responses are denoted by `regular` text. The workstation's Internet address is mana.soest.hawaii.edu, or `128.171.154.9` (either address should work).

```
Prompt>  ftp 128.171.154.9

Name (.....) :  anonymous

Password:  type your own Internet address

ftp>  cd /pub/hot

ftp>  ls
```

A directory of files and subdirectories will appear here.

```
ftp>  get Readme.first

ftp>  quit
```